Spring 2021

DEVELOPMENT OF OPEN LACTAM AND CAPTOPRIL ANALOGUES FOR THE COVALENT INHIBITION OF METALLO-β-LACTAMASES

Marie-Josiane Ohoueu
University of New Hampshire, Durham

DEVELOPMENT OF OPEN LACTAM AND CAPTOPRIL ANALOGUES FOR THE COVALENT INHIBITION OF METALLO-β-LACTAMASES

BY

MARIE-JOSIANE OHOUEU
B.S., American International College, 2013
M.S., New Mexico Highlands University, 2015

DISSERTATION

Submitted to the University of New Hampshire
in Partial Fulfillment of
the Requirement for the Degree of

Doctor of Philosophy
in
Chemistry

May, 2021

This dissertation was examined and approved in partial fulfillment of the requirements for the degree of Doctor of Philosophy in Chemistry by:

Dissertation Director, Marc A. Boudreau, Assistant Professor, Department of Chemistry

Arthur Greenberg, Professor, Department of Chemistry

Richard P. Johnson, Professor, Department of Chemistry

Christopher Bauer, Professor, Department of Chemistry

Krisztina Varga, Associate Professor, Department of Molecular, Cellular, and Biomedical Sciences

On April 12th, 2021

Approval signatures are on file with the University of New Hampshire Graduate School.

DEDICATION

To my parents, brothers, Drou, and all my family members,

For their constant support and encouragements.

Thank you.

ACKNOWLEDGMENTS

I would like to thank my research advisor, Marc Boudreau, for his support and guidance. He has helped me grow as a chemist and expand my knowledge and understanding in the field of chemistry. Also, I thank my committee members for the time and support they have dedicated me during this process.

To my friends close and far, all across the globe, thank you for making grad school what it has been with your messages and calls of encouragement. And a special thanks to Dr. Deisy Pena-Romero and Dr. Sharon Song for always being there to guide and cheer me up during grad school. I would like to acknowledge the past and present Boudreau group members for making these years in lab fun. I thank especially my parents, my brothers, Drou and his family for being there during these years whenever I needed them.

Cindi and Laura, I would like to thank you for the support you have provided me during my time at UNH and helping in every way you could to make it smooth administratively but also with all the kind and supportive words and gestures you had. It was always greatly appreciated.

To the university instrument center, particularly Dr. Patricia Wilkinson and Jon Wilderman, thank you for providing help to set up NMR experiments and troubleshooting any related issues whenever I needed it.

TABLE OF CONTENTS

LIST OF SCHEMES

LIST OF FIGURES

LIST OF TABLES

ABSTRACT

DEVELOPMENT OF OPEN LACTAM AND CAPTOPRIL ANALOGUES FOR THE COVALENT INHIBITION OF METALLO-β-LACTAMASES

By

MARIE-JOSIANE OHOUEU

University of New Hampshire, May 2021

The synthesis of a series of compounds designed to act as inhibitors of metallo-β-lactamase enzymes (MBLs), a sub-class of β-lactamases found in several clinically difficult to treat bacteria that are responsible for the widespread β-lactam antibiotic resistance, are described. The strategy involves the introduction of a functional group, such as an epoxide or thiirane, in the designed inhibitors capable of covalently binding the MBL targets and shutting them down irreversibly. This would prevent the enzymes from hydrolyzing the antibiotic drugs which would maintain their efficacy as a form of treatment.

This was first attempted through the development of a convergent synthesis which involved the formation of L- and D-vinylglycine methyl ester, serving for the incorporation of the 3-membered ring, in a five-step synthetic pathway. This was subsequently introduced using coupling chemistry to a dipeptide. The intermediate dipeptide precursor synthesized through amino acid coupling was phenylglycine-serine (Phg-Ser) followed by a phenylacetic acid-serine (PAA-Ser), which both mimic an open lactam structure. They were subjected to halogenation to convert the serine alcohol functional group to a bromide for the alkylation reaction with the amino group contained in the protected vinylglycine. However, the bromination of Phg-Ser proved to be difficult while the formation of the desired tripeptide with the brominated PAA-Ser was not observed. Evidence of an alkene product was observed which was attributed to the acidic proton at the α-position favoring the elimination of the bromine. Those limitations led to the modification

of the serine core to aspartic acid which was thought to circumvent the elimination issue by introducing the vinylglycine by amide bond formation rather than alkylation. Investigation with the phenylacetic-acid-aspartic acid dipeptide led to a promising route in which the coupling of the vinylglycine was achieved efficiently. The subsequent last steps of epoxidation of the alkene and deprotection seemed to be successful although optimization of these is still required.

Another strategy for the development of covalent inhibitors was the synthesis of compounds inspired from L-captopril, an inhibitor of angiotensin converting enzyme (ACE) inhibitors which plays a role in heart attack. Here, the strategy involves the synthesis of an alkene-containing intermediate with 2-methylprop-2-enoic acid or 2-methyl-3-butenoic acid through acylation of proline ethyl ester with the corresponding acyl chlorides. The intermediates were successfully obtained, enabling the formation of the epoxide and thiirane compounds. Subsequently, the ethyl ester hydrolysis was done to provide the final derivatives 1-(2-methyloxirane-2-carbonyl) pyrrolidine-2-carboxylic acid (**82)** and 1-(2-methylthiirane-2-carbonyl) pyrrolidine-2-carboxylic acid **(83)** with evidence of the formation of the desired **82** and **83.** In the case of the longer chain analogues, 1-[2-(oxirane-2yl)propanoyl] pyrrolidine-2-carboylic acid (**84**) and 1-[2-(thiirane-2yl)propanoyl] pyrrolidine-2-carboylic acid (**85**), the deprotection led to the isolation of the final thiirane compound **85** in an overall 5% yield while this last deprotection step remains to be optimized to obtain **84**.

The synthetic pathway of the open lactam derivatives was overall successful with only the last two steps requiring further optimization which would provide a new class of β-lactamase inhibitors. The pathway for the development of the proline derivatives afforded efficiently one of the desired captopril derivatives while the purification of last step to isolate the remaining compounds needs to be improved. The strategy presented could be used in the future to provide further library compounds for MBL inhibition for further studies.

General Introduction

This dissertation is composed of three separate chapters: (I) Introduction to β-lactamases and antimicrobial resistance, (II) Development of open lactam analogues as covalent inhibitors targeting metallo-β-lactamases, (III) Development of captopril-inspired compounds as covalent inhibitors of metallo-β-lactamases. The first chapter serves as introduction to the subject under the form of a mini review. The subsequent chapters investigate the strategies which have been explored in order to obtain the desired targets. They each are comprised of an introduction, results and discussion, and conclusion. Following the chapters is an appendix of relevant spectroscopic data related to the experimental procedures of the different chapters.

Chapter I. Introduction to β-lactamases and antimicrobial resistance

Bacterial infections: a life-threatening issue

Microorganisms are diverse, comprising fungi, viruses, protozoa, algae, archaea, and bacteria, and they are ubiquitous in our environment. Humans are in constant interaction with microorganisms, particularly bacteria. These unicellular organisms are divided in two major bacterial types: Gram-positive and Gram-negative. The main difference between these two categories lies in the structural features of the bacterial cell wall. In the case of Gram-positive bacteria, layers of a rigid macromolecule known as peptidoglycan, 20 layers on average, are present in addition to the inner cell membrane. In Gram-negative bacteria the peptidoglycan layer is thinner, 1.5 layers on average, and has in addition to the inner membrane a semipermeable outer membrane. Thus, Gram-negative bacteria are thought to be relatively more flexible and more sensitive to lysis.[1] It is estimated that about 3.8×10^{13} bacterial cells are found in the human body,[2] and they can live in symbiosis with human beings and animals in anatomic areas such as the skin, and the gastrointestinal, upper respiratory, genital, and urinary tracts. They can be essential to the proper functioning of physiological processes such as maintaining normal intestinal development or stimulating the development of their host defense, among others.[1]

However, bacteria can also be harmful to their host if they penetrate tissue barriers which are normally free of microorganisms. In this case, the bacterium is able to multiply and damage tissues, resulting in an infection. Serious infections, for instance those known as nosocomial, are common and usually contracted within hospital sites.[1] In the United States alone it has been reported that at least 2.8 million people are infected by drug resistant bacteria every year. Among those, an average of 35,000 end up dying as a direct consequence of their contracted infection.[3] Globally, as of today, on average 700,000 people die annually due to infections involving antimicrobial resistance and that number has been predicted to reach an average of 10 million deaths worldwide yearly by 2050.[4] It is important to be able to diagnose and treat bacterial

infections rapidly to avoid lethal outcomes in the worst case scenario, which is not always easy to achieve. Indeed, the development of antibiotics as a remedy to bacterial infections has been pursued for many decades.

Antibiotics and their modes of action against bacteria

The term antibiotics was first proposed by Selman Waksman who developed one of the first effective therapeutic treatments for tuberculosis in the early 1940s.[5] Antibiotics were initially defined as chemical compounds produced by microorganisms capable of selectively inhibiting the growth of bacteria in dilute media conditions. In the late 1920s several discoveries helped the era of antimicrobial development, notably that by Sir Alexander Fleming who accidentally found that the fungus *Penicilllium notatum* (Figure 1A) was able to inhibit bacterial growth in 1928.[6,1] Around the same time, the development of one of the first antimicrobial drugs used clinically was accomplished by Domagk and co-workers from Bayer pharmaceutical. The sulfonamide based drug, Prontosil, was among the first effective antimicrobial treatments for which Domagk received the Nobel Prize in 1939 (Figure 1B).[7]

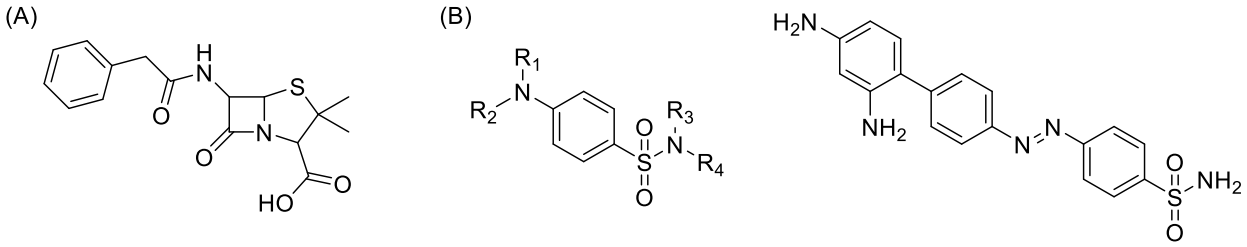

Figure 1: Early antimicrobial compounds: Penicillin (A) and sulfa base structure (left) and Prontosil (right) (B)

The industrial development of antibiotics as it is known nowadays has also been contributed to by Paul Ehrlich, who in addition to synthesizing the first antimicrobial molecule Salvarsan (Arsphenamine) for the treatment of syphilis in 1907[8], introduced a systematic screening approach which resulted in the discovery of many other drugs through time.[9] Most of the antibiotics known have been isolated primarily from studied soil samples; Gramicidin,

discovered by Rene Dubos, was among the first to be isolated through systematic search and manufactured commercially.[10,11] The early definition of antibiotics by Waksman through time has been subject to change as studies and understanding of antibiotics has evolved. More recently, antibiotics have been defined by many, but not all, as synthetically or naturally obtained chemicals capable of preventing bacterial growth with minimal toxicity to hosts.[12,13]

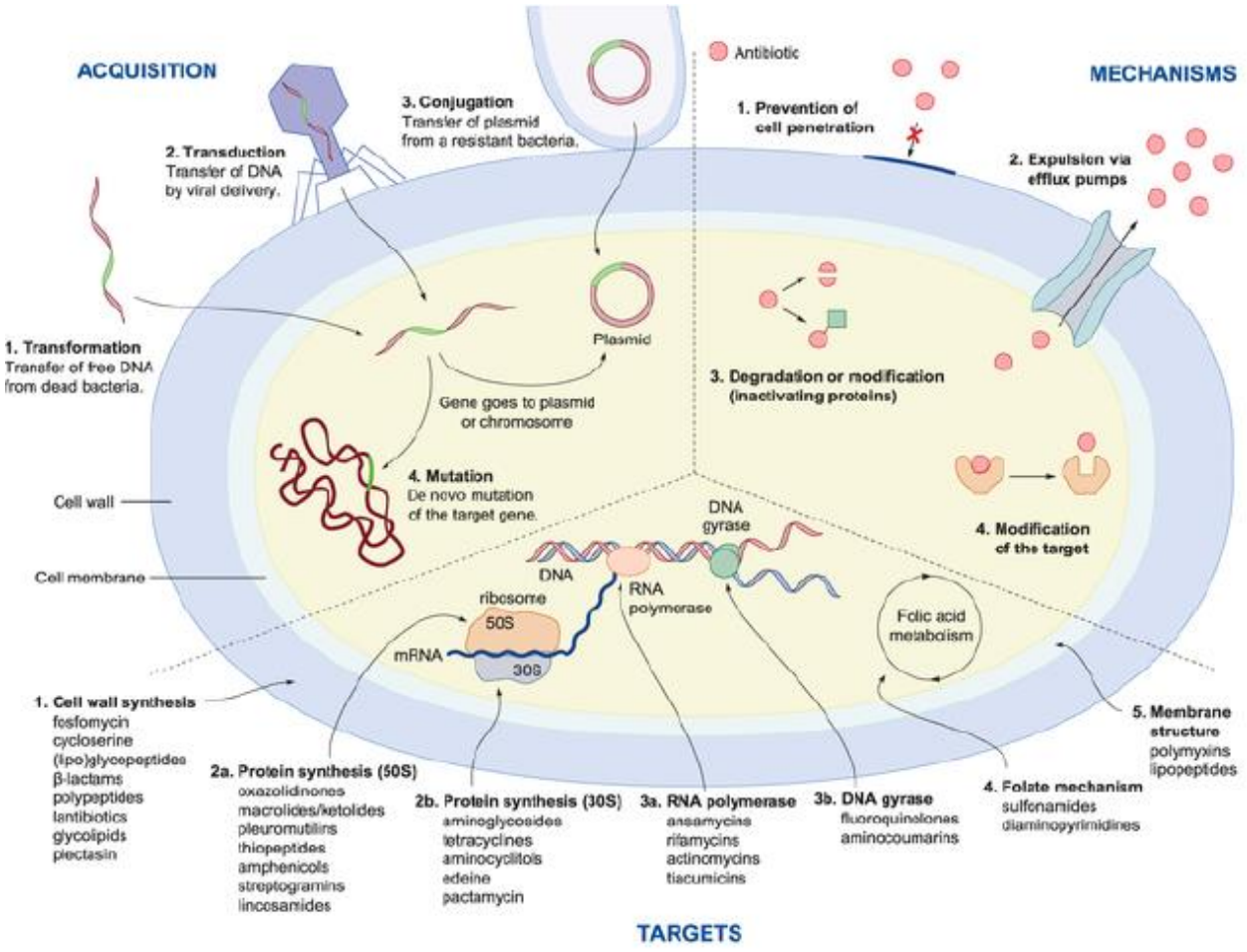

Figure 2: Illustration of the different mechanisms of bacterial antimicrobial resistance and antibiotic modes of action.[14]

Antibiotics are identified based on the mechanism and impact they have on bacteria as either bacteriostatic, which prevent continuous growth, or bactericidal, which kill the bacteria. Studies of antibiotics have shown that they operate through five principal mechanisms against bacteria (Figure 2). Three of those mechanisms in which antibiotics are involved prevent the

synthesis of vital metabolites for bacteria cell survival. Oxazolidinones, macrolides, aminoglycosides and tetracyclines can interfere with protein synthesis in bacterial cells. Protein synthesis involves four main stages: the initiation step with ribosomes binding to messenger ribonucleic acid (mRNA) to translate the sequence to amino acids by decoding to transfer ribonucleic acid (tRNA), the elongation step consisting in extending the peptide chain by binding together each amino acid decoded by the ribosome, the termination step which halts the formation of the protein is triggered by a particular mRNA sequence (stop codon) which stops the addition of amino acid residues to the protein, and the recycling step is the release of the ribosome from the completed protein which is ready to bind to another mRNA to start a new protein synthesis cycle.[14,15] Those drugs inhibit the first two steps of the synthesis by inhibiting the ribosome function or by interfering with the decoding of the amino acid to be synthesized (Figure 3A-D).

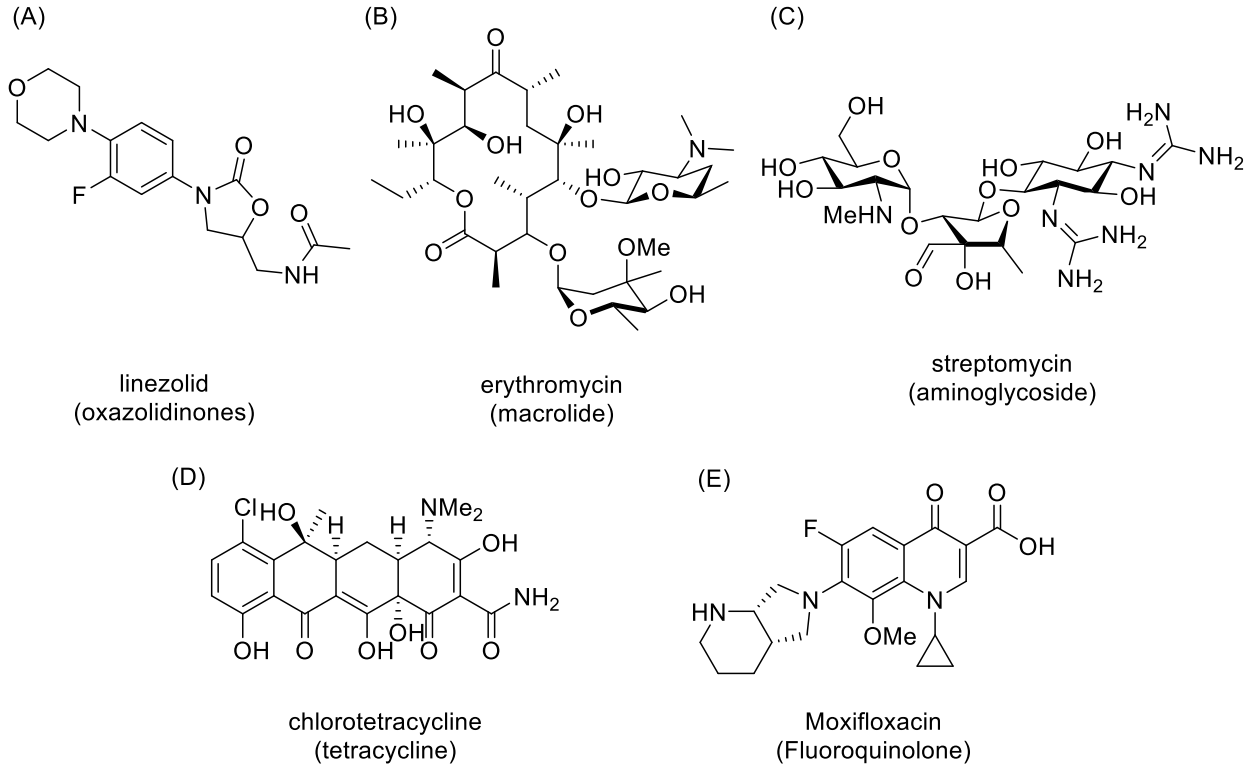

Figure 3: Molecular structure of selected antibiotics inhibiting protein synthesis pathway (A-D) and DNA/RNA synthesis (E)

Deoxyribonucleic acid (DNA) and RNA synthesis is known to be disrupted by fluoroquinolone compounds (Figure 3E).[14] Fluoroquinolone antibiotics tend to alter the process of transcription of genetic material which consists of a DNA strand being copied to an RNA strand by an enzyme to express a gene which will have a specific role in the cell. The antibiotics bind to the designated transcription factor site, thus preventing the enzyme to do so and the process from taking place.

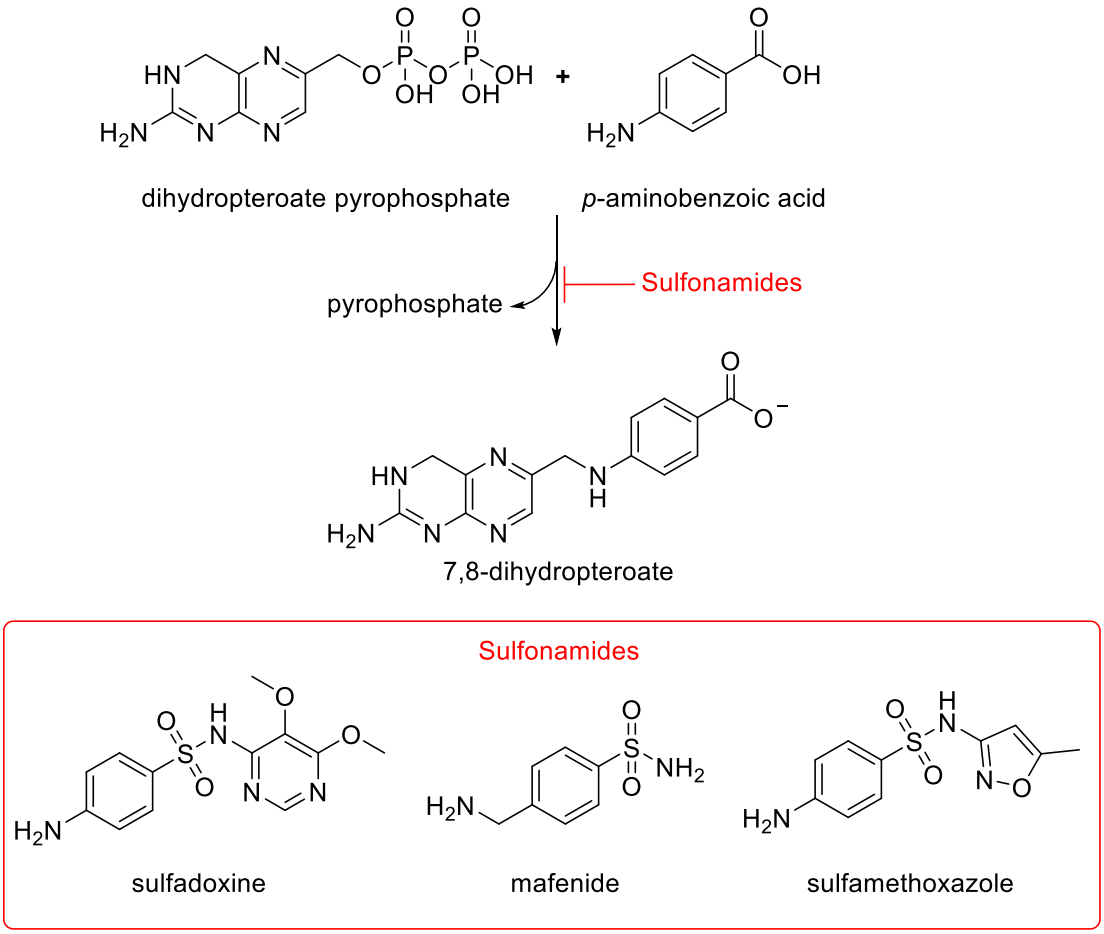

Scheme 1: Inhibition of the reaction catalyzed by dihydropteroate synthase (DHPS) in the early step of folic acid synthesis by sulfonamides.

The production of folates, which are precursors of several metabolites needed in bacterial cells can be inhibited by sulfonamides (Scheme 1). Sulfonamides, referred to as antifolates, target the first enzymes involved in the folic acid biosynthesis, dihydropteroate synthase (DHPS). Sulfonamides attach to the binding pocket of DHPS preventing any substrates that are used by

this enzyme for the metabolic pathway to do so. This prevents the formation of a folate intermediate, 7,8-dihydropteroate, to be formed, thus halting the folate synthesis (Scheme 1).[14,16]

Another approach is to provoke the disruption of the cell membrane in bacteria with the presence of antibiotics which can accomplish that through various mechanisms. Daptomycin (Figure 4A), a lipopeptide drug, can insert itself into the phospholipid bilayer of the cell membrane and cause it to rupture. As it accumulates, the formation of holes in the bacterial cell membrane are created which provoke a dysfunction of vital metabolic pathways preventing them from being synthesized.[17,18] An antibiotics class that is known as the glycopeptides, e.g. Vancomycin (Figure 4B), can disrupt peptidoglycan synthesis by inhibiting transglycosylase enzymes involved at an early stage of the cell wall synthesis.[19]

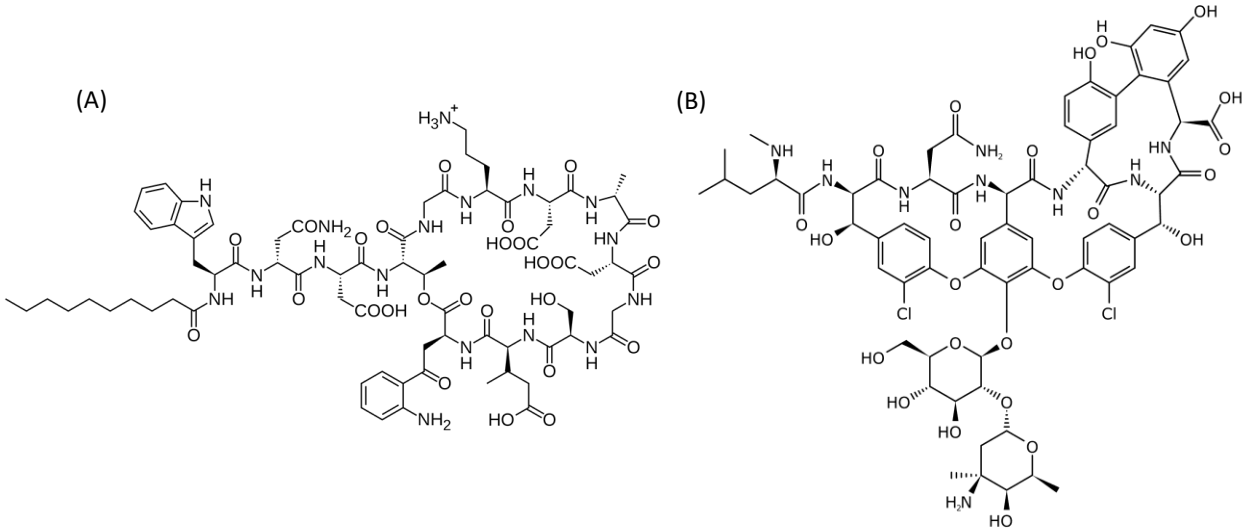

Figure 4: Structure of the Daptomycin (A) and Vancomycin (B)

Other compounds, such as β-lactams, can interrupt peptidoglycan synthesis by inhibiting the penicillin binding proteins (PBPs) which play an important role in the later stages of peptidoglycan cell wall formation. PBPs are responsible for the reaction involving peptide bond formation and transglycosylation notably between the peptide and glycosidic bond in the peptidoglycan.[20] Both glycopeptides (i.e. streptomycin, Figure 3) and β-lactams prevent the formation of the rigid bacterial cell wall structure which is necessary to prevent osmotic lysis due

to its inability to regulate the osmotic pressure created by the flow of water coming into of the cell. As a consequence the bacterial cells lacking peptidoglycan are killed by osmotic burst.[21] The role of β-lactams is of particular relevance for the current project and will be discussed in more details in the subsequent sections.

Certain characteristics have to be taken into consideration when developing efficient antibiotics, including target selectivity, water solubility, low side reactions, stability, low cost, and slow resistance development. In general, antibiotics are extremely effective to cure infections when first developed and used, but with time it is observed that some diseases persist in patients despite the administration of antibiotic drugs. This is due to bacteria developing or acquiring the ability to circumvent antibiotics' mechanisms of action (Figure 2). A minimum inhibitory concentration (MIC) test can assess the effectiveness of studied antibiotics to determine if a particular strain becomes resistant to it. The adaptation of bacteria to antibiotics has been a recurrent issue which has caught the attention of many in this field. Although a great number of scientists have intensively conducted research into this problem, few successful breakthroughs have been reported in the last few decades for high-risk pathogens. Moreover, the number of antibiotics developed yearly has decreased by almost 90% over the last several decades.[3] In order to find an appropriate solution to this problem, it is necessary to understand how bacterial resistance is acquired and works in these microorganisms.

Mechanisms of antimicrobial resistance in bacteria

In certain bacteria intrinsic resistance is observed and consists of resistance against antibiotics without prior exposure to them. It is usually due to transport proteins found in their outer membrane acting as a natural barrier to large antibiotics (e.g. vancomycin in *E. coli*) while smaller ones (e.g. β-lactams) are able to bypass this natural filter.[22–24] On the other hand, acquired resistance is observed in bacteria exposed to antibiotics and developed through adaptation. Bacteria that acquire resistance proliferate exponentially in the environment as a result of misused

antimicrobial agents, leading to selection of the most life-threatening bacterial strains while eradicating sensitive bacterial strains. One manner in which bacteria can pass on acquired resistance is via the transfer of genetic material between bacterial cells. It was found that some bacterial strains acquire genes coding for the factors of resistance by transfer from live or dead viruses or bacterial cells via plasmids, via a conjugation process, which are then passed on through one generation to the next.[25,26] As well, epigenetic inheritance is suspected to play an important role in antibiotic resistance in bacteria. This consists of the transfer of an environmentally induced modification of genetic material from a mother to a daughter cell.[27,28] When exposed to a gradual increase of concentration of antibiotics, bacteria can methylate their DNA via deoxyadenosine methyl transferase (DAM) enzyme which can provide them with antibiotic resistance by preventing lethal DNA damages resulting from the presence of antibiotics in their environment.[29,30]

Usually, the genetic material acquired gives bacteria the ability to exhibit three major mechanisms of resistance. First, they can reduce the amount of antibiotic in their cell in two ways: 1) by decreasing the permeability of the cell to antibiotics by reducing the number of outer-membrane proteins acting as a point of entry (in the case of Gram-negative bacteria) or 2) by expressing more efflux pumps excreting antibiotic molecules out of the cell. A second mechanism involves the activation of alternative pathways that are not affected by the presence of antibiotics. The new pathway involves biomolecules, such as catalytic enzymes with receptors different than the one originally targeted by the antibiotics, thus preventing it from being shut down. In this manner, the bacteria can still function normally even in the presence of the drug. A good example of this mechanism is with the mutated version of penicillin-binding-proteins (PBP), exogenous enzymes which will be discussed in more detail in the subsequent sections and commonly found in methicillin-resistant *Staphylococcus aureus* (MRSA). PBP2a, the mutated enzyme, has a low affinity for the β-lactam antibiotics due to misalignment of the active serine residue preventing for

the antibiotic to be acylated. As a result the antibiotic does not bind to the active site and cannot inhibit the mutated PBP2a. [31]

Lastly, the production of enzymes which can modify or completely inactivate the action of antibiotics is the most widely-studied and well-understood mechanism of resistance for bacteria (Figure 1).[14,32] There are 3 principle classes of enzymes involved in antimicrobial drug inactivation: transferases, redox enzymes, and hydrolases.[33] First, transferases modify the antibiotics by altering them through covalently binding functional groups which in turns leads to a loss of activity. A common transferase enzyme is *N*-acetyltransferase which can alter aminoglycosides through acetylation, preventing the resulting acetylated compound from binding to its target.[33]

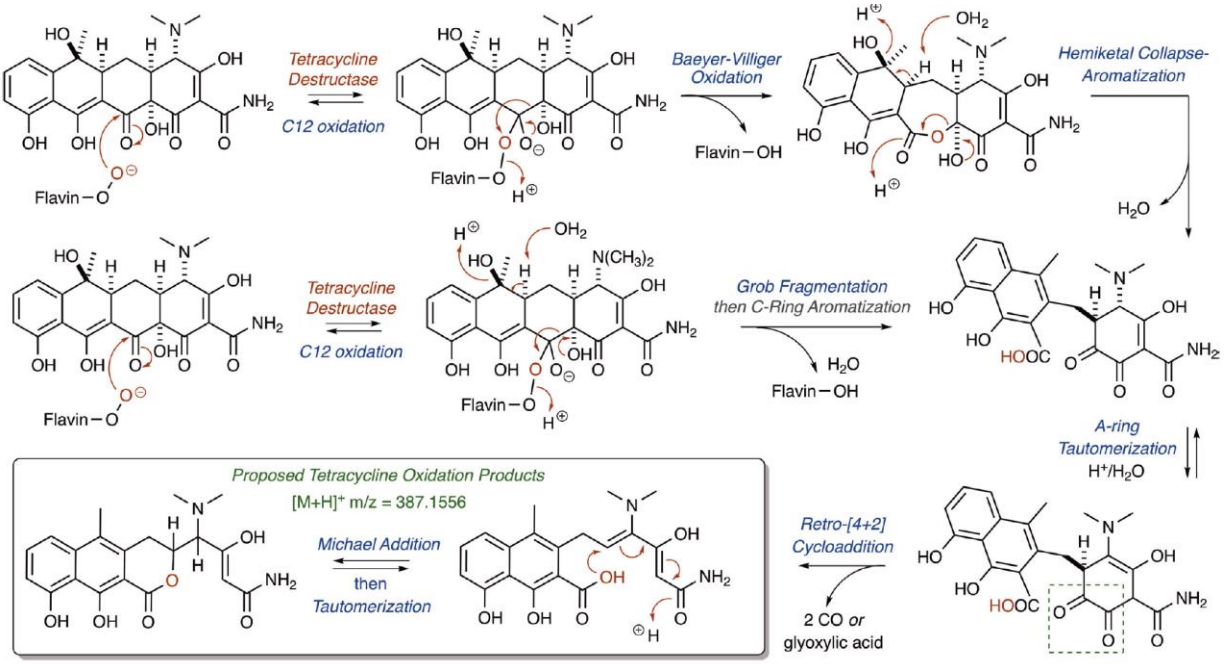

Scheme 2: Tetracycline inactivation by oxidation at C_{12} by monooxygenase TetX.[34]

The second class of enzymes are monooxygenases such as flavin-dependent tetracycline enzymes (TetX) and are redox enzymes providing bacteria with resistance to tetracycline drugs (Scheme 2). The oxidation reaction of the substrate can occur at multiple positions (C_{11a}, C_{12}, C_1, C_2, or C_3) leading to cyclization and series of degradation reactions of the molecule (Scheme 2).[34,35] The third largest class of enzyme inactivation category is hydrolases which is comprised

principally of macrolide esterases and β-lactamases. Macrolide esterases, as the name implies, perform an esterification of the 14- and 15- membered ring of the macrolide lactones (Figure 5A), and the resulting ring-opened product has no antibacterial activity. β-Lactamases are a type of hydrolases[33] which target β-lactam antibiotics (Figure 5B) and are the main focus of this work. These will be discussed in greater detail in the following section.

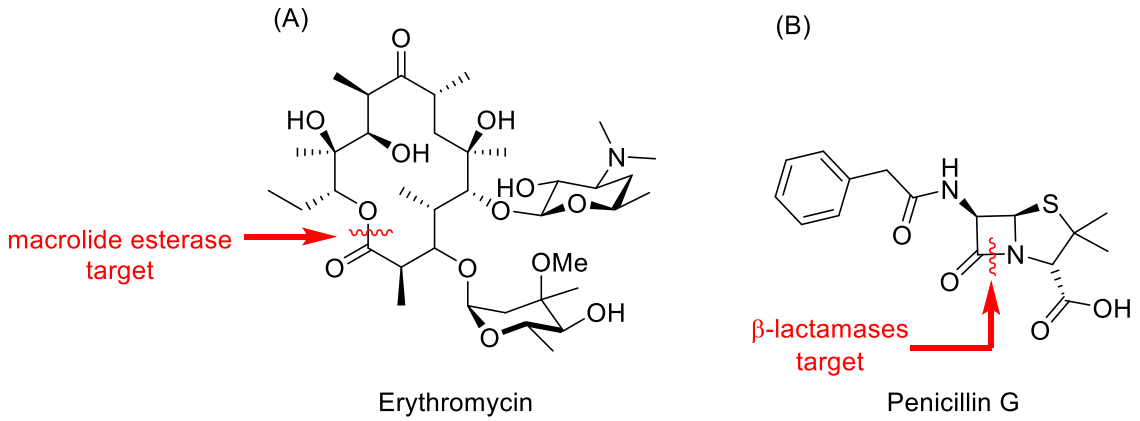

Figure 5: Targets of hydrolase enzymes in the inactivation of antibiotics

The strategy utilized by bacteria to inactivate antibiotics using enzymes has been investigated extensively by researchers as it is a very effective manner for bacteria to acquire resistance. Studies have shown promise of finding an efficient solution to antimicrobial resistance when tackling enzyme inhibition. However, more work must be done to understand the mechanism of β-lactamase enzymes in order to develop efficient inhibitors.

β-Lactam antibiotics and β-lactamases enzymes

β-Lactams are among the first antibiotics to have been used to treat infections, penicillin being the first one to be isolated in 1928 by Alexander Fleming.[36] Their mode of action consists of mimicking the peptidoglycan chain by having structural similarities to the terminal D-Ala-D-Ala chain (Figure 6). The peptidoglycan is the natural substrate of penicillin-binding-proteins (PBPs) catalyzing the reaction of transglycolation is responsible for the continued cell wall extension through transpeptidation forming cross-links between two *N*-acetylmuramic (NAM or MurNAc)

side chains (Figure 6). Thus, β-lactams act as competitive inhibitors to peptidoglycan for PBPs as they can be catalyzed in its place and halt its formation by preventing the transpeptidation reaction between NAM residues.

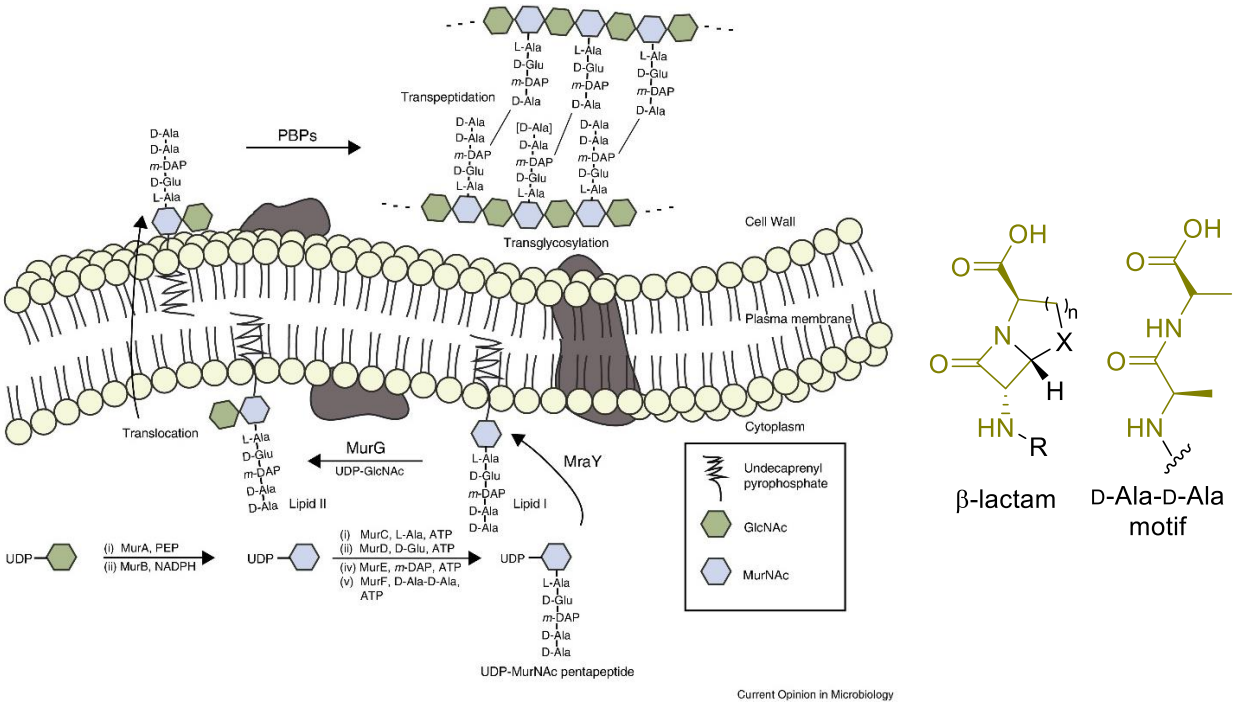

Figure 6: Illustration of bacterial cell wall synthesis[37] and the structural similarities (green) between β-lactam antibiotics and the D-Ala-D-Ala motif in peptidoglycan.

As mentioned earlier, the peptidoglycan makes up the bacterial cell wall and is vital as it prevents cell burst resulting from unregulated osmotic pressure.[38] The core structure β-lactam ring is found in all β-lactam antibiotics and is a 4-membered ring containing an amide functionality (Figure 7). The lactam ring is an important part of the recognized sequence of the antibiotic by the PBPs with which the serine residue can react instead of the NAM side chain D-Ala-D-Ala terminal dimer motif in the peptidoglycan.[39,40]

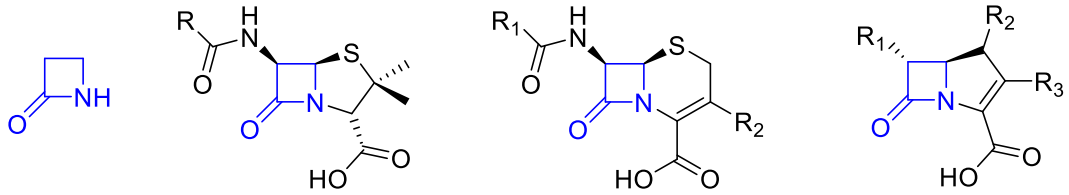

Figure 7: β-Lactam and examples of β-lactam antibiotics

As a response to the lethal effect caused by β-lactams, bacteria have expressed β-lactamases enzymes. These enzymes have the ability to inactivate antibiotics via hydrolysis mechanisms, rendering them inefficient as a treatment method. The acquisition of β-lactamases by Gram-negative bacteria can be attributed to genetic modifications occurring over time. They developed these enzymes as a defense mechanism as far back as several million years ago, based on dating analysis of encoded plasmids to fight against β-lactams present naturally in the environment.[41] As with other enzymes, β-lactamases are substrate specific and interact solely with molecules containing defined structural features. The binding interaction with a particular substrate depends on the enzyme's primary amino acid sequence and its resulting 3-D structure exposing certain amino residues in the void space of the active site capable to uniquely bound to the substrate. β-Lactamases have been divided into four classes (Amber class), A, B, C, and D, according to their amino acid sequence. Class A, C, and D enzymes possess a common feature as they all contain a catalytic, nucleophilic serine (Ser) residue in their active site. The hydroxyl group on the serine residue is able to catalyze hydrolysis by initial nucleophilic attack on the carbonyl of the antibiotic β-lactam (**1**, Scheme 3) to form a tetrahedral intermediate (**2**, Scheme 3) followed by lactam ring opening (**3**, Scheme 3) rendering it inactive.[42]

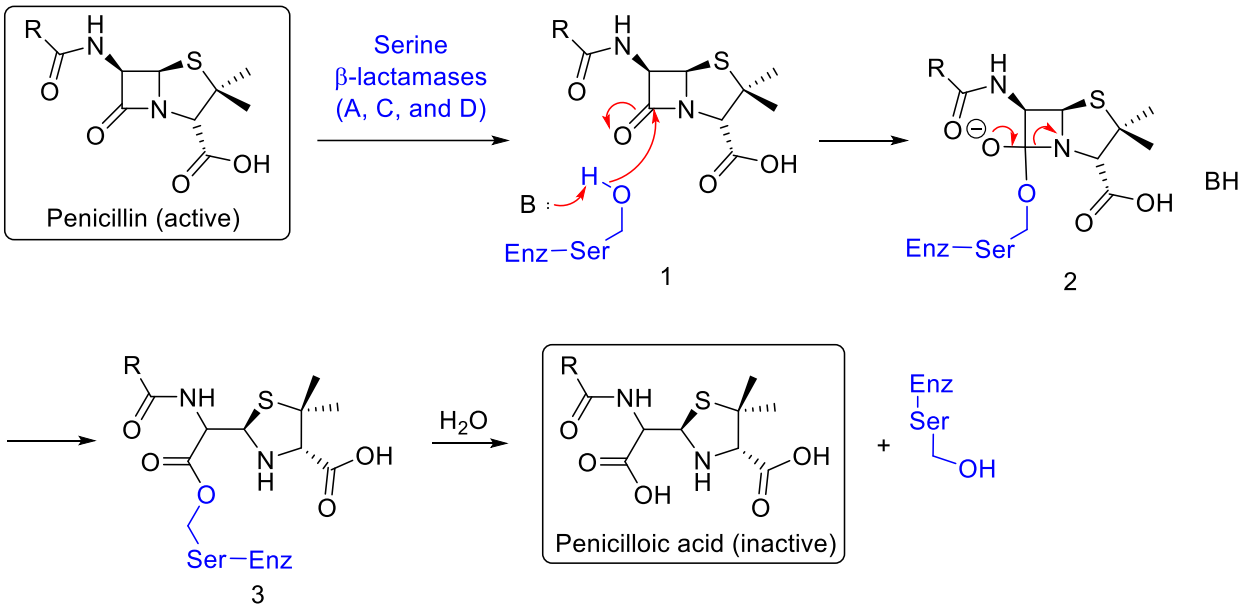

Scheme 3 : Hydrolysis mechanism of penicillin by serine (Ser)-containing β-lactamase enzymes (class A, C, and D)

The case of class B enzymes, the focus of this research, differ considerably structurally and mechanistically. Their structures, mechanism of action, and inhibition will be discussed in more detail in the subsequent sections.

Metallo-β-lactamases (MBLs)

The particularity of metallo-β-lactamases (MBLs) as compared to the serine containing enzymes is the presence of one or two zinc (Zn^{2+}) cations in the binding pocket which catalyze the hydrolysis of the antibiotics rather than a serine amino acid. MBLs can be sub-divided into three groups, B1, B2, and B3, according to their amino acid sequence influencing their 3-D structure and the number of zinc cations interacting in the binding pocket (Figure 8). In the sub-class B1 and B3, two zinc cations are chelated in the active site while in the B2 sub-class only one Zn^{2+} is found. In all three sub-classes, aspartic acid (Asp_{120}) and three histidines (His_{118}, His_{196}, His_{263}) amino acids are present in the enzyme's active site and are involved in the coordination of the zinc atom(s). Both, B1 and B2 sub-classes possess a cysteine (Cys_{221}) bound to one of the zinc cations in what is known as the DCH site while in B3 this residue is replaced by

a histidine (His_{121}; Figure 8A in green), and the B2 sub-class presents a lysine (Lys_{116}) residue. It is important to note that the great majority of clinically relevant MBLs are identified as B1 type.[43,44]

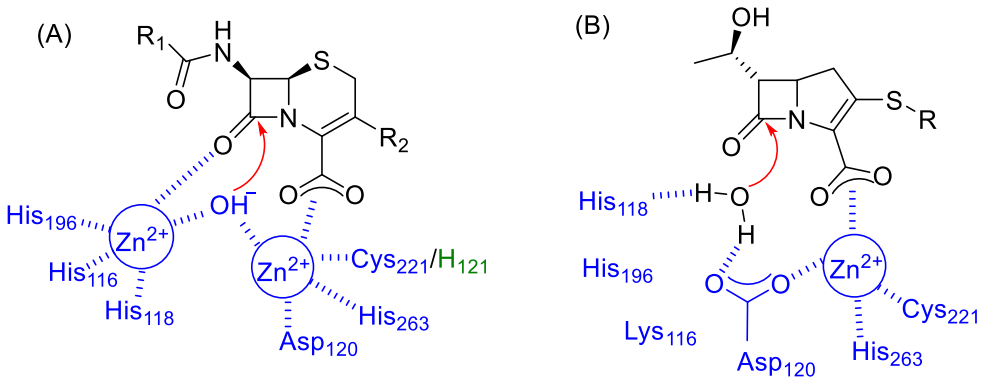

Figure 8: Coordination of zinc atoms in MBLs (blue) in sub-class (A) B1and B3 with a bound cephalosporin (variation for B3 in green); (B) B2 with a bound carbapenem

Class B enzymes have the particularity to have two flexible mobile loops implicated in substrate binding in proximity of their wide active site (Figure 9). It gives them the ability to accommodate substrate varying in sizes. This is in addition to the presence of zinc cations performing the hydrolysis of drugs without being covalently bound to the enzyme providing them with more flexibility compared to serine-β-lactamases.[43,45,46]

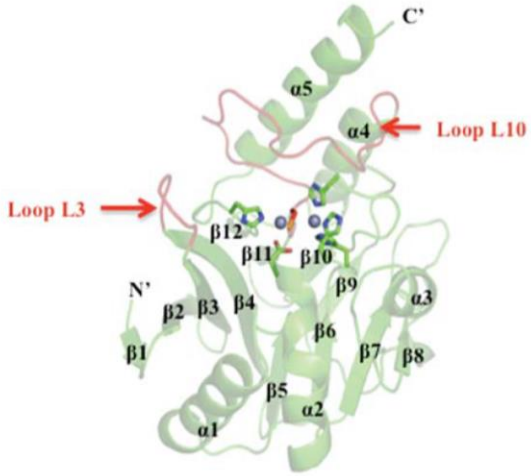

Figure 9: Crystal structure of the NDM-1 enzyme (green) with L3 and L10 loops highlighted (red) and zinc cations (grey)[47]

Metallo- β-lactamases are able to hydrolyze a large range of substrates. Indeed, the majority of β-lactam antibiotics were found to be hydrolyzed by MBLs B1 and B3, while B2 hydrolyze carbapenems principally.[48] Hydrolysis by the sub-classes B1 and B2 is similar starting with the zinc cations guiding a hydroxide ion to perform a nucleophilic attack on the carbonyl of the antibiotic's β-lactam ring (**4**, Scheme 4) giving a tetrahedral intermediate (**5**, Scheme 4); thus the amide bond is subsequently broken.

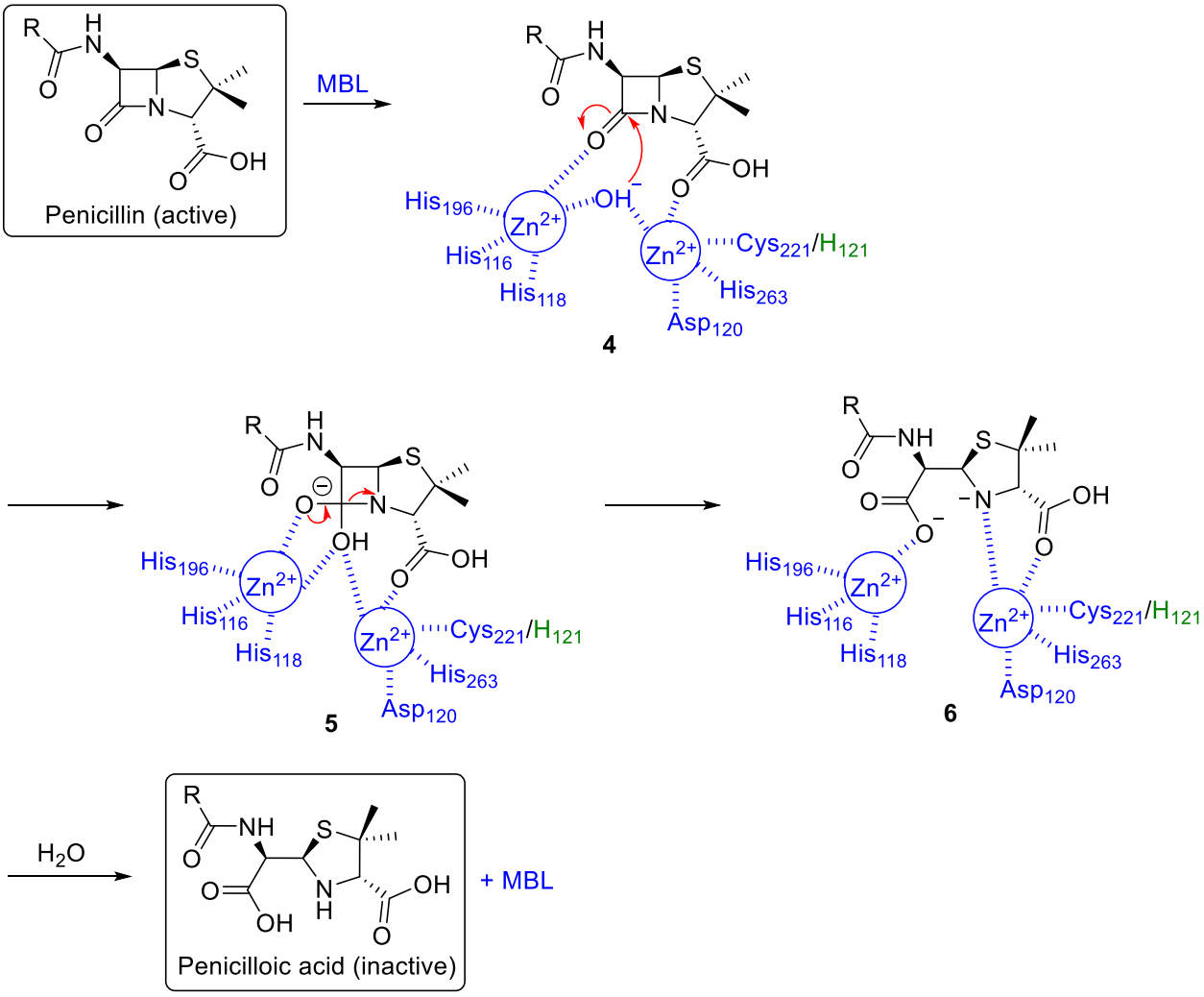

Scheme 4: Hydrolysis mechanism of a penicillin by MBLs containing β-lactamase enzyme type B1 and B3

The anionic intermediate (**6**, Scheme 4) obtained and stabilized by Zn^{2+} can be protonated. This leads to the formation of a hydrolyzed inactive product which is released from the active site in

presence of a water molecule. This way the enzyme is ready to perform another hydrolysis (Scheme 4).[44]

In the case of B2 enzymes a water molecule, as opposed to a hydroxide, is performing the hydrolysis guided by the zinc ion and one of the histidine residues (His_{118}) in the active site (Figure 8B), otherwise the mechanism follows similar steps as with di-zinc enzymes.[44] Among the metallo-β-lactamase subclasses, the B1 subclass is found to be the most widespread. This subclass contains some of the most important enzymes found clinically[49,50] including Imipenemase (IMP), Verona Integron-encoded Metallo-β-lactamase (VIM), and New-Delhi Metallo-β-lactamase (NDM). IMP-1, which was encountered in Japan in 1988, was the first observed and isolated transferrable enzyme via plasmid.[51] They have been able to inactivate all β-lactam drugs, making them a primary concern.[50] Later on, VIM-1 was found in Verona University Hospital (northern Italy) in 1999[52] and has become the largest B1 subgroup with almost 46 variants as of 2018.[41] Variants are differentiated based on their amino acid sequence. NDM-1 variants, as the name indicates, originated in 2008 from New Delhi, India[53] and have spread to a large number of countries. The gene coding for NDM-1 enzymes is often found in addition to other genes encoding for different types of β-lactamases, thus NDM-1 variants are able to hydrolyze a broad range of antibiotics, making them multi-drug resistant.[50] Despite a large variability between each variant, conserved residues in these enzymes have been observed as mentioned above with residues coordinating zinc cations in the binding pocket. As well, B1 and B2 enzymes, with the exception of VIM variants, have a conserved lysine residue at the amino acid position 224 (Lys224) which was found to be important in the binding of antibiotics.[54] Lys224 is able to form electrostatic interactions with the carboxylate group of the β-lactam to position them appropriately in the active site and favor their inactivation. VIM-2, VIM-4, VIM-5, and VIM-38 variants on the other hand carry an arginine amino acid residue (Arg228), containing a terminal amine group as for lysine, which is believed to play a similar role to Lys224 in drug inactivation.[55]

All these enzymes are able to hydrolyze the latest carbapenem-based drugs which are considered last resort drug treatment options, making bacteria containing MBLs an important threat. The challenges faced in the development of MBL inhibitors is an increasing concern as resistance of bacteria containing MBLs has been more commonly observed over the years. Currently, the development of more efficient inhibitors against MBLs is an intense area of research and although it is showing promise, it has yet to be very successful. Thus, there is an urgent need for more investigations toward the development of new MBL inhibitors acting as adjuvants to antibiotics with the hope to render them potent.

Inhibitors of metallo-β-lactamases

The serine residue in the active sites of class A, C, and D of serine-containing β-lactamase enzymes is part of the design of efficient inhibitor molecules which would be trapped very efficiently in the enzyme binding pocket and act as competitive molecules to the active drug. However, the case of MBLs, class B, is more challenging for inhibition due to the fact that they do not contain a covalently bond amino acid residue as for serine-β-lactamases directly involved in the degradation of antibiotics.[44] The emergence of β-lactamase enzymes has forced scientists to quickly look for a solution to the problems that arise when inactivating β-lactam antibiotics. β-Lactamase inhibitors have been used for a long period of time to combat β-lactam resistance. The first generation of inhibitors, notably clavulanic acid, sulbactam, and tazobactam (Figure 10), are well suited for inhibiting serine-based β-lactamases but cannot inhibit the activity of class B enzymes. This is due to the structural differences of the active site and the mechanism of inactivation of drugs relying on the covalently bound serine residue absent in MBLs.[49] Indeed, the effectiveness of the inhibitors developed earlier on (Figure 10) rely on trapping a covalently bound enzyme-substrate adduct, key step for the hydrolysis. Thus, the lack of covalently bond residues involve in the MBLs' hydrolysis mechanism renders serine inhibitor ineffective for class B.[49] In

recent years, many prospective candidates as MBL inhibitors have been reported in the literature, but no effective MBL inhibitors have been clinically approved as of today.[56,57]

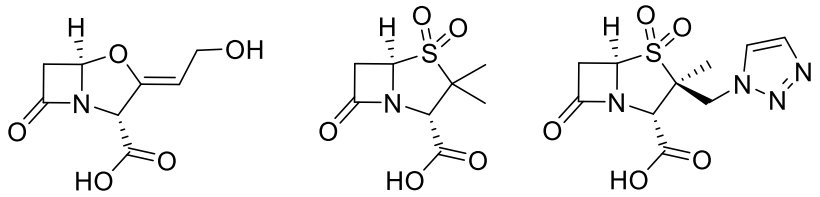

Figure 10: Structure of clavulanic acid, sulbactam, and tazobactam

The enzyme-substrate binding interaction is specific requiring a particular molecular motif in the substrate to allow binding in the enzyme active site which often form a tightly bond covalent intermediate.[58] As stated previously, Zn cations located in the MBLs' binding pocket play an important role in the enzyme-substrate interaction for β-lactam hydrolysis. Therefore, most approaches for the development of efficient inhibitors involve a Zn-dependent mechanism. The first inhibitor not relying on zinc cations for inhibition was reported by Schofield and co-workers in 2017[59]; however zinc-independent inhibitors have very few candidates reported thus far. At the opposite, zinc-dependent mechanisms of inhibition of MBLs has extensively been studied and can be broadly divided in four categories as illustrated in Scheme 5.[60]

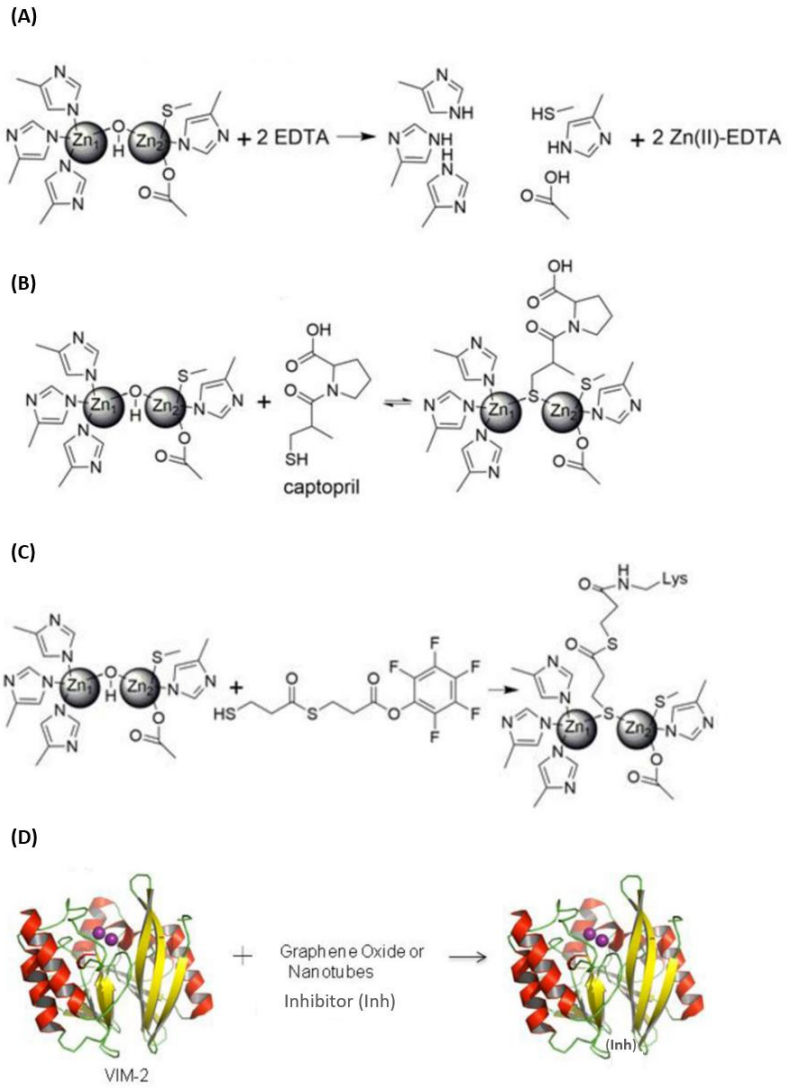

Scheme 5: Various modes of inhibition of MBLs with representation of the active site (A-D) and overall quaternary structure (D). (A) Zinc abstraction from the active site. (B) Zinc ion binding by ternary enzyme complex between the MBL, Zn, and inhibitor). (C) Covalent bond formation between MBL and inhibitor. (D) Allosteric inhibitors bind to MBL exosite, modifying the MBL active site[60]

One successful strategy involves the complete stripping of Zn cations from the enzyme binding pocket (Scheme 5A) using metal chelating agents, such as EDTA, preventing the hydrolysis of antibiotics. Other ion stripping approaches involve small inhibitors capable of zinc removal as reported for the well-studied natural product Aspergillomarasmine A.[61–65] Researchers have also incorporated elements in inhibitor structures designed to interfere with the nucleophilic catalytic Zn-water complex by bridging of functional group such as thiols or acids (Scheme 5B&C).

The majority of reported prospective MBL inhibitors using the ion binding strategy include principally non-β-lactam based inhibitors belonging to one of the following classes: cyclic boronates,[66–69] sulfamoyl carboxylates,[70–72] dicarboxylic acids,[73–75] and thioacid-containing molecules[76–78] (Figure 11).

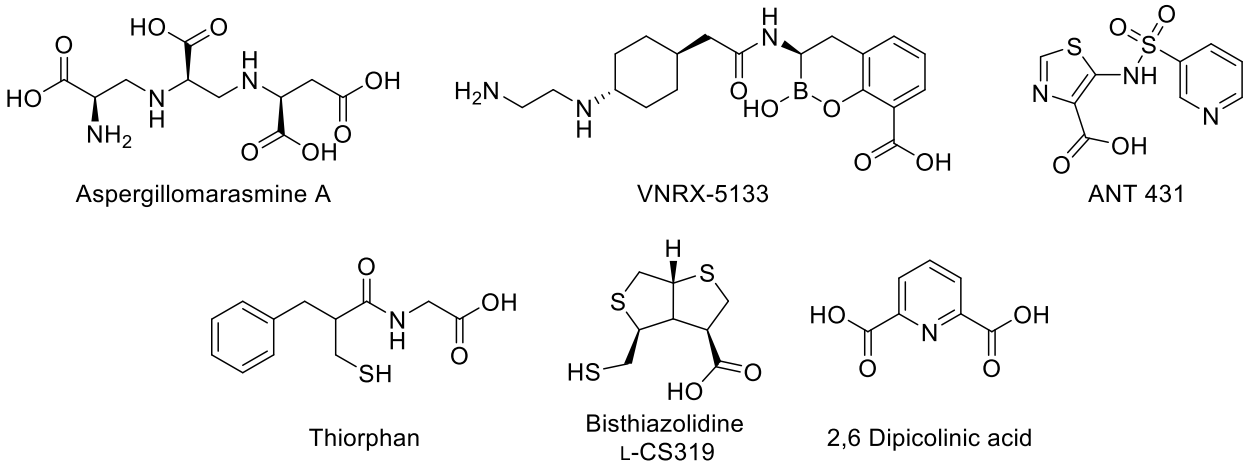

Figure 11: Various MBL inhibitors from the reported major classes of compounds

Taniborbactam (VNRX-5133, Figure 11), a boron-based compound, was reported to be efficient as a broad spectrum inhibitor against serine and MBL enzymes and is one of the few compounds to have advanced to the clinic as a promising therapeutic for MBL inhibition.[79] Everett and colleagues reported in 2018 the 5-(pyridine-3-sulfonamido)-1,3-thiazole-4-carboxylic acid (ANT431, Figure 11), a sulfamoyl carboxylic acid based compound, which exhibited inhibitory activity against NDM-1, VIM-1, VIM-2, or IMP-1 via ion binding strategy. ANT 431 showed that when combined with meropenem, it enables for the antibiotic to be active against bacterial strains presenting the 4 MBLs investigated; while meropenem alone is ineffective.[71] Certain molecules have been repurposed as MBL inhibitors, notably malic acid, citric acid and ascorbic acid, as shown by the work conducted by Abbas and co-workers. They showed that those acids were able to synergistically restore imipenem and meropenem activities in their presence (Figure 12).[80]

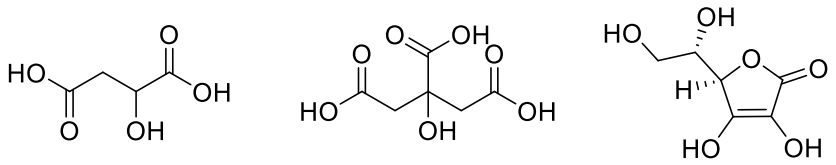

Malic acid Citric acid Ascorbic acid

Figure 12: Structure of repurposed compounds: malic acid, citric acid, and ascorbic acid

In addition to zinc-dependent mechanisms, covalent binding strategies for the inhibition of β-lactamases have been explored. This method has been effective in covalent inhibition of serine-β-lactamase due the serine residue (S64, Scheme 6) involved in the hydrolysis mechanism being covalently bound to the active site. Additionally, the presence of other nucleophilic residues in proximity, notably lysine (K315, Scheme 6), enable this mechanism as reported for the inhibition by cross-linking hydroxamate derivatives.[81–83]

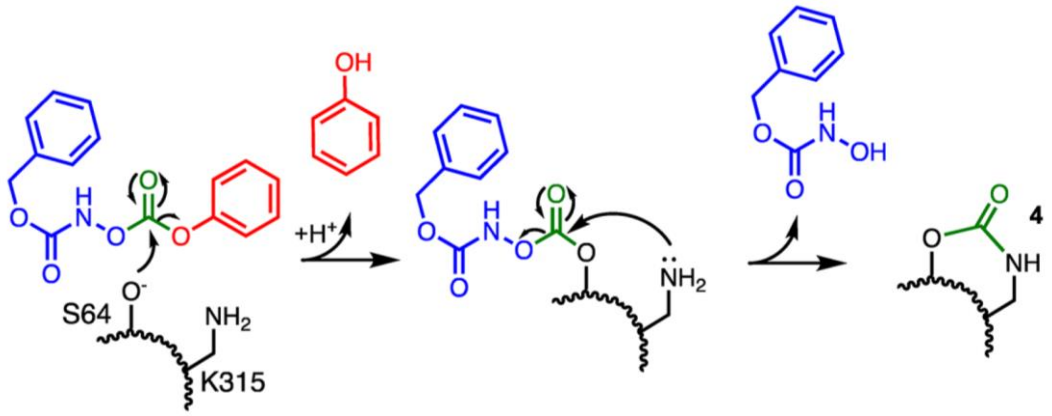

Scheme 6: Mechanism of covalent inhibition in serine-β-lactamases using hydroxamate derivatives forming a cross-linked enzyme active site[83]

This approach relies heavily on the presence of a nucleophilic moiety in the enzyme active site which can interact with an inhibitor containing an electrophilic site. Application of this strategy to MBLs (Scheme 5C) has been explored although not as extensively as for SBLs. In the case of MBLs, the nucleophilic site targeted for covalent binding is generally a conserved amino acid in the enzyme binding pocket. In recent years, Thomas and co-workers also highlighted how essential are conserved amino acids for effective inhibitor development via covalent binding studies targeting Lys211 in NDM-1.[83,84] In their research, the strategy to analyze the role of Lys211

relied on the presence of an electrophilic carbonyl carbon from a hydroxamate derivative which upon attack by the amino group of the lysine 211 (K211, Scheme 7) residue leads to the loss of a phenol group. In later work, they also investigated possible future routes for inactivation of NDM-1 via high-throughput screening of compounds by targeting a cysteine residue (Cys208) which is known to be conserved in the B1 subclass of MBLs.[85]

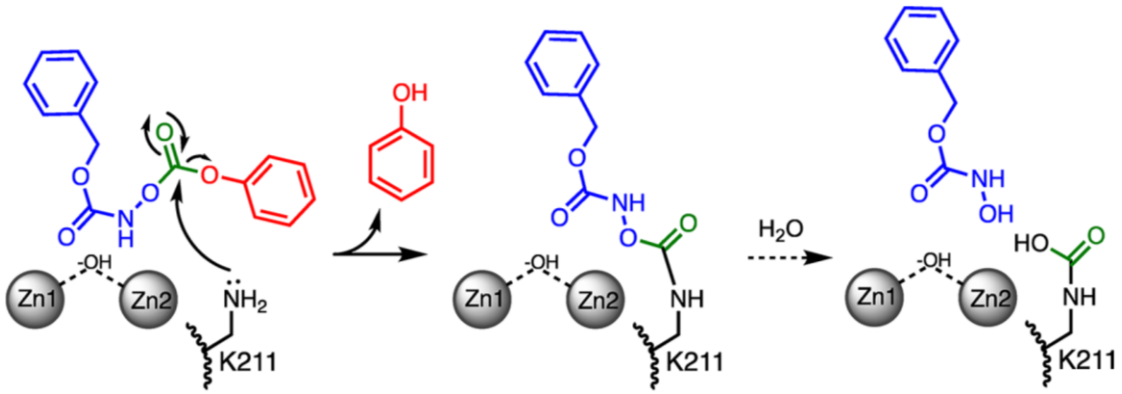

Scheme 7: Proposed mechanism for the covalent inhibition of MBLs applying the serine- β-lactamase covalent inhibition approach with hydroxamate derivatives[83]

Similarly, Christopeit *et al*. demonstrated the importance of conserved lysine Lys224 in the mechanism of inhibition via covalent binding. Indeed, mutation of native enzymes leading to the deletion of this lysine residue resulted in the loss of inhibitory effect by covalent binding.[86] Such a strategy, involving a nucleophilic attack on a carbonyl of an inhibitor with an adjacent good leaving group to allow the nucleophilic group Lys244 to form a covalent bond with the inhibitor, was also seen in prior work by Kurosaki and co-workers for the inhibition of IMP-1.[87]

The difficulty in creating efficient covalent inhibitors interacting in a predictable manner for most MBLs is made more difficult due to several factors: 1) the non-covalently bond enzyme catalytic hydrolytic site, 2) the small overlap of conserved amino acid across all subclasses as mentioned earlier. However, the large success in inhibiting serine-based enzymes relied on the understanding and predictability of the role of the serine hydroxyl in the hydrolysis mechanism of β-lactams. Recent studies on the mechanism of hydrolysis of β-lactam antibiotics by MBLs, the

few conserved amino acids in the enzyme active site, and the mechanisms of inhibition of MBLs, have inspired further research to develop covalent inhibitors of metallo-β-lactamases.

Overall research goal

The strategy of covalent inhibition of metalloenzymes, with the exception of metallo-β-lactamases (MBLs), through use of a strained ring has been reported, notably with epoxide- and thiirane-based inhibitors. Irreversible inhibitors such as fumagillin (Figure 13A) and its derivatives have been studied for the down-regulation and inhibition of the dimetalloenzyme methionine aminopeptidase involved in rheumatoid arthritis. They possess an epoxide which can be ring opened by a glutamic acid residue located near the catalytic metal center metal.[88,89] Mobashery and co-workers have been studying zinc-dependent endopeptidases, which are involved in cancer and ulcers among other diseases. They have developed thiirane- and epoxide-containing molecules such as (*R*)-ND-336 (Figure 13B) which have been shown to inhibit matric matrix metalloproteinase (MMP) through covalent interaction with nucleophilic residues in the active site.[90,91] Metallocarboxypeptidases (MCPs) are involved in diseases such as Alzheimer's disease and suspected to be involved in various cancers. Their inhibition has been studied by Testero and co-workers, who tested an extensive series of thiirane and epoxide derivatives inspired by (2*S*, 3*R*)-2-benzyl-3,4-epoxybutanoic acid (BEBA, Figure 13C), in which they modified the original BEBA phenyl ring to alkyl side chains or rings (Figure 13C).[92] Some recent studies have reported the application of epoxide compounds toward the inhibition of bacterial enzymes. Class A β-lactam inhibition involving an epoxy cephalosporin derivative was reported by Lebedev and colleagues showing promising inhibitory activities. However, their study was inconclusive on the exact mechanism by which the inhibition took place.[93] Fosfomycin (or Phosphomycin; Figure 13D), which is the only phosphonate in the clinic, can bind to the uridine diphosphate-N-acetylglucosamine enolpyruvyl transferase enzyme (MurA) which is involved in peptidoglycan

synthesis. This takes place by nucleophilic attack of the MurA's cysteine residue found in its active site on the fosfomycin epoxide ring, thus being a bactericidal compound.[94,95]

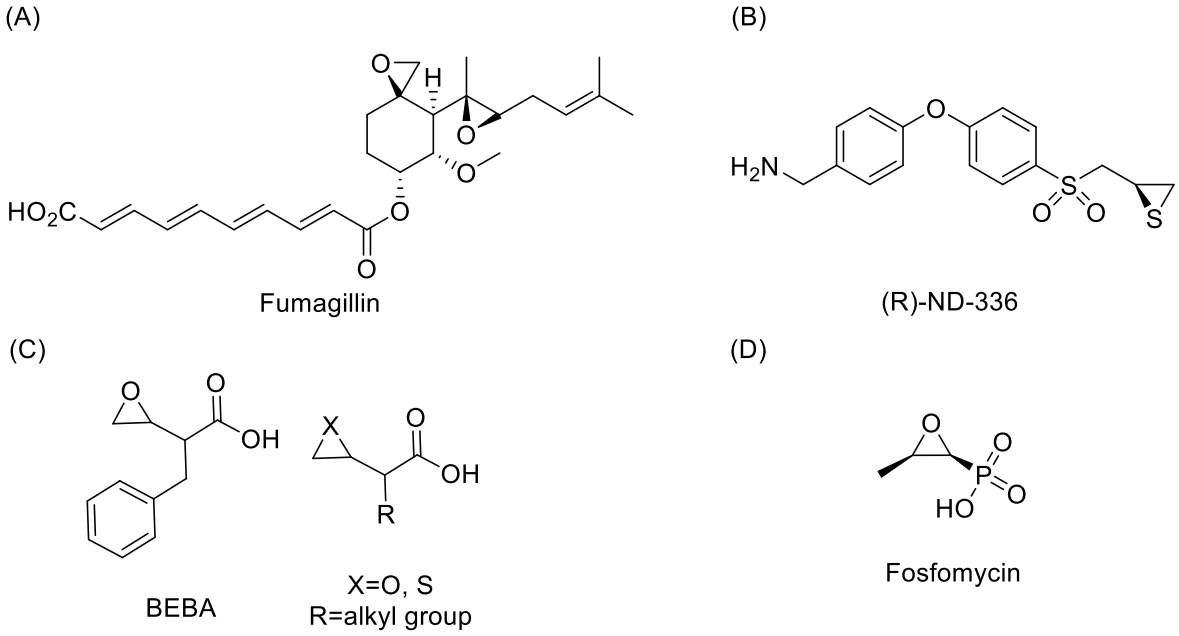

Figure 13: Epoxide and thiirane covalent inhibitors of metalloenzymes

Although the reported covalent inhibitors have not targeted metallo-β-lactamase enzymes and proceed by a different mechanism than the traditional hydrolysis of a substrate, the study and application of strained 3-membered-ring-containing molecules is believed to have relevance in the development of efficient irreversible covalent MBL inhibitors.

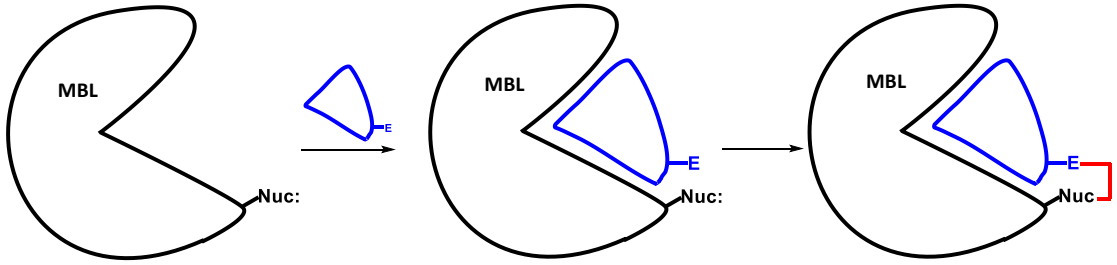

Scheme 8: Covalent binding strategy illustrated for an MBL. Black: MBL; Blue: inhibitor; Nuc: nucleophilic amino acid; E: thiirane/epoxide electrophile.

The use of strained 3-membered rings such as epoxides or thiiranes as a warhead for covalent enzyme inhibition has not been investigated in the context of MBLs. Therefore, this work

aims at developing a series of newly-designed potential inhibitors containing an epoxide or thiirane and a zinc-coordinating functional group(s) in order to efficiently inhibit covalently the MBL class (Scheme 8). Several strategies are explored in this work to achieve covalent binding with different newly designed inhibitors. Also, the use of a metal ion binding strategy by incorporation of coordinating functional groups (thioacid and carboxylic acid) to those newly designed inhibitors is of interest.

Chapter II. Open β-lactam analogues as covalent inhibitors targeting metallo-β-lactamases

Introduction: From closed lactam ring to modification into the open β-lactam analogues

The project for the development of covalent open β-lactam inhibitors arose from investigations during preceding work on traditional β-lactam inhibitors derived from clavulanic acid (Scheme 9). This clavulanic acid-based project which did not lead to a successful outcome provided insights for synthetic strategies and direction for the current work presented below. The initial goal was to make a series of clavulanic acid inspired inhibitors effective against class B which is not normally affected by the traditional clavulanic acid targeting principally class A β-lactamases very efficiently. The approach was to incorporate an anchor in the designed inhibitor for covalent interactions with metallo-β-lactamases (MBLs) using a 3-membered ring such as an epoxide, thiirane, or aziridine.

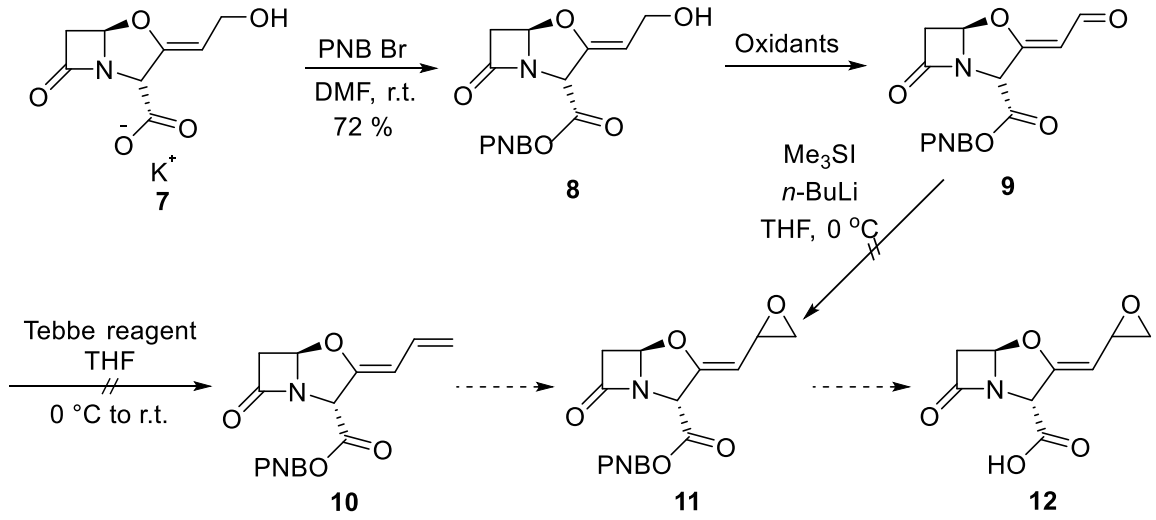

Scheme 9: Attempted synthesis of clavulanic acid derivative containing an epoxide

Starting with potassium clavulanate (**7**), a benzyl ester protection of the carboxylic acid functional group was performed[96] to give **8** in 72% yield leading to the next step, the oxidation of

the allylic alcohol. Surprisingly, the use of manganese dioxide as oxidant,[97] known to be very selective for allylic alcohols, did not provide a significant yield of the desired product **9**. The reaction conditions led to low percent conversions (2-15%) as determined by nuclear magnetic resonance spectroscopy (NMR). Other reagents were explored for the oxidation reaction including 2,2,6,6-tetramethyl-1-piperidinyloxy (TEMPO),[98] Dess-Martin Periodinane (DMP),[99] and its precursor 2-iodoxybenzoic acid (IBX).[100] Attempted oxidation with TEMPO did not lead to conclusive results, but the use of DMP and IBX reagents provided a range of percent conversions of the corresponding aldehyde **9** between 0 to 70%, as determined by NMR. Two sets of doublets were observed at 7.8 ppm and 8.0 ppm with J = 0.9 Hz and J = 8.3 Hz, respectively, when the oxidation was performed with DMP while only one peak at 8.0 ppm was observed with IBX. This suggests that *E* and *Z* isomers of the allyl aldehyde were formed with DMP while IBX afforded only one. Although the aldehyde proton characteristic peak of the nitro benzyl protected clavulanic **9** was observe at around 8.0 ppm, the purification happened to be challenging and they were not isolated satisfactorily.

A crude sample of **9** was subjected to the Tebbe reagent[101] for an attempted methylenation reaction from the aldehyde. These conditions led to a complex mixture with the loss of the nitro benzyl protecting group. The formation of the corresponding alkene compound was not confirmed, and the inconsistent results pushed us towards an alternative strategy. The new approach was to bypass the olefination step and attempt a direct epoxidation[102] of the crude aldehyde product collected. This would have shortened the synthesis pathway and avoided issues encountered with the Tebbe reaction conditions, but despite multiple attempts, the reaction did not form the epoxide **11**.

It was thought that since 3-membered ring formation was proving to be challenging with the current substrate, a change in the target structure was necessary which led to the project detailed below in this chapter.

Research Objectives: Covalent inhibition of MBLs with strained 3-membered ring open lactam analogues

As reported previously, the introduction of a strained 3-membered ring strategy in the Metallo-β-lactamase (MBL) inhibitors has not been applied as of right now to the best of our knowledge. Thus, it was of interest to investigate it and determine the potential benefits which could be observed toward efficient inhibition of MBLs. MBLs found in antibiotic-resistant bacterial strains are known to have conserved amino acid residues which can be used as leverage in the development of small inhibitor molecules of these enzymes. Some of the conserved amino acids in the most prevalent MBL, B1 subclass, include lysine ($-NH_2$) and aspartic acid (-COOH) which have been important for the catalytic mechanism of MBLs as reviewed in chapter 1 (Figure 8A). These amino acid residues might interact with the designed inhibitors through nucleophilic reaction to lead to the formation of a covalent bond between the inhibitor and enzyme, rendering the interaction irreversible.

The new compounds designed are the opposite of a traditional lactam ring structure, an open version of the ring containing a coordinating functional group (thioacid) in addition to a 3-membered ring. This idea was thought to provide a stronger interaction with class B lactamases and allow for a more achievable synthesis pathway than the original clavulanic acid derivative. The approach that was taken when designing the target molecules include for this series of inhibitors (Figure 14) a thioacid functional group which could enhance the positive interaction with the targeted enzymes, a phenyl moiety, and the strained 3-membered ring as covalent anchoring group.

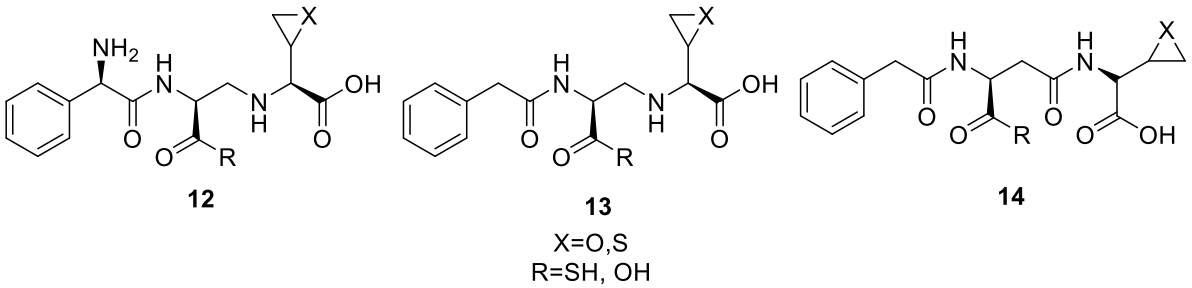

Figure 14: Structure of the proposed covalent 3-membered ring open lactam analogues

Experimental and *in silico* studies of MBL inhibition from all 3 subclasses, including NDM-1 (B1), IMP-1 (B1), BCII (B1), CphA (B2), L1 (B3), FEZ-1 (B3) among others, reported the presence of hydrophobic moieties contained in the molecule, i.e. alkyl chain, cyclopropyl, benzyl, or phenyl group, stabilize the binding in the active site through hydrophobic interactions with loop structures in MBLs.[103–107] Loop L3 (Figure 15) present in the B1 and B3 subclass can include hydrophobic residues such as valine, methionine, tryptophan, or phenylalanine which can favorably interact with hydrophobic moieties in inhibitors.[44] An in-depth study of ampicillin, which is a well-known and commonly used antibiotic containing a phenyl group, with B1 subclass NDM-1 showed the structural interaction after hydrolysis of ampicillin (Figure 15) and the importance of the presence of the phenyl ring in the binding pocket through hydrophobic interactions. The hydrophobic interaction of the phenyl ring with methionine (M67) and leucine (L65) residues lead to the appropriate positioning and tight binding of the hydrolyzed ampicillin in the active site, essential for efficient enzyme inhibition (Figure 15).[46]

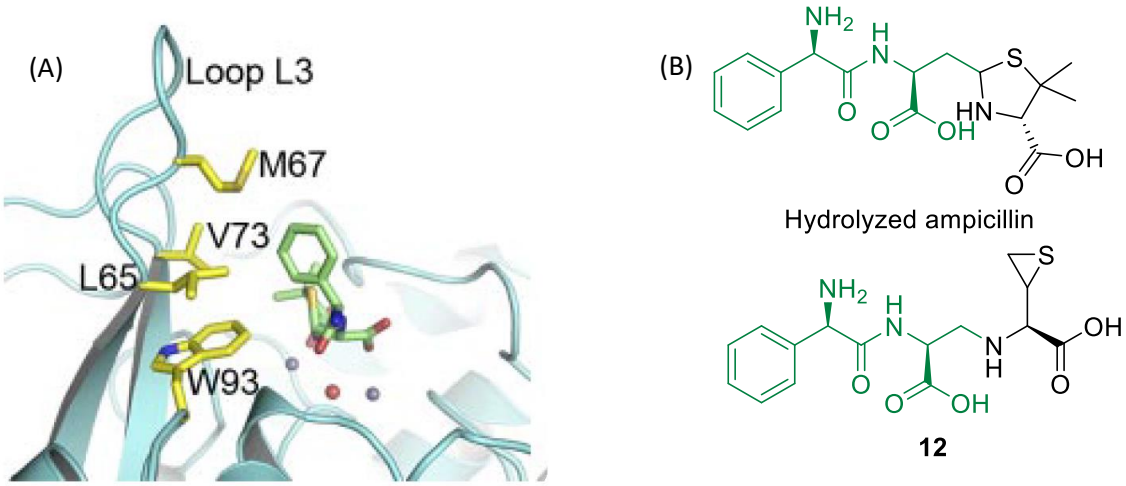

Figure 15: X-ray crystal structure of the hydrophobic interactions of hydrolyzed ampicillin (green) in the active site of NDM-1 (A).Structural similarities between compound **12** and hydrolyzed ampicillin (B)[46]

Considering the structural features of MBLs and the reported results, it was decided to incorporate a phenyl group which would serve to promote hydrophobic interactions as with hydrolyzed ampicillin, which the designed derivatives were inspired from. The initial approach, in addition to the hydrophobic moiety, was to incorporate a thioacid, but the synthesis was constrained to a carboxylic acid due to synthetic challenges.

Proposed mechanism of action of covalent 3-membered ring open lactam analogues

The proposed inhibitors are believed to have the ability to interact covalently with MBLs, leading to an irreversible inhibition of the metallo enzymes. These derivatives, when administrated simultaneously with an antibiotic to the patient, will ideally have a higher affinity for the bacterial MBL enzyme than the antibiotic does. Thus, the activity of the MBL will be inhibited, preventing it from inactivating the β-lactam antibiotic.

The presence of a conserved amino acid residue, i.e. aspartic acid (Figure 16), in the binding pocket of metallo-β-lactamases could allow for the development of more effective

inhibitors, as they contain a nucleophilic carboxylate group that can form covalent interactions with electrophilic chemical species.

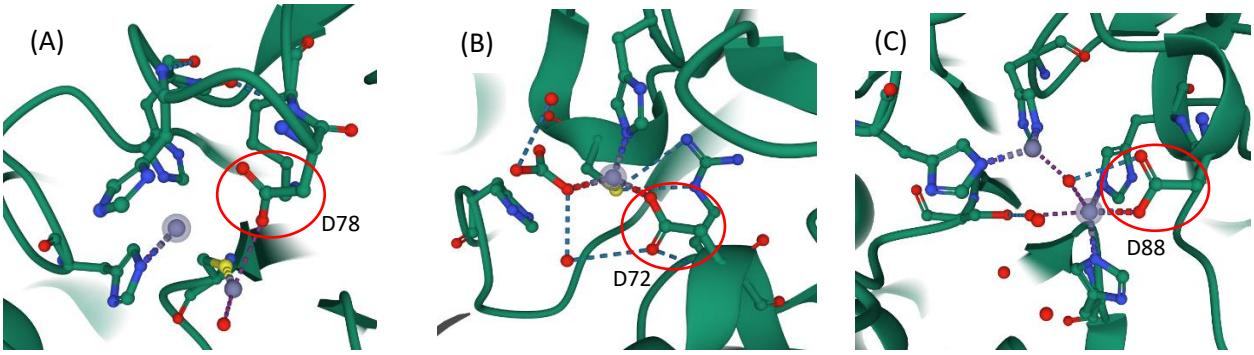

Figure 16: Crystal structure of the active site of MBL highlighting the presence of aspartic acid (D) residues circled in red. (A) B1 (NDM-1, PDB: 3S0Z); (B) B2 (CphA, PDB: 1XBG); (C) B3 (L1, PDB: 15ML).

The designed compounds could reach the enzyme binding pocket where they would be positioned appropriately through hydrogen bonding and hydrophobic interactions between the various MBL's active site amino acids and the functional groups of the target inhibitor. The analogues containing a 3-membered ring introduced using organic synthesis could potentially interact covalently with the nucleophilic residue in MBLs. The proposed mechanism involves a conserved residue, aspartic acid for instance, acting as a nucleophile for the formation of a covalent bond. This can take place through an elimination reaction by deprotonation of an acidic proton in **13** (Scheme 10) leading to the thiirane ring opening followed by nucleophilic attack by the aspartic acid residue on the elimination product (**14**, Scheme 3) to form a covalent bond for an irreversible interaction (**15**, Scheme 10). Another plausible mechanism can be through direct ring opening of the thiirane of the inhibitor (**16**, Scheme 11) to give the covalently bound inhibitor (**17**, scheme 11).

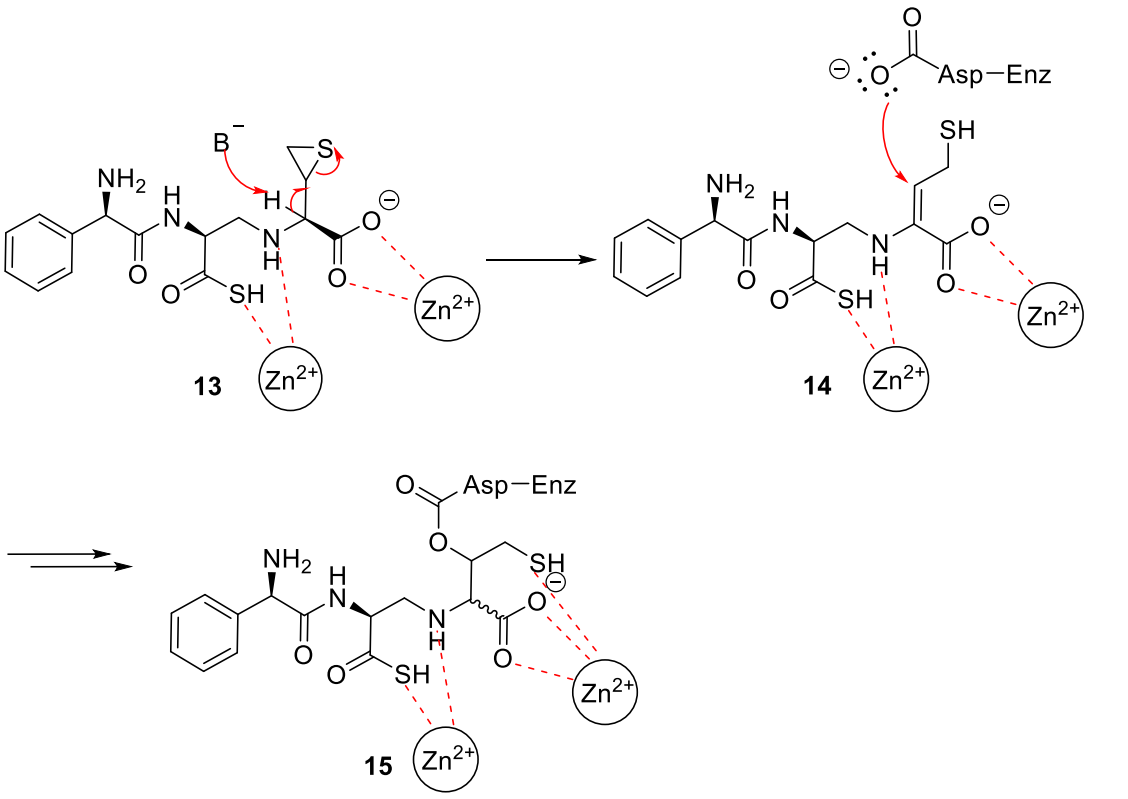

Scheme 10: Mode of action of analogue **7** for the inhibition of MBL via elimination.

Scheme 11: Mode of action of the covalent inhibitor **7** via a direct thiirane ring opening mechanism

Result and Discussion

Synthesis of Vinylglycine methyl ester hydrochloride (23)

Multiple convergent synthetic routes were explored in attempts to synthesize the acid containing analogues, and these will be discussed in detail in the present section. All pathways explored involved a convergent synthesis of a vinylglycine derivative (**23a**, **23b**) used for the formation of a 3-membered ring, which is introduced to a dipeptide fragment in attempt to obtain the final target molecules presented in Figure 14. The investigation of different dipeptide fragments was done leading to several generations of targets which will be detailed.

Vinylglycine (VG) is a costly commercially available compound, thus it was decided that it would be synthesized following a modified literature method reported by A. Afzali and H. Rapoport in 5 steps.[108] Through this multistep synthesis (Scheme 12), the methyl ester protected D-VG (**23a**) and L-VG (**23b**) were synthesized in an overall 54% yield. Esterification of D-methionine methyl ester HCl (**18a**) and L-methionine methyl ester HCl (**18b**) with benzyl chloroformate afforded the corresponding Cbz-protected methionine methyl esters **19a** and **19b** in 88% yield.

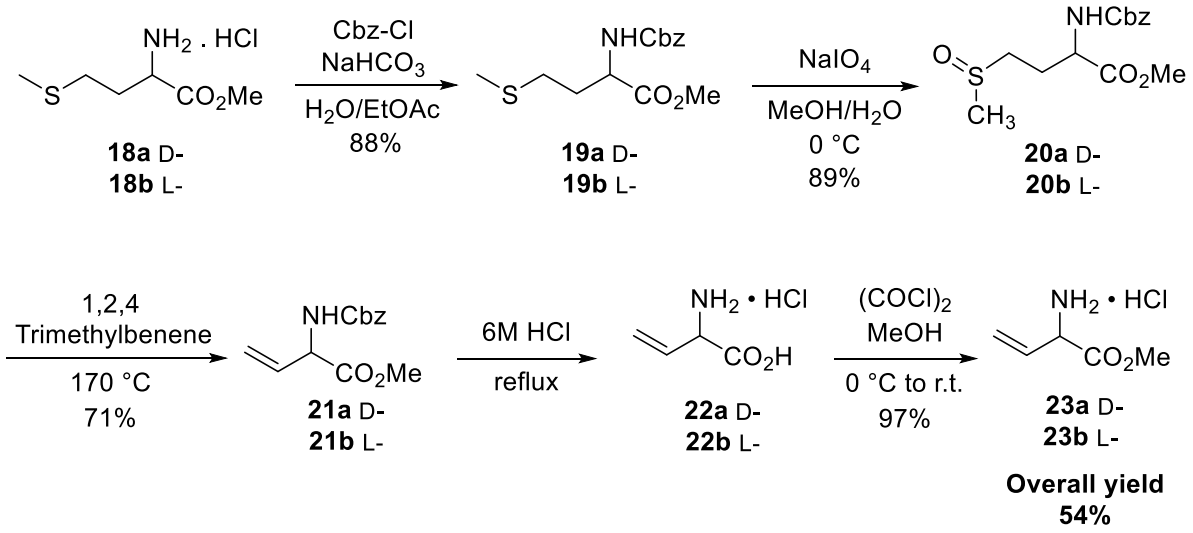

Scheme 12: Synthesis of L- and D-VG methyl esters HCl (**23a**, **23b**)

Entry	Deprotection Conditions	Observation	Yield
1	Et_3SiH, $Pd(OAc)_2$,Et_3N	No Deprotection SM recovered	--
2	Et_3SiH, $PdCl_2$, Et_3N	No Deprotection SM recovered	--
3	6M HCl, Reflux	Cbz and methyl ester deprotection	97%

Table 1: Reaction summary for the Cbz removal of **21**

Oxidation of the methionine sulfides using $NaIO_4$ led to the corresponding sulfoxides **20a** and **20b** in 89% yield. Pyrolysis of protected methionine sulfoxides at 170 ^oC afforded through a β-elimination the L- and D-Cbz-VG methyl esters **21a** and **21b** respectively in 71% yield. Removal of the Cbz group (Table 1) was first attempted using $Pd(OAc)_2$[109] and $PdCl_2$[110] with Et_3SiH to obtain the desired protected VG methyl ester (**23a**, **23b**) without deprotecting the methyl ester which was not proposed in the route by Afzali and Rapoport. As the attempted palladium-catalyzed deprotections were unsuccessful, the removal of both protecting groups was accomplished with 6 M HCl under refluxing conditions and afforded the vinylglycine hydrochloride **22a** and **22b** in 97% yield. The fully deprotected VG was esterified to give the desired VG methyl ester hydrochloride final compounds (**23a**, **23b**) in quantitative yields (p. 124 ^1H NMR; p.125 ^{13}C NMR). At that point, the VG methyl ester was to be used as part of the convergent synthesis to obtain the desired MBL inhibitors proposed in Figure 14 and discussed below.

Attempted synthesis of (2S)-(2-amino-2-phenylacetamido)-3-oxo-(3-sulfanylpropyl)amino-(oxiran-2-yl)acetic acid (12)

The original target in the development of covalent inhibitors of MBLs was compound **12** (Figure 14). Through retrosynthetic analysis it was understood that the ampicillin-mimicking moiety in **12** could be introduced via the non-essential amino acid phenylglycine (**24**) by coupling it with the amino group of a dehydroalanine moiety, obtained from **26**, and used to incorporate the thioacid functional group in the analogue (Scheme 13). As mentioned previously, the 3-

membered ring portion was designed to be incorporated into the molecule from vinylglycine methyl ester hydrochloride (**23a**, **23b**) synthesized from methionine (**27**) in which the alkene bond would undergo epoxidation or indirect episulfidation to serve as an anchor for covalent interactions with MBLs. Those two moieties were to be linked together through a conjugate addition reaction between the primary amine of **23** and the alkene **25**.

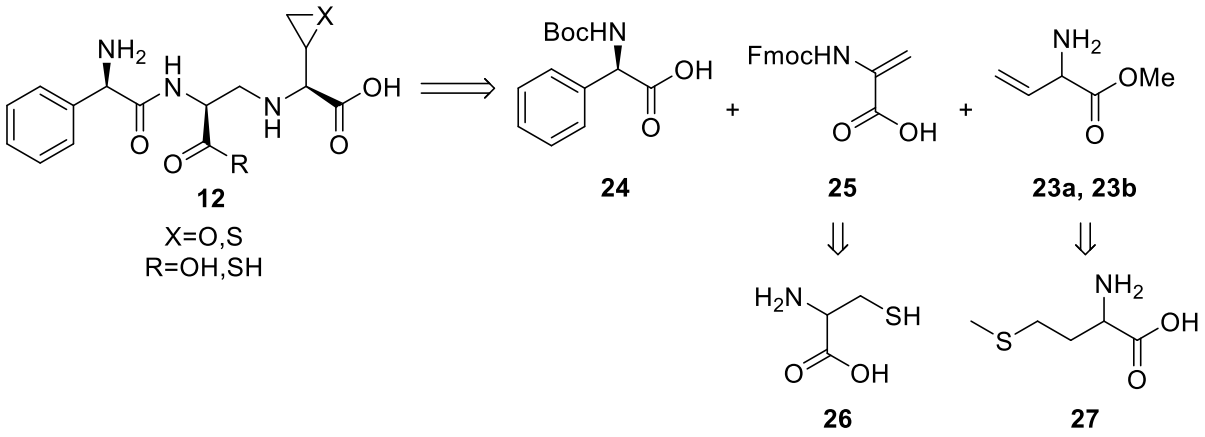

Scheme 13: Retrosynthetic analysis of **12**.

N-Boc phenylglycine (**24**) is commercially available for use in the coupling reaction with dehydroalanine. Therefore, synthesis of **12** began with the attempted synthesis of dehydroalanine from L-cysteine. A diamide **30** was synthesized in a two-step reaction[111] (Scheme 14a) via formation of dibrominated acyl chloride intermediate **29** from adipic acid (**28**) followed by nucleophilic addition reaction with ammonia to afford **30** in 29% yield. This was to be used for the formation of dehydroalanine (Scheme 14b), however the synthesis from Fmoc-cysteine **31** failed to provide the desired compound **25**.[112] The results of the reaction suggested that the Fmoc protecting group was cleaved under the applied conditions which was confirmed by NMR analysis which presented the dibenzofulvene characteristic peaks in addition to what seems to be a cysteine dipeptide.

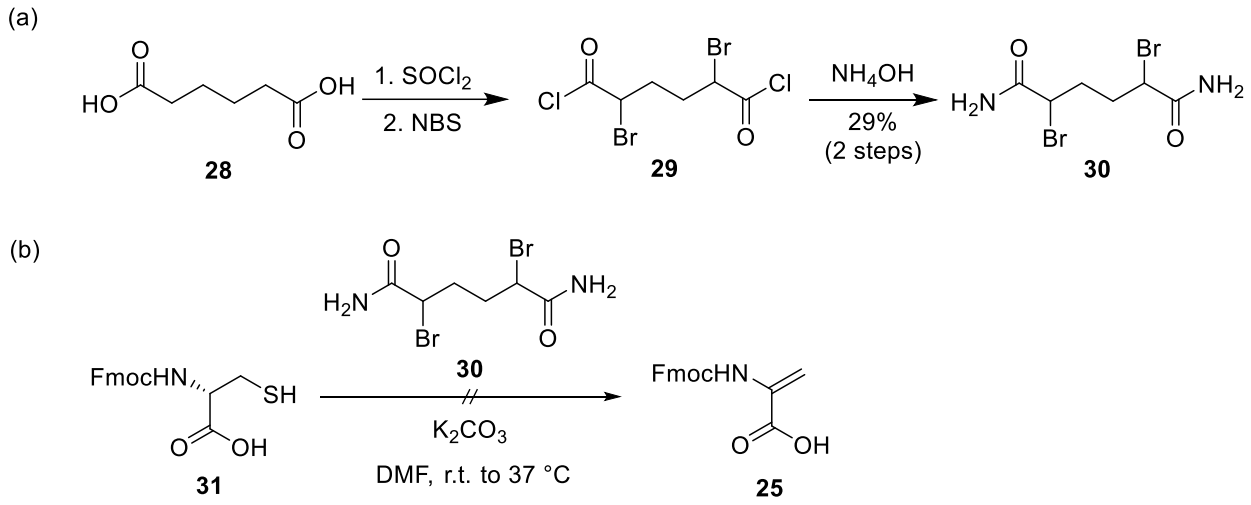

Scheme 14: (a) Synthesis of diamide **30**; (b) Attempted synthesis of Fmoc-dehydroalanine (**25**)

In attempt to obtain **12** and avoid the encountered issues with the previously discussed synthesis of dehydroalanine, it was decided to replace it by a bromoalanine core which would be used to incorporate the acid functionality and to converge the previously synthesized VG methyl ester in the desired target molecule (Scheme 12). The bromoalanine core moiety is derived from the amino acid serine rather than cysteine used initially for the formation of dehydroalanine. The protected VG **23a** or **23b** can be added in the synthesis via an *N*-alkylation reaction with the protected brominated dipeptide intermediate **37** rather than the previously planned conjugate addition reaction with the alkene of dehydroalanine derivative **25**.

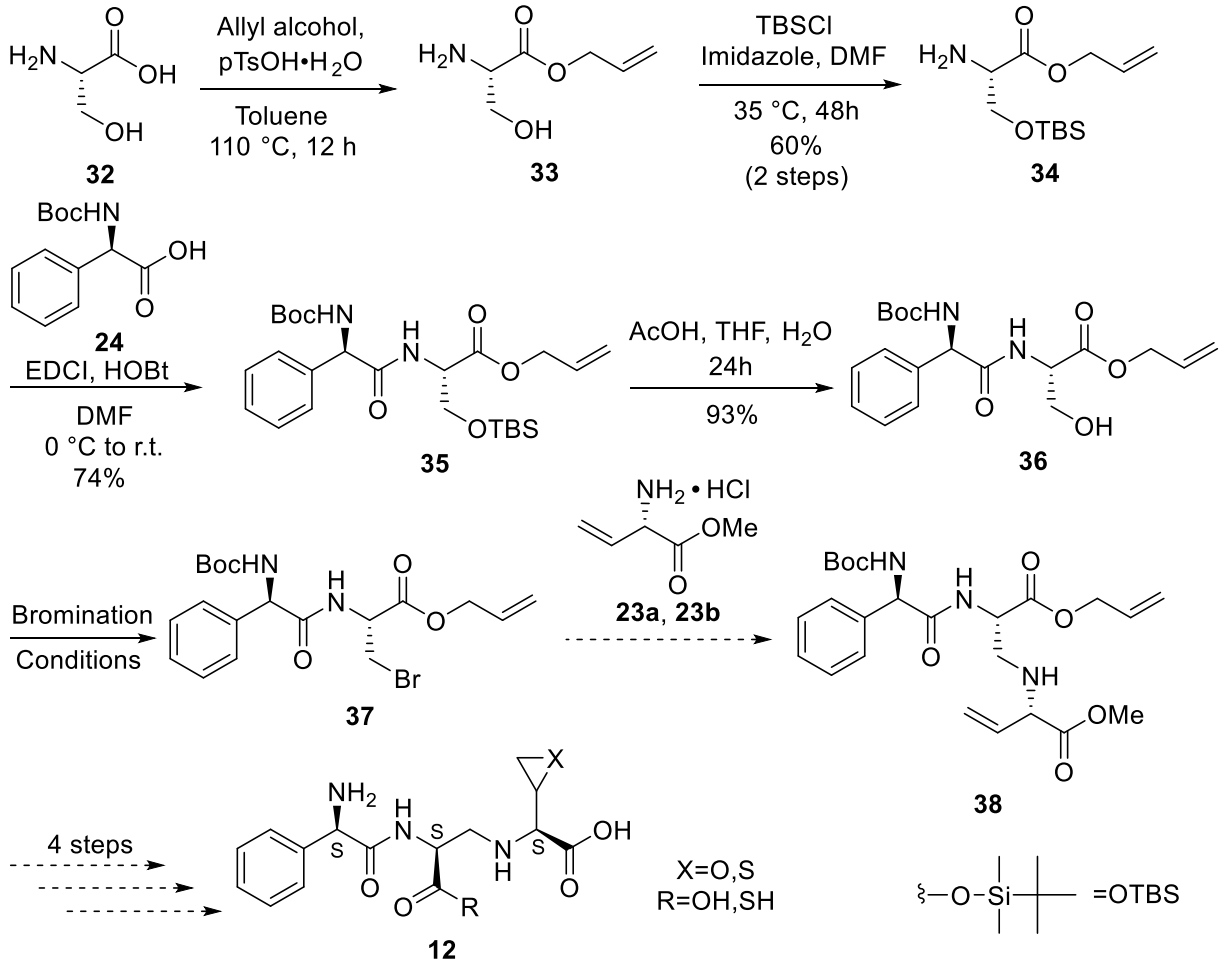

Scheme 15: Attempted synthesis of **12** via bromo dipeptide **37**

Entry	Bromination Conditions	Solvent	Temperature /Time	Observation	Purification
1	CBr_4, PPh_3	CH_2Cl_2	0 °C to 35 °C 4h	No reaction completion	Required- side products after workup
2	NBS, PPh_3	CH_2Cl_2	r.t. 4h	No starting material remaining	Required- side products after workup
3	PBr_3	Et_2O	0 °C 1h	No starting material remaining- groups missing	Cleaner than NBS after workup

Table 2: Reaction summary for the bromination of **36**

The synthesis of **12** following the new proposed pathway involved a two-step reaction for the protection of L-serine (**32**). An allyl ester formation of the carboxylic acid followed by silylation of the alcohol side chain gave the desired L-serine allyl ester O-*tert*-butyldimethylsilyl ether (**34**) in a 60% yield over 2 steps.[113,114] Amino acid coupling[115] of *N*-Boc protected phenylglycine (**24**) with the synthesized protected serine (**34**) afforded the desired dipeptide **35** in 74% yield (p. 127 ^{1}H NMR; p.128 ^{13}C NMR; p. 129 HRMS). Subsequently, a highly efficient and clean mild acid cleavage of the *tert*-butyldimethylsilyl ether of dipeptide **35** led to the corresponding free alcohol **36** in 94% yield without further purification required.[114] At this point, **36** was to be brominated using a brominating agent in the presence of triphenylphosphine. Multiple changes of the reaction variables for the bromination were applied in order to obtain an optimized conversion of the alcohol (Table 2) to bromide **37**. The reaction of **36** with CBr_4[116] did not lead to complete conversion of the alcohol, which was mostly recovered. When subjected to the reaction conditions using *N*-bromosuccinimide (NBS), the starting alcohol was fully consumed contrarily to CBr_4 as seen by thin layer chromatography (TLC). Unfortunately, the bromination conditions using NBS[117] contributed to some impurities in the product which required purification prior to moving onto the next reaction step. Compound **37** is not stable as the product lose its bromine group after manipulation through the purification by column chromatography to form an alkene. Proton Nuclear Magnetic Resonance (^{1}H NMR) analysis of the collected product suggested the observed outcome. Indeed, the diastereotopic protons of the methyl group geminal to the alcohol in the serine moiety of the dipeptide **36** are observed at 4.0-3.9 ppm, but upon bromination to give **37**, these diastereotopic protons shift downfield after a period of time to 6.6-5.9 ppm. This was indicative of the formation of the desired bromine **37** although unstable to manipulation post reaction. Thus, it was of interest to seek a more efficient and cleaner option for the formation of bromide **37**.

Phosphorus tribromide[118] was used alternatively as the brominating agent instead of CBr_4 or NBS. In this case there was evidence of complete consumption of the alcohol **36** with minor side products observed upon aqueous workup which was desired to avoid manipulation through purification steps. However, the NMR spectroscopy analysis of the isolated product of the reaction showed a loss of peaks for part of the desired compound: the phenylglycine group and evidence of the deprotection of the Boc protected amine. The outcome obtained with PBr_3 as generating less side products was an useful insight for the subsequent synthetic work. However, the loss of functionalities in the molecule using **36** led us to focus on the synthesis pathway to develop compound **13** which was developed simultaneously and will be described in detail below.

Attempted synthesis of (2*S*)-(2-phenylacetamido)-3-oxo-(3-sulfanylpropyl)amino-(oxiran-2-yl)acetic acid (13)

In parallel to the synthesis using phenylglycine as the ampicillin-mimicking moiety to form **12** (Scheme 15), it was decided to use phenylalanine (**40**) as another derivative which gives compound **13** in this case. As it does not contain an amino group, it was of interest to use it for both the ease of handling through the synthetic steps and the eventual variation in the interaction and inhibition of MBL in comparison to **12**. The synthetic path follows a similar approach to the one reported for **12**, with the majority of the synthetic steps leading to comparable yields except for the formation of alcohol **42** (Scheme 16). Phenylalanine (**40**) was introduced into the synthesis by reaction with the previously made protected serine **34** providing **41** in 85% yield followed by deprotection of the *tert*-butyldimethylsilyl ether group to give alcohol **42** in a 88% yield (p. 135 ^{1}H NMR; p.136 ^{13}C NMR), slightly lower than what was obtained for amine containing analogue **36** (Scheme 15). Based on the results of the bromination conditions investigated for **12** it was decided to employ the reaction conditions using PBr_3 for the bromination reaction of **42**. This led to the formation of the desired compound in 10% conversion as observed by ^{1}H NMR analysis which

was used as is without further purification. The next step was the attempted alkylation reaction with **43** for the incorporation of the VG moiety.

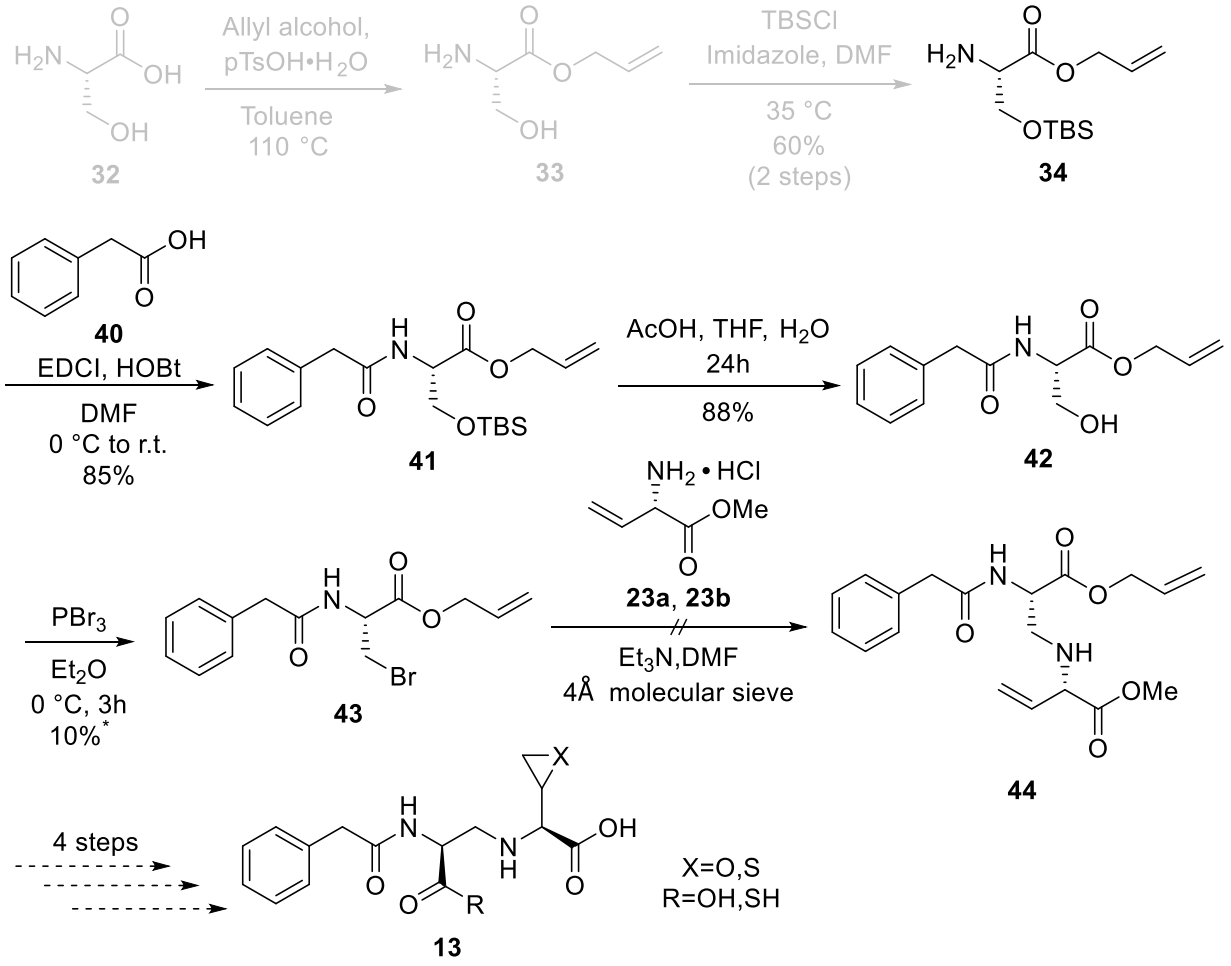

*Percent conversion by ^{1}H NMR

Scheme 16: Attempted synthesis of **13** with bromo dipeptide intermediate **43**

In anticipation of possible undesired over-alkylated side products in the reaction of bromide **43** and L-VG methyl ester hydrochloride (**23**), the reaction conditions followed were those described by S. Bhattacharyya and co-workers.[119] The strategy used relies on a chemoselective deprotonation of primary amines in the presence of secondary amines, preventing them from being alkylated. The reaction conditions were controlled by slow addition of Et_3N/dry dimethylformamide (DMF) solution (1/40th) over an extended period of time of 8 hours into the

alkyl bromide solution in DMF in the presence of 4Å molecular sieves. They reported an *N*-alkylation of bromide salts of primary amines with alkyl bromides with a 9:1 ratio of monoalkylated to dialkylated product observed, reaction often providing undesired over-alkylated product at much higher ratio. However, following the above conditions for the *N*-alkylation of **43** with **23** did not lead to conclusive results for the formation of the desired product **44** despite modification of the reaction variables such as the number of equivalents of base or reaction time. Consumption of the amine **23** and new product formation were observed, but the ^{1}H NMR spectroscopic analysis did not confirm the formation of the desired monoalkylated product in the crude mixture, or any of the fractions collected after purification by column chromatography. Interestingly, the ^{1}H NMR spectrum obtained only showed the presence of a portion of the expected molecule. The vinylglycine moiety seemed to be missing, as the expected peak for the methine group at ~5.0 ppm and the vinylic protons at 5.2-6.0 ppm were not observed (Figure 17). The spectrum suggests that the brominated dipeptide (**43**) underwent elimination of HBr leading to the formation of an alkene product (**45**) as the geminal vinylic protons in the 6.5-5.9 ppm region were present (Figure 17). This would be expected due to the presence of the acidic α-proton adjacent to the ester, which can be deprotonated under basic conditions, followed by elimination of the bromide. After several trials and the encountered issues following this pathway, it was clear that the strategy undertaken needed to be altered in order to incorporate the VG moiety effectively. The presence of an acidic proton next to the bromine, which is a very good leaving group, causes its elimination. Therefore, it was decided to attempt a reductive amination of an aldehyde instead of an *N*-alkylation of a bromide.

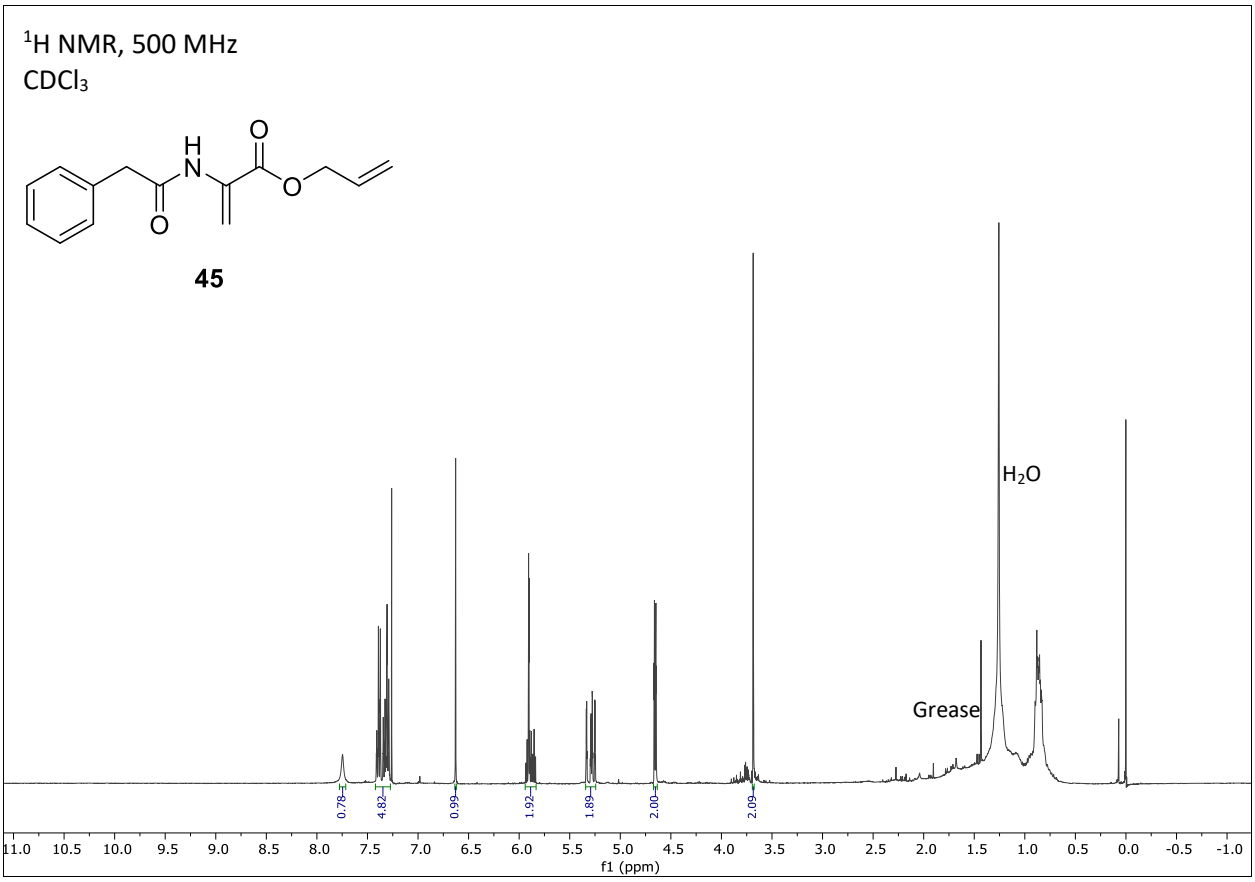

Figure 17: ^{1}H NMR spectrum of the proposed unexpected product **45** during attempted reaction of **45** with **23**.

For the reductive amination, the oxidation of alcohol **42** is required to obtain the corresponding aldehyde. It was decided to use a model system to determine the best reaction conditions to achieve the oxidation (Scheme 17). *N*-(*tert*-butoxycarbonyl)serine allyl ester (**46**) was synthesized as the model system in 17% over 2 steps from **38**[113,120] followed by an oxidation reaction to obtain the corresponding aldehyde **47.** Dess Martin periodinane reagent was used to convert alcohol **46** to its corresponding aldehyde **47**. After unfruitful attempts, optimization of the reaction conditions led to the desired aldehyde **47** in a low yield of 14%, requiring 4 equivalents of DMP reagent in a 0.1 M solution (Scheme 17).

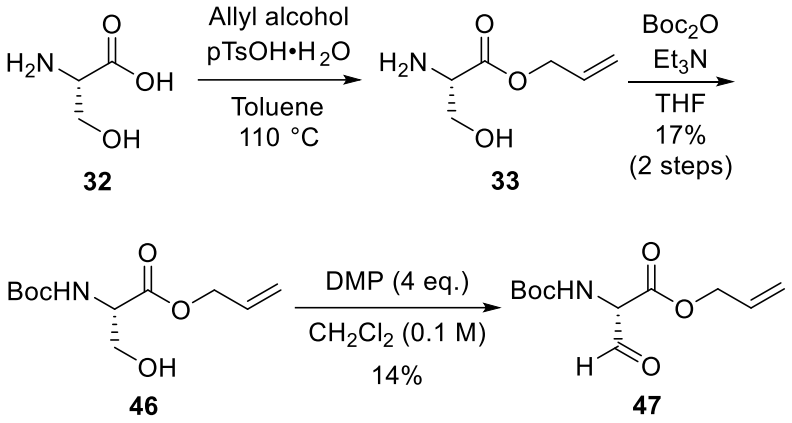

Scheme 17: Synthesis of alcohol **46** and oxidation to **47** using optimized conditions

To form the aldehyde dipeptide **48** (Scheme 18), the oxidation of alcohol **42** was attempted with DMP following the optimized conditions determined with the model system, however, the desired aldehyde was not obtained despite multiple changes of the reaction parameters (DMP equivalents, concentration, etc.). Another oxidant, pyridinium chlorochromate (PCC)[121], was also explored in attempts to oxidize **42.** This did not lead to desired aldehyde **48**, and only alcohol **42** was recovered.

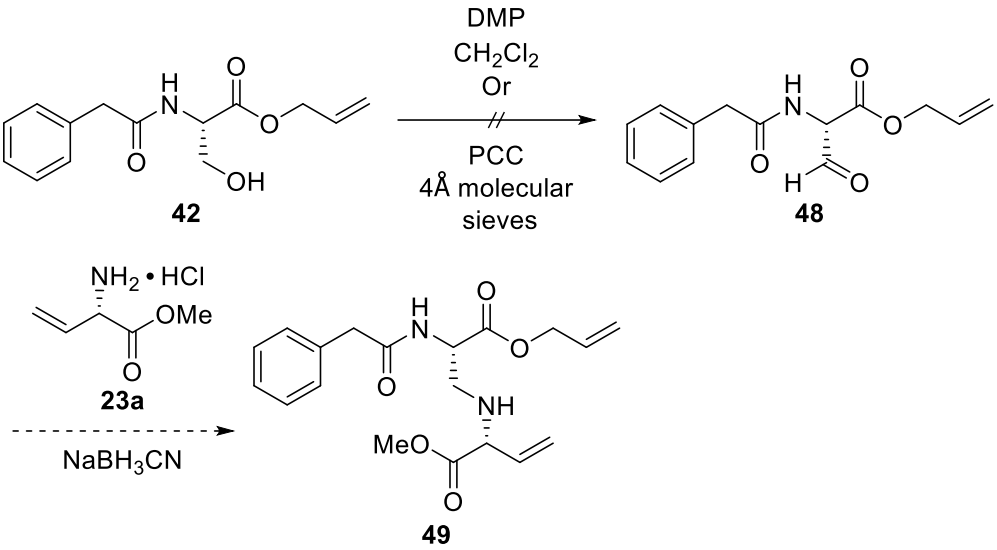

Scheme 18: Attempted synthesis of aldehyde dipeptide **49**

Since the strategies involving *N*-alkylation with a bromide and reductive amination of an aldehyde to incorporate the vinylglycine moiety were both unsuccessful, it became clear that the

core structure had to be changed and the synthetic pathway modified to obtain open β-lactam inhibitors structure for MBLs. The results obtained to this point gave essential information to move in a more promising direction with the choice of molecule to work with. Knowing the difficulties encountered with the acidic proton at the α-position of previous substrates, it was decided to move away from using serine as the core structure and choose an amino acid core with which the issue of the acidic proton would not be encountered over the synthetic steps followed.

Attempted synthesis of (2*S*)-2-({[9*H*-fluoren-9-yl)methoxy]carbonyl]amino)-4-oxo-(1-methoxy-1-oxobut-3-en-2-yl)amino)-1-oxo-1-[(prop-2-en-yl)oxy]butanoate (14)

Aspartic acid was thought to be an appropriate substitute to the serine core. Compared to serine, aspartic acid does not have a free hydroxy group which could be utilized for reductive amination or *N*-alkylation strategies presented above. Instead, an alternative route was explored with the use of a protected aspartic acid starting material **50** as core molecule to incorporate VG methyl ester **23a** or **23b** in the synthesis which lead to compound **14** (Figure 19). This was possible by taking advantage of the carboxylic acid functional group in the aspartic acid to perform an amino acid coupling.

The Fmoc protecting group is commonly used and known to be practical for orthogonal peptide synthesis, so the original proposed pathway to synthesize **14** involved *N*-fluorenylmethoxycarbonyl- (Fmoc-)-L-aspartic acid allyl ester (**50**, Scheme 19). The free carboxylic acid side chain of the starting compound being unprotected enables for the coupling of the VG methyl ester (**23b**) using benzotriazol-1-yl-oxytripyrrolidinophosphonium hexafluorophosphate (PyBOP) as a coupling agent and diisopropylethylamine (*i*-Pr_2NEt). The reaction is moderately efficient with the desired product **51** easily collected after purification by column chromatography in 36% yield. The subsequent step is the deprotection of the amino group in order to introduce the ampicillin mimicking portion by coupling of phenylacetic acid to **50**.

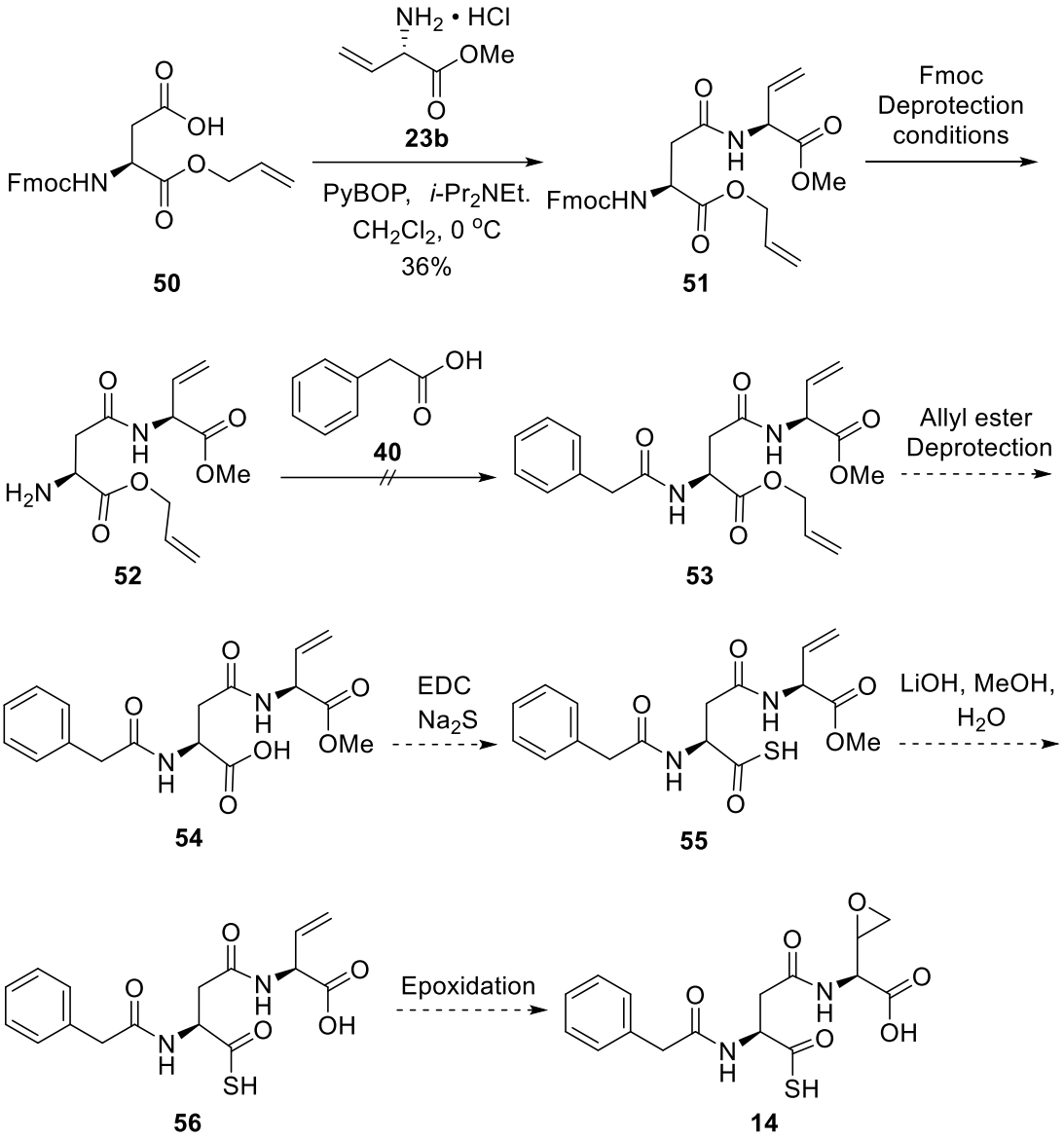

Scheme 19: Attempted synthesis of **14** using a Fmoc protected aspartic acid allyl ester **50**

Entry	Fmoc Deprotection Conditions	Time	Observations	Purification
1	50% *i*-Pr_2NEt, CH_2Cl_2	>24h	SM remaining	Not isolated
2	10% piperidine	4h	No SM	Not isolated
3	20% piperidine	10 mins	No SM	Not isolated Impure

Table 3: Attempted Fmoc deprotection reaction conditions of **51**

Following the mild reaction conditions reported by Chang and co-workers[122] using *i*-Pr_2Net did not lead to Fmoc removal with starting material **51** recovered. Alternatively, the traditional approach with piperidine[123] for Fmoc deprotection was used instead in the hope to get the reaction to completion and facilitate the isolation of the product. Multiple conditions were explored with piperidine for the Fmoc removal reaction which seemed to lead to the complete deprotection of the amino group (Table 3). However, the suspected free amine **52** proved to be difficult to isolate and the collection of the purified desired product was not achieved despite a series of purification attempts. The NMR analysis of the collected crude product suggested that the deprotection reaction of **51** was successful. Indeed, the characteristic dibenzofulvene by-product peaks were present in the NMR spectrum. Therefore, it was decided to use the crude material for the next step which was the coupling reaction with phenylacetic acid **40**. Standard amine coupling conditions were used on the crude material collected which led to a complex mixture as the reaction progressed. The desired product was not observed upon spectral analysis of the isolated product spots. The pitfalls encountered in the presented path with the *N*-Fmoc protected aspartic acid allyl ester **50** as the starting material demonstrated that working with the free amine **52** as an intermediate was more challenging than expected and an alternative which would avoid such manipulation should be more malleable. The order of the steps to be taken to achieve the synthesis of **14** needed to be revisited and starting with a free amine should give a more feasible pathway.

L-Aspartic acid 4-*tert*-butyl-1-methyl ester hydrochloride (**57**) was chosen as the starting material for the modified pathway to **14** as it was desired to keep the same amino acid core structure (Scheme 20). In order to avoid working with a free amine intermediate through the synthetic steps, the free amine starting material **57** was first coupled to phenylacetic acid (**40**) using the same conditions as discussed previously. This led to the dipeptide **58** in a high yield of 91% after purification by column chromatography. Subsequently, the methyl ester deprotection

with lithium hydroxide in a 3:1 mixture of methanol/water[124] gave the free carboxylic acid **59** in 48% yield. This was then coupled to VG methyl ester hydrochloride (**23b**) leading to **60** in a yield of 38% and a mixture of diastereomers (d.r. 2:1) although the reaction was carried through with PyBOP which should minimize racemization. Subsequently, the use of trifluoroacetic acid (TFA) with triethylsilane as the carbocation scavenger for the removal of the *t*-butyl ester protecting group[125] of compound **59** provided the free carboxylic acid **61** in a satisfying 97% yield (p. 150 ^{1}H NMR; p.151 ^{13}C NMR; p. 152 HRMS).

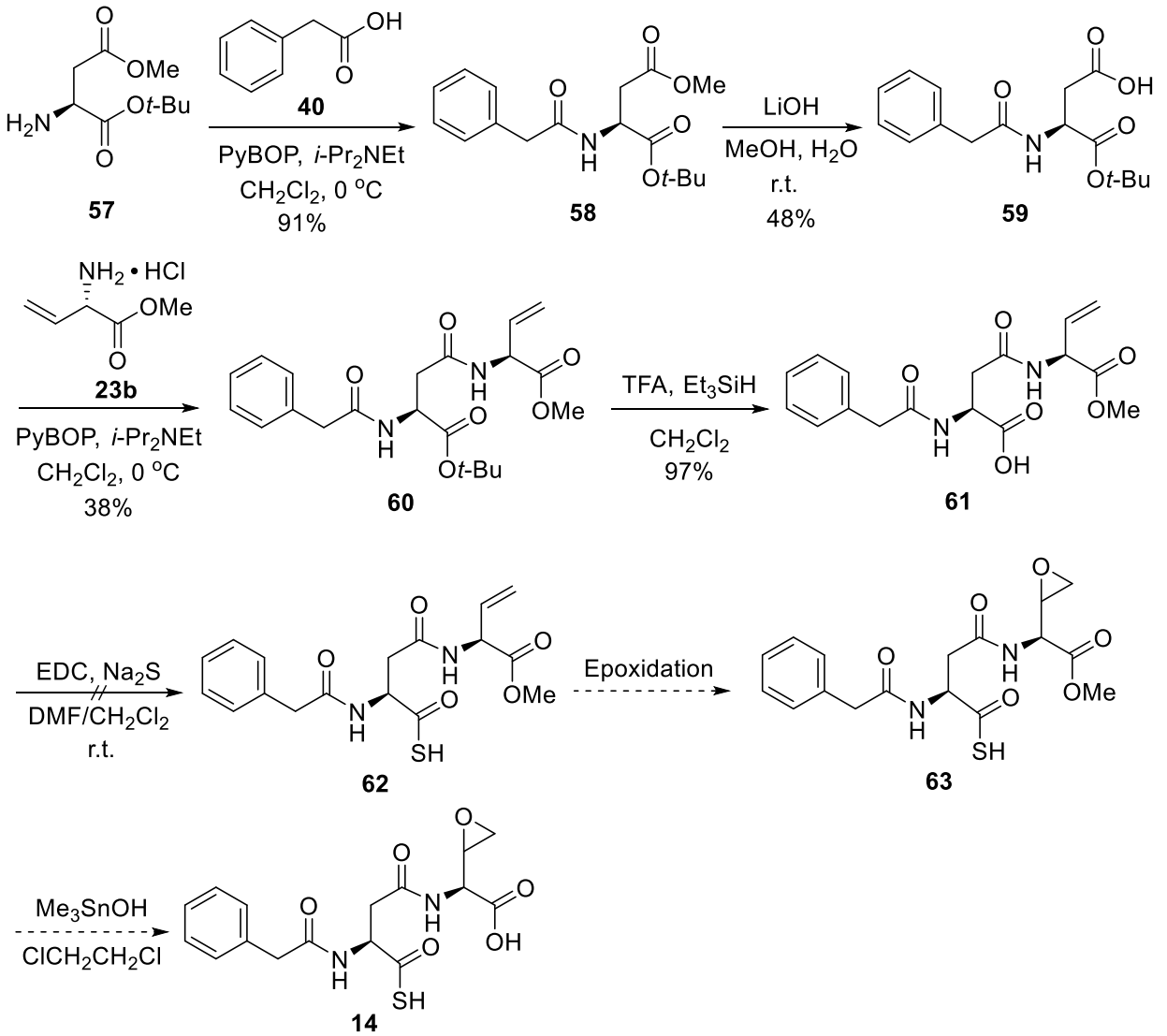

Scheme 20: Synthesis of **14** from L-Aspartic acid 4-*tert*-butyl 1-methyl ester hydrochloride **57**

From there the carboxylic acid **61** was to be converted to the corresponding thioacid which happened to be challenging. The initial reaction conditions followed are those reported by Vishwanatha T.M. *et al.* and use sodium sulfide in DMF in the presence of *N*-ethyl-*N*'-(3-dimethylaminopropyl)carbodiimide (EDC) as the coupling agent.[126] The reaction was attempted with **61**, but the vinylglycine moiety in the expected product **62** was not observed by NMR analysis. Subsequently, an attempt towards the optimization of the reaction conditions was done, however the results obtained did not confirm the formation of **62**. The same outcomes were observed, and the NMR data collected suggested that a cyclized product **64** was formed. This could have occurred through a 5-exo trig ring closure by attack of the carboxylate group of **61** on the amide carbonyl and loss of the VG portion (Scheme 21). The calculated mass for thioacid **62** is *m/z* 364, and the analysis of the crude product by electrospray ionization mass spectrometry (ESI-MS+) did not present evidence of this product. Instead, the expected cyclized product with a calculated *m/z* 233 seemed to be present as a molecular ion peak at that a *m/z* 234 [M+H] was observed in the mass spectrum.

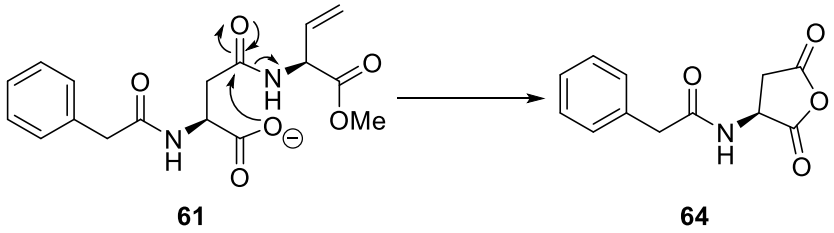

61 **64**

Scheme 21: Proposed mechanism for the formation the undesired product **64** during attempted formation of **62** from **61**

In light of the provided results and the time constraint, it was of interest to attempt the remaining reaction steps of the synthesis, the epoxidation and methyl ester deprotection, with the carboxylic acid version rather than the thioacid (Scheme 22). Since both the acid and thioacid have zinc-coordinating abilities, it was hypothesized that it would be a good alternative and could eventually allow for comparison of the inhibitory abilities of both analogues against MBLs, in the case that the thioacid could be synthesized at a later time.

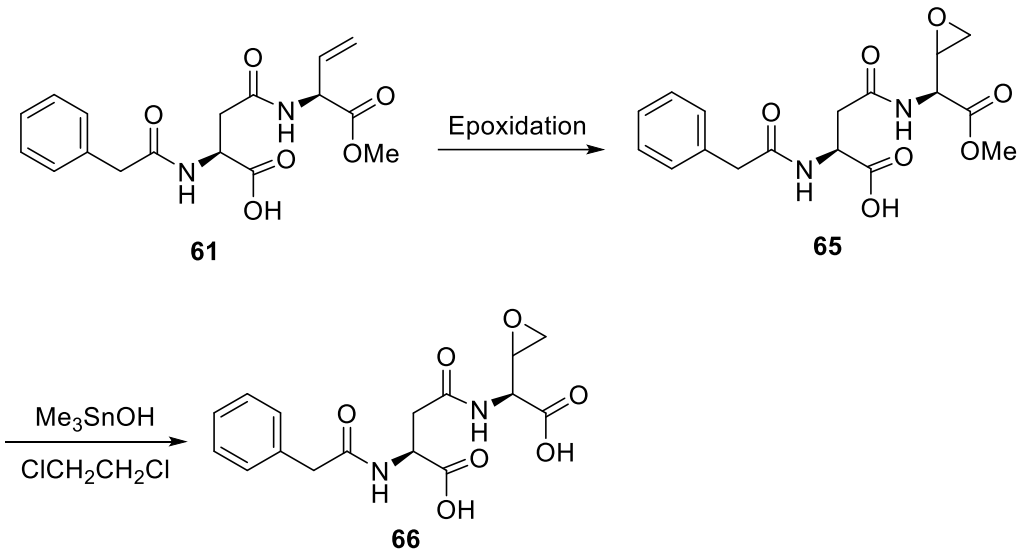

Scheme 22: Synthesis of **66** starting from previously made **61**

The epoxidation of alkene **61** using standard Prilezhaev conditions with *m*-chloroperbenzoic acid (*m*-CPBA)[127] was performed in attempt to obtain **65**, however the alkene was left unreacted as the NMR of the collected crude material showed the characteristic proton peak for the alkene. Starting material **64** was subjected to alternative epoxidation conditions involving trifluoroacetone and potassium peroxymonosulfate (Oxone ®).[128] Through this method, 3-methyl-3-(trifluoromethyl)dioxirane is formed *in situ* which is known to be more reactive with alkenes than the traditional dimethyldioxirane (DMDO). The ^{1}H and ^{13}C NMR data of the crude material collected **65** confirmed that the alkene in the vinylglycine moiety in **61** had reacted as the vinyl protons at 6.0 ppm were not present in the spectrum. The ^{13}C NMR obtained as well showed that the alkene carbons were not present at 132 ppm and 117 ppm, reinforcing the thought that the desired epoxide was indeed synthesized. Multiple purifications of the crude product by chromatography were attempted to confirm the formation of **65**, but the isolation of the pure compound was unsuccessful. Therefore, it was decided to analyze the crude product by ESI-MS to help determine if **65** was actually formed as the ^{1}H NMR data of the crude suggested. Thus, a two-step reaction to get to the final desired compound **66** could potentially be carried on.

The ESI-MS+ provided interesting results supporting the NMR analysis findings. The epoxide **65** *m/z* 364 was found as the base peak *m/z* 365 [M+H] in the presence of some impurities in low ratio (Figure 18).

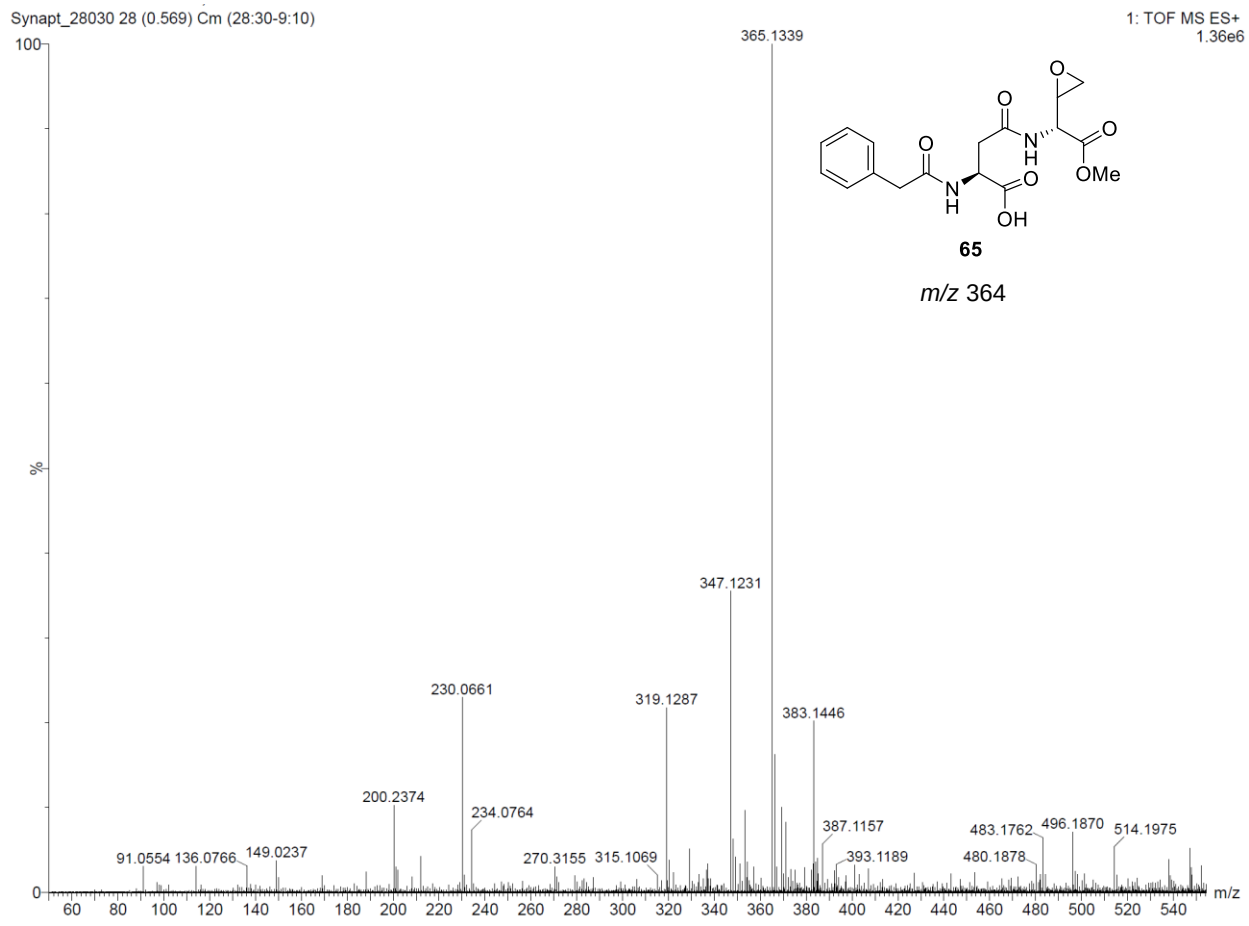

Figure 18: ESI-MS+ spectrum of **65**

The confirmation of the formation of the epoxide enabled the final synthetic step to be performed in order to obtain **66**. It was necessary for the methyl ester deprotection step to be selective to avoid any undesired reactions with functionalities contained in the molecule such as the epoxide. Trimethyltin hydroxide which is known to be mild and selective for the hydrolysis of esters was used in an attempt to deprotect the carboxylic acid to give **66**.[129] The methyl ester deprotection reaction using Me_3SnOH performed was challenging due to the fact that the outcome of the reaction did not clearly show evidence of the final desired product. The ^1H NMR analysis of

the crude product of the deprotection reaction showed the presence of minor peaks corresponding to the expected product suggesting that the deprotection had taken place. However, the peak to noise ratio in the ^{1}H NMR interfered to confirm in a conclusive manner that the desired compound was present in the crude mixture, and additional analysis was needed before manipulating the compound through purification methods in the case where the epoxide ring could ring open. An ESI-MS analysis was performed to help clarify the ^{1}H NMR data obtained, and the expected product *m/z* 351 was not conclusively detected as a *m/z* 347.1241 $[M-H]^-$ was observed as low abundance peak representative of a deprotonated specie (Figure 19). This suggested that the results for the removal of the methyl ester group was unclear and further investigation required to confirm the formation of the desired product of reaction **66**.

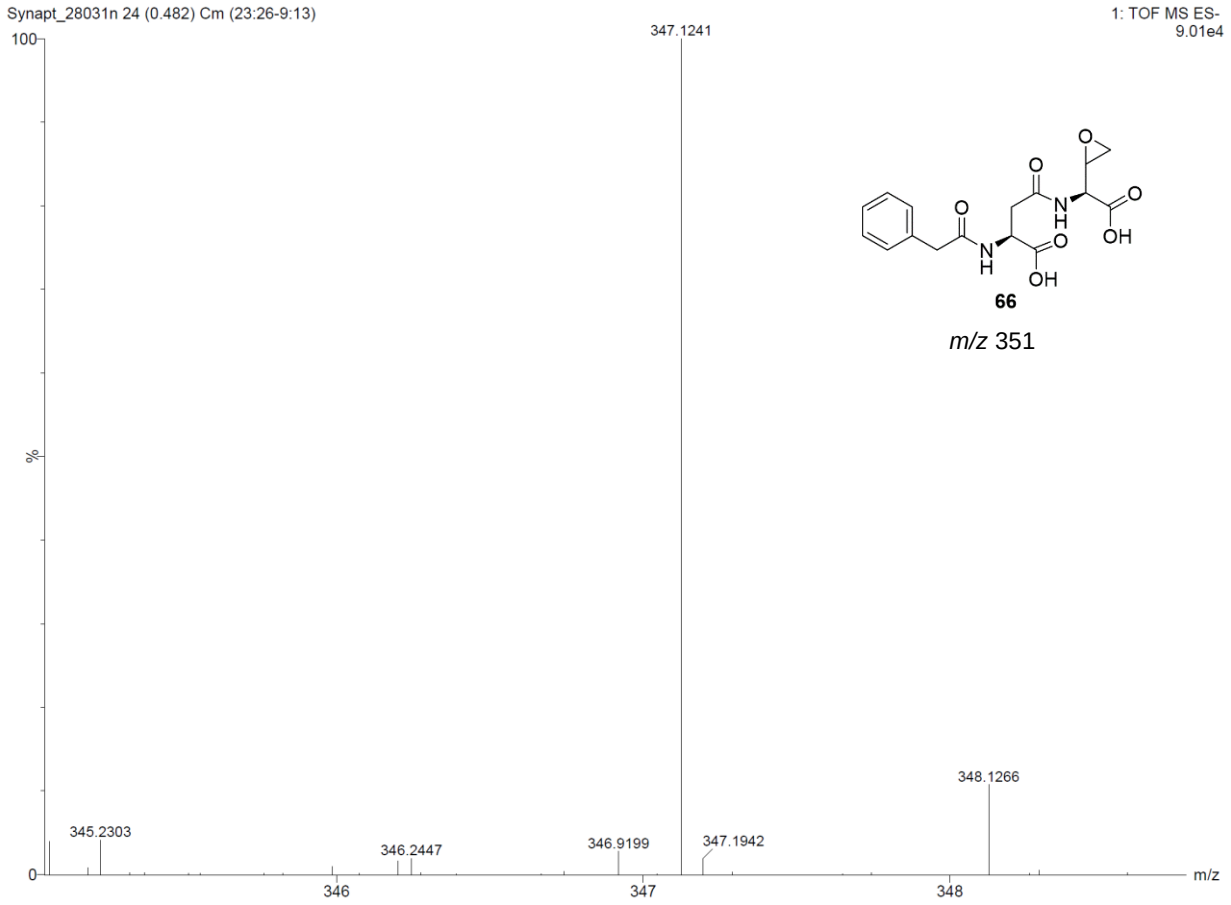

Figure 19: ESI-MS- results for compound **66**

The current results of the pathway followed to get to the desired target **66** were promising as the final compound calculated *m/z* was observed by ESI-MS reinforcing what the preliminary NMR data have suggested for the epoxide formation and the potential methyl ester deprotection. The minimal amount of product to run the last reaction steps was a limitation, thus optimization and scale up of the reactions performed should help achieve the isolation and characterization of the pure final compound **66** which we hope to do in the near future.

Conclusions and prospective work

The designed synthesis to get to the thioacid derivatives to MBLs has proven to be complex with challenges requiring a series of modifications to the initial target goal. The pathway followed to access **12** starting with L-cysteine was attempted, however the preliminary steps being unsuccessful forced us to step away from that route. The approach taken to circumvent the encountered issues consisted of using L-serine as the core structure of the dipeptide instead, followed by coupling to phenylglycine and introduction of the L- or D-VG methyl ester (**23a**, **23b**), previously synthesized as the anchor for the 3-membered ring. The first half of that synthesis pathway was accomplished successfully until arriving at the halogenated intermediate, which is difficult to handle and move forward with. As well, the alternative compound using phenylacetic acid instead of phenylglycine to get **13** showed similar problems. Thus, the pathway to obtained compound **14** was designed subsequently which did not include a halogenated intermediate. The route for the attempted synthesis of thioacid **62** and carboxylic acid **66** was the most successful. The attempted thioacid formation was unsuccessful, with a suspected cyclization of intermediate **61** to anhydride **64**, leading us to exclude the thioacid formation step in the synthetic route. The acid taken to the final steps did not pose major issues. However, the products obtained after epoxidation and methyl ester deprotection were not isolated pure. The analysis of the crude product by NMR and ES-HRMS for the epoxide suggest its formation, but the final synthetic step for the methyl ester deprotection was inconclusive. Thus, additional investigation of these last two

steps could give the final compound. From a synthetic standpoint, it would be interesting to synthesize the thiirane version of the target **66** to see if the possible inhibitory activity is altered in any way. More time would need to be allocated in order to find a way to obtain the thioacid compound **62** as it would be interesting to determine how the chelating effect changes the inhibition.

An optimization of the isolation of the epoxide intermediate and final compound **66** remain to be performed to collect pure molecule in order to use it for any inhibitory assessment. The preliminary test to be done to determine if the synthesized molecule has a potential for future application in antibiotic development is to subject the inhibitor to a with biochemical assay with nitrocefin, a chromogenic cephalosporin. Nitrocefin assay with various metallo enzymes could be done to measure enzyme inhibition indicated by a change of color from yellow to red which can be quantified by spectrometry techniques. Then, in hope of a successful outcome a minimum inhibitory concentration (MIC) assay would enable to determine the ability of bacteria strain growth to be inhibited.

Chapter III. Captopril-inspired compounds as covalent Inhibitors of metallo-β-lactamases

Introduction: Development of captopril and applications to enzyme inhibition

In the late 1960s and early 1970s, the collaborative work conducted by scientists associated with Bristol-Myers Squibb Pharmaceutical Research Institute (Princeton, NJ) on antihypertensive drug development led to the first efficient one, L-captopril (**67**, Figure 20) which was originally inspired by teprotide (**68**, Figure 20).[130]

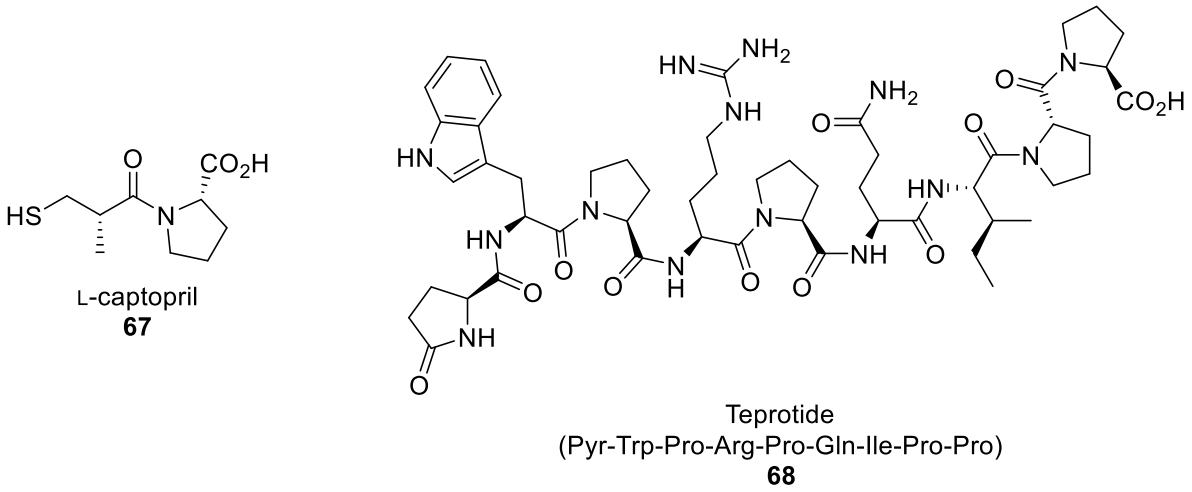

Figure 20: Structures of L-captopril **(67)** and teprotide **(68)**

Teprotide (**68,** Figure 20), a nonapeptide isolated from a Brazilian arrow head viper by Ferreira and co-worker[131] for application with carboxypeptidase enzymes, was found to be efficient at inhibiting angiotensin-converting enzymes (ACE) responsible for the conversion of angiotensin I to angiotensin II; angiotensin II being responsible for vasoconstriction and possible cardiovascular fatal issues (Scheme 23). The obstacle in applying the efficient finding of teprotide due to its lack of oral availability when administrated to patients and its cost, limited it's application as a practical treatment which inspired Bristol-Myers Squibb scientists to develop an alternative option.[132]

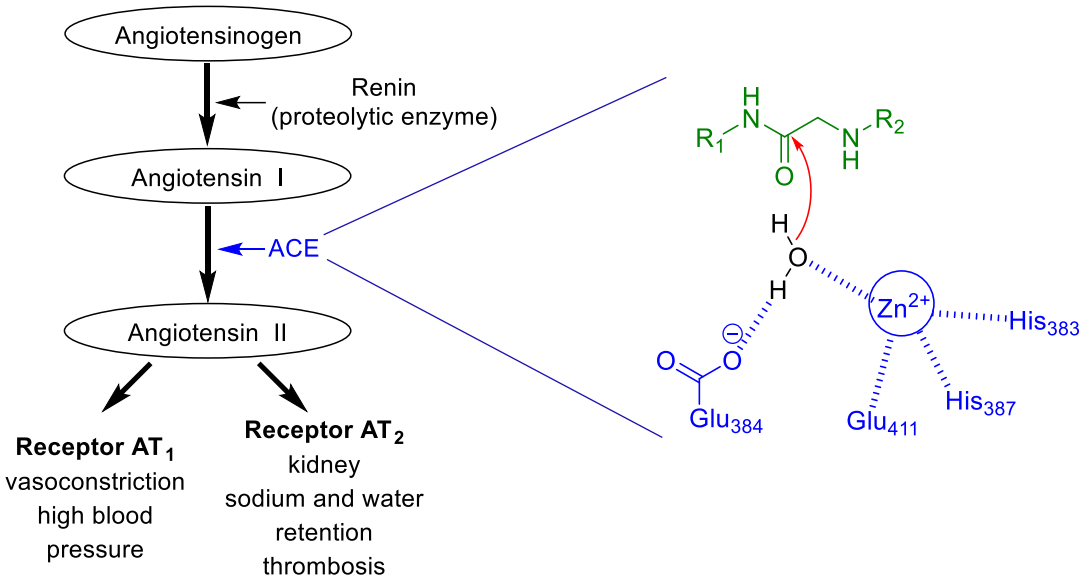

Scheme 23: Renin–angiotensin system involving ACE (left); enzyme-substrate interaction in ACE active site (right, blue) with a representative substrate (right, green)

D- and L-Captopril (Figure 20), (2*S*)-1-[(2*R*)-2-methyl-3-sulfanylpropanoyl] pyrrolidine-2-carboxylic acid and (2*S*)-1-[(2*S*)-2-methyl-3-sulfanylpropanoyl] pyrrolidine-2-carboxylic acid respectively, were obtained as a response to the search for a suitable angiotensin-converting-enzyme inhibitor which could be easily administrated orally rather than intravenously as it was necessary with teprotide.[133]

Ondetti, Rubin, and Cushman designed L-captopril through screening of a series of potential ACE inhibitors starting from the core structure benzylsuccinyl carboxylate (**69,** Figure 21), that Byer and Wolfenden had published several months earlier.[134] Ondetti and co-workers speculated that the role of the carboxylate group was a key factor in the observed inhibition of the bovine carboxypeptidase reported by Beyer due to the presence of a zinc cation lodged in the binding pocket of the enzyme.[134]

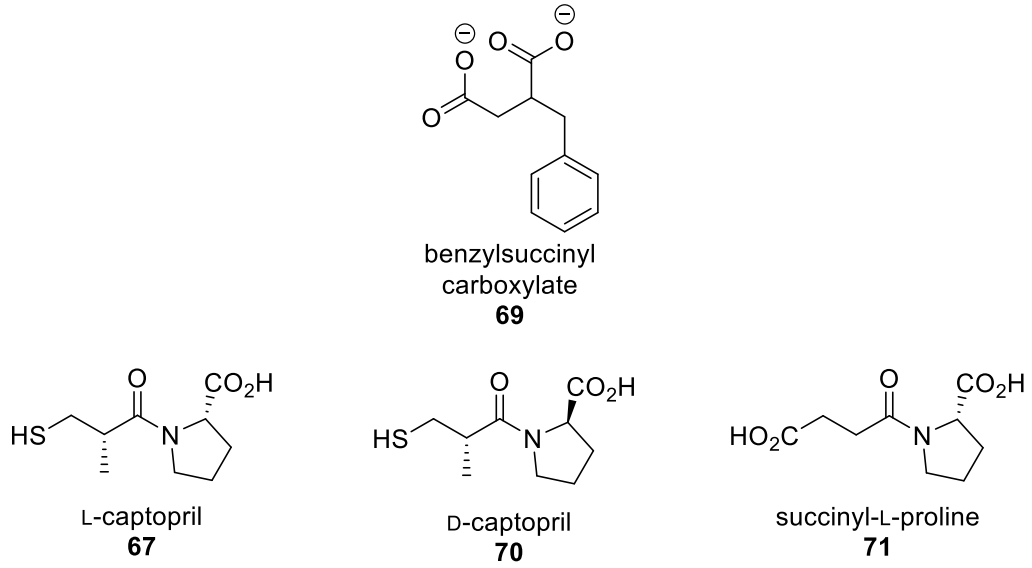

Figure 21: Structures of D- and L-captopril and succinyl-L-proline

In light of the observations from the investigation with benzylsuccinyl carboxylate as well as the study of the ACE binding site structure, they decided to modify functionalities of succinyl-L-proline (**71,** Figure 21) as their starting point for the development of an orally available compound mimicking teprotide (**68**, Figure 20). They observed a "mild" inhibitory activity with a 50% maximal inhibitory concentration (IC_{50}) of 135 μg/mL when succinyl-L-proline was tested against rabbit lung ACE. A series of derived molecules were tested through systematic screening against rabbit lung ACE which revealed successful inhibition of the latter with the synthesized captopril. Testing of D- (**70**) and L-captopril (**67**) resulted in an IC_{50} of 0.04 μg/mL and 0.005 μg/mL, respectively. The outcome showed a 10-fold decrease in IC_{50} for the L-isomer, thus demonstrating a greater inhibitory activity with L-captopril than D-captopril. This gave important insight on the type of binding interaction required between the enzyme and designed inhibitors. The key factor they found which enhanced the inhibitory activity of captopril was the incorporation of a sulfhydryl group which has the ability to coordinate to the zinc atom of the enzyme binding pocket.

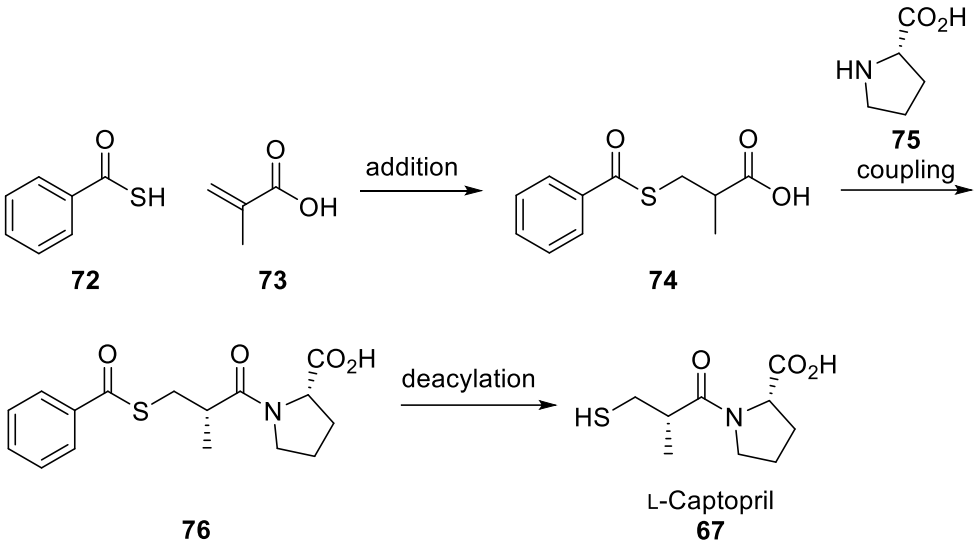

Scheme 24: Synthesis of L-captopril developed by Cushman and co-worker in 1977[132]

The synthetic approach of captopril reported by Cushman and co-worker (Scheme 24) begins with a Michael addition of thiobenzoic acid (**72**) to methacrylic acid (**73**) to obtain the mercapto-2-methylpropanoic acid intermediate **74**. Then, coupling of **74** to L-proline (**75**) provided a mixture of diastereomers of proline coupled product **76**. The two diastereomers were separated by crystallization of their diastereomeric dicyclohexylammonium salts. The deacylation of the resolved diastereomer provided the desired captopril compound (**67**).[132] Multiple synthetic pathways toward captopril have been designed since to circumvent the necessary classical resolution presented in the original synthesis. Notably, Shimazaki and colleagues had shortly thereafter developed a synthesis using an optically active starting material not leading to the formation of multiple diastereomers.[135]

Captopril has been for a long period of time successfully used in ACE enzyme inhibition. More recently, its use has been extended to applications other than inhibition of cardiovascular related enzymes, notably with metallo-β-lactamases. It is not surprising that captopril has drawn scientists' interest in the field of MBL inhibition due to one common structural feature with ACE. Indeed, both ACE[136] and MBL[137] are metalloproteinases, which rely on zinc cations for their

mechanism of action. Therefore, the insights provided by prior studies of ACE inhibition with L-captopril revealed a possibility of successful application to MBLs which have been difficult to inhibit and for which no inhibitor has been approved for clinical use thus far.

Captopril belongs to the thiol containing compound class, one of the 4 major classes known to inhibit MBLs including cyclic boronates,[69] sulfamoyl carboxylates,[70–72] and dicarboxylates presented in chapter 1 (Figure 11).[73,75] In the early 2000s, interesting computational and experimental studies of captopril with various MBL subclasses[138,139] revealed the ability of the compound to inhibit moderately the enzyme. Indeed, computational work presented by Jen Anthony and co-workers used *ab initio* Hartree Fork (HF) and density functional theory (DFT) calculations as well as molecular dynamics methods to study binding site interactions in a D-captopril-MBL complex with B1 MBL enzyme from *Bacteroides fragilis*. Although two possible binding modes are probable, monodentate through the thiolate S^- or bidentate through the proline carboxylate group, they focused on the monodentate binding through the thiol for this study (Figure 21, left). They reported that the calculated binding energies of D-captopril to MBL was higher, and thus has a greater affinity for the active site than the corresponding L-diastereomer through the binding of the thiolate to both zinc cations. Heinz Uwe and colleagues studied the interaction of D- and L-captopril with cadmium and cobalt-substituted MBLs, both mononuclear (B2 subclass) and binuclear (B1 subclass) enzymes, in place of the native zinc dependent MBL. Their investigation revealed that the D- and L-captopril molecules presented an inhibitory activity against both types of MBL subclasses tested. However, D-captopril has demonstrated a greater efficiency at inhibiting the cadmium substituted MBLs than L-captopril had, which is consistent with the computational results with the native zinc enzyme reported by Anthony *et al.* mentioned earlier.[138] It was noted that the D-diastereomer has a similar structural backbone as a hydrolyzed penicillin, which would explain the greater inhibition (**70** and **77**, Figure 22).

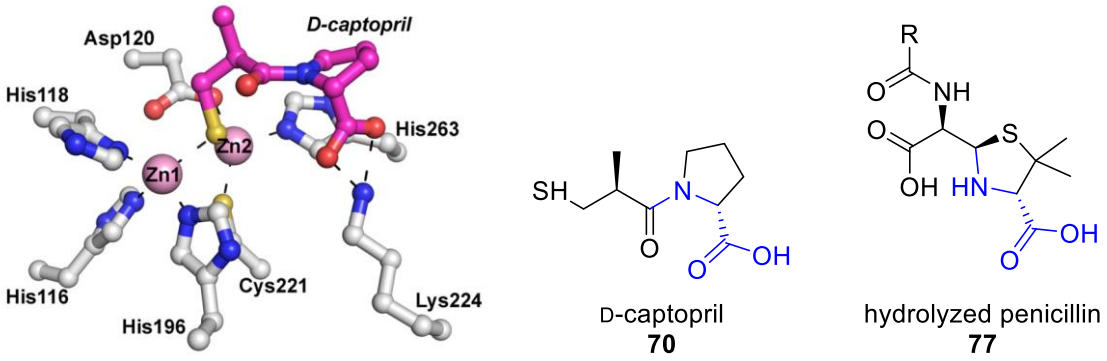

Figure 22: Crystal structure of the active site of IMP-1 (MBL B1 subclass) with D-captopril (pink);[66] comparative structure of D-captopril (**70**) with hydrolyzed penicillin (**77**)

Interestingly, the binding mode of captopril differs considerably for the inhibition of B1 and B2 subclasses, revealing that the development of efficient MBL inhibitors across all subclasses presents a real challenge. These results were also confirmed later by other in-depth crystallography studies of all stereoisomers of captopril[66] along with other thiol-containing compounds with all three classes: B1, B2, and B3 MBLs. These investigations looked at the required structural aspect to be taken into consideration for the development of a broad-spectrum MBL drug.[104]

These studies led to the emergence of a growing interest for the compound and structure-design studies with MBL for which a series of derivatives has been reported. Captopril contains two main fragments, the 3-mercapto-2-methylpropanoyl (**70**, blue portion, Figure 23) and the pyrrolidine moiety (**70**, green portion, Figure 23) for which modifications have been reported in attempts to improve the inhibitory efficiency against MBLs. Altering the chain by modifying the length between 1 to 3 carbons of the 3-mercapto-2-methylpropanoyl portion or removal of the methyl group at the 2 position led to a minimal decrease in the inhibition of the IMP-1 (B1 subclass MBL) as compared to L-captopril.[140] However, substitution of the methyl group by a phenyl ring (**78**, Figure 23) at the 2 position was shown to slightly improve the inhibitory effect against the MBL NDM-1.[140] The substitution to a thiol group[141] at that position, leading to a dithiol captopril

derivative, is not effective and suspected to change the proper conformational interaction in the binding pocket unlike what is observed with dicarboxylate MBL inhibitors.

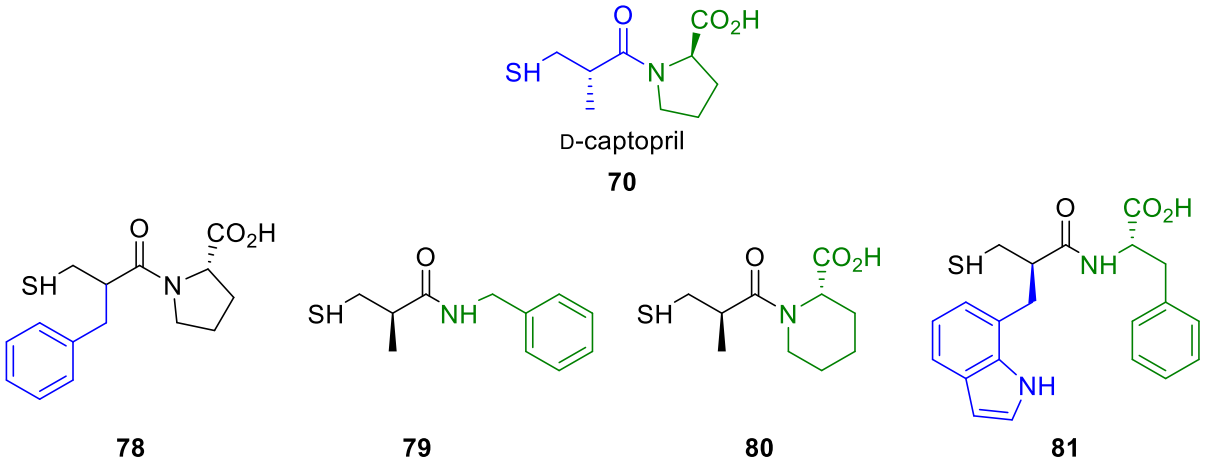

Figure 23: Selected captopril derivatives as efficient inhibitors of MBLs

Analogues with a modified pyrrolidine ring (Figure 23, green) have been investigated by multiple groups, notably Li and co-workers[142] who screened a series of derivatives against NDM-1. A benzylamide alternative to the L-proline was shown to improve the inhibition of the enzymes considerably (**79**, Figure 23).[142] When the ring is replaced by pipecolinic acid (**80**, Figure 23),[141] a 6-membered ring as opposed to the traditional 5-membered ring, a better inhibition is also demonstrated. The hydrophobic interaction initially observed between the proline ring and hydrophobic amino acid residues in the active site is enhanced which is thought to lead to the observed results. Additionally, alteration of both 3-mercapto-2-methylpropanoyl and pyrrolidine has also led to relevant discoveries with compounds of high potential as MBL inhibitors. One compound reported by Meng and co-workers (**81**, Figure 23) containing an indole in place of a methyl group and a benzyl group rather that the 5-membered proline proved to inhibit efficiently the NDM-1 enzyme.[143] For the compounds discussed above, in some occasions they were tested against other B1 MBL enzymes such as VIM-1 and IMP-1 without showing improvement of the inhibition. This shows that some work remains to be done in this area with inspired captopril derivatives as it is shown by the increasing studies reported.

Research project goals: Covalent inhibition of MBLs using new captopril derivatives containing a thiirane or epoxide functional group

The work to be discussed in the following section emerged as a result of the observations of the capability of captopril and its current derivatives as potential MBL enzymes inhibitors. Although the recent literature has shown promise in this area, there is more to explore when it comes to MBL inhibition with captopril derivatives as shown by many challenges discussed above, notably the inhibition of multiple MBLs with a single molecule. In the aim to address these issues, we decided to apply the strategy of enzyme covalent modification using a strained 3-membered ring, explored for the development of open lactam analogue in chapter 2, to design captopril inhibitors for MBLs. It was decided to keep the pyrrolidine moiety (D-captopril) unaltered while the 3-mercapto-2-methylpropanoyl would be modified to incorporate a 3-membered ring. The synthesis of 4 captopril derivatives was investigated in this project (Figure 24).

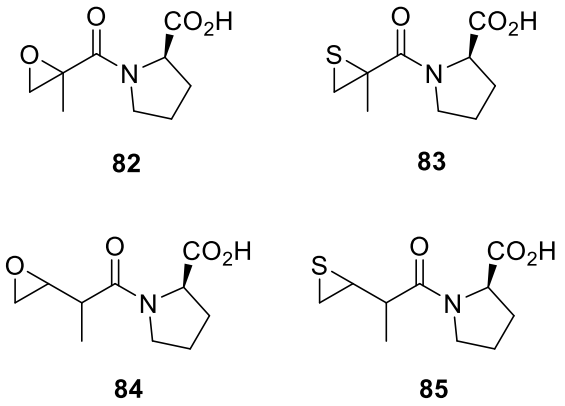

Figure 24: Structures of the newly designed captopril inhibitors (**82**, **83**, **84**) and reported epoxide compound (**85**) for the study of MBLs inhibition.

We designed and synthesized captopril derivatives with unaltered pyrrolidine moieties but with a modified chain length in addition to the strained ring. The epoxide **82** and thiirane **83** have an ethanoyl chain leading to no carbon spacer between the methyl group and the strained ring unlike **84** and **85**. This was done to determine if the proximity of the 3-membered ring to the proline ring would impact the possible inhibition of MBLs. Upon developing potential inhibitors, it was

discovered that one epoxide derivative of captopril (**84**, Figure 23), the only one to this date known to the best of our knowledge, was reported in the literature by Choo and co-workers in 1998 for application to ACE inhibition.[144] In these studies, a series of 22 epoxy amides, esters, and ketones were investigated. In the case of the epoxy amides, multiple amino acids were coupled among which proline was a candidate leading to the epoxy-captopril derivative **84**.[144] However, this compound was not yet been studied for the inhibition of MBLs, so it was of interest to determine its eventual inhibitory ability. Furthermore, we were interested in synthesizing a thiirane version, compound **85**, which has never been synthesized in the past, in order to study the effect of the sulfur atom in relation to the binding interaction within the active site as compared to the oxygen analogue.

Here again, the presence of a conserved amino acid such as aspartic acid in the MBL binding pocket is key to the strategy of the captopril derivatives we aim to develop. Additionally, lysine or glutamic acid residues identified in the active site of crystal structures of clinically relevant MBLs (NDM-1,[137] VIM-1,[145] IMP-1,[146] BcII,[147] CcrA[148]) might also play a central role for the strategy to be implemented. The type and position of the amino acid residues located in the binding pocket of MBL, particularly in the B1 subclass, gave insight on the possible interactions of the developed inhibitors in this project. It is thought that the captopril-inspired derivatives would interact through the negatively charged carboxylate group at physiological pH in a manner where it is coordinating to the two zinc atoms in a bidentate mode. This would allow for a possible nucleophilic attack of the 3-membered ring for and formation of a covalent bond.

Proposed mechanism of action for the captopril derivatives containing a strained 3-membered ring for covalent inhibition

If the predicted interactions mentioned previously occur, it would allow for a proper insertion of the derivative **86** (Scheme 25) in an MBL active site with the alkyl side chain containing the 3-membered ring accessible to residues such as aspartic acid, glutamic acid, or lysine. Lysine being protonated to an ammonium at physiological pH, this might hydrogen bonding with the epoxide or thiirane and help position it such that the conserved aspartic acid residue could therefore perform a direct ring opening of the strained ring through nucleophilic attack forming a covalently bond inhibitor (**87**). A glutamic acid residue, which is found in proximity to the metal center in some MBL binding sites, might also ring open the thiirane ring through nucleophilic attack since it is negatively charged at pH 7.4. Alternatively, the covalent bond formation can take place indirectly via deprotonation of the α-proton of the mercapto chain (**86**) leading to the ring opening and the double bond formed in the intermediate **88** subsequently attacked by the nucleophilic aspartate residue leading to a covalently bond inhibitor (**89**) (Scheme 25).

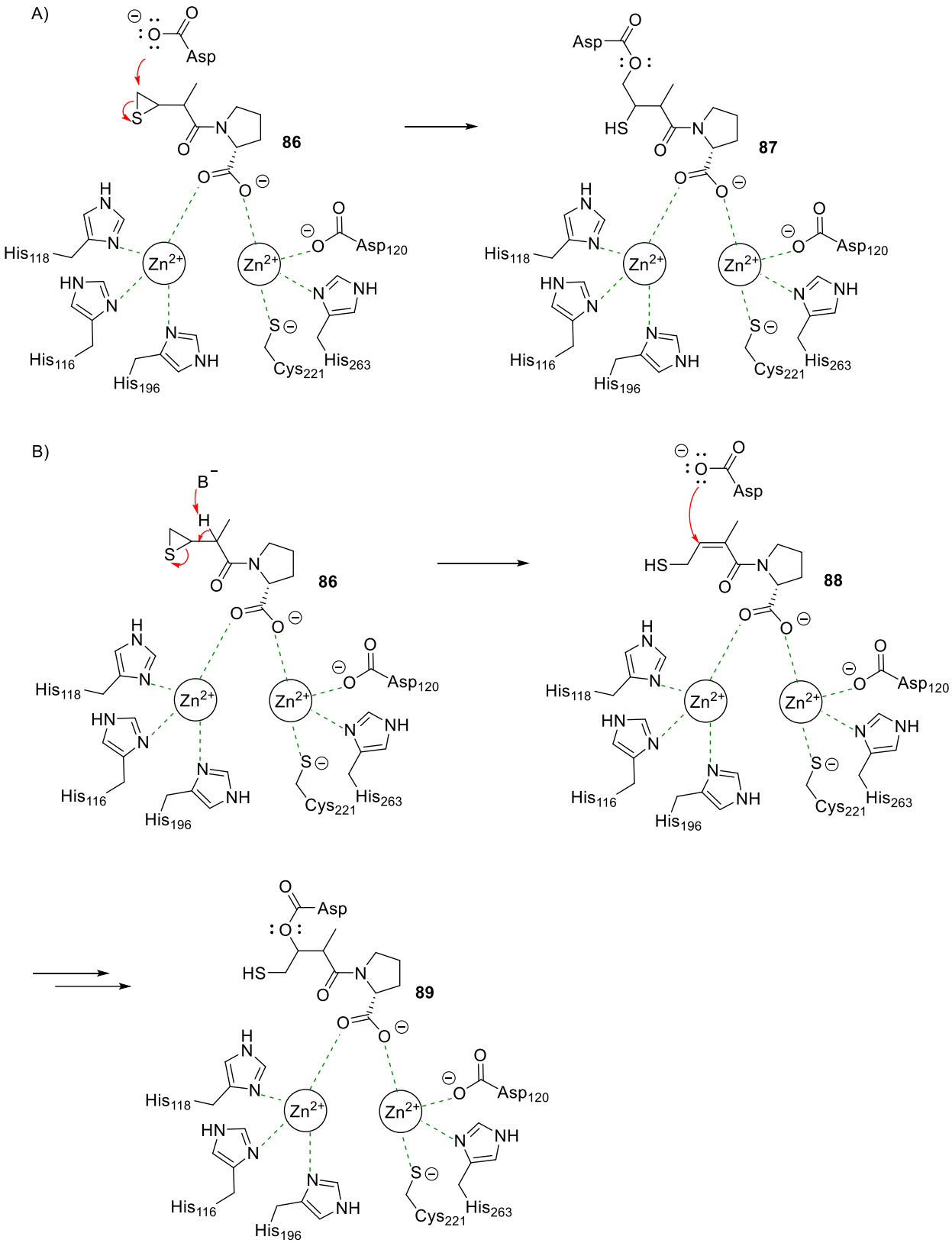

Scheme 25: Possible mechanisms of action for the designed inhibitors through direct ring opening (A) or indirect ring opening (B)

Results and discussion

Synthesis of 1-(2-methyloxirane-2-carbonyl)pyrrolidine-2-carboxylic acid (82) and 1-(2-methylthiirane-2-carbonyl)pyrrolidine-2-carboxylic acid (83)

The synthesis of epoxide **82** and thiirane **83** as D-captopril analogues started from commercially available 2-methylprop-2-enoic acid **(90)** and is summarized in Scheme 25. Following a modified procedure reported by Choo and co-workers,[144] the proline coupled intermediate **91** was formed via acylation of D-proline ethyl ester with 2-methylprop-2-enoyl chloride **(90)**, formed in situ from **90** (Scheme 26).

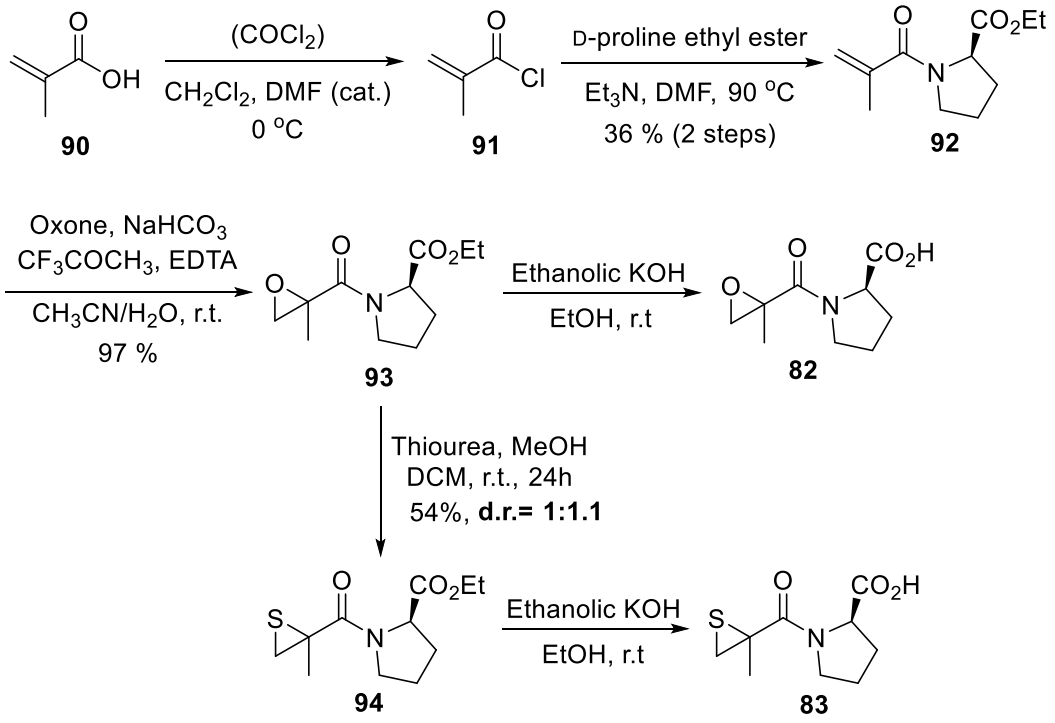

Scheme 26: Optimized conditions for the synthesis of captopril derivatives **82** and **83**

Entry	Solvent	Temperature (° C)	Time (h)	Yield (%)
1	Dichloromethane	r.t.	18	7
2	Dichloromethane	35	28	8
3	Dichloromethane	45	12	28
4	Acetonitrile	60	48	23
5	DMF	90	22	36

Table 4: Reaction conditions surveyed for the substitution step in the formation of **92**

The original reaction conditions for the substitution step used dichloromethane as the solvent of choice at 0 °C, providing **92** in a low yield of 7% which was attributed to the low solubility of D-proline ethyl ester. Optimization of the reaction conditions afforded the desired coupled product in a 36% yield (p.156 ^{1}H NMR, p.157 ^{13}C NMR) which required at 90 °C with DMF as the solvent (Table 4). Direct coupling conditions, which would have shortened the synthetic pathway, were also investigated using HATU[149] as the coupling agent without any desired product observed.

The NMR spectrum of compound **92** suggested the presence of rotamers by the presence of two sets of doublets at 5.3 and 5.1 ppm corresponding to the vinylic methylene group (Figure 24). This was confirmed by variable temperature (VT) NMR analysis showing coalescence of the two sets of doublets. Thus, demonstrating that the slow exchange rate due to the rotational barrier around the C-N bond transition toward a fast-exchange rate as the temperature increases enabling signal averaging and coalescence of the peaks (Figure 25).

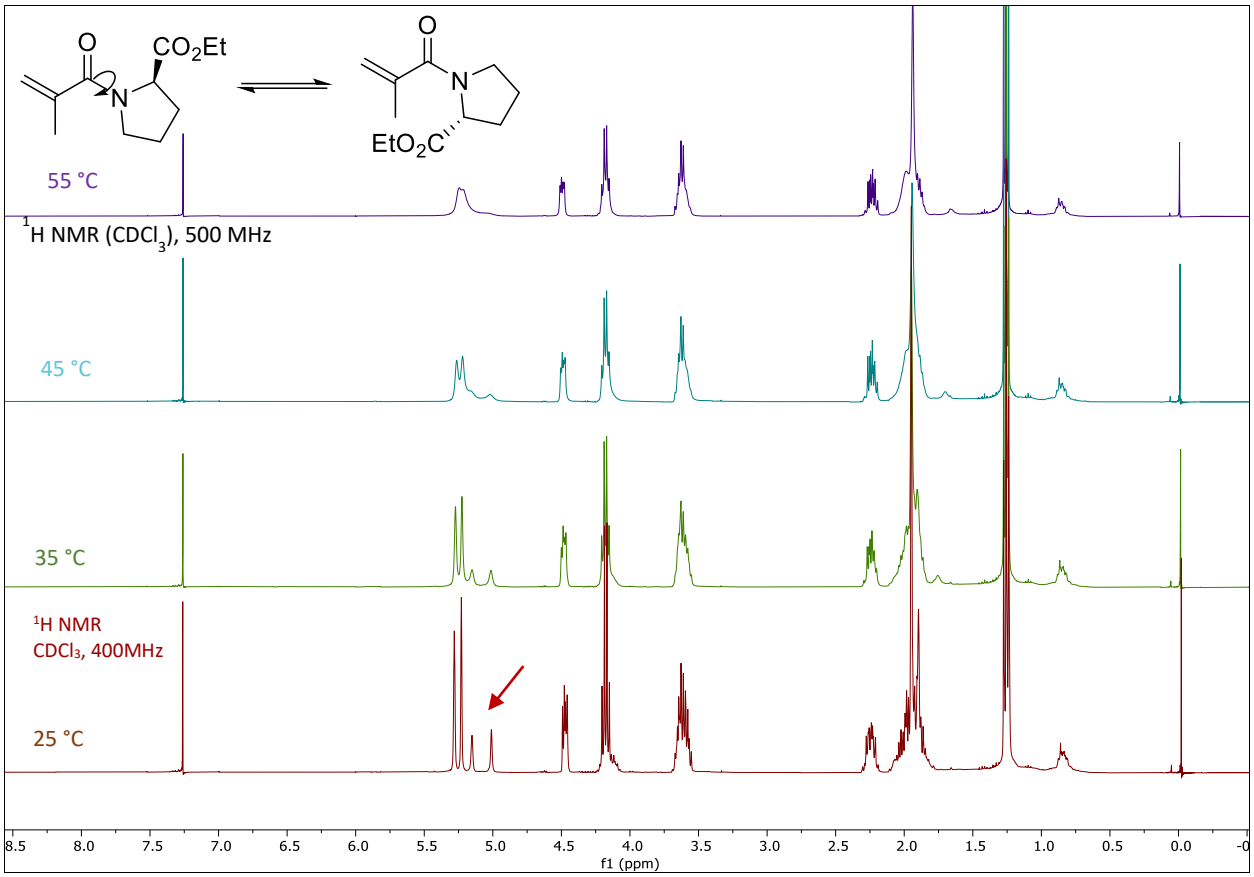

Figure 25: ^{1}H NMR spectra of the variable temperature analysis of compound **92**

After the unsaturated amide **92** was synthesized, it was subjected to various oxidation conditions in order to convert the alkene to the desired ethyl ester-protected epoxide **93** (Table 4). Initially, standard conditions using a common peracid, *m*-chloroperoxybenzoic acid (mCPBA) were explored, however, this only provided a low 20% starting material conversion to the desired product as observed by ^{1}H NMR. It was decided to apply more reactive reagents for the epoxidation including H_2O_2,[127] *t*-BuOOH,[150] dioxirane derivatives,[128,144] as well as NiOAc with NaOH.[151] The most efficient epoxidation conditions found for the formation of **93** were with 3-methyl-3-fluoromethyldioxirane which easily afforded the epoxide in over 90% yield confirmed by the absence of the vinylic protons peaks in the 5.0-5.3 ppm region and presence of the characteristic methylene proton of the epoxide at 2.4-2.8 ppm in the ^{1}H NMR (p.157 ^{1}H NMR, p.158 ^{13}C NMR, p.159 HRMS).

Entry	Oxidative Reagents	Solvent	Temperature	Time	%Yield
1	mCPBA	CH_2Cl_2	0 °C	48h	20*
2	H_2O_2/NaOH	CH_3OH	0 °C to r.t.	20h	NR
3	*t*-BuOOH /KMHDS	THF	-15 °C	2h	NR
4	$Ni(OAc)_2$/NaOH/ cold bleach	CH_2Cl_2	0 °C	12h	0 to 20*
5	$Ni(OAc)_2$/cold bleach	CH_2Cl_2	0 °C	12h	NR
6	Oxone/acetone	H_2O	r.t.	24h	0 to 50*
7	Oxone/trifluoroacetone	H_2O	r.t.	2h	97

*Percent conversion determined by ^{1}H NMR; NR= no reaction with starting material fully or partially recovered

Table 5: Summary of the epoxidation conditions used for the synthesis of **92**

In order to obtain the final desired compound **82**, cleavage of the ethyl ester protecting group by hydrolysis[152] with ethanolic KOH was performed. The ^{1}H NMR spectrum (p.160 ^{1}H NMR) of the product collected suggested that the deprotection occurred, with the ethyl ester peaks at 1.2 ppm (-CH_3) and 4.1 (-CH_3) ppm were not present in addition to the broad singlet at 9.56 ppm, corresponding to the carboxylic hydroxyl proton. The epoxide was stable under the hydrolysis conditions, giving the final desired compound **82** with the presence of a side product, observed in the ^{1}H NMR spectrum of the crude product. However, the removal of the side product attempted by columns chromatography was unsuccessful (Figure 26, top) with one side product co-eluting. The ^{13}C NMR of the material collected after the column show the absence of the ethyl ester group at 14 ppm and 61 ppm for the methylene and methyl proton respectively The subsequent attempt for purification by preparative TLC seemed to lead to a ring opening and formation of the

corresponding diol **95** as seen by the downshift of the methylene protons from 2.4-2.8 ppm to 3.9-4.1 ppm (Figure 26, bottom).

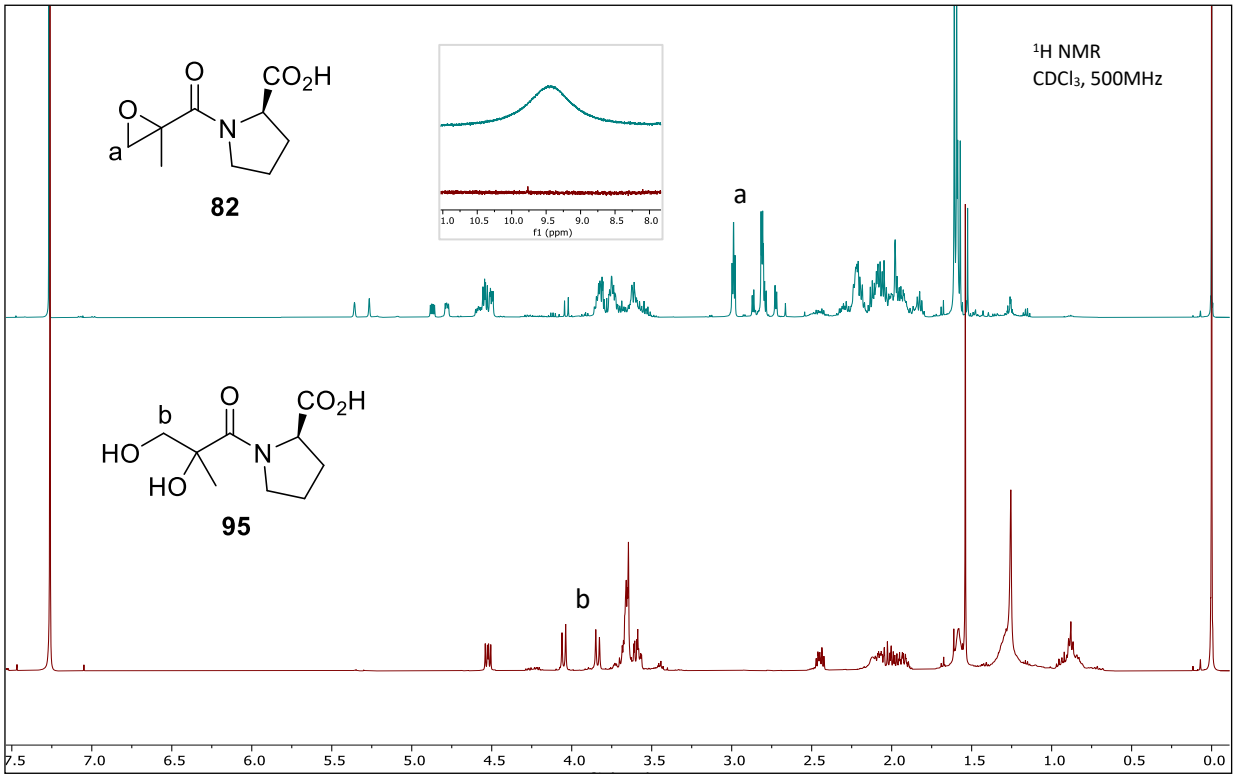

Figure 26: ^{1}H NMR spectra for the impure product after column (**82**, top, blue) and purified product collected (**95**, bottom, red) in the attempted isolation of compound **82**

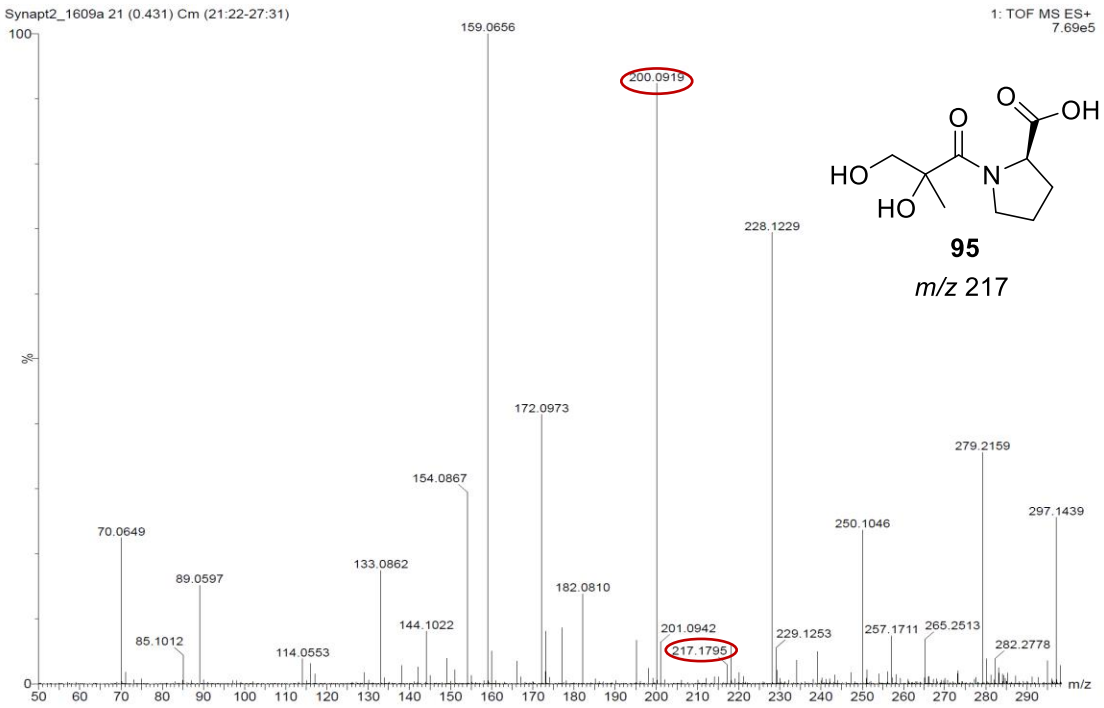

Figure 27: HRMS-(ES+) spectrum of the suspected diol **95**

This was further confirmed by the results of the ESI-MS of the purified compound collected (Figure 27) which showed the presence of peaks at m/z 217.1785 representative of the diol **95** with a calculated *m/z* 217.10 as well as the ionized fragment with loss of water with a m/z 200.0919. In light of these results, it is promising to see that the ethyl ester deprotection can be achieved under these conditions, however a optimization of the column chromatography purification is required to isolate the pure product **82** as it is suspected that preparative TLC could be the main issue for the ring opening.

The sulfur analogue **83** was obtain by converting the ethyl ester protected epoxide to a thiirane which occurs through a ring opening with thiourea[153] as the nucleophile and subsequently forming a stable intermediate which cyclizes to form the thiirane ring. The reaction led to the observation of separable diastereomers as a 1:1 ratio, based on isolated yield, by column chromatography which was not the case for the epoxide analogue. The two diastereomers were obtained in a moderate 54% yield (p. 161 ^{1}H NMR, p.162 ^{13}C NMR, p.163 HRMS). The reaction for the removal of the acid protecting group showed removal cleavage of the ethyl ester with

presence of a side product as observed in the ^{1}H NMR spectrum of the crude product. Thus, a more suitable purification technique than the one used for the epoxide version is to be investigated to isolate the clean thiirane compound **83**. In addition, the ES-MS of the crude sample collected of **83** confirmed the presence of the expected molecular ion *m/z* 215.06 found at *m/z* 216.0687 for $[M+H]^{+}$.

The overall steps for the formation of **82** and **83** are promising for future scale up attempts of the synthesis, with the exception of the final step of deprotection for which a better purification procedure is required. However, due to time constraints this was not investigated further. The final step in the synthesis of both products could eventually be optimized by exploring alternative deprotection conditions which would prevent the formation of the side product which has yet to be identified. This would ultimately allow a cleaner reaction and might not require further manipulation of the product through purification to help obtain **82** and **83** in higher yields.

Synthesis of 1-[2-(oxiran-2yl)propanoyl] pyrrolidine-2-carboxylic acid (84) and 1-[2-(thiirane-2yl)propanoyl] pyrrolidine-2-carboxylic acid (85)

The investigations for the optimization of the synthetic pathway to **82** and **83** provided useful insight to tackle the synthesis of 1-[2-(oxirane-2yl)propanoyl] pyrrolidine-2-carboylic acid (**84**) and 1-[2-(thiirane-2yl)propanoyl] pyrrolidine-2-carboylic acid (**85**). Here, a racemic mixture of the starting 2-methyl-3-butanoic acid (**96**), as opposed to the enantiomerically pure compound, was used for cost-effectiveness purposes of the synthetic pathway. It was planned to separate the diastereomers formed as we move through the synthesis if possible (Scheme 27).

The synthesis began with the amine coupling of compound **96** to D-proline ethyl ester using the previously optimized two-step reaction conditions involving the formation of the acyl chloride **97** formed from the carboxylic acid **96** and subsequent acylation reaction of to get the coupling coupled product **98** in 31% yield over two steps (Scheme 27).

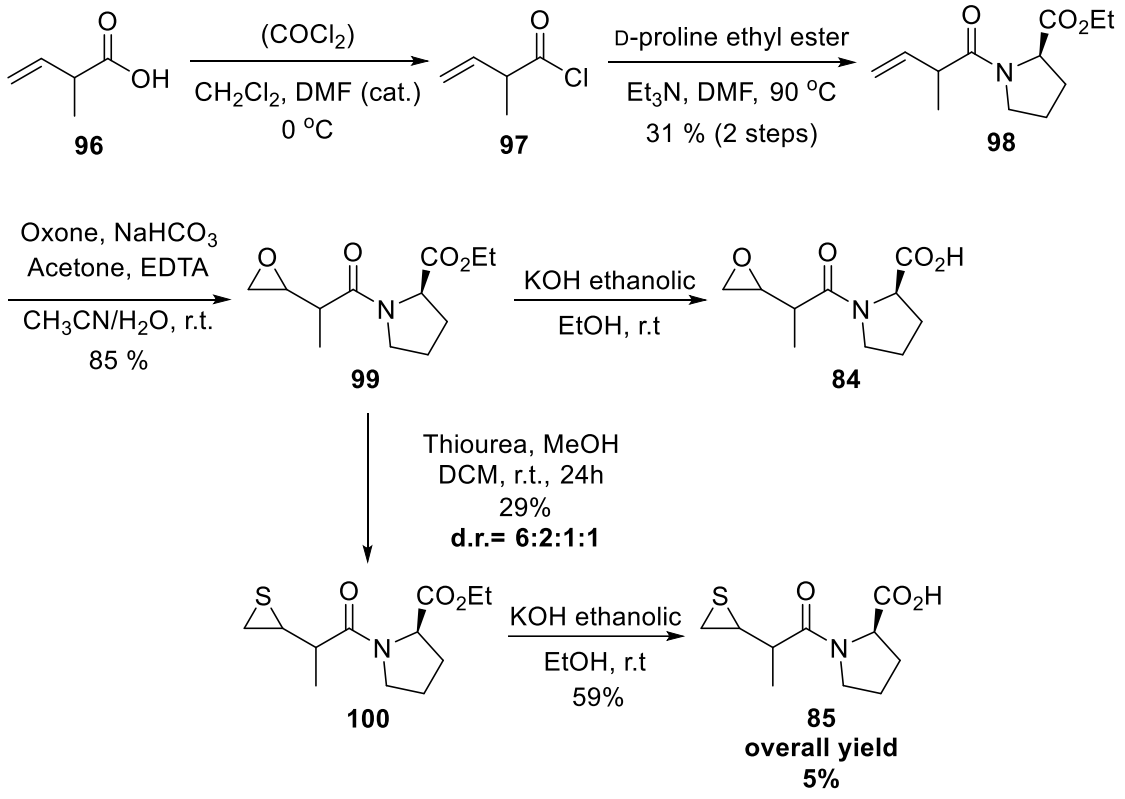

Scheme 27: Synthesis of compounds **84** and **85** from 2-methyl-3-butanoic acid (**96**)

Subsequently, the formation of the epoxide **98** using dimethyldioxirane formed *in situ* showed evidence of multiple diastereomers by ^{1}H NMR (p.169 ^{1}H NMR, p.170 ^{13}C NMR, p. 171 HRMS), with peak broadening and duplication observed. This was noticeable at 2.4 to 2.8 ppm and 4.2 to 4.6 ppm representative of the methylene epoxy protons (H_a) and the methine proton at the proline stereogenic center, respectively (Figure 28). Although observable by NMR, they were not separable using chromatography techniques and the mixture of diastereomers was used as is in the following steps.

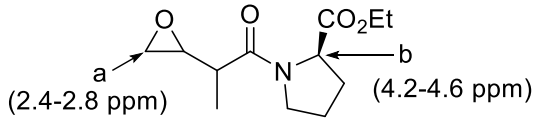

Figure 28: Epoxide **99** and observable protons in ^{1}H NMR giving evidence of the formation of additional diastereomers

The hydrolysis of the ethyl ester in **99** with ethanolic KOH gave unconclusive results with the observation of a complex mixture by ^{1}H NMR. The data analysis by ESI-MS of the collected material of reaction suggested the presence of the corresponding molecular ion of the deprotect compound *m/z* 213.10 and found for $[M+H]^{+}$ at *m/z* 214.1070. Several attempts to get a clean reaction and facilitate the isolation of the desired epoxide **84** led to similar results and an alternative method required.

The conversion of the ethyl ester epoxide **99** to the thiirane analogue was performed with thiourea to afford **100** in 38% yield. This was followed by hydrolysis of the ethyl ester to provide the final target compound **85** in 59% yield (p.179 ^{1}H NMR, p.180 ^{13}C NMR, p.181 HRMS). The ^{1}H NMR and ^{13}C NMR analysis of the two collected product fractions suggested that a set of 3 diastereomers were not separable while one diastereomer seemed to be found in which was not clean and presented impurities. The ^{1}H NMR showed two distinguishable proton peaks at the 4.2-4.6 ppm region (H_b, Figure 27) which suggested only two diastereomers, however the ^{13}C NMR was consistent with the presence of three diastereomers as each carbon peaks were present in set of 3. At this point, additional data analysis such as NOE and 2D NMR experiments are to be run in attempt to assign the stereochemistry of the diastereomers. The overall synthetic pathway was achieved for thiirane analogues compound **85** in 5% yield, while the last step for the deprotection of the epoxide needs to be optimized in order to get more accurate data.

Conclusions and prospective work

The syntheses of both series of analogues were overall successful, with the synthesis of the longer chain compounds **85** achieved completely while some investigation for the deprotection of **99** to obtain the final product **84** is needed. Regarding compound **82** and **83**, the final steps have been shown to be promising with the evidence of their formation, however, milder deprotection conditions or a better suited purification method is required to isolate them as pure products.

Additionally, the experimental spectral data obtained for the final compounds were in good agreement with the predicted NMR spectra calculated using DFT calculation. The next step in this project would be the determination of the inhibitory potential of **82**, **83**, **84**, and **85** against most prevalent MBLs such as NDM-1 once all derivatives are isolated. Some prospective work would involve the modification of the pyrrolidine ring structure as it has been demonstrated in the literature that more hydrophobic moieties could help enhance the interaction in the binding site, as mentioned earlier. This could include a phenyl or indole ring which could potentially interact with hydrophobic residues in the MBL binding site such as phenylalanine or tryptophan through pi-pi stacking. As well, it would be interesting to determine if the conversion of the carboxylic acid on the pyrrolidine ring to a thioacid would affect the binding affinity and increase or decrease the inhibitory effect.

Chapter IV. Experimental

General procedures

Solvents

Anhydrous solvents, diethyl ether, dichloromethane, and tetrahydrofuran (THF), were obtained from an innovative Technology, Inc. Solvent Delivery System before use and stored over 4 Å molecular sieves. THF was purified further by distillation over sodium and benzophenone under an atmosphere of dry nitrogen prior to use. Other solvents, hexanes, ethyl acetate, trimethylbenzene, methanol, ethanol were purchased as ACS grade from Pharmco (Brookfield, CT), VWR (Bridgeport, NJ), MilliporeSigma Chemical Company (St. Louis,MO), and Alfa Aesar (Haverhill, MA), and used without further purifications unless otherwise stated. Deionized water was obtained from the university water system.

Reagents and reaction conditions

All reagents were and purchased from Acros Organics Ltd. (Hampton, NH), Alfa-Aesar Chemicals. (Haverhill, MA), AK Scientific Inc. (Union City, CA), Santa Cruz Biotechnology, Inc (Dallas, TX) Ambeed Inc. (Arlington Hts, IL), Thermo Fisher Scientific (Waltham, MA), MilliporeSigma Chemical Company (St. Louis, MO), Oakwood Products, Inc. (Estill, SC), or TCI American Chemicals. (Portland, OR). They were all American Chemical Society (ACS) grade and used without further purification unless otherwise stated. All processes involving air or moisture sensitive reactants and/or requiring anhydrous conditions were performed under a positive pressure of nitrogen using oven or flame-dried glassware. The removal of solvent *in vacuo* refers to evaporation under reduced pressure below or at 40 °C using a Büchi rotary evaporator followed by evacuation (< 0.1 mm Hg) to a constant sample mass. Unless otherwise specified, solutions of NH_4Cl, $NaHCO_3$, HCl, citric acid, LiOH, and $Na_2S_2O_3$ refer to aqueous solutions. Brine refers to a saturated aqueous solution of NaCl.

Purification techniques

Unless stated otherwise, all reactions and fractions from column chromatography were monitored by thin layer chromatography (TLC) using glass-backed plates (1.5 x 5 cm) pre-coated (0.25 mm) with silica gel containing a UV fluorescent indicator (normal silica gel, 60 F254; reverse-phase, C18 SiO_2 F254) from Sorbent Technologies, Inc. (Norcross, GA). Compounds were visualized by exposing the plates to UV light, or by dipping the plates in solutions of potassium permanganate, *p*-anisaldehyde, or phosphomolybdic acid/ethanol (5:95) followed by heating on a hot plate. Flash chromatography was performed using grade 60 silica gel (Rose Scientific, 230-400 mesh) or with a Teledyne Isco CombiFlash Rf 200 purification system. Purification using CombiFlash used RediSep® silica gel columns (20-70 μm particle size). Mobile phases were prepared per use.

Instrumentation for compound characterization

Nuclear Magnetic Resonance (NMR) spectra were measured on a Varian Mercury Plus 400 FT-NMR operating at 400 MHz for ^{1}H NMR and 100 MHz for ^{13}C NMR spectroscopy, a Bruker 500 FT-NMR operating at 500 MHz ^{1}H and 126 MHz for ^{13}C NMR spectroscopy, or a Bruker 700 FT-NMR operating at 700 MHz ^{1}H and 176 MHz for ^{13}C spectroscopy. Deuterated solvents for NMR analysis were purchased from Cambridge Isotope Laboratory and stored over 4 Å molecular sieves. All ^{1}H NMR chemical shifts are reported in parts per million (ppm) downfield relative to tetramethylsilane (TMS) using the residual proton resonance of solvents as the reference: $CDCl_3$, δ 7.24; CD_3OD, δ 3.30; D_2O, δ 4.79. All ^{13}C NMR chemical shifts are reported relative to: $CDCl_3$, δ 77.0; CD_3OD, δ 49.0. Additional assignments were made using pulsed field gradient versions of shift correlation spectroscopy (gCOSY), heteronuclear single quantum coherence (gHSQC), and heteronuclear multiple quantum coherence spectroscopy (gHMQC). ^{1}H NMR data are reported in the following order: multiplicity (app, apparent, s, singlet; d, doublet; t, triplet; q, quartet; quin, quintet; and m, multiplet), number of protons, coupling constant (*J*) in Hertz (Hz), and assignment.

When appropriate, the multiplicity is preceded by br, indicating that the signal was broad. The coupling constants reported are within an error range of 0.2-0.4 Hz and have been rounded to the nearest 0.1 Hz. All literature compounds had ^{1}H NMR, ^{13}C NMR, and mass spectra consistent with the assigned structures. The temperature for the variable temperature study were calibrated using a varian model L900 temperature controller.

Mass spectra (MS) were performed at the University of Illinois and recorded on a Micromass 70-VSE high resolution mass spectrometer (HRMS), using a Micromass ZabSpec Hybrid Sector-TOF positive or negative mode electrospray ionization (ESI).

Detailed Experimental Section Chapter II

Cbz-L-methionine methyl ester hydrochloride (19b)*

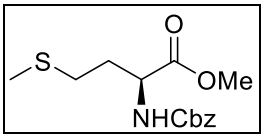

This compound was prepared following by a modification of the procedure by Afzali-Ardakani *et al.*[108] L-Methionine methyl ester hydrochloride (**18b**) (2.00 g, 10.00 mmol) was dissolved in ethyl acetate (50 mL), then $KHCO_3$ (5.01 g, 0.050 mmol) in water (50.0 mL) was added at 0 °C, followed by dropwise addition of Cbz-chloride (2.2 mL, 11 mmol) over 30 mins. The reaction mixture was stirred for 3.5h . The organic layer was separated, washed with HCl (0.5 M, 4 x 5 mL) and water (3 x 5 mL), dried (Na_2SO_4), and the solvent evaporated *in vacuo*. The product was purified by column chromatography (SiO_2, hexanes/ethyl acetate, 3:1) to yield the protected compound **19b** as an off-white solid (2.6252 g, 88%): R_f= 0.48 (hexanes/ ethyl acetate, 3:1); ^{1}H NMR (400 MHz, $CDCl_3$) δ 7.41–7.27 (m, 5H, ArH), 5.40 (br d, 1H, *J* = 8.2 Hz, NH), 5.11 (s, 2H, $PhCH_2$), 4.51 (td, 1H, *J* = 7.9, 5.0 Hz, H-2), 3.76 (s, 3H, CO_2CH_3), 2.53 (app t, 2H, *J* = 6.8, 7.4 Hz, $CH_3S\underline{CH_2}CH_2$), 2.23-2.10 (m, 1H, $CH_3SCH_2C\underline{H_a}H_b$), 2.09 (s, 3H, CH_3S), 2.06-1.90 (m, 1H, $CH_3SCH_2CH_a\underline{H_b}$); ^{13}C NMR (126 MHz, $CDCl_3$) δ 172.5, 155.9, 136.2, 128.6, 128.2, 128.1, 67.1, 53.1, 52.5, 32.0, 29.9, 15.5.

Cbz-L-Methionine methyl ester sulfoxide (20b)*

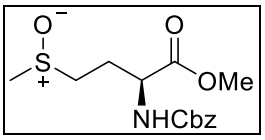

This compound was prepared following by a modification of the procedure by Afzali-Ardakani *et al.*[108] Cbz-L-methionine methyl ester hydrochloride (**19b**) (6.15 g, 20.69 mmol) was dissolved in methanol (64.0 mL) to which was added a solution of sodium periodate (4.66 g, 21.79 mmol) in

water (25.0 mL) at 0 °C. The reaction mixture was allowed to warm to r.t. and stirred vigorously for 2.5 h. It was then filtered through a pad of celite and the solvent was partially evaporated under vacuum. The resulting concentrate was extracted with chloroform (4 x 15 mL), and the combined organic layers were washed with brine (2 x 30 mL), dried (Na_2SO_4), and concentrated *in vacuo*. The crude product was purified by column chromatography (SiO_2, CH_2Cl_2/MeOH, 95:5) to give the product **20b** as a clear oil (6.19 g, 96%): R_f= 0.41 (CH_2Cl_2/MeOH, 95:5), ^{1}H NMR (400 MHz, $CDCl_3$) δ 7.41-7.29 (m, 5H, ArH), 5.61 (dd, 1H, *J* = 7.8, 8.0 Hz, NH), 5.11 (s, 2H, $PhCH_2$), 4.57-4.40 (m, 1H, H-2), 3.77 (s, 3H, CO_2CH_3), 2.86-2.62 (m, 2H, $CH_3S\underline{CH_2}CH_2$), 2.56 (d, 3H, *J* = 2.5 Hz, CH_3S), 2.47-2.32 (m, 1H, $CH_3SCH_2C\underline{H_a}H_b$), 2.22-2.07 (m, 1H, $CH_3SCH_2CH_a\underline{H_b}$). ^{13}C NMR (126 MHz, $CDCl_3$) δ 171.7, 156.1, 136.08, 136.0, 128.6, 128.6, 128.3, 128.3, 128.2, 67.2, 67.2, 53.1, 52.8, 52.8, 50.8, 50.3, 50.2, 38.6, 26.3, 25.9.

Synthesis of Cbz-L-Vinylglycine methyl ester (21b)*

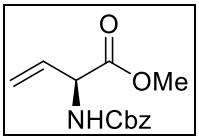

This compound was prepared following by a modification of the procedure by Afzali-Ardakani *et al.*[108] L-Methionine methyl ester sulfoxide (**20b**) (3.44 g, 10.98 mmol) was suspended in 1, 2, 3-trimethylbenzene (44.0 mL) and heated to 170 °C. After 16h, the dark reaction mixture was cooled to r.t. and the product was purified by column chromatography (SiO_2, hexanes/ethyl acetate, 100% hexanes to 8:2) to give the product **21b** as an orange oil (1.73 g, 63 %): R_f= 0.38 (hexanes/ ethyl acetate, 8:2), ^{1}H NMR (400 MHz, $CDCl_3$) δ 7.38 (m, 5H, ArH), 5.92 (ddd, 1H, *J* = 6.0 Hz, H-3), 5.46 (br d, 1H, NH), 5.38 (dd, 1H, *J* = 17.1, 1.8 Hz, $\underline{H_a}H_bC$=CH), 5.29 (dd, 1H, *J* = 10.4, 1.8 Hz, $H_a\underline{H_b}C$=CH), 5.14 (s, 2H, $PhCH_2$), 4.96 (t, 1H, H-2), 3.78 (s, 3H, CO_2CH_3); ^{13}C NMR (126 MHz, $CDCl_3$) δ 170.9, 155.4, 136.2, 132.3, 128.6, 128.2, 128.2, 117.8, 67.2, 56.1, 52.8.

Synthesis of L-vinylglycine hydrochloride (22b)*

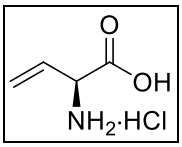

This compound was prepared following by a modification of the procedure by Afzali-Ardakani *et al.*[108] Cbz-vinylglycine methyl ester (**21b**) (2.01 g, 8.07 mmol) was suspended in HCl (6 M, 41.0 mL) and heated to reflux for 4 h. The reaction mixture was cooled, and the aqueous layer was washed with chloroform (2 x 25 mL) and ethyl acetate (2 x 25 mL), followed by lyophilization to collect the pure product **22b** as a white powder (1.05 g, 94%): R_f= 0.04 (hexanes/ethyl acetate, 1:1), ^{1}H NMR (400 MHz, D_2O) δ 5.60-5.46 (m, 1H, H-3), 5.15-5.11 (m, 2H $\underline{H_2C}$=CH), 4.23 (d, 1H, *J* = 7.4 Hz, H-2). ^{13}C NMR (126 MHz, D_2O) δ 171.0, 128.4, 122.6, 55.4.

Synthesis of L-vinylglycine methyl ester (23b)*

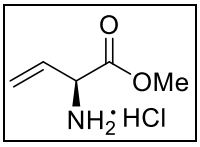

This compound was prepared following by a modification of the procedure by vinylglycine hydrochloride (**22b**) (0.1927 g, 1.40 mmol) was dissolved in dry methanol (7.5 mL) to which was added oxalyl chloride (0.270 mL) at 0 °C under N_2. The reaction mixture was allowed to warm to r.t. After 25h, the solvent was evaporated *in vacuo* and the remaining solid was dried on high vacuum to afford the desired product as an off-white solid (0.2260 g, quant.): R_f= 0.06 (hexanes/ethyl acetate, 1:1); ^{1}H NMR (400 MHz, D_2O) δ 5.82 (m, 1H, H-3), 5.45 (dd, 1H, *J* = 2.7, 1.2 Hz, $H_a\underline{H_b}$C=CH), 5.42 (dd, 1H, *J* = 11.2, 1.2 Hz, $\underline{H_a}H_b$C=CH), 3.69 (s, 3H, CO_2CH_3); ^{13}C NMR (126 MHz, D_2O) δ 169.0, 127.2, 123.5, 54.8, 54.1, 53.8, 48.9.

*The synthesis of the d- enantiomer was completed under the same conditions and gave the same results.

Synthesis of prop-2-enyl- (2*S*)-2-amino-3(*tert*-butyl(dimethylsilyl)oxypropanoate (34)

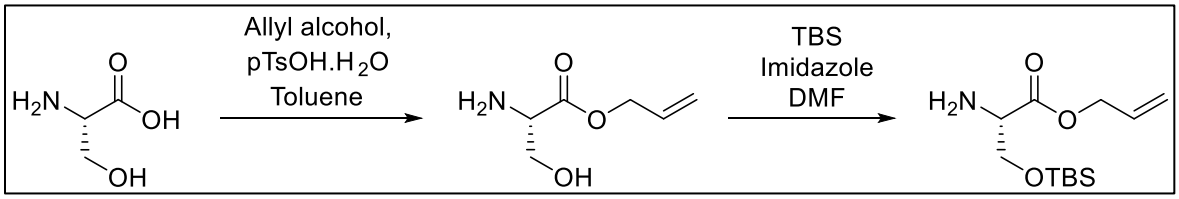

The following reaction procedure was adapted from Pattabiraman *et al.*[113] and Corey *et al.*[114] L-Serine (**32**) (3.01 g, 28.61 mmol) was suspended in toluene (90.0 mL) and *p*-TsOH·H_2O (5.94 g, 34.48 mmol) followed by allyl alcohol (20 mL, 292.7 mmol) were added to the mixture. The reaction mixture was left to stir for 24 h at 115 ^oC, after which the solvent was evaporated, and the concentrate dissolved in CH_2Cl_2 (62.0 mL). *t*- Butyldimethylsilyl chloride (9.5051 g, 63.06 mmol) and imidazole (4.78 g, 70.25 mmol) were added to the flask which was stirred for 18h at 35 ^oC. The reaction mixture was concentrated under vacuum, and the residue was dissolved in ethyl acetate (100 mL). This was washed with NaOH (1 M, 4 x 50mL) and brine (50 mL), then dried (Na_2SO_4), and the solvent evaporated under vacuum. The product was purified by column chromatography (SiO_2; 10:90 to 30:70 ethyl acetate/hexanes) to yield **34** as a yellow oil (5.24 g, 60% (2 steps)): R_f= 0.13 (hexanes/ethyl acetate, 1:1); ^{1}H NMR (400 MHz, $CDCl_3$) δ 5.92 (dddd, 1H, *J* = 17.1, 10.4, 5.7, 5.7 Hz, H_2C=C$\underline{H}$), 5.33 (dq, 1H, *J* = 17.2, 1.5 Hz, $\underline{H_a}H_bC$=C), 5.24 (dq, 1H, *J* = 10.4, 1.3 Hz, $H_a\underline{H_b}C$=C), 4.62 (dq, 2H, *J* = 5.8, 1.2 Hz, OCH_2), 3.95 (dd, 1H, *J* = 9.7, 4.3 Hz, $\underline{H_a}H_bC$-OTBS), 3.82 (dd, 1H, *J* = 9.7, 3.7 Hz, $H_a\underline{H_b}C$-OTBS), 3.54 (t, 1H, *J* = 4.0 Hz, H-2), 1.68 (br s, 2H, NH_2), 0.87 (s, 9H, $Si(CH_3)_3$), 0.04 (d, 6H, *J* = 5.5 Hz, $Si(CH_3)_2$)).

Synthesis of 3-(prop-2-en-1-yl)-2-[(2*S*)-2-*N*-*tert*-butoxycarbonylamino-2-phenylacetamido]-1-tert-butyl(dimethylsilyl)oxypropanoate (35)

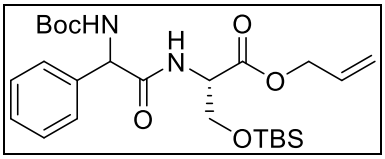

The following procedure was adapted from Quéléver *et al.*[115] *N*-Boc phenylglycine **(24)** (0.5148 g, 2.05 mmol), EDC (0.7934 g, 5.11 mmol), and HOBt (0.5675 g, 4.20 mmol) were dissolved in DMF (9.2 mL) and the mixture was cooled to 0 ^{o}C. The amino acid **34** (0.5122 g, 0.961 mmol) was dissolved in DMF (0.91 mL) and *i*-Pr_2NEt (0.5 mL) at 0 ^{o}C and added dropwise to the mixture containing the activated phenylglycine. The reaction mixture was allowed to warm to r.t. and stirred for 18h. The reaction mixture was diluted with ethyl acetate (10 mL), washed with brine (5 x 10 mL), dried (Na_2SO_4), and the organic layer was concentrated *in vacuo*. The product was purified by column chromatography (SiO_2; ethyl acetate /hexanes, 1:1) to give a pale-yellow oil (0.7229 g, 74%) as a mixture of diastereomers (d.r. = 1:2): R_f= 0.80 (ethyl acetate /hexanes, 1:1); ^{1}H NMR (400 MHz, $CDCl_3$) δ 7.41-7.27 (m, 7.5H, both isomers, ArH), 6.55 (br s, 1H, major isomer, NH), 6.46 (d, 0.5H, *J* = 8.1 Hz, minor isomer, NH), 5.89 (dddd, 1H, *J* = 17.2, 10.4, 5.8, 5.8, major isomer, Hz, H_2C=C$\underline{H}$), 5.84-5.70 (m, 1.5H, major isomer, NH, and minor isomer, H_2C=C$\underline{H}$), 5.32 (dq, 1H, *J* = 17.2, 1.5 Hz, major isomer, $\underline{H_a}H_bC$=C), 5.28-5.15 (m, 3.5H, major isomer, $H_a\underline{H_b}C$=C and PhC$\underline{H}$ of, $\underline{H_2}C$=C and minor isomer, PhC$\underline{H}$), 4.68-4.61 (m, 3H, both isomers, OCH_2), 4.60-4.56 (dt, 0.5H, *J* = 8.2, 2.7 Hz, minor isomer, H-2), 4.53 (dt, 1H, *J* = 5.8, 1.4 Hz, minor isomer, H-2), 4.09-4.04 (dd, 0.5H, *J* = 10.2, 2.4 Hz, minor isomer, $\underline{H_a}H_b$C-OTBS), 4.02 (dd, 1H, *J* = 10.0, 2.5 Hz, major isomer, $\underline{H_a}H_b$C-OTBS), 3.82 (dd, 0.5H, *J* = 10.1, 3.1 Hz, minor isomer, $H_a\underline{H_b}$C-OTBS), 3.66 (d, 1H, *J* = 10.1 Hz, major isomer, $H_a\underline{H_b}$C-OTBS), 1.41 (s, 13H, both isomers, $CO_2C(CH_3)_3$), 0.80 (s, 4.5H, minor isomer, Si(C$\underline{H_3}$)(CH_3)), 0.75 (s, 9H, major isomer, $SiC(CH_3)_3$), 0.01 (s, 1.5H, Si(C$\underline{H_3}$)(CH_3) of minor isomer), -0.03 (s, 1.5H, Si(CH_3)(C$\underline{H_3}$) of minor isomer), -0.10 (s, 3H,

Si(C<u>H</u>$_3$)(CH$_3$) of major isomer); -0.16 (s, 3H, Si(CH$_3$)(C<u>H</u>$_3$) of major isomer); ^{13}C NMR (126 MHz, cdcl$_3$) δ 169.7, 169.5, 131.5, 131.4, 129.1, 129.1, 128.4, 128.4, 127.3, 127.2, 119.00, 118.8, 66.2, 66.1, 63.2, 63.1, 54.5, 54.4, 28.3, 25.7, 25.6, 18.1, 18.0, -5.6, -5.7, -5.8, -5.9; HRMS (ES+) *m/z* calculated for $C_{25}H_{41}N_2O_6Si$ 493.2734 $[M+H]^+$ found 493.2739.

Synthesis of 3-(prop-2-en-1-yl)-2-[(2*S*)-2-N-*tert*-butoxycarbonylamino-2-phenylacetamido]-1-hydroxypropanoate (36)

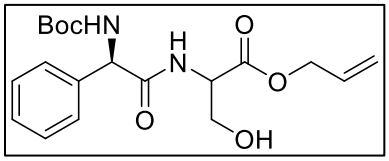

This procedure was modified from Corey, E, J. *et al*.[114] The TBS protected dipeptide **(35)** (1.71 g, 3.47 mmol) was dissolved in a solution mixture of THF/H_2O/acetic acid (35 ml, 1:1:3) and warmed up to 35 ^oC. After, 48h the reaction mixture was neutralized to pH 6 using sat. $NaHCO_3$ and extracted with CH_2Cl_2 (4 x 15 mL). The combined organic layers were washed with brine (3 x 30 mL), dried (Na_2SO_4), and the solvent evaporated *in vacuo.* The product **(36)** was isolated by column chromatography (SiO_2; ethyl acetate/hexanes, 1:1) as white solid (1.22 g, 93 %) and a mixture of diastereomers (d.r. 2:1): R_f= 0.55 (ethyl acetate /hexanes, 1:1); ^{1}H NMR (400 MHz, $CDCl_3$) δ 7.44 – 7.28 (m, 8H, both isomers, ArH), 7.02 (d, 1H, *J* = 7.5 Hz, major isomer NH), 6.93 (d, 0.5H, *J* = 7.5 Hz, minor isomer NH), 5.89 (dddd,1H, *J* = 17.3, 10.4, 5.8, 5.8 Hz, major isomer, H_2C=C<u>H</u>), 5.84 – 5.76 (m, 0.5H, minor isomer, H_2C=C<u>H</u>), 5.69 (d, 0.5H, *J*= 6.8 Hz, minor isomer NH), 5.60 (s, 1H, major isomer NH), 5.33 (dq, 1H, *J* = 17.2, 1.4 Hz, major isomer <u>H$_a$</u>H$_b$C=C), 5.30 – 5.23 (m, 1.6H, minor isomer H_2C=C and PhC<u>H</u>), 5.21 (dq, 1H, *J* = 10.4, 1.2 Hz, major isomer, H$_a$<u>H$_b$</u>C=C), 5.18 (s, 1H, major isomer, PhC<u>H</u>), 4.68 – 4.61 (m, 4H, both isomers, OCH_2, and minor isomer H-2), 4.61 – 4.56 (dd, 1H, *J*= 5.7, 1.3 Hz, major isomer, H-2), 3.94 (d, 3H, *J* = 16.8 Hz, both isomers, H_2C-OH), 3.13 (br s, 0.5H, minor isomer, OH), 2.75 (br s, 1H, major isomer, OH); ^{13}C NMR (126 MHz, $CDCl_3$) δ 170.5, 170.3, 169.9, 169.7, 155.6, 155.5, 137.2, 131.3, 131.2, 131.2,

129.2, 129.1, 128.7, 128.7, 128.6, 127.3, 119.1, 119.1, 119.0, 118.9, 80.9, 80.5, 66.5, 66.4, 62.8, 62.6, 59.6, 58.8, 55.1, 55.0, 28.3, 28.3, 20.5.

Synthesis of 3-(prop-2-en-1-yl)-(2-phenylacetamido)-1-tert-butyl(dimethylsilyl)oxypropanoate (41)

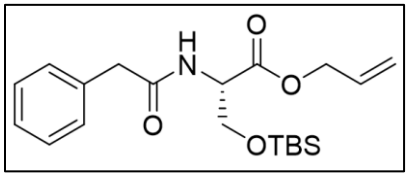

The following reaction procedure was adapted from Corey *et al.*[114] Phenylacetic acid **(40)** (0.2660 g, 1.95 mmol) was dissolved in CH_2Cl_2 (5.0 mL) to which was added PyBOP (2.01 g, 3.97 mmol) and *i*-Pr_2NEt (2.2 mL) at 0 ^oC. Protected serine **(34)** (0.5018 g, 1.93 mmol) dissolved in CH_2Cl_2 (5.0 mL) was then added to the reaction mixture and stirred under N_2 for 3h. The solvent was evaporated *in vacuo* and the product was purified by column chromatography (SiO_2; ethyl acetate/hexanes, 3:7) to a pale orange solid (0.6239 g, 85%): R_f= 0.72 (ethyl acetate /hexanes, 1:1); ^1H NMR (400 MHz, $CDCl_3$) δ 7.38 – 7.28 (m, 5H), 6.25 (d, 1H, J = 8.3 Hz, NH), 5.87 (dddd, 1H, J = 17.2, 10.4, 5.5, 5.5 Hz, H_2C=C$\underline{H}$), 5.30 (dq, 1H, J = 17.2, 1.5 Hz, $\underline{H_a}H_bC$=C), 5.23 (dq, 1H, J = 10.4, 1.3 Hz, $H_a\underline{H_b}C$=C), 4.66 (dt,1H, J = 8.4, 2.7 Hz, H-2), 4.60 (dt, 2H, J = 5.7, 1.4 Hz, OCH_2), 4.03 (dd, 1H, J = 10.0, 2.4 Hz, $\underline{H_a}H_bC$-OTBS), 3.73 (dd, 1H, J = 10.0, 3.0 Hz, $H_a\underline{H_b}C$-OTBS), 3.64 (d, 2H, J = 3.2 Hz, $PhCH_2$), 0.75 (s, 9H, $SiC(CH_3)_3$), -0.07 (s, 3H, J = 7.8 Hz, $SiC(C\underline{H_3})(CH_3)$), -0.09 (s, 3H, J = 7.8 Hz, $SiC(CH_3)(C\underline{H_3})$); ^{13}C NMR (101 MHz, $CDCl_3$) δ 170.7, 169.9, 134.4, 131.52, 129.5, 129.1, 127.4, 118.7, 66.0, 63.3, 54.1, 43.7, 25.6, 18.0, -5.7, -5.8; HRMS (ES) *m/z* calculated for $C_{20}H_{31}NO_4Si$ $[M+Na]^+$ 400.1920, found 400.1919.

Synthesis of 3-(prop-2-en-1-yl)-(2-phenylacetamido)-1-hydroxypropanoate (42)

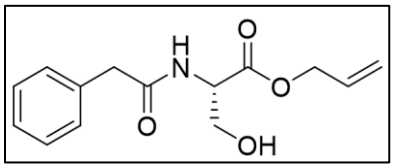

The following reaction procedure was adapted from Corey *et al.*[114] The serine dipeptide **(41)** (0.3771 g, 1.00 mmol) was dissolved on a solution mixture of THF/H_2O/acetic acid (10 ml, 1:1:3) and warmed up to 40 ^oC. After, 22h the reaction was neutralized using sat. $NaHCO_3$ and extracted with ethyl acetate (4 x 25 mL). The combined organic layers were washed with brine (3 x 30 mL), dried (Na_2SO_4), and the solvent evaporated *in vacuo.* The product **42** was isolated by column chromatography (SiO_2; ethyl acetate/hexanes, 1:1) as a white solid (0.2318 g, 88%): R_f= 0.28 (ethyl acetate /hexanes, 1:1); ^1H NMR (400 MHz, $CDCl_3$) δ 7.39 – 7.28 (m, 5H, ArH), 6.36 (d, 1H, *J* = 7.0 Hz, NH), 5.87 (dddd, 1H, *J* = 17.2, 10.4, 5.7, 5.7 Hz, H_2C=C<u>H</u>), 5.31 (dq, 1H, *J* = 17.2, 1.5 Hz, <u>H_a</u>H_bC=C), 5.26 (dq, 1H, *J* = 10.5, 1.2 Hz, H_a<u>H_b</u>C=C), 4.67 (dd, 1H, *J* = 7.2, 3.6 Hz, H-2), 4.64 (dq, 2H, *J* = 5.8, 1.2 Hz, OCH_2), 4.00 – 3.88 (m, 2H, C<u>H_2</u>OH), 3.64 (s, 2H, PhC<u>H_2</u>), 2.30 (s, 1H, OH); ^{13}C NMR (126 MHz, $CDCl_3$) δ 171.6, 169.9, 134.3, 131.2, 129.4, 129.0, 127.5, 119.04, 66.4, 63.4, 63.4, 55.0, 43.5, 29.7.

Synthesis of 3-(prop-2-en-1-yl)-(2*S*)-2-phenylacetamido-1-bromopropanoate (43)

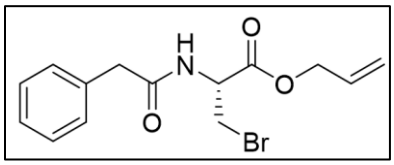

The procedure followed was adapted from the one reported by Adachi, M. *et al.*[118] Deprotected serine dipeptide **42** (0.0884 g, 0.34 mmol) was dissolved in Et_2O (13.5 mL) at 0 ^oC to which was added PBr_3 (90 µL, 0.94 mmol) under N_2. The reaction was tracked by TLC until completion, 1h, and poured over ice-cold water (20 mL). The quenched reaction mixture was extracted with

Et_2O/hexanes (1:1, 2 x 10 mL), the combined organic layers washed with water (3 x 20 mL), and dried (Na_2SO_4). The solvent evaporated under vacuum and the product **43** was collected as a crude white gel (0.0261 g): R_f= 0.05 (ethyl acetate /hexanes, 1:1) The product was used as is without further purification.

Synthesis of prop-2-en-1-yl-(2*S*)-[(*tert*-butoxycarbonyl)amino]-3-hydroxy propanoate (46)

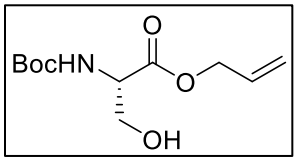

The reaction followed was adapted from Shendage *et al*.[154] Ally ester protected amine **33** (0.9388 g, 6.47 mmol) was dissolved in THF (21.5 mL) along with Boc anhydride (2.16 g, 9.88 mmol) to which was added Et_3N (3.2 mL) at 0 ^oC. The reaction mixture was warmed up to r.t. and stirred for 18h. Upon completion as seen by TLC, the mixture was diluted with water (20 mL), extracted with ethyl acetate (3 x 15 mL), and the combined organic layers washed with brine (2 x 10 mL) and dried (Na_2SO_4). The solvent was evaporated *in vacuo* and compound **46** collected by column chromatography (SiO_2, CH_2Cl_2/MeOH, 95:5) as a pale-yellow oil (0.2589 g, 17%): R_f= 0.50 (CH_2Cl_2/MeOH, 95:5); ^1H NMR (400 MHz, $CDCl_3$) δ 5.91 (dddd, 1H, *J* = 17.2, 10.4, 5.7, 5.7 Hz, H_2C=C<u>H</u>), 5.43 (br s, 1H, NH), 5.35 (dq, 1H, *J* = 17.2, 1.5 Hz, 1H, <u>H_a</u>H_bC=C), 5.27 (dq, 1H, *J* = 10.5, 1.3 Hz, H_a<u>H_b</u>C=C), 4.68 (dt, 2H, *J* = 5.8, 1.4 Hz,), 4.42 (br s, 1H, C<u>H</u>CH_2OH), 4.11 – 3.79 (m, 2H), 2.30 (s, 1H, OH), 1.41 (s, 9H, $NHCO_2C$(<u>CH_3</u>)<u>$_3$</u>).

Synthesis of prop-2-en-1-yl-(2*S*)-[(*tert*-butoxycarbonyl)amino]-3-oxopropanoate (47)

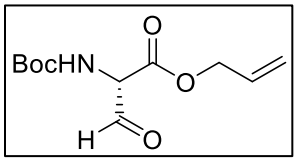

The following procedure was adapted from Taewoo *et al*.[99] Compound **46** (0.1438 g, 0.58 mmol) was dissolved in CH_2Cl_2 (5.8 mL) to which was added Dess-Martin periodinane (DMP, 0.9947 g, 2.35 mmol) at r.t. The reaction mixture was left to stir for 20h and neutralized with sat. $NaHCO_3$ followed by dilution with ethyl acetate (8 mL). The mixture was washed with water (2 x 10 mL), brine (3 x 5 mL), dried (Na_2SO_4), and the solvent evaporated *in vacuo*. Purification by column chromatography (SiO_2, ethyl acetate/hexanes, 4:6) then preparative TLC (SiO_2, ethyl acetate/hexanes, 15:85) afforded the product **47** as a pale yellow oil (0.0279 g, 1.4%): R_f= 0.69 (ethyl acetate /hexanes, 4:6); ^{1}H NMR (400 MHz, $CDCl_3$) δ 8.69 (br s, 1H, C<u>H</u>O), 5.91 (dddd, 1H, *J* = 17.2, 10.4, 5.7, 5.7 Hz, H_2C=C<u>H</u>), 5.43 (br s, 1H, NH), 5.35 (dq, 1H, *J* = 17.2, 1.5 Hz, 1H, <u>H</u>$_a$H$_b$C=C), 5.27 (dq, 1H, *J* = 10.5, 1.3 Hz, H$_a$<u>H</u>$_b$C=C), 4.68 (dt, 2H, *J* = 5.8, 1.4 Hz,), 4.42 (br s, 1H, C<u>H</u>CHO), 4.11 – 3.79 (m, 2H), 2.30 (s, 1H, OH), 1.41 (s, 9H, NHCO$_2$C<u>(CH$_3$)$_3$</u>).

Synthesis of (2*S*)-2-({[9*H*-fluoren-9-yl)methoxy]carbonyl]amino)-4-oxo-(1-methoxy-1-oxobut-3-en-2-yl)amino)-1-oxo-1-[(prop-2-en-yl)oxy]butanoate (51)

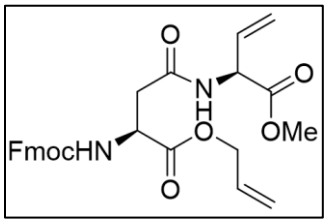

The following procedure was adapted from Quéléver *et al.*[115] Fmoc-Asp-OAllyl **(50)** (0.7874 g, 1.99 mmol) was dissolved in CH_2Cl_2 (10.0 mL) followed by *i*-Pr_2NEt (2.1 mL), PyBOP (2.0687 g, 3.98 mmol), and cooled to 0 ^{o}C. Vinylglycine methyl ester **(23b)** (0.3228 g, 2.13 mmol) was added to the reaction mixture and left to stir under N_2. After completion as seen by TLC, 2h, the reaction

was concentrated *in vacuo*. The product **51** was purified by column chromatography (SiO_2, ethyl acetate/hexanes, 6:4) collected as pale yellow flakes (0.3503 g, 36%) mixture of diastereomers (d.r. 3:10): R_f= 0.47 (ethyl acetate /hexanes, 1:1); ^{1}H NMR (500 MHz, $CDCl_3$) δ 7.76 (d, 3H, *J* = 7.5 Hz, both isomers, PhF ArH), 7.60 (q, 3H, *J* = 5.4, 4.0 Hz, both isomers, PhF ArH), 7.39 (t, 3H, *J* = 7.5 Hz, both isomers, PhF ArH), 7.30 (t, 3H, *J* = 7.4 Hz, both isomers, PhF ArH), 6.38 (d, 0.3H, *J* = 7.8 Hz, minor isomer, NH), 6.34 (d, 1H, *J* = 7.7 Hz, major isomer, NH), 6.13 (d, 1H *J* = 8.7 Hz, major isomer, NH), 6.07 (d, 0.3H, *J* = 8.4 Hz, minor isomer, NH), 5.88 (ddt, 3H, *J* = 17.1, 10.3, 5.1 Hz, both isomers, 2 x H_2C=C<u>H</u>), 5.32 (d, 2.8H, *J* = 17.2 Hz, both isomers, vinylglycine <u>H_2</u>C=CH), 5.26 (dd, 1.7H, *J* = 10.4, 1.8 Hz, both isomers, <u>H_a</u>H_bC=CH), 5.22 (d, 1.5H, J= 20.3 Hz, both isomers, H_a<u>H_b</u>C=CH), 5.16 – 5.10 (d, 1.3H, *J*= 10.7 Hz, both isomers, NHC<u>H</u>(CO_2CH_3)), 4.67 (t, 4H, *J* = 5.2 Hz, both isomers, H-2, OCH_2), 4.37 (ddd, 2.9H, *J* = 39.4, 10.6, 7.1 Hz, both isomers, PhFCHC<u>H_2</u>), 4.23 (t, 1.6H, *J* = 7.1 Hz, PhFC<u>H</u>), 3.76 (s, 0.9H, minor isomer, CO_2C<u>H_3</u>), 3.75 (s, 3H, major isomer, CO_2C<u>H_3</u>), 3.07 (dd, 1.3H, *J* = 15.9, 4.5 Hz, both isomers, C<u>H_a</u>H_b-3), 2.86 (dt, 1.3H, *J* = 15.8, 4.2 Hz, both isomers, CH_a<u>H_b</u>-3). ^{13}C NMR (100 MHz, $CDCl_3$) δ 170.7, 169.5, 169.3, 156.2, 143.9, 143.8, 141.3, 141.3, 131.7, 131.6, 131.6, 131.6, 127.7, 127.1, 125.3, 125.2, 120.0, 119.0, 118.7, 118.7, 118.1, 118.1, 67.3, 66.4, 66.4, 54.6, 54.6, 52.9, 52.1, 50.9, 47.1, 37.6, 29.7; HRMS (ES+) *m/z* calculated for $C_{27}H_{28}N_2O_7$ $[M+H]^+$ 493.1975, found 493.1976.

Synthesis of 1-*tert*-butyl 4-methyl (2*S*)-(2-phenylacetamido)butanedioate (58)

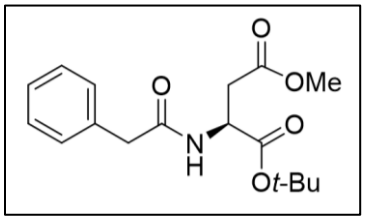

The reaction followed was adapted from Quéléver *et al*.[115] Phenylacetic acid **(40)** (0.2843 g, 2.09 mmol) was dissolved in CH_2Cl_2 (10.5 mL) at 0 °C to which was added PyBOP (2.16 g, 4.15 mmol) and *i*-Pr_2NEt (2.2 mL). After 10 mins, 1-(*tert*-butyl) 4-methyl L-aspartate hydrochloride **(57)**

(0.4990 g, 2.08 mmol) was added to the reaction mixture and left to stir under N_2 until completion as seen by TLC. After, 2.5h the reaction was concentrated *in vacuo* and the product **58** isolated by column chromatography (SiO_2, ethyl acetate/hexanes, 1:1) as an off-white solid powder (0.6096 g, 91%): R_f= 0.71 (ethyl acetate /hexanes, 1:1); ^{1}H NMR (500 MHz, $CDCl_3$) δ 7.39 – 7.26 (m, 5H, ArH), 6.37 (d, 1H, *J* = 7.8 Hz, NH), 4.70 (dt, 1H, *J* = 7.8, 4.6 Hz,), 3.61 (s, 3H, $CO_2C\underline{H}_3$), 3.59 (s, 2H, PhC$\underline{H}$), 2.93 (dd, 1H, *J* = 16.7, 4.3 Hz, C$\underline{H}_a$H$_b$-3), 2.78 (dd, 1H, *J* = 16.7, 4.9 Hz, CH$_a\underline{H}_b$-3), 1.41 (s, 9H, C(CH_3)$_3$); ^{13}C NMR (126 MHz, $CDCl_3$) δ 171.2, 170.5, 169.4, 134.5, 129.4, 128.9, 127.3, 82.6, 51.8, 49.3, 43.6, 36.3, 27.8; HRMS (ES+) *m/z* calculated for $C_{17}H_{23}NO_5Na$ $[M+Na]^+$ 344.1474 found 344.1473.

Synthesis of 4-*tert*-butoxy-4-oxo- (3*S*)-(2-phenylacetamido)butanoic acid (59)

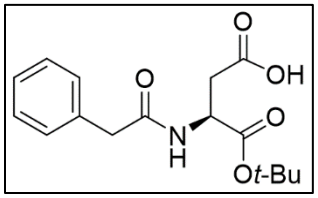

The procedure followed was adapted from Ghosh and Liu.[155] The methyl ester protected dipeptide **(58)** (0.3611 g, 1.12 mmol) was dissolved in a mixture of MeOH/H_2O (3:1, 42.5 mL) and cooled to 0 ^{o}C. LiOH·H_2O solution (1 M, 6.1 mL) was added to the reaction under vigorous stirring. The reaction was tracked by TLC, and after 2h it was partially evaporated, acidified to pH 3 using saturated citric acid (4 mL), followed by extraction with ethyl acetate (3 x 40 mL). The combined organic layers were dried (Na_2SO_4) and solvent evaporated *in vacuo*. The collected product **59** was purified by column chromatography (SiO_2, CH_2Cl_2/MeOH, 95:5) collected as a yellow oil (0.1897 g, 48%): R_f= 0.39 (CH_2Cl_2/MeOH, 95:5); ^{1}H NMR (400 MHz, CD_3OD) δ 7.34 – 7.16 (m, 5H, ArH), 4.62 (td, *J* = 6.0, 1.3 Hz, 1H, C$\underline{H}CO_2t$Bu), 3.54 (s, 2H, PhC$\underline{H}$), 2.83 (d, 1H, 1.9 Hz, C$\underline{H}_a$H$_b$-3), 2.68 (d, 1H, 2.1 Hz, CH$_a\underline{H}_b$-3), 1.40 (s, 9H, C(CH_3)$_3$). ^{13}C NMR (100 MHz, $CDCl_3$) δ

172.3, 171.0, 169.8, 135.2, 128.8, 126.5, 81.7, 49.8, 42.1, 35.6, 26.7; HRMS (ES-) *m/z* calculated for $C_{16}H_{20}NO_5$ $[M-H]^-$ 306.1341 found 306.1342.

Synthesis of 1-*tert*-butyl -4-[(2*S*)-(1-methoxy-1-oxobut-3-en-2-yl)amino]-4-oxo-(2*S*)-(2-phenylacetamido)butanedioate (60)

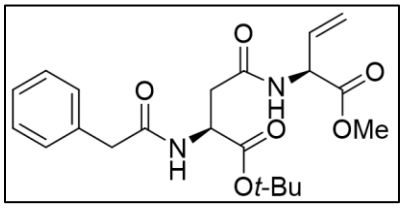

The reaction followed was adapted from Quéléver *et al*.[115] The carboxylic acid **(59)** (0.0905 g, 0.29 mmol) was suspended in CH_2Cl_2 (1.5 mL) followed by *i*-Pr_2NEt (0.310 mL) and cooled to 0 ^oC. PyBOP (0.3204 g, 0.62 mmol) and vinylglycine methyl ester (0.0443 g, 0.29 mmol) were added to the reaction mixture and left to stir under N_2. After reaction completion as seen by TLC, 2.5h, the reaction was concentrated *in vacuo*. The product **(60)** was collected as a pale yellow solid (0.0452 g, 38%) after purification by column chromatography (SiO_2, ethyl acetate/hexane, 6:4) as a 2:1 diastereomers mixture: R_f= 0.50 (ethyl acetate/hexanes, 6:4); ^1H NMR (400 MHz, $CDCl_3$) δ 7.37 – 7.21 (m, 9.5H, both isomers overlapping $CDCl_3$ solvent, ArH), 6.70 (d, 1H, *J* = 7.9 Hz, major isomer NH), 6.65 (d, 0.5H, *J* = 7.6 Hz, minor isomer, NH), 6.39 (br d, 1.5H, *J* = 7.4 Hz, both isomers, NH), 5.90-5.80 (m, 1.5H, both isomers, C<u>H</u>=CH_2), 5.31 (dd, 1H, *J* = 17.2, 1.8 Hz, major isomer, C<u>H</u>=C<u>H</u>$_a$H$_b$), 5.27 – 5.22 (m, 2H, major isomers, C<u>H</u>=CH$_a$<u>H</u>$_b$, and minor isomer, CH=C<u>H</u>$_2$), 5.10-5.03 (m, 1.5H, both isomers. C<u>H</u>CH=CH_2), 4.72-4.64 (m, 1.5H, both isomers, C<u>H</u>CO_2*t*Bu), 3.78 (s, 3H, major isomer, CO_2C<u>H</u>$_3$), 3.76 (s, 1.5H, minor isomer, CO_2C<u>H</u>$_3$), 3.58 (s, 2H, major isomer, PhC<u>H</u>), 3.56 (s, 1H, minor isomer, PhC<u>H</u>), 2.94-2.87 (m, both isomers, 1.5H, C<u>H</u>$_a$H$_b$-3), 2.82-2.75 (m, 1.5H, both isomers, CH$_a$<u>H</u>$_b$-3), 1.41 (s, 4.5H, minor isomer, $C(CH_3)_3$), 1.40 (s, major isomer, 9H, $C(CH_3)_3$); ^{13}C NMR (101 MHz, $CDCl_3$) δ 170.8, 170.8, 170.7, 169.6, 169.5, 169.5, 169.3, 134.6, 134.5, 131.8, 131.7, 129.4, 129.3, 128.9, 128.8, 127.2, 127.2, 118.0,

117.9, 82.5, 82.5, 77.3, 77.2, 77.0, 76.7, 54.5, 52.8, 52.8, 49.6, 49.6, 43.6, 43.53, 37.6, 37.6, 27.8, 27.8; HRMS (ES-) *m/z* calculated for $C_{17}H_{20}N_2O_6$ $[M-H]^-$ 347.13 found 347.1240.

Synthesis of 4-[(1-methoxy-1-oxobut-3-en-2-yl)amino]-4-oxo-(2*S*)-(2-phenylacetamido)butanoic acid (61)

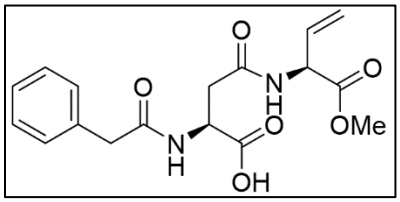

The following reaction was adapted from Martin *et* al.[125] Butanedioate **(60)** (0.0565 g, 0.14 mmol) was dissolved in CH_2Cl_2 (350 µL) to which was added Et_3SiH (30 µL) at 0 ^oC. TFA (320 µL, 4.12 mmol) was added to the reaction which was let to stir under N_2. The reaction was tracked by TLC, and after 5h, concentrated *in vacuo*. The product was isolated by column chromatography (SiO_2, 95:5 DCM/ methanol) as a white solid (0.0470 g, 97%): R_f= 0.27 (SiO_2, CH_2Cl_2/MeOH, 95:5); ^1H NMR (400 MHz, $CDCl_3$) δ 11.88 (br s, 1.5H, both isomers, CO_2H), 7.37 – 7.21 (m, 11H, both isomers overlapping $CDCl_3$ solvent, ArH), 5.87-5.75 (m, 1.5H, both isomers, C<u>H</u>=CH_2), 5.34 – 5.21 (m, 3H, both isomer, CH=C<u>H</u>$_2$), 5.06-4.99 (m, 1.5H, both isomers, C<u>H</u>CH=CH_2), 4.74-4.65 (m, 1.5H, both isomers, C<u>H</u>CO_2tBu), 3.74 (s, 3H, major isomer, CO_2C<u>H</u>$_3$), 3.72 (s, 1.5H, minor isomer, CO_2C<u>H</u>$_3$), 3.64 (s, 2H, major isomer, PhC<u>H</u>), 3.62 (s, 1H, minor isomer, PhC<u>H</u>), 3.02-2.95 (m, 1.5H, both isomers, C<u>H</u>$_a$H$_b$-3), 2.91-2.82 (m, 1.5H, both isomers, CH$_a$<u>H</u>$_b$-3); ^{13}C NMR (101 MHz, $CDCl_3$) δ 173.3, 173.2, 172.7, 172.6, 170.9, 170.9, 170.6, 170.6, 133.8, 133.8, 131.1, 131.0, 129.4, 129.3, 128.9, 127.4, 118.6, 118.5, 77.4, 77.0, 76.7, 55.0, 53.0, 52.9, 49.5, 42.8, 36.8, 36.7; HRMS (ES+) *m/z* calculated for $C_{17}H_{21}N_2O_6$ $[M+H]^+$ 349.1400 found 349.1397.

Synthesis of 4-{[2-methoxy-2-oxo-1-(oxiran-2-yl)-2-oxoethyl]amino}-4-oxo-2-(2-phenulacetamido)butaneoic acid (62)

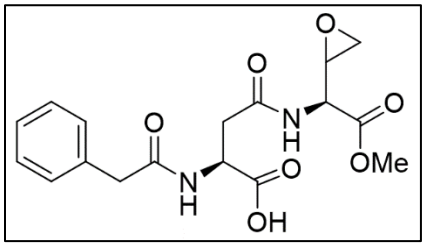

The reaction followed was adapted from Yang *et* al. The alkene **(62)** (0.0155 g, 0.045 mmol) was dissolved in CH_3CN (0.5 mL) and EDTA (4×10^{-4} M, 0.20 mL). The mixture was cooled to 8 ^oC followed by addition of trifluoroacetone acid (20 µL, 0.04 mmol), $NaHCO_3$ (0.1567 g, 1.87 mmol), and Oxone ® (0.0614 g, 0.73 mmol). After 3.5h, anhydrous Na_2SO_4 was added to the reaction mixture and CH_2Cl_2 (10.0 mL) used to collect the product. The solvent was evaporated *in vacuo* and the white solid product **(62)** isolated by purification using reverse phase preparative TLC (C18, CH_3CN:H_2O, 1:1): R_f= 0.05 (C18, CH_3CN:H_2O, 1:1); HRMS (ES+) *m/z* calculated for $C_{17}H_{21}N_2O_7$ $[M+H]^+$ 365.1349 found 365.1339.

Synthesis of 4-{[2-methoxy-2-oxo-1-(oxiran-2-yl)-2-oxoethyl]amino}-4-oxo-2-(2-phenulacetamido)butaneoic acid (63)

The following procedure was adapted from Nicolaou *et al*.[129] The epoxide **(62)** was dissolved in 1,2 dichloroethane (360 µL) to which was added Me_3SnOH (0.0199 g, 010 mmol) and the mixture was warmed up to 60 ^oC for 2.5h. The reaction mixture was then concentrated *in vacuo*, redissolved in ethyl acetate (5 mL), and washed with $KHSO_4$ (0.01 M, 3 x 5 mL) and water (1 x 5 mL). The solvent was evaporated in vacuo to give the crude product **(63)**: R_f= ~1 (C18, CH_3CN:H_2O, 1:1); HRMS (ES+) *m/z* calculated for $C_{17}H_{19}N_2O_6$ [M-3H] 347.1243 found 347.1241.

Detailed Experimental Section Chapter. III

Synthesis of ethyl-1-(2-methylprop-2-enoyl)pyrrolidine-2-carboxylate (92)

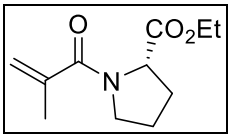

The following procedure was modified from the one reported in O'Daniel *et al* and Choo *et al*.[144,156] Methacrylic acid **(90)** (740 µL, 8.63 mmol) was dissolved in CH_2Cl_2 (89 mL) to which was added DMF (4 drops) and oxalyl chloride (0.9 mL, 10.5 mmol) at 0 °C under N_2. After 1.5 h, the reaction mixture was concentrated *in vacuo* and dissolved in DMF (5 mL). A mixture of D-proline ethyl ester (1.06 g, 5.92 mmol) and NEt_3 (1.6 mL, 11.3 mmol) in DMF (3 mL) at 0 °C was prepared, added to the acid chloride solution, warmed to 90 °C, and the mixture stirred under N_2 for 18h. The reaction mixture was filtered through a pad of celite, the solvent was evaporated *in vacuo*, and the product purified by column chromatography (SiO_2, ethyl acetate/hexanes, 1:1) to give **92** as a dark yellow oil (0.6606 g, 36% over 2 steps) as a ~2.5:1 mixture of rotamers: R*f*= 0.50 (ethyl acetate/hexanes, 1:1); ^{1}H NMR (400 MHz, $CDCl_3$) δ 5.32-5.27 (s, 0.7H, major isomer, C=C$\underline{H_a}$CH_b), 5.24 (s, 0.7H, major isomer, C=CH_aC$\underline{H_b}$), 5.17 (s, 0.3H, minor isomer, C=C$\underline{H_a}$CH_b), 5.02 (s, 0.3H, minor isomer, C=CH_aC$\underline{H_b}$), 4.49 (dd, 1H, *J* = 8.5, 5.1 Hz, both isomers, H-2), 4.19 (q, 2H, *J* = 7.2 Hz, both isomers, $CO_2C\underline{H_2}CH_3$), 3.69-3.52 (m, 2H, both isomers, CH_2-5), 2.31-2.20 (m, 1H, both isomers, C$\underline{H_a}H_b$), 2.11-1.79 (m, 6H, both isomers, $CH_a\underline{H_b}$-3, CH_2-4, C=CCH_3), 1.31-1.21 (t, 3H, both isomers, $CO_2CH_2C\underline{H_3}$); ^{13}C NMR (126 MHz, $CDCl_3$) δ 172.3, 170.5, 141.8, 141.0, 116.9, 115.9, 61.4, 61.1, 61., 58.7, 49.1, 46.2, 31.5, 29.3, 25.1, 22.7, 20.0, 19.8, 18.1, 14.1 (3 carbon signals not observed due to overlap).

Synthesis of ethyl-1-(2-methyloxirane-2carbonyl)pyrrolidine-2-carboxylate (93)

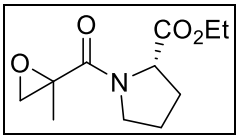

This procedure was modified from the one reported by Yang *et al.*[128] EDTA (950 µL) was added to a solution of compound **92** (0.0510 g, 0.24 mmol) in CH_3CN (2.4 mL) at 8 ^oC. Trifluoroacetone (490 µL) was then added to the reaction mixture using a pre-cooled syringe followed by oxone (1.4650 g, 2.39 mmol) and $NaHCO_3$ (0.2893 g, 3.44 mmol). The mixture was monitored by TLC until completion, 2h, upon which anhydrous Na_2SO_4 (5 g) was added. The reaction mixture was diluted with CH_2Cl_2 (25 mL), filtered through a thin plug of celite, and the filtrate was concentrated *in vacuo* to afford the product **93** as a pale-yellow oil (0.0520 g, 97%) and a set of rotamers of two diastereomers (1:1.5:2.5): R*f*= 0.06 (ethyl acetate/hexanes, 7:3); ^1H NMR (400 MHz, $CDCl_3$) δ 4.78 (dd, ~0.2H, *J* = 8.6, 4.3 Hz, minor isomer, H-2), 4.69 (dd, ~0.3H, *J* = 8.5, 1.8 Hz, second isomer, H-2), 4.46-4.37 (m, ~0.5H, major isomers, H-2), 4.17 (m, 2H, all isomers, $CO_2C\underline{H_2}CH_3$), 3.83-3.45 (m, 2H, all isomers, H-5), 2.94-2.66 (m, 2H, all isomers, epoxide CH_2), 2.30-1.67 (m, 4H, all isomers, CH_2-3, all isomers, CH_2-4), 1.55 (dd, 4H, *J* = 10.6, 6.8 Hz, all isomers, CH_3), 1.30-1.17 (m, 12H, 4 x $CO_2CH_2C\underline{H_3}$); ^{13}C NMR (126 MHz, $CDCl_3$) δ 172.7, 171.9, 171.8, 169.9, 169.1, 169.0, 168.5, 61.5, 61.2, 61.2, 61.1, 59.8, 59.5, 59.3, 59.0, 57.7, 57.6, 57.3, 57.0, 53.1, 53.1, 52.8, 52.5, 52.5, 47.3, 47.2, 46.8, 31.9, 31.5, 28.6, 28.5, 25.4, 24.8, 23.7, 21.9, 21.8, 21.3, 19.6, 19.2, 19.0, 18.8, 14.2, 14.2, 14.1; HRMS (ES+) *m/z* calculated for $C_{11}H_{18}NO_4$ $[M+H]^+$ 228.1236 found 228.1234.

Synthesis of 1-(2-Methyloxirane-2-carbonyl)pyrrolidine-2-carboxylic acid (82)

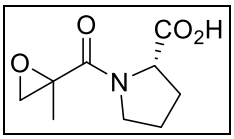

The deprotected compound was obtained following similar reaction conditions as those presented by Orrling *et al.*[152] The ethyl ester protected epoxide compound **93** (0.0417 g, 0.18 mmol) was dissolved in ethanol (260 µL) to which was added ethanolic KOH (1.07 M, 320 µL) and stirred at r.t. After 25 min, the reaction mixture was diluted with sat. $NaHCO_3$ (0.5 mL), acidified to pH 8 with HCl (0.5 M). and washed with ethyl acetate (3 x 8 mL). The aqueous layer was acidified to pH 1 with HCl (0.5 M) and extracted with ethyl acetate (3 x 4 mL). The combined organic layers were dried ($MgSO_4$) and the solvent was evaporated *in vacuo* to afford the crude product **82**: R*f*= 0.04 (CH_2Cl_2/MeOH, 95:5); HRMS (ES+) *m/z* calculated for $C_{11}H_{18}NO_4$ $[M+H]^+$ 228.1236 found 228.1234.

Synthesis of ethyl-1-(2-methylthiirane-2-carbonyl)pyrrolidine-2-carboxylate (94)

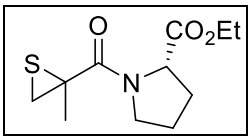

This compound was prepared of Gooyit *et al*.[153] The epoxide **93** (0.0520 g) was dissolved in CH_2Cl_2 (75 µL) and a solution of thiourea (0.1847 g, 2.43 mmol) in MeOH (2.1 mL) was added. The mixture was stirred at r.t. under N_2 for 23h and concentrated *in vacuo*. The concentrate was dissolved in Et_2O/water mixture (1:1, 20 mL), then the organic layer was separated, washed with water (2 x 20 mL), and dried ($NaSO_4$). The solvent was evaporated *in vacuo* followed by purification by column chromatography (SiO_2, ethyl acetate/hexanes, 1:1) to give the desired product as a clear oil (0.0298 g, 54 %) and separable diastereomers in a 1:1 ratio: Data for **94a** : R*f*= 0.57 (ethyl acetate/hexanes, 7:3); ^{1}H NMR (400 MHz, $CDCl_3$) δ 4.47-4.42 (dd, 1H, H-2), 4.18 (q, 2H, *J* = 7.1 Hz, $CO_2C\underline{H_2}CH_3$), 3.93-3.86 (dt, 1H, *J* = 10.4, 6.1 Hz, $C\underline{H_a}H_b$-5), 3.73 (dt, 1H, *J* =

10.0, 6.7 Hz, CH_aH_b-5), 3.09 (d, 1H, *J* = 1.2 Hz, thiirane CH_aH_b), 2.40 (d, 1H, *J* = 1.2 Hz, thiirane CH_aH_b), 2.28-2.17 (m, 1H, CH_aH_b-3), 2.13-2.03 (m, 1H, CH_aH_b-4), 2.01-1.90 (m, 2H, CH_aH_b-3, CH_aH_b-4), 1.82 (s, 3H, CH_3), 1.27 (t, 3H, *J* = 7.2 Hz, $CO_2CH_2CH_3$); ^{13}C NMR (126 MHz, $CDCl_3$) δ 171.75, 168.83, 60.98, 59.87, 47.55, 42.40, 31.62, 28.83, 24.86, 23.37, 14.09; HRMS (ES+) *m/z* calculated for $C_{11}H_{18}NO_3S$ $[M+H]^+$ 244.1007 found 244.1010. Data for **94b**:R*f*= 0.50 (ethyl acetate/hexanes, 7:3); ^{1}H NMR (400 MHz, $CDCl_3$) δ 4.41 (dd, 1H, *J* = 8.6, 3.5 Hz, H-2), 4.25-4.05 (m, 2H, *J* = 7.1 Hz, $CO_2CH_2CH_3$), 3.94 (app ddd, 1H, *J* = 9.8, 7.6, 4.7 Hz, CH_aH_b-5), 3.68 (dt, 1H, *J* = 10.3, 7.0 Hz, CH_aH_b-5), 3.09 (d, 1H, *J* = 1.2 Hz, thiirane CH_aH_b), 2.40 (d, 1H, *J* = 1.2 Hz, thiirane CH_aH_b), 2.26-1.92 (m, 4H, CH_2-3, CH_2-4), 1.78 (s, 3H, CH_3), 1.22 (t, 3H, *J* = 7.2 Hz, $CO_2CH_2CH_3$). ^{13}C NMR (100 MHz, $CDCl_3$) δ 171.8, 168.8, 61.0, 59.9, 47.6, 42.4, 31.6, 28.8, 24.9, 23.4, 14.1. HRMS (ES+) *m/z* calculated for $C_{11}H_{18}NO_3S$ $[M+H]^+$ 244.1007 found 244.1011.

Synthesis of 1-(2-methylthiirane-2-carbonyl)pyrrolidine-2-carboxylic acid (83)

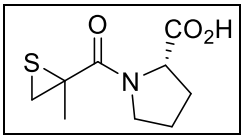

The deprotected compound was obtained following similar reaction conditions as those presented by Orrling *et al.*[152] The epoxide (0.0168 g, 0.069 mmol) was dissolved in ethanol (120 µL) to which was added ethanolic KOH (1.05 M, 150 µL) and stirred at r.t. After 2h, the reaction mixture was diluted with sat. $NaHCO_3$ (0.5 mL), acidified to pH 8 with HCl (0.5 M), and washed with ethyl acetate (3 x 8 mL). The aqueous layer was acidified to pH 1 with HCl (0.5 M) and extracted with ethyl acetate (3 x 4 mL). The combined organic layers were dried (Na_2SO_4) and the solvent was evaporated *in vacuo* to afford the crude product: Data for **83a**: R*f*= 0.08 (CH_2Cl_2/MeOH, 95:5); HRMS (ES+) *m/z* calculated for $C_9H_{14}NO_3S$ $[M+H]^+$ 216.0694 found 216.0687; Data for **83b**: R*f*= 0.11 (CH_2Cl_2/MeOH, 95:5); HRMS (ES+) *m/z* calculated for $C_9H_{14}NO_3S$ $[M+H]^+$ 216.0694 found 216.0689.

Synthesis of ethyl-1-(2-methylbut-3-enoyl)pyrrolidine-2-carboxylate (98)

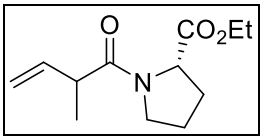

The following procedure was modified from the one reported in Choo *et al*.[144] The 2-methyl-3-butenoic acid **(96)** (780 µL, 7.50 mmol) was dissolved in CH_2Cl_2 (75 mL) at 0 °C to which was added DMF (4 drops) and oxalyl chloride (0.9 mL, 10.5 mmol) under N_2. After 1.5 h, the reaction mixture was concentrated *in vacuo* and dissolved in DMF (5 mL). A mixture of D-proline ethyl ester (0.9692 g, 9.68 mmol) and NEt_3 (1.4 mL, 11.3 mmol) in DMF (4 mL) was prepared at 0 °C and added to the acid chloride solution. Then, the reaction mixture was warmed to 90 °C and stirred under N_2 for 18 h. The reaction mixture was filtered through a pad of celite, the solvent was evaporated *in vacuo*, and the product purified by column chromatography (SiO_2, ethyl acetate/hexanes, 7:3) to yield a dark yellow oil (0.5591 g, 31% over 2 steps). The product **98** was isolated as a mixture of diastereomers: R*f*= 0.64 (ethyl acetate/hexanes, 1:1); ^{1}H NMR (400 MHz, $CDCl_3$) δ 5.90-5.74 (m, 1H, CH_2=C<u>H</u>), 5.22-4.95 (m, 2H, C<u>H$_2$</u>=CH), 4.50-4.41 (m, 1H, H-2), 4.23-4.10 (m, 2H, $CO_2C\underline{H_2}CH_3$), 3.72-3.46 (m, 2H, H-5), 3.23 (m, 1H, COC<u>H</u>CH_3), 2.27-1.81 (m, 4H, CH_2-3, CH_2-4), 1.30-1.14 (m, 6H, CH_3, $CO_2CH_2C\underline{H_3}$); ^{13}C NMR (101 MHz, $CDCl_3$) δ 172.6, 172.4, 172.4, 172.3, 138.3, 138.1, 138.0, 137.5, 115.8, 115.6, 115.5, 115.2, 61.5, 61.4, 60.9, 60.9, 59.5, 59.0, 46.7, 46.7, 46.5, 43.4, 43.1, 42.9, 42.5, 31.5, 31.3, 29.1, 29.1, 24.8, 24.8, 22.4, 22.3, 18.3, 17.6, 17.5, 17.4, 17.1, 14.2, 14.1 (8 carbon signals not observed due to overlap); HRMS (ES+) *m/z* calculated for $C_{12}H_{20}O_3$ $[M+H]^+$ 226.1443 found 226.1441.

Synthesis of ethyl-1-[2-(oxiran-2-yl)propanoyl]pyrrolidine-2-carboxylate (99)

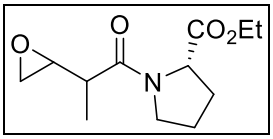

This procedure was adapted from the procedure reported by Choo *et al.*[144] The alkene **(98)** (0.1011 g, 0.45 mmol) was dissolved in a mixture of acetone/water (3:5, 3.6 mL) to which was added oxone (1.1118 g, 1.81 mmol) and $NaHCO_3$ (0.5228 g, 6.22 mmol). After being stirred for 1h at r.t. the reaction mixture was acidified to pH 1-2 using conc. HCl and extracted with EtOAc (2 x 8 mL), and the combined organic layers were dried ($NaSO_4$). Evaporation of the solvent *in vacuo* and high vacuum afforded the desired epoxide as a yellow oil (0.0909 g, 85%) as a mixture of 4 diastereomers: R*f*= 0.11 (CH_2Cl_2/MeOH, 95:5); ^{1}H NMR (400 MHz, $CDCl_3$) δ 4.61 (dd, 1H, *J* = 8.5, 2.4 Hz, H-2), 4.51-4.36 (m, 6H, 6 x H-2), 4.34 (dd, 0.5H, *J* = 8.5, 2.4 Hz, 0.5 x H-2), 4.26 (dd, 0.5H, *J* = 8.3, 2.4 Hz, 0.5 x H-2), 4.19-4.07 (m, 16H, 8 x $CO_2C\underline{H}_2CH_3$), 3.87-3.72 (m, 2H, H-5), 3.70-3.42 (m, 14H, 7 x H-5'), 3.23-2.98 (m, 8H, 8 x $COC\underline{H}CH_3$), 2.79-2.67 (m, 8H, 8 x epoxide CH), 2.78-2.44 (m, 16H, 8 x epoxide CH_2), 2.27-1.83 (m, 32H, 8 x CH_2-3, 8 x CH_2-4), 1.36-1.01 (m, 48H, 8 x CH_3, 8 x $CO_2CH_2C\underline{H}_3$). ^{13}C NMR (100 MHz, $CDCl_3$) δ 172.8, 172.58, 172.4, 172.3, 172.2, 172.1, 172.0, 172.0, 171.8, 61.7, 61.6, 61.5, 61.2, 61.0, 61.0, 61.0, 59.6, 59.4, 59.2, 59.2, 59.1, 58.9, 58.8, 58.9, 54.9, 54.2, 54.2, 54.0, 53.8, 53.8, 53.6, 47.1, 47.0, 47.0, 46.9, 46.7, 46.5, 46.5, 46.4, 46.4, 46.1, 46.0, 45.3, 45.2, 42.1, 41.6, 41.1, 40.8, 40.8, 40.7, 40.2, 31.4, 31.3, 31.3, 31.2, 29.1, 29.01, 24.7, 24.7, 24.6, 22.5, 22.4, 22.3, 14.6, 14.5, 14.2, 14.1, 13.54, 13.3, 13.2, 12.7 (25 carbon signals not observed due to overlap); HRMS (ES+) *m/z* calculated for C_{12} $H_{20}NO_4$ [M+H] 242.1392 found 242.1387.

Synthesis of 1-[2-(oxiran-2-yl)propanoyl]pyrrolidine-2-carboxylic acid (84)

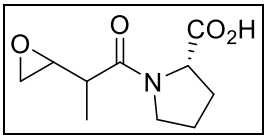

The deprotected compound # was obtained following similar reaction conditions as those presented by Orrling *et al.*[152] The protected epoxide **99** (0.0157g, 0.066 mmol) was dissolved in ethanol (100 µL) at r.t. to which was added ethanolic KOH solution (1.05 M, 110 µL). After stirring for 2h, the reaction mixture was diluted with sat. $NaHCO_3$ (0.5 mL), acidified to pH 8 with HCl (0.5 M). and washed with ethyl acetate (3 x 2 mL). The aqueous layer was acidified to pH 1 with HCl (0.5 M) and extracted with ethyl acetate (3 x 4 mL). The combined organic layers were dried (Na_2SO_4) and the solvent was evaporated *in vacuo* to afford the crude product **85**: R*f*= 0.05 (CH_2Cl_2/MeOH, 95:5); HRMS (ES+) *m/z* calculated for $C_{10}H_{16}NO_4$ $[M+H]^+$ 214.1079 found 214.1070.

Synthesis of ethyl-1-[2-(thiirane-2-yl)propanoyl]pyrrolidine-2-carboxylate (100)

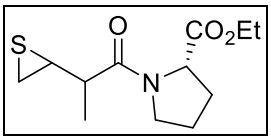

The epoxide **99** (0.1284 g, 0.53 mmol) was dissolved in CH_2Cl_2 (1.7 mL) to which a solution of thiourea (0.4205 g, 5.52 mmol) in MeOH (3.4 mL) was added, and the mixture was stirred at r.t. under N_2 for 24h. The reaction mixture was concentrated *in vacuo* re-dissolved in a mixture of Et_2O/water (1:1, 20 mL), then the organic layer was separated and dried ($NaSO_4$). The solvent was evaporated *in vacuo* followed by purification by column chromatography (SiO_2, 1:1 ethyl acetate/hexanes) to give the desired product as a clear oil (0.0514 g, 38%) and two set of separable diastereomers in a 6:2:1:1 ratio: R*f*= 0.47 (ethyl acetate/hexanes, 1:1); ^{1}H NMR (400 MHz, $CDCl_3$) δ 4.53 (dd, ~0.2H *J* = 8.8, 4.0 Hz, one isomer, H-5), 4.48 (dd, ~0.6H, *J* = 8.8, 4.2

Hz, one isomer, H-5), 4.40 (dd, ~0.1H, *J* = 8.5, 2.5 Hz, one isomer, H-5), 4.27 (dd, ~0.1H *J* = 8.3, 2.6 Hz, one isomer, CH-5), 4.28-4.07 (m, 2H, $CO_2C\underline{H}_2CH_3$), 3.90-3.72 (m, 1H, H-2), 3.72-3.58 (m, 1H, H-2), 3.51-3.39 (m, 1H, $COC\underline{H}CH_3$), 3.22-3.10 (m, 1H, thiirane CH), 2.54 (ddd, 1H, *J* = 11.5, 6.3, 1.4 Hz, thiirane $C\underline{H}_aH_b$), (1H, *J* = 8.6, 6.9 Hz, thiirane $CH_a\underline{H}_b$), 2.33-2.13 (m, 3H, thiirane $CH_a\underline{H}_b$, $C\underline{H}_aH_b$-3, $C\underline{H}_aH_b$-4), 2.10-1.77 (m, 2H, $CH_a\underline{H}_b$-3, $CH_a\underline{H}_b$-4), 1.45-1.32 (m, 3H, CH_3) 1.30-1.24, 3H, $CO_2CH_2C\underline{H}_3$); ^{13}C NMR (126 MHz, CDCl3) δ 173.95, 173.2, 173.2, 173.0, 172.5, 172.3, 172.2, 172.1, 61.8, 61.8, 61.7, 61.1, 61.1, 61.0, 59.5, 59.1, 58.9, 58.8, 47.1, 47.1, 47.0, 46.4, 46.4, 46.3, 45.7, 45.6, 45.2, 38.4, 38.3, 38.0, 37.9, 31.4, 29.1, 29.1, 25.3, 25.3, 25.0, 24.8, 24.8, 24.1, 24.1, 23.2, 22.5, 22.4, 18.5, 18.0, 17.7, 16.8, 14.2, 14.1 ; HRMS (ES+) *m/z* calculated for $C_{12}H_{20}NO_3S$ $[M+H]^+$ 258.1164 found. 258.1171.

Synthesis of 1-[2-(thiirane-2-yl)propanoyl]pyrrolidine-2-carboxylic acid (85)

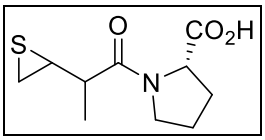

The deprotected compound **85** was obtained following similar reaction conditions as those presented by Orrling *et al.*[152] The protected thiirane compound **100** (0.0116 g, 0.045 mmol) was dissolved in ethanol (70 µL) at r.t. to which was added ethanolic KOH solution (1.05 M, 100 µL). After stirring for 2h, the reaction mixture was diluted with sat. $NaHCO_3$ (0.5 mL), acidified to pH 8 with HCl (0.5 M). and washed with ethyl acetate (3 x 2 mL). The aqueous layer was acidified to pH 1 with HCl (0.5 M) and extracted with ethyl acetate (3 x 4 mL). The combined organic layers were dried (Na_2SO_4) and the solvent was evaporated *in vacuo* to afford the product **85** as an off white solid (0.0282 g, 59%) and mixture of diastereomers: R*f*= 0.05 (CH_2Cl_2/MeOH, 95:5); ^{1}H NMR (700 MHz, $CDCl_3$) δ 4.67 (dd, ~0.3H, *J* = 8.0, 2.5 Hz, minor isomer, CH-5), 4.60 – 4.57 (m, ~0.7H, major isomer, CH-5), 3.66 – 3.54 (m, 1H, H-2), 3.52 – 3.44 (m, 1H, H-2), 3.24 – 3.09 (m, 1H, $COC\underline{H}CH_3$), 3.22-3.10 (m, 1H, thiirane CH), 2.54 (ddd, 1H, *J* = 11.5, 6.3, 1.4 Hz, thiirane $C\underline{H}_aH_b$),

2.46 – 2.21(m, 3H, thiirane $CH_a\underline{H}_b$, $C\underline{H}_aH_b$-3, $C\underline{H}_aH_b$-4), 2.12 – 1.98 (m, 2H, $CH_a\underline{H}_b$-3, $CH_a\underline{H}_b$-4), 1.47 – 1.35 (m, 3H, CH_3); ^{13}C NMR (176 MHz, $CDCl_3$) δ 176.3, 175.8, 175.6, 172.7, 172.5, 172.5, 59.9, 59.9, 59.7, 47.9, 47.8, 47.8, 45.9, 45.1, 44.5, 37.0, 36.5, 27.6, 27.6, 27.4, 24.8, 24.8, 24.8, 24.7, 24.4, 24.4, 17.8, 17.5, 17.1; HRMS (ES+) *m/z* calculated for $C_{10}H_{16}NO_3S$ $[M+H]^+$ 230.0851 found 230.0844.

References

(1) Talaro, K.; Talaro, A. *Foundation in Microbiology: Basic Principles*, 5th ed.; McGraw-Hill: New-York, 2005.

(2) Ron, S.; Shai, F.; Ron, M. Revised Estimates for the Number of Human and Bacteria Cells in the Body Ron. *PLoS Biol.* **2016**, *8*, e1002533.

(3) CDC. Antibiotic Resistance Threats in the United States, 2019. Atlanta, GA: U.S. Department of Health and Human Services, CDC. **2019**.

(4) American Chemical Society National Historic Chemical Landmarks. *Selman Waksman and Antibiotics*; 2005.

(5) Aminov, R. I. A Brief History of the Antibiotic Era: Lessons Learned and Challenges for the Future. *Front. Microbiol.* **2010**, *1*, 1–7.

(6) Sengupta, S.; Chattopadhyay, M. K.; Grossart, H. P. The Multifaceted Roles of Antibiotics and Antibiotic Resistance in Nature. *Front. Microbiol.* **2013**, *4*, 1–13.

(7) Otten, H. Domagk and the Development of the Sulphonamides. *J. Antimicrob. Chemother.* **1986**, *17*, 689–690.

(8) Williams, K. J. The Introduction of “chemotherapy” Using Arsphenamine - The First Magic Bullet. *J. R. Soc. Med.* **2009**, *102*, 343–348.

(9) Walsh, C. T.; Wencewicz, T. A. Prospects for New Antibiotics: A Molecule-Centered Perspective. *J. Antibiot. (Tokyo).* **2014**, *67*, 7–22.

(10) Dubos, R. J. Studies on a Bactericidal Agent Extracted from a Soil Bacillus: I. Preparation of the Agent. Its Activity in Vitro. *J. Exp. Med.* **1939**, *70*, 1–10.

(11) Van Epps, H. L. René Dubos: Unearthing Antibiotics. *J. Exp. Med.* **2006**, *203*, 259.

(12) Bhattacharjee, M. K. *Chemistry of Antibiotics and Related Drugs*; Springer: Switzerland, 2016.

(13) Chatwal, G. R.; Arora, M. *Pharmaceutical Chemistry-- Organic. Vol. II*, 2nd Ed.; Arora, M., Ed.; HIMALAYA BOOKS PVT. LTD.: New Dehli, 2007.

(14) Chellat, M. F.; Raguž, L.; Riedl, R. Targeting Antibiotic Resistance. *Angew. Chemie - Int. Ed.* **2016**, *55*, 6600–6626.

(15) Kiel, M. C.; Kaji, H.; Kaji, A. Ribosome Recycling: An Essential Process of Protein Synthesis. *Biochem. Mol. Biol. Educ.* **2007**, *35*, 40–44.

(16) Fernández-Villa, D.; Aguilar, M. R.; Rojo, L. Folic Acid Antagonists: Antimicrobial and Immunomodulating Mechanisms and Applications. *Int. J. Mol. Sci.* **2019**, *20*, 1–30.

(17) Lohani, C. R.; Taylor, R.; Palmer, M.; Taylor, S. D. Solid-Phase Total Synthesis of Daptomycin and Analogs. *Org. Lett.* **2015**, *17*, 748–751.

(18) Robbel, L.; Marahiel, M. A. Daptomycin, a Bacterial Lipopeptide Synthesized by a Nonribosomal Machinery. *J. Biol. Chem.* **2010**, *285*, 27501–27508.

(19) Walsh, C. Deconstructing Vancomycin. *Science (80-.).* **1999**, *284*, 442 LP – 443.

(20) Sauvage, E.; Terrak, M.; Ayala, J. A.; Charlier, P. The Penicillin-Binding Proteins : Structure and Role in Peptidoglycan Biosynthesis. **2008**, *32*, 234–258.

(21) Wood, J. M. Bacterial Responses to Osmotic Challenges. *J. Gen. Physiol.* **2015**, *145*, 381–388.

(22) Epand, R. M.; Walker, C.; Epand, R. F.; Magarvey, N. A. Molecular Mechanisms of Membrane Targeting Antibiotics. *Biochim. Biophys. Acta - Biomembr.* **2016**, *1858*, 980–987.

(23) Pira, A.; Scorciapino, M. A.; Bodrenko, I. V.; Bosin, A.; Acosta-Gutiérrez, S.; Ceccarelli, M. Permeation of β-Lactamase Inhibitors through the General Porins of Gram-Negative Bacteria. *Molecules* **2020**, *25*, 5747.

(24) Vergalli, J.; Bodrenko, I. I.; Masi, M.; Moynie, L.; Acosta-Guitierrez, S.; Naismith, J. H.; Davin-Regli, A.; Ceccarelli, M.; Van den Berg, B.; Winterhalter, M.; Pagès, M. Porins and Small-Molecule Translocation across the Outer Membrane of Gram-Negative Bacteria. *Nat. Rev. Microbiol.* **2020**, *18*, 164–176.

(25) Stephens, C.; Arismendi, T.; Wright, M.; Hartman, A.; Gonzalez, A.; Gill, M.; Pandori, M.; Hess, D. F Plasmids Are the Major Carriers of Antibiotic Resistance Genes in Human-Associated Commensal Escherichia Coli. *mSphere* **2020**, *5*, e00709-20.

(26) Darphorn, T. S.; Bel, K.; Koenders-van Sint Anneland, B. B.; Brul, S.; Ter Kuile, B. H. Antibiotic Resistance Plasmid Composition and Architecture in Escherichia Coli Isolates from Meat. *Sci. Rep.* **2021**, *11*, 2136.

(27) Motta, S. S.; Cluzel, P.; Aldana, M. Adaptive Resistance in Bacteria Requires Epigenetic Inheritance, Genetic Noise, and Cost of Efflux Pumps. *PLoS One* **2015**, *10*, 3–8.

(28) Lind, M. I.; Spagopoulou, F. Evolutionary Consequences of Epigenetic Inheritance. *Heredity (Edinb).* **2018**, *121*, 205–209.

(29) Adam, M.; Murali, B.; Glenn, N. O.; Potter, S. S. Epigenetic Inheritance Based Evolution of Antibiotic Resistance in Bacteria. *BMC Evol. Biol.* **2008**, *8*, 52.

(30) Cohen, N. R.; Ross, C. A.; Jain, S.; Shapiro, R. S.; Gutierrez, A.; Belenky, P.; Li, H.; Collins, J. J. A Role for the Bacterial GATC Methylome in Antibiotic Stress Survival. *Nat. Genet.* **2016**, *48*, 581–586.

(31) Peterson, E.; Kaur, P. Antibiotic Resistance Mechanisms in Bacteria: Relationships between Resistance Determinants of Antibiotic Producers, Environmental Bacteria, and Clinical Pathogens. *Front. Microbiol.* **2018**, *9*, 1–21.

(32) Drawz, S. M.; Papp-Wallace, K. M.; Bonomo, R. A. New β-Lactamase Inhibitors: A Therapeutic Renaissance in an MDR World. *Antimicrob. Agents Chemother.* **2014**, *58*, 1835–1846.

(33) Egorov, A. M.; Ulyashova, M. M.; Rubtsova, M. Y. Bacterial Enzymes and Antibiotic Resistance. *Acta Naturae* **2018**, *10*, 33–48.

(34) Markley, J. L.; Wencewicz, T. A. Tetracycline-Inactivating Enzymes. *Front. Microbiol.* **2018**, *9*, 1–22.

(35) Yang, W.; Moore, I. F.; Koteva, K. P.; Bareich, D. C.; Hughes, D. W.; Wright, G. D. TetX Is a Flavin-Dependent Monooxygenase Conferring Resistance to Tetracycline Antibiotics.

J. Biol. Chem. **2004**, *279*, 52346–52352.

(36) Fleming, A. On the Antibacterial Action of Cultures of a Penicillium, with Special Reference to Their Use in the Isolation of B. Influenzæ. *Br. J. Exp. Pathol.* **1929**, *10*, 226–236.

(37) Gale, R. T.; Brown, E. D. New Chemical Tools to Probe Cell Wall Biosynthesis in Bacteria. *Curr. Opin. Microbiol.* **2015**, *27*, 69–77.

(38) Zapun, A.; Contreras-Martel, C.; Vernet, T. Penicillin-Binding Proteins and β-Lactam Resistance. *FEMS Microbiol. Rev.* **2008**, *32*, 361–385.

(39) Tipper, D. J.; Strominger, J. L. Mechanism of Action of Penicillins: A Proposal Based on Their Structural Similarity to Acyl-D-Alanyl-D-Alanine. *Proc. Natl. Acad. Sci. U. S. A.* **1965**, *54*, 1133–1141.

(40) Llarrull, L. I.; Testero, S. A.; Fisher, J. F.; Mobashery, S.; Dame, N.; States, U. The Future of the Beta-lactams. *Curr. Opin. Microbiol.* **2010**, *13*, 551–557.

(41) Bush, K. Past and Present Perspective on Beta-Lactamases. *Antimicrob. Agents Chemother.* **2018**, 1–20.

(42) Tooke, Catherine L. Hinchliffe, P.; Bragginton, Elis C. Colenso, C. K.; Hirvonen, V. H. A.; Takebayashi, Y.; Spence, J. β-Lactamases and β-Lactamase Inhibitors in the 21st Century. *J. Mol. Biol.* **2019**, *18*, 3472–3500.

(43) Boyd, S. E.; Livermore, D. M.; Hooper, D. C.; Hope, W. W. Metallo-β-Lactamases: Structure, Function, Epidemiology, Treatment Options, and the Development Pipeline. *Antimicrob. Agents Chemother.* **2020**, *64*, e00397-20.

(44) Palzkill, T. Metallo-β-Lactamase Structure and Function. *Ann. N. Y. Acad. Sci.* **2013**, *1277*, 91–104.

(45) Palacios, A. R.; Mojica, M. F.; Giannini, E.; Taracila, M. A.; Bethel, C. R.; Alzari, P. M.; Otero, L. H.; Klinke, S.; Llarrull, L. I.; Bonomo, R. A.; Vila, A. J. The Reaction Mechanism of Metallo-β-Lactamases Is Tuned by the Conformation of an Active-Site Mobile Loop. *Antimicrob. Agents Chemother.* **2019**, *63*, e01754-18.

(46) Zhang, H.; Hao, Q. Crystal Structure of NDM-1 Reveals a Common B-lactam Hydrolysis Mechanism. *FASEB J.* **2011**, *25*, 2574–2582.

(47) King, D. T.; Worrall, L. J.; Gruninger, R.; Strynadka, N. C. J. New Delhi Metallo-β-Lactamase: Structural Insights into β-Lactam Recognition and Inhibition. *J. Am. Chem. Soc.* **2012**, *134*, 11362–11365.

(48) Drawz, S. M.; Bonomo, R. A. Three Decades of β-Lactamase Inhibitors. *Clin. Microbiol. Rev.* **2010**, *23*, 160–201.

(49) Mojica, M. F.; Bonomo, R. A.; Fast, W. B1-Metallo-β-Lactamases: Where Do We Stand? *Curr. Drug Targets* **2016**, *17*, 1029–1050.

(50) Meini, M. R.; Llarrull, L. I.; Vila, A. J. Evolution of Metallo-β-Lactamases: Trends Revealed by Natural Diversity and in Vitro Evolution. *Antibiotics* **2014**, *3*, 285–316.

(51) Watanabe, M.; Iyobe, S.; Inoue, M.; Mitsuhashi, S. Transferable Imipenem Resistance in Pseudomonas Aeruginosa. *Antimicrob. Agents Chemother.* **1991**, *35*, 147–151.

(52) Lauretti, L.; Riccio, M. L.; Mazzariol, A.; Cornaglia, G.; Amicosante, G.; Fontana, R.; Rossolini, G. M. Cloning and Characterization of BlaVIM, a New Integron-Borne Metallo-Beta-Lactamase Gene from a Pseudomonas Aeruginosa Clinical Isolate. *Antimicrob. Agents Chemother.* **1999**, *43*, 1584–1590.

(53) Yong, D.; Toleman, M. A.; Giske, C. G.; Cho, H. S.; Sundman, K.; Lee, K.; Walsh, T. R. Characterization of a New Metallo-β-Lactamase Gene, Bla NDM-1, and a Novel Erythromycin Esterase Gene Carried on a Unique Genetic Structure in Klebsiella Pneumoniae Sequence Type 14 from India. *Antimicrob. Agents Chemother.* **2009**, *53*, 5046–5054.

(54) Bebrone, C.; Anne, C.; Kerff, F.; Garau, G.; De Vriendt, K.; Lantin, R.; Devreese, B.; Van Beeumen, J.; Dideberg, O.; Frère, J.-M.; Galleni, M. Mutational Analysis of the Zinc- and Substrate-Binding Sites in the CphA Metallo-β-Lactamase from Aeromonas Hydrophila. *Biochem. J.* **2008**, *414*, 151–159.

(55) Makena, A.; Düzgün, A.; Brem, J.; McDonough, M. A.; Rydzik, A. M.; Abboud, M. I.; Saral, A.; Çiçek, A.; Sandalli, C.; Schofield, C. J. Comparison of Verona Integron-Borne Metallo-β-Lactamase (VIM) Variants Reveals Differences in Stability and Inhibition Profiles. *Antimicrob. Agents Chemother.* **2016**, *60*, 1377–1384.

(56) Linciano, P.; Tondi, D.; Cendron, L.; Gianquinto, E.; Spyrakis, F. Ten Years with New Delhi Metallo-β-Lactamase-1 (NDM-1): From Structural Insights to Inhibitor Design. *ACS Infect. Dis.* **2019**, *5*.

(57) Khan, A. U.; Maryam, L.; Zarrilli, R. Structure, Genetics and Worldwide Spread of New Delhi Metallo-β-Lactamase (NDM): A Threat to Public Health. *BMC Microbiol.* **2017**, *17*, 1–12.

(58) Voet, D.; Voet, J. G.; Pratt, C. W. *Fundamentals of Biochemistry Life at the Molecular Level*, 5th ed.; Voet, D., Voet, J. G., Pratt, C. W., Eds.; Wiley: Hoboken, NJ, 2016.

(59) Li, G.-B.; Abboud, M. I.; Brem, J.; Someya, H.; Lohans, C. T.; Yang, S.-Y.; Spencer, J.; Wareham, D. W.; McDonough, M. A.; Schofield, C. J. NMR-Filtered Virtual Screening Leads to Non-Metal Chelating Metallo-β-Lactamase Inhibitors. *Chem. Sci.* **2017**, *8*, 928–937.

(60) Ju, L.-C.; Cheng, Z.; Fast, W.; Bonomo, R. A.; Crowder, M. W. The Continuing Challenge of Metallo-β-Lactamase Inhibition: Mechanism Matters Lin-Cheng. *Trends Pharmacol Sci.* **2018**, *39*, 635–647.

(61) King, A. M.; Reid-Yu, S. A.; Wang, W.; King, D. T.; De Pascale, G.; Strynadka, N. C.; Walsh, T. R.; Coombes, B. K.; Wright, G. D. Aspergillomarasmine A Overcomes Metallo-β-Lactamase Antibiotic Resistance. *Nature* **2014**, *510*, 503–506.

(62) Liao, D.; Yang, S.; Wang, J.; Zhang, J.; Hong, B.; Wu, F.; Lei, X. Total Synthesis and Structural Reassignment of Aspergillomarasmine A. *Angew. Chemie Int. Ed.* **2016**, *55*, 4291–4295.

(63) Koteva, K.; King, A. M.; Capretta, A.; Wright, G. D. Total Synthesis and Activity of the Metallo-β-Lactamase Inhibitor Aspergillomarasmine A. *Angew. Chemie - Int. Ed.* **2016**, *55*, 2210–2212.

(64) Zhang, J.; Wang, S.; Wei, Q.; Guo, Q.; Bai, Y.; Yang, S.; Song, F.; Zhang, L.; Lei, X. Synthesis and Biological Evaluation of Aspergillomarasmine A Derivatives as Novel

NDM-1 Inhibitor to Overcome Antibiotics Resistance. *Bioorganic Med. Chem.* **2017**, *25*, 5133–5141.

(65) Rotondo, C. M.; Sychantha, D.; Koteva, K.; Wright, G. D. Suppression of β-Lactam Resistance by Aspergillomarasmine A Is Influenced by Both the Metallo-β-Lactamase Target and the Antibiotic Partner. *Antimicrob. Agents Chemother.* **2020**, *64*, e01386-19.

(66) Brem, J.; Van Berkel, S. S.; Zollman, D.; Lee, S. Y.; Gileadi, O.; McHugh, P. J.; Walsh, T. R.; McDonough, M. A.; Schofield, C. J. Structural Basis of Metallo-β-Lactamase Inhibition by Captopril Stereoisomers. *Antimicrob. Agents Chemother.* **2016**, *60*, 142–150.

(67) Krajnc, A.; Brem, J.; Hinchliffe, P.; Calvopiña, K.; Panduwawala, T. D.; Lang, P. A.; Kamps, J. J. A. G.; Tyrrell, J. M.; Widlake, E.; Saward, B. G.; Walsh, T. R.; Spencer, J.; Schofield, C. J. Bicyclic Boronate VNRX-5133 Inhibits Metallo- and Serine-β-Lactamases. *J. Med. Chem.* **2019**, *62*, 8544–8556.

(68) Hecker, S. J.; Reddy, K. R.; Lomovskaya, O.; Griffith, D. C.; Rubio-Aparicio, D.; Nelson, K.; Tsivkovski, R.; Sun, D.; Sabet, M.; Tarazi, Z.; Parkinson, J.; Totrov, M.; Boyer, S. H.; Glinka, T. W.; Pemberton, O. A.; Chen, Y.; Dudley, M. N. Discovery of Cyclic Boronic Acid QPX7728, an Ultrabroad-Spectrum Inhibitor of Serine and Metallo-β-Lactamases. *J. Med. Chem.* **2020**, *63*, 7491–7507.

(69) Parkova, A.; Lucic, A.; Krajnc, A.; Brem, J.; Calvopiña, K.; Langley, G. W.; McDonough, M. A.; Trapencieris, P.; Schofield, C. J. Broad Spectrum β-Lactamase Inhibition by a Thioether Substituted Bicyclic Boronate. *ACS Infect. Dis.* **2020**, *6*, 1398–1404.

(70) Everett, M.; Sprynski, N.; Davies, D. T.; Leiris, S.; Zalacain, M.; Morrissey, I.; Magnet, S.; Holden, K.; Warn, P. Discovery of a Novel Metallo- Beta-Lactamase Inhibitor That Potentiates Meropenem Activity Against Carbapenem Resistant Enterobacteriaceae. *Antimicrob. Agents Chemother.* **2018**, *62*, 1–11.

(71) Leiris, S.; Coelho, A.; Castandet, J.; Bayet, M.; Lozano, C.; Bougnon, J.; Bousquet, J.; Everett, M.; Lemonnier, M.; Sprynski, N.; Zalacain, M.; Pallin, T. D.; Cramp, M. C.; Jennings, N.; Raphy, G.; Jones, M. W.; Pattipati, R.; Shankar, B.; Sivasubrahmanyam, R.; Soodhagani, A. K.; Juventhala, R. R.; Pottabathini, N.; Pothukanuri, S.; Benvenuti, M.; Pozzi, C.; Mangani, S.; De Luca, F.; Cerboni, G.; Docquier, J. D.; Davies, D. T. SAR Studies Leading to the Identification of a Novel Series of Metallo-β-Lactamase Inhibitors for the Treatment of Carbapenem-Resistant Enterobacteriaceae Infections That Display Efficacy in an Animal Infection Model. *ACS Infect. Dis.* **2019**, *5*, 131–140.

(72) Wachino, J.; Jin, W.; Kimura, K.; Kurosaki, H.; Sato, A.; Arakawa, Y. Sulfamoyl Heteroarylcarboxylic Acids as Promising Metallo-Beta- Lactamase Inhibitors for Controlling Bacterial Carbapenem Resistance. *MBio* **2020**, *11*, 1–17.

(73) Chen, A. Y.; Thomas, P. W.; Stewart, A. C.; Bergstrom, A.; Cheng, Z.; Miller, C.; Bethel, C. R.; Marshall, S. H.; Credille, C. V; Riley, C. L.; Page, R. C.; Bonomo, R. A.; Crowder, M. W.; Tierney, D. L.; Fast, W.; Cohen, S. M. Dipicolinic Acid Derivatives as Inhibitors of New Delhi Metallo-β-Lactamase-1. *J. Med. Chem.* **2017**, *60*, 7267–7283.

(74) Chen, A. Y.; Thomas, P. W.; Cheng, Z.; Xu, N. Y.; Tierney, D. L.; Crowder, M. W.; Fast, W.; Cohen, S. M. Investigation of Dipicolinic Acid Isosteres for the Inhibition of Metallo-β-Lactamases. *ChemMedChem* **2019**, *14*, 1271–1282.

(75) Tehrani, K. H. M. E.; Bruchle, N. C.; Wade, N.; Mashayekhi, V.; Pesce, D.; van Haren, M.

J.; Martin, N. I. Small Molecule Carboxylates Inhibit Metallo-β-Lactamases. *ACS Infect. Dis.* **2020**, *6*, 1366–1371.

(76) Klingler, F. M.; Wichelhaus, T. A.; Frank, D.; Cuesta-Bernal, J.; El-Delik, J.; Müller, H. F.; Sjuts, H.; Göttig, S.; Koenigs, A.; Pos, K. M.; Pogoryelov, D.; Proschak, E. Approved Drugs Containing Thiols as Inhibitors of Metallo-β-Lactamases: Strategy to Combat Multidrug-Resistant Bacteria. *J. Med. Chem.* **2015**, *58*, 3626–3630.

(77) González, M. M.; Kosmopoulou, M.; Mojica, M. F.; Castillo, V.; Hinchliffe, P.; Pettinati, I.; Brem, J.; Schofield, C. J.; Mahler, G.; Bonomo, R. A.; Llarrull, L. I.; Spencer, J.; Vila, A. J. Bisthiazolidines: A Substrate-Mimicking Scaffold as an Inhibitor of the NDM-1 Carbapenemase. *ACS Infect. Dis.* **2016**, *1*, 544–554.

(78) Hinchliffe, P.; González, M. M.; Mojica, M. F.; González, J. M.; Castillo, V.; Saiz, C.; Kosmopoulou, M.; Tooke, C. L.; Llarrull, L. I.; Mahler, G.; Bonomo, R. A.; Vila, A. J.; Spencer, J. Cross-Class Metallo-β-Lactamase Inhibition by Bisthiazolidines Reveals Multiple Binding Modes. *Proc. Natl. Acad. Sci. U. S. A.* **2016**, *113*, E3745–E3754.

(79) Liu, B.; Trout, R. E. L.; Chu, G. H.; Mcgarry, D.; Jackson, R. W.; Hamrick, J. C.; Daigle, D. M.; Cusick, S. M.; Pozzi, C.; De Luca, F.; Benvenuti, M.; Mangani, S.; Docquier, J. D.; Weiss, W. J.; Pevear, D. C.; Xerri, L.; Burns, C. J. Discovery of Taniborbactam (VNRX-5133): A Broad-Spectrum Serine- And Metallo-β-Lactamase Inhibitor for Carbapenem-Resistant Bacterial Infections. *J. Med. Chem.* **2020**, *63*, 2789–2801.

(80) Abbas, H. A.; Kadry, A. A.; Shaker, G. H.; Goda, R. M. Impact of Specific Inhibitors on Metallo-β-Carbapenemases Detected in Escherichia Coli and Klebsiella Pneumoniae Isolates. *Microb. Pathog.* **2019**, *132*, 266–274.

(81) Wyrembak, P. N.; Babaoglu, K.; Pelto, R. B.; Shoichet, B. K.; Pratt, R. F. O-Aryloxycarbonyl Hydroxamates: New β-Lactamase Inhibitors That Cross-Link the Active Site. *J. Am. Chem. Soc.* **2007**, *129*, 9548–9549.

(82) Tilvawala, R.; Pratt, R. F. Covalent Inhibition of Serine β-Lactamases by Novel Hydroxamic Acid Derivatives. *Biochemistry* **2013**, *52*, 3712–3720.

(83) Thomas, P. W.; Cammarata, M.; Brodbelt, J. S.; Monzingo, A. F.; Pratt, R. F.; Fast, W. A Lysine-Targeted Affinity Label for Serine-β-Lactamase Also Covalently Modifies New Delhi Metallo-β-Lactamase-1 (NDM-1). *Biochemistry* **2019**, *58*, 2834–2843.

(84) Thomas, P. W.; Cammarata, M.; Brodbelt, J. S.; Fast, W. Covalent Inhibition of New Delhi Metallo-β-Lactamase-1 (NDM-1) by Cefaclor. *ChemBioChem* **2014**, *15*, 2541–2548.

(85) Thomas, P. W.; Spicer, T.; Cammarata, M.; Brodbelt, J. S.; Hodder, P.; Fast, W. An Altered Zinc-Binding Site Confers Resistance to a Covalent Inactivator of New Delhi Metallo-Beta-Lactamase-1 (NDM-1) Discovered by High-Throughput Screening. *Bioorganic Med. Chem.* **2013**, *21*, 3138–3146.

(86) Christopeit, T.; Albert, A.; Leiros, H. K. S. Discovery of a Novel Covalent Non-β-Lactam Inhibitor of the Metallo-β-Lactamase NDM-1. *Bioorganic Med. Chem.* **2016**, *24*, 2947–2953.

(87) Kurosaki, H.; Yamaguchi, Y.; Higashi, T.; Soga, K.; Matsueda, S.; Yumoto, H.; Misumi, S.; Yamagata, Y.; Arakawa, Y.; Goto, M. Irreversible Inhibition of Metallo-β-Lactamase (IMP-1) by 3-(3-Mercaptopropionylsulfanyl)Propionic Acid Pentafluorophenyl Ester. *Angew. Chemie* **2005**, *117*, 3929–3932.

(88) Bernier, S. G.; Lazarus, D. D.; Clark, E.; Doyle, B.; Labenski, M. T.; Thompson, C. D.; Westlin, W. F.; Hannig, G. A Methionine Aminopeptidase-2 Inhibitor, PPI-2458, for the Treatment of Rheumatoid Arthritis. *Proc. Natl. Acad. Sci. U. S. A.* **2004**, *101*, 10768–10773.

(89) Farrell, P. J.; Zopf, C. J.; Huang, H. J.; Balakrishna, D.; Holub, C.; Bilakovics, J.; Fanjul, A.; Matuszkiewicz, J.; Plonowski, A.; Rolzin, P.; Banerjee, U.; Ermolieff, J.; Cheruvallath, Z. S.; McBride, C.; Bartkowski, D.; Mazur, C.; Pachori, A.; Larson, C. J. Using Target Engagement Biomarkers to Predict Clinical Efficacy of MeTAP2 Inhibitors. *J. Pharmacol. Exp. Ther.* **2019**, *371*, 299–308.

(90) Ikejiri, M.; Bernardo, M. M.; Bonfil, R. D.; Toth, M.; Chang, M.; Fridman, R.; Mobashery, S. Potent Mechanism-Based Inhibitors for Matrix Metalloproteinases. *J. Biol. Chem.* **2005**, *280*, 33992–34002.

(91) Peng, Z.; Nguyen, T. T.; Song, W.; Anderson, B.; Wolter, W. R.; Schroeder, V. A.; Hesek, D.; Lee, M.; Mobashery, S.; Chang, M. Selective MMP-9 Inhibitor (R)-ND-336 Alone or in Combination with Linezolid Accelerates Wound Healing in Infected Diabetic Mice. *ACS Pharmacol. Transl. Sci.* **2021**, *4*, 107–117.

(92) Testero, S. A.; Granados, C.; Fernández, D.; Gallego, P.; Covaleda, G.; Reverter, D.; Vendrell, J.; Avilés, F. X.; Pallarès, I.; Mobashery, S. Discovery of Mechanism-Based Inactivators for Human Pancreatic Carboxypeptidase A from a Focused Synthetic Library. *ACS Med. Chem. Lett.* **2017**, *8*, 1122–1127.

(93) Lebedev, G. V.; Grigorenko, V. G.; Antipin, R. L.; Rubtsova, M. Y.; Egorov, A. M. Novel Chromogenic Substrate for Bacterial β-Lactamases Based on Cephalosporin Modified with an Epoxy Group. *Moscow Univ. Chem. Bull.* **2018**, *73*, 34–38.

(94) Trinh, T. D.; Smith, J. R.; Rybak, M. J. Parenteral Fosfomycin for the Treatment of Multidrug Resistant Bacterial Infections: The Rise of the Epoxide. *Pharmacotherapy* **2019**, *39*, 1077–1094.

(95) Cao, Y.; Peng, Q.; Li, S.; Deng, Z.; Gao, J. The Intriguing Biology and Chemistry of Fosfomycin: The Only Marketed Phosphonate Antibiotic. *RSC Adv.* **2019**, *9*, 42204–42218.

(96) Brown, A. G.; Corbett, D. F.; Goodacre, J.; Harbridge, J. B.; Howarth, T. T.; Ponsford, R. J.; Stirling, I.; King, T. J. Clavulanic Acid and Its Derivatives. Structure Elucidation of Clavulanic Acid and the Preparation of Dihydroclavulanic Acid, Isoclavulanic Acid, Esters and Related Oxidation Products. *J. Chem. Soc.* **1984**, *Perkin Tra*, 635–650.

(97) Fürstner, A.; Gastner, T. Total Synthesis of Cristatic Acid. *Org. Lett.* **2000**, *2*, 2467–2470.

(98) Ho, X. H.; Oh, H. J.; Jang, H. Y. Multistep Organocatalysis for the Asymmetric Synthesis of Multisubstituted Aldehydes from Allylic Alcohols. *European J. Org. Chem.* **2012**, No. 29, 5655–5659.

(99) Kim, T.; Han, Y. T.; An, H.; Kim, K.; Lee, J.; Suh, Y. G. Diastereoselective Total Synthesis of (-)-Galiellalactone. *J. Org. Chem.* **2015**, *80*, 12193–12200.

(100) O'Rourke, N. F.; Davies, K. A.; Wulff, J. E. Cascading Radical Cyclization of Bis-Vinyl Ethers: Mechanistic Investigation Reveals a 5-Exo/3-Exo /Retro-3-Exo/5-Exo Pathway. *J. Org. Chem.* **2012**, *77*, 8634–8647.

(101) Pine, S. H.; Shen, G. S.; Hoang, H. Ketone Methylenation Using the Tebbe and Wittig Reagents - A Comparison. *Synthesis (Stuttg).* **1991**, *1991*, 165–167.

(102) Corey, E. J.; Chaykovsky, M. Dimethyloxosulfonium Methylide ((CH3)2SOCH2) and Dimethylsulfonium Methylide ((CH3)2SCH2). Formation and Application to Organic Synthesis. *J. Am. Chem. Soc.* **1965**, *87*, 1353–1364.

(103) Horsfall, L. E.; Garau, G.; Lie, B. M. R.; Dideberg, O.; Schofield, C. J.; Galleni, M. Competitive Inhibitors of the CphA Metallo-β-Lactamase from Aeromonas Hydrophila □. **2007**, *51*, 2136–2142.

(104) Liénard, B. M. R.; Garau, G.; Horsfall, L.; Karsisiotis, A. I.; Damblon, C.; Lassaux, P.; Papamicael, C.; Roberts, G. C. K.; Galleni, M.; Dideberg, O.; Frère, J. M.; Schofield, C. J. Structural Basis for the Broad-Spectrum Inhibition of Metallo-β- Lactamases by Thiols. *Org. Biomol. Chem.* **2008**, *6*, 2282–2294.

(105) Kang, J. S.; Zhang, A. L.; Faheem, M.; Zhang, C. J.; Ai, N.; Buynak, J. D.; Welsh, W. J.; Oelschlaeger, P. Virtual Screening and Experimental Testing of B1 Metallo-β-Lactamase Inhibitors. *J. Chem. Inf. Model.* **2018**, *58*, 1902–1914.

(106) Jin, W. Bin; Xu, C.; Cheung, Q.; Gao, W.; Zeng, P.; Liu, J.; Chan, E. W. C.; Leung, Y. C.; Chan, T. H.; Wong, K. Y.; Chen, S.; Chan, K. F. Bioisosteric Investigation of Ebselen: Synthesis and in Vitro Characterization of 1,2-Benzisothiazol-3(2H)-One Derivatives as Potent New Delhi Metallo-β-Lactamase Inhibitors. *Bioorg. Chem.* **2020**, *100*, 103873.

(107) Toney, J. H.; Hammond, G. G.; Fitzgerald, P. M. D.; Sharma, N.; Balkovec, J. M.; Rouen, G. P.; Olson, S. H.; Hammond, M. L.; Greenlee, M. L.; Gao, Y. Succinic Acids as Potent Inhibitors of Plasmid-Borne IMP-1. **2001**, *276*, 31913–31918.

(108) Afzali-Ardakani, A.; Rapoport, H. L-Vinylglycine. *J. Org. Chem.* **1980**, *45*, 4817–4820.

(109) Wipf, P.; Uto, Y. Total Synthesis of the Putative Structure of the Marine Metabolite Trunkamide A. *Tetrahedron Lett.* **1999**, *40*, 5165–5169.

(110) Sakaitani, M.; Kurokawa, N.; Ohfune, Y. N-Carboxylate Ion Equivalent. II. Novel Transformations of N-Benzyloxycarbonyl (Z) Group and N-Allyloxycarbonyl Group into N-t-Butyldimethylsilyloxycarbonyl Intermediate. *Tetrahedron Lett.* **1986**, *27*, 3753–3754.

(111) Chalker, J. M.; Lercher, L.; Rose, N. R.; Schofield, C. J.; Davis, B. G. Conversion of Cysteine into Dehydroalanine Enables Access to Synthetic Histones Bearing Diverse Post-Translational Modifications. *Angew. Chemie - Int. Ed.* **2012**, *51*, 1835–1839.

(112) Chalker, J. M.; Gunnoo, S. B.; Boutureira, O.; Gerstberger, S. C.; Fernández-González, M.; Bernardes, G. J. L.; Griffin, L.; Hailu, H.; Schofield, C. J.; Davis, B. G. Methods for Converting Cysteine to Dehydroalanine on Peptides and Proteins. *Chem. Sci.* **2011**, *2*, 1666–1676.

(113) Pattabiraman, V. R.; McKinnie, S. M. K.; Vederas, J. C. Solid-Supported Synthesis and Biological Evaluation of the Lantibiotic Peptide Bis(Desmethyl) Lacticin 3147 A2. *Angew. Chemie - Int. Ed.* **2008**, *47*, 9472–9475.

(114) Corey, E. J.; Venkateswarlu, A. Protection of Hydroxyl Groups as Tert-Butyldimethylsilyl Derivatives. *J. Am. Chem. Soc.* **1972**, *94*, 6190–6191.

(115) Quéléver, G.; Burlet, S.; Garino, C.; Pietrancosta, N.; Laras, Y.; Kraus, J. L. Simple Coupling Reaction between Amino Acids and Weakly Nucleophilic Heteroaromatic

Amines. *J. Comb. Chem.* **2004**, *6*, 695–698.

(116) Baughman, T. W.; Sworen, J. C.; Wagener, K. B. The Facile Preparation of Alkenyl Metathesis Synthons. *Tetrahedron* **2004**, *60*, 10943–10948.

(117) Brenneman, J. B.; Ginn, J. D.; Sarko, C. R.; Westbrook, J.; Zhang, Z.; Yu, M.; Hopkins, T. D.; Lowe, M. D. Heterocyclic Carboxylic Acids as Acitvators of Soluble Guanylate Cyclase. WO 2016/014463 A1, 2016.

(118) Adachi, M.; Zhang, Y.; Leimkuhler, C.; Sun, B.; LaTour, J. V.; Kahne, D. E. Degradation and Reconstruction of Moenomycin A and Derivatives: Dissecting the Function of the Isoprenoid Chain. *J. Am. Chem. Soc.* **2006**, *128*, 14012–14013.

(119) Bhattacharyya, S.; Pathak, U.; Mathur, S.; Vishnoi, S.; Jain, R. Selective N-Alkylation of Primary Amines with R-NH2·HBr and Alkyl Bromides Using a Competitive Deprotonation/Protonation Strategy. *RSC Adv.* **2014**, *4*, 18229–18233.

(120) Pan, X.; Bai, S.; Yu, W.; Ding, D.; Zhao, D.; Liu, F. Efficient Synthesis of 3-R-Boc-Amino-4-(2,4,5-Trifluorophenyl)Butyric Acid. *Synth. Commun.* **2015**, *45*, 1451–1456.

(121) Corey, E. J.; Schmidt, G. Useful Procedures for the Oxidation of Alcohols Involving Pyridinium Dichromate in Approtic Media. *Tetrahedron Lett.* **1979**, *20*, 399–402.

(122) Chang, C.-D.; Waki, M.; Ahmad, M.; Meienhofer, J.; Lundell, E.; Haug, J. D. Preparation and Properties of Nalpha-9-Fluorenylmethyloxycarbonylamino Acids Bearing Tert.-Butyl Side Chain Protection. *Int. J. Pept. Protein Res.* **1980**, *15*, 59–66.

(123) Carpino, L. A.; Han, G. Y. The 9-Fluorenylmethoxycarbonyl Amino-Protecting Group. *J. Org. Chem.* **1972**, *37*, 3404–3409.

(124) Bagley, M. C.; Bashford, K. E.; Hesketh, C. L.; Moody, C. J. Total Synthesis of the Thiopeptide Promothiocin A. *J. Am. Chem. Soc.* **2000**, *122*, 3301–3313.

(125) Martin, S. F.; Chen, K. X.; Eary, C. T. An Enantioselective Total Synthesis of (+)-Geissoschizine. *Org. Lett.* **1999**, *1*, 79–81.

(126) Vishwanatha, T. M.; Samarasimhareddy, M.; Sureshbabu, V. V. Facile N-Urethane-Protected α-Amino/Peptide Thioacid Preparation Using EDC and Na 2S. *Synlett* **2012**, No. 1, 89–92.

(127) Porto, R. S.; Vasconcellos, M. L. A. A.; Ventura, E.; Coelho, F. Diastereoselective Epoxidation of Allylic Diols Derived from Baylis-Hillman Adducts. *Synthesis (Stuttg).* **2005**, No. 14, 2297–2306.

(128) Yang, D.; Wong, M. K.; Yip, Y. C. Epoxidation of Olefins Using Methyl(Trifluoromethyl)Dioxirane Generated in Situ. *J. Org. Chem.* **1995**, *60*, 3887–3889.

(129) Nicolaou, K. C.; Estrada, A. A.; Zak, M.; Lee, S. H.; Safina, B. S. A Mild and Selective Method for the Hydrolysis of Esters with Trimethyltin Hydroxide. *Angew. Chemie Int. Ed.* **2005**, *44*, 1378–1382.

(130) Cushman, D. W.; Ondetti, M. A. History of the Design of Captopril and Related Inhibitors of Angiotensin Converting Enzyme. *Hypertension* **1991**, *17*, 589–592.

(131) Ferreira, S. H.; Bartelt, D. C.; Greene, L. J. Isolation of Bradykinin-Potentiating Peptides from Bothrops Jararaca Venom. *Biochemistry* **1970**, *9*, 2583–2593.

(132) Ondetti, M. A.; Rubin, B.; Cushman, D. W. Design of Specific Inhibitors of Angiotensin-Converting Enzyme: New Class of Orally Active Antihypertensive Agents. *Science (80-.).* **1977**, *196*, 441–444.

(133) Cushman, D. W.; Cheung, H. S.; Sabo, E. F.; Ondetti, A. Design of Potent Competitive Inhibitors of Angiotensin-Converting Enzyme. Carboxyalkanoyl and Mercaptoalkanoyl Amino Acids. *Biochemistry* **1977**, *16*, 5484–5491.

(134) Byers, L. D.; Wolfenden, R. Binding of the By-Product Analog Benzylsuccinic Acid by Carboxypeptidase A. *Biochemistry* **1973**, *12*, 2070–2078.

(135) Shimazaki, M.; Hasegawa, J.; Kan, K.; Nomura, K.; Nose, Y.; Kondo, H.; Ohashi, T.; Watanabe, K. Synthesis of Captopril Starting from Optically Active Beta-Hydroxy Acid. *Chem. Pharm. Bull.* **1982**, *30*, 3139–3146.

(136) Natesh, R.; Schwager, S. L. U.; Sturrock, E. D. Crystal Structure of the Human Angiotensin-Converting Enzyme – Lisinopril Complex. *Nature* **2003**, *421*, 551–554.

(137) King, D.; Strynadka, N. Crystal Structure of New Delhi Metallo-β-Lactamase Reveals Molecular Basis for Antibiotic Resistance. *Protein Sci.* **2011**, *20*, 1484–1491.

(138) Antony, J.; Gresh, N.; Olsen, L.; Hemmingsen, L.; Schofield, C. J.; Bauer, R. Binding of D- and L-Captopril Inhibitors to Metallo-β-Lactamase Studied by Polarizable Molecular Mechanics and Quantum Mechanics. *J. Comput. Chem.* **2002**, *23*, 1281–1296.

(139) Heinz, U.; Bauer, R.; Wommer, S.; Meyer-Klaucke, W.; Papamichaels, C.; Bateson, J.; Adolph, H. W. Coordination Geometries of Metal Ions in D- or L-Captopril-Inhibited Metallo-β-Lactamases. *J. Biol. Chem.* **2003**, *278*, 20659–20666.

(140) Büttner, D.; Kramer, J. S.; Klingler, F. M.; Wittmann, S. K.; Hartmann, M. R.; Kurz, C. G.; Kohnhäuser, D.; Weizel, L.; Brüggerhoff, A.; Frank, D.; Steinhilber, D.; Wichelhaus, T. A.; Pogoryelov, D.; Proschak, E. Challenges in the Development of a Thiol-Based Broad-Spectrum Inhibitor for Metallo-β-Lactamases. *ACS Infect. Dis.* **2018**, *4*, 360–372.

(141) Ma, G.; Wang, S.; Wu, K.; Zhang, W.; Ahmad, A.; Hao, Q.; Lei, X.; Zhang, H. Structure-Guided Optimization of D-Captopril for Discovery of Potent NDM-1 Inhibitors. *Bioorganic Med. Chem.* **2021**, *29*, 115902.

(142) Li, N.; Xu, Y.; Xia, Q.; Bai, C.; Wang, T.; Wang, L.; He, D.; Xie, N.; Li, L.; Wang, J.; Zhou, H. G.; Xu, F.; Yang, C.; Zhang, Q.; Yin, Z.; Guo, Y.; Chen, Y. Simplified Captopril Analogues as NDM-1 Inhibitors. *Bioorganic Med. Chem. Lett.* **2014**, *24*, 386–389.

(143) Meng, Z.; Tang, M. L.; Yu, L.; Liang, Y.; Han, J.; Zhang, C.; Hu, F.; Yu, J. M.; Sun, X. Novel Mercapto Propionamide Derivatives with Potent New Delhi Metallo-β-Lactamase-1 Inhibitory Activity and Low Toxicity. *ACS Infect. Dis.* **2019**, *5*, 903–916.

(144) Choo, H. Y. P.; Yoon, H. R.; Park, H. S.; Kim, D. H.; Park, J.; Kim, D. H. Epoxyalkanoyls as Novel ACE Inhibitors. *Arch. Pharm. Res.* **1998**, *21*, 168–173.

(145) Salimraj, R.; Hinchliffe, P.; Kosmopoulou, M.; Tyrrell, J. M.; Brem, J.; van Berkel, S. S.; Verma, A.; Owens, R. J.; McDonough, M. A.; Walsh, T. R.; Schofield, C. J.; Spencer, J. Crystal Structures of VIM-1 Complexes Explain Active Site Heterogeneity in VIM-Class Metallo-β-Lactamases. *FEBS J.* **2019**, *286*, 169–183.

(146) Concha, N. O.; Janson, C. A.; Rowling, P.; Pearson, S.; Cheever, C. A.; Clarke, B. P.; Lewis, C.; Galleni, M.; Frère, J.-M.; Payne, D. J.; Bateson, J. H.; Abdel-Meguid, S. S.

Crystal Structure of the IMP-1 Metallo β-Lactamase from Pseudomonas Aeruginosa and Its Complex with a Mercaptocarboxylate Inhibitor: Binding Determinants of a Potent, Broad-Spectrum Inhibitor,. *Biochemistry* **2000**, *39*, 4288–4298.

(147) Carfi, A.; Pares, S.; Duée, E.; Galleni, M.; Duez, C.; Frère, J. M.; Dideberg, O. The 3-D Structure of a Zinc Metallo-Beta-Lactamase from Bacillus Cereus Reveals a New Type of Protein Fold. *EMBO J.* **1995**, *14*, 4914–4921.

(148) Concha, N. O.; Rasmussen, B. A.; Bush, K.; Herzberg, O. Crystal Structure of the Wide-Spectrum Binuclear Zinc β-Lactamase from Bacteroides Fragilis</Em>. *Structure* **1996**, *4*, 823–836.

(149) Dunetz, J. R.; Magano, J.; Weisenburger, G. A. Large-Scale Applications of Amide Coupling Reagents for the Synthesis of Pharmaceuticals. *Org. Process Res. Dev.* **2016**, *20*, 140–177.

(150) Knight, S. D.; Overman, L. E.; Pairaudeau, G. Enantioselective Total Synthesis of (−)-Strychnine. *J. Am. Chem. Soc.* **1993**, *115*, 9293–9294.

(151) Chekler, E. L. P.; Unwalla, R.; Khan, T. A.; Tangirala, R. S.; Johnson, M.; St. Andre, M.; Anderson, J. T.; Kenney, T.; Chiparri, S.; McNally, C.; Kilbourne, E.; Thompson, C.; Nagpal, S.; Weber, G.; Schelling, S.; Owens, J.; Morris, C. A.; Powell, D.; Verhoest, P. R.; Gilbert, A. M. 1-(2-Hydroxy-2-Methyl-3-Phenoxypropanoyl) Indoline-4-Carbonitrile Derivatives As Potent and Tissue Selective Androgen Receptor Modulators. *J. Med. Chem.* **2014**, *57*, 2462–2471.

(152) Orrling, K. M.; Marzahn, M. R.; Gutiérrez-de-Terán, H.; Åqvist, J.; Dunn, B. M.; Larhed, M. α-Substituted Norstatines as the Transition-State Mimic in Inhibitors of Multiple Digestive Vacuole Malaria Aspartic Proteases. *Bioorganic Med. Chem.* **2009**, *17*, 5933–5949.

(153) Gooyit, M.; Lee, M.; Hesek, D.; Boggess, B.; Oliver, A. G.; Fridman, R.; Mobashery, S.; Chang, M. Synthesis, Kinetic Characterization and Metabolism of Diastereomeric 2-(1-(4-Phenoxyphenylsulfonyl)Ethyl)Thiiranes as Potent Gelatinase and MT1-MMP Inhibitors. *Chem. Biol. Drug Des.* **2009**, *74*, 535–546.

(154) Shendage, D. M.; Fröhlich, R.; Haufe, G. Highly Efficient Stereoconservative Amidation and Deamidation of α-Amino Acids. *Org. Lett.* **2004**, *6*, 3675–3678.

(155) Ghosh, A. K.; Liu, C. Total Synthesis of Antitumor Depsipeptide (-)-Doliculide. *Org. Lett.* **2001**, *3*, 635–638.

(156) O'Daniel, P. I.; Peng, Z.; Pi, H.; Testero, S. A.; Ding, D.; Spink, E.; Leemans, E.; Boudreau, M. A.; Yamaguchi, T.; Schroeder, V. A.; Wolter, W. R.; Llarrull, L. I.; Song, W.; Lastochkin, E.; Kumarasiri, M.; Antunes, N. T.; Espahbodi, M.; Lichtenwalter, K.; Suckow, M. A.; Vakulenko, S.; Mobashery, S.; Chang, M. Discovery of a New Class of Non-β-Lactam Inhibitors of Penicillin-Binding Proteins with Gram-Positive Antibacterial Activity. *J. Am. Chem. Soc.* **2014**, *136*, 3664–3672.

Appendices

Appendix A: Spectra

^{1}H NMR (400 MHz, $CDCl_3$)

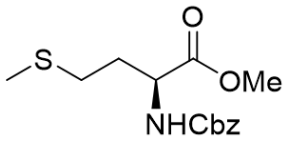

19b

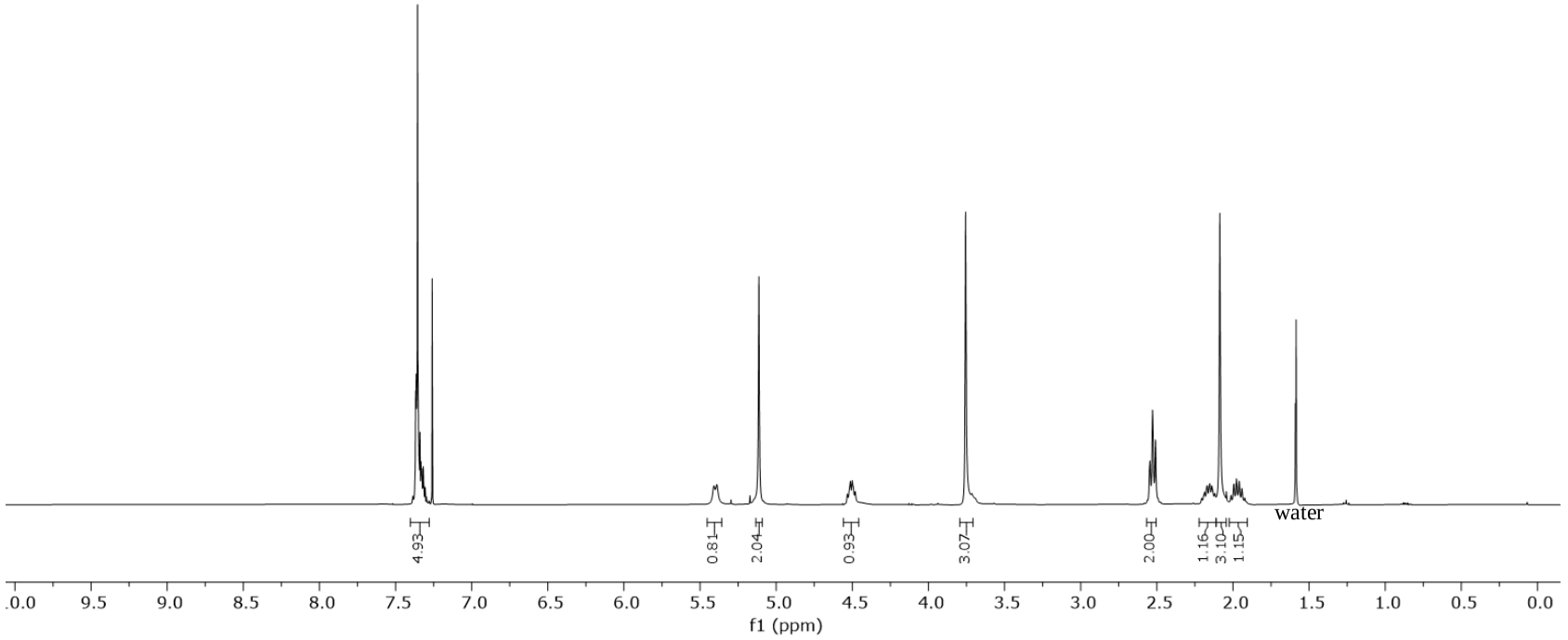

^{13}C NMR (126 MHz, $CDCl_3$)

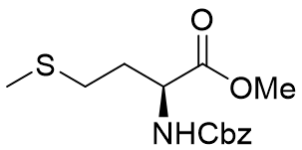

19b

^{1}H NMR (400 MHz, CDCl3)

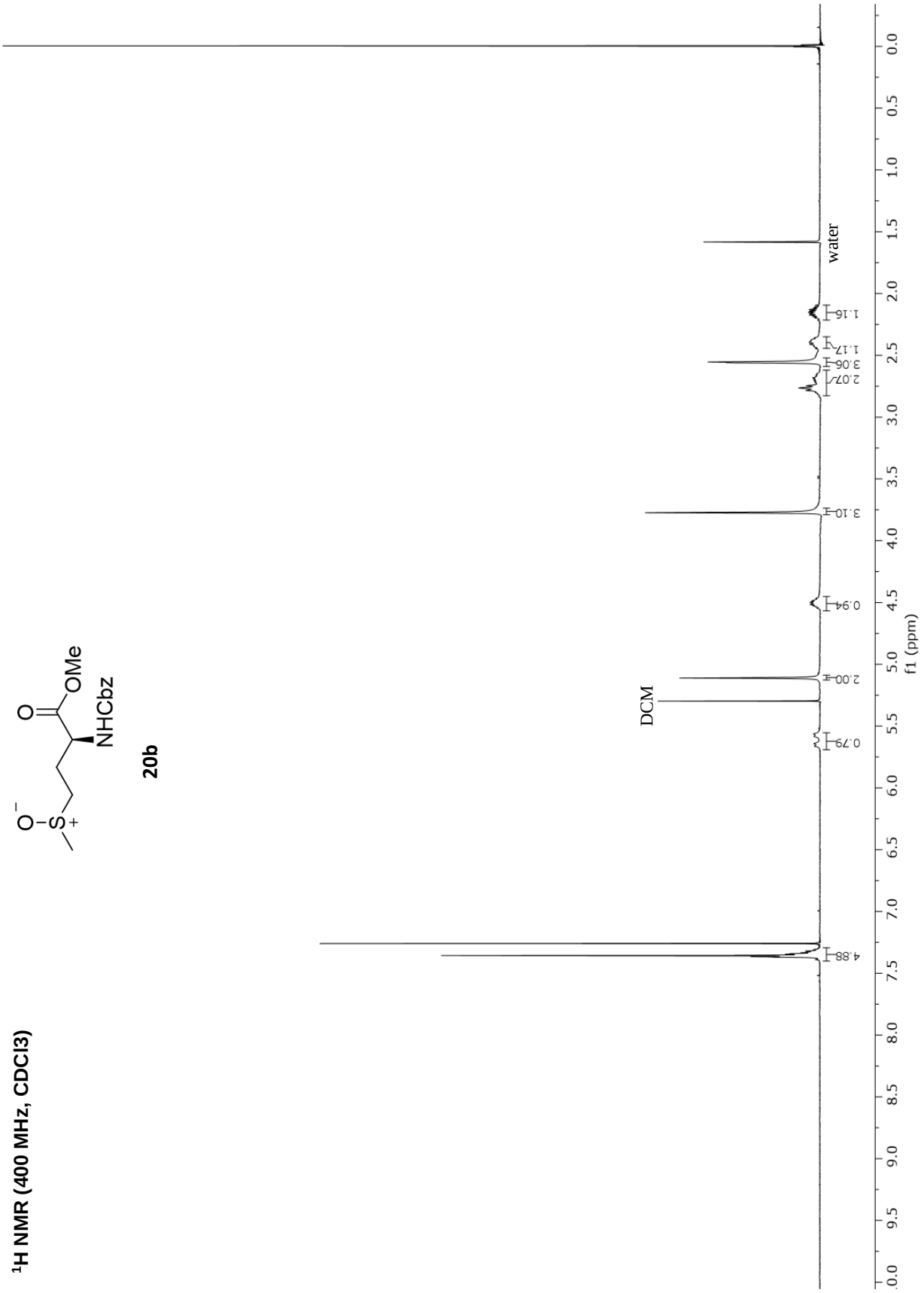

^{13}C NMR (126 MHz, $CDCl_3$)

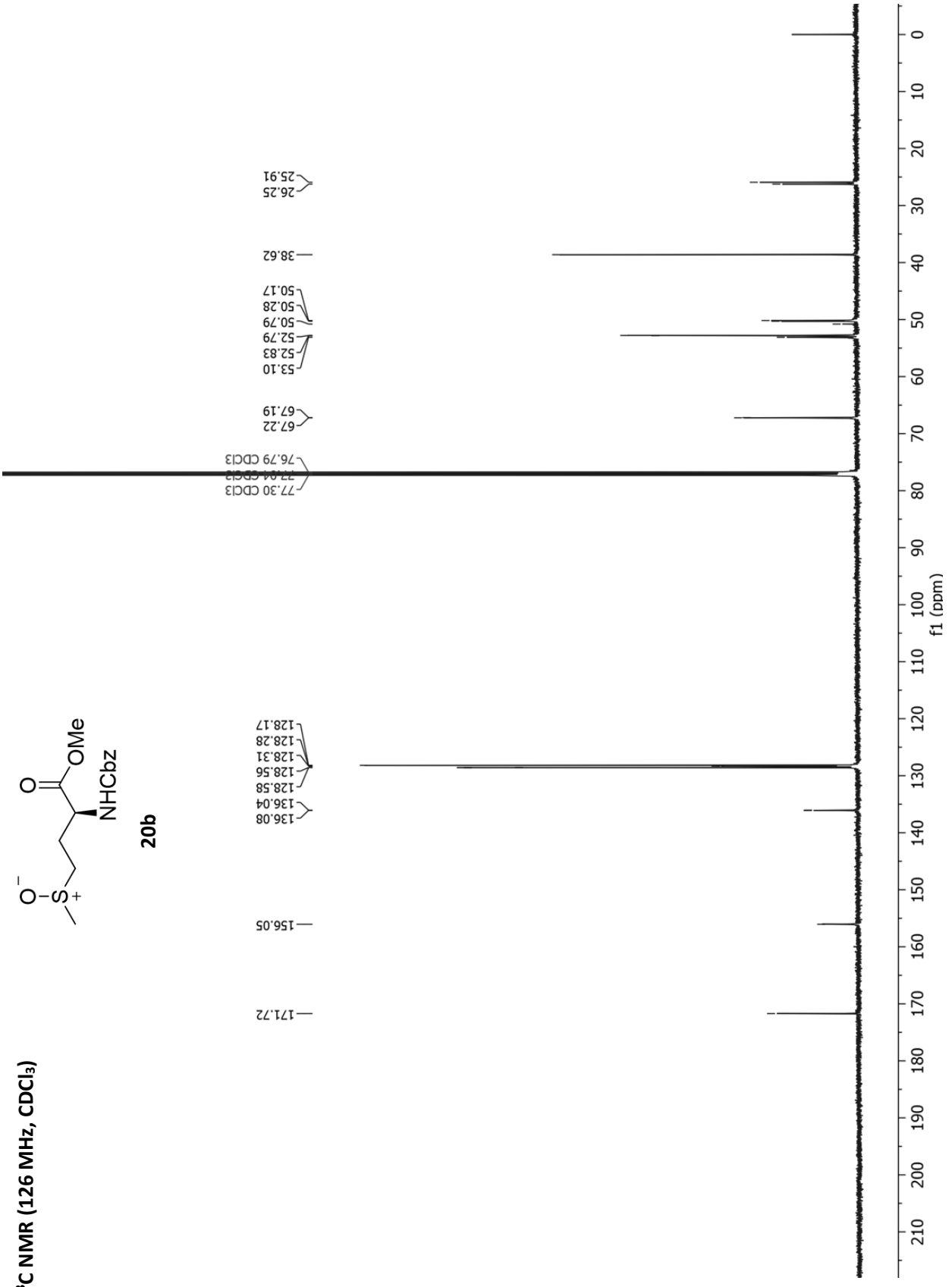

^{1}H NMR (400 MHz, $CDCl_3$)

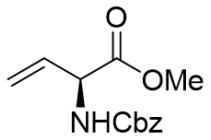

21b

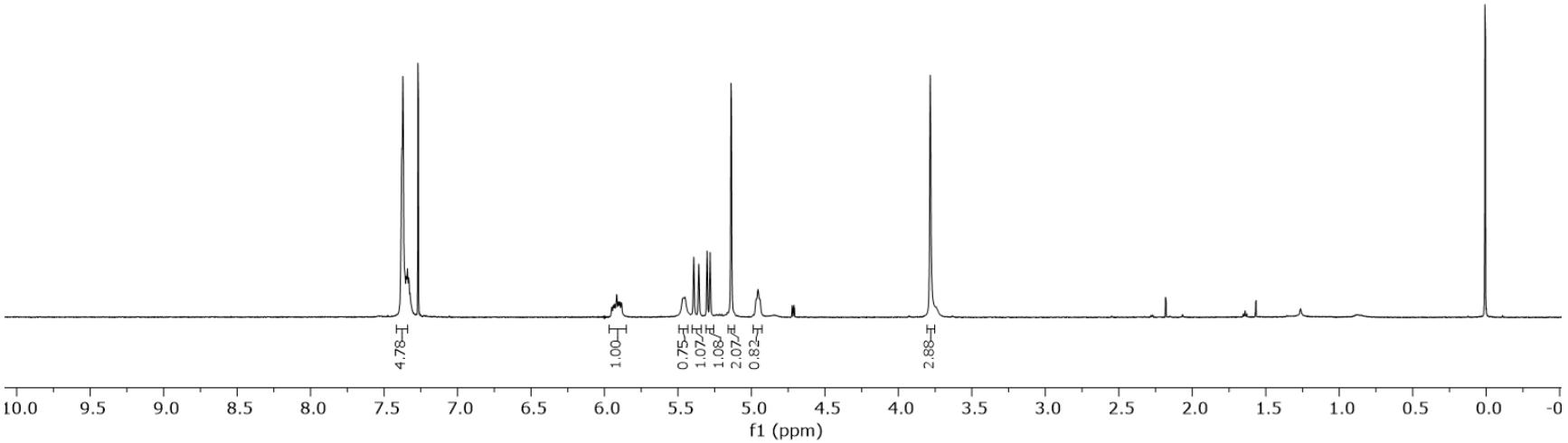

^{13}C NMR (126 MHz, $CDCl_3$)

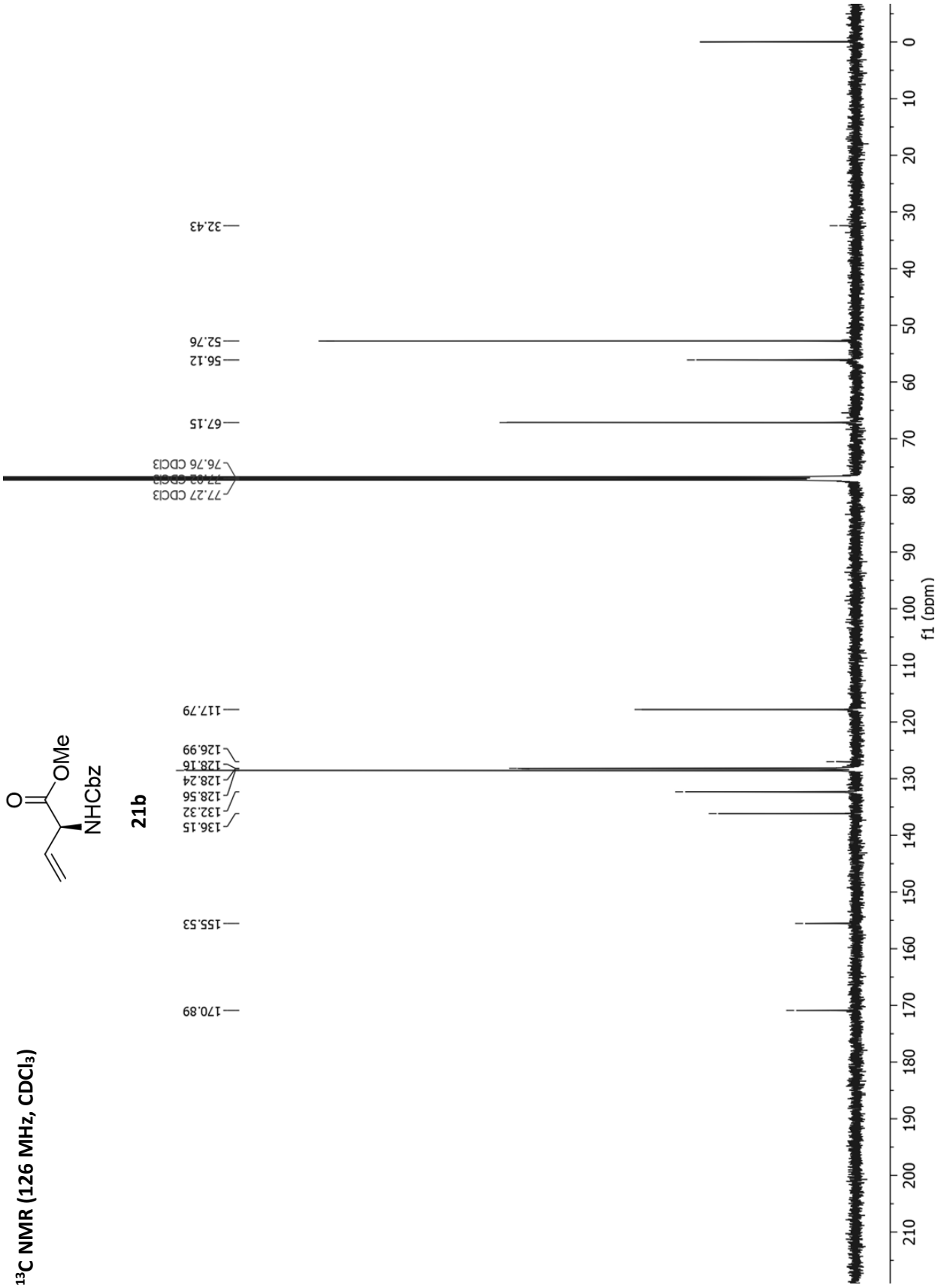

^{1}H NMR (400 MHz, D_2O)

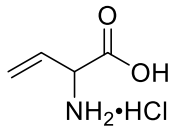

22b

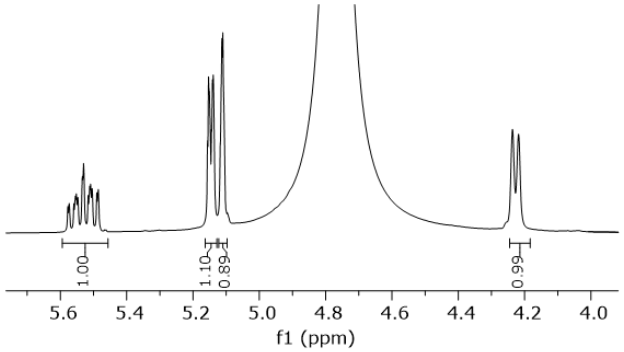

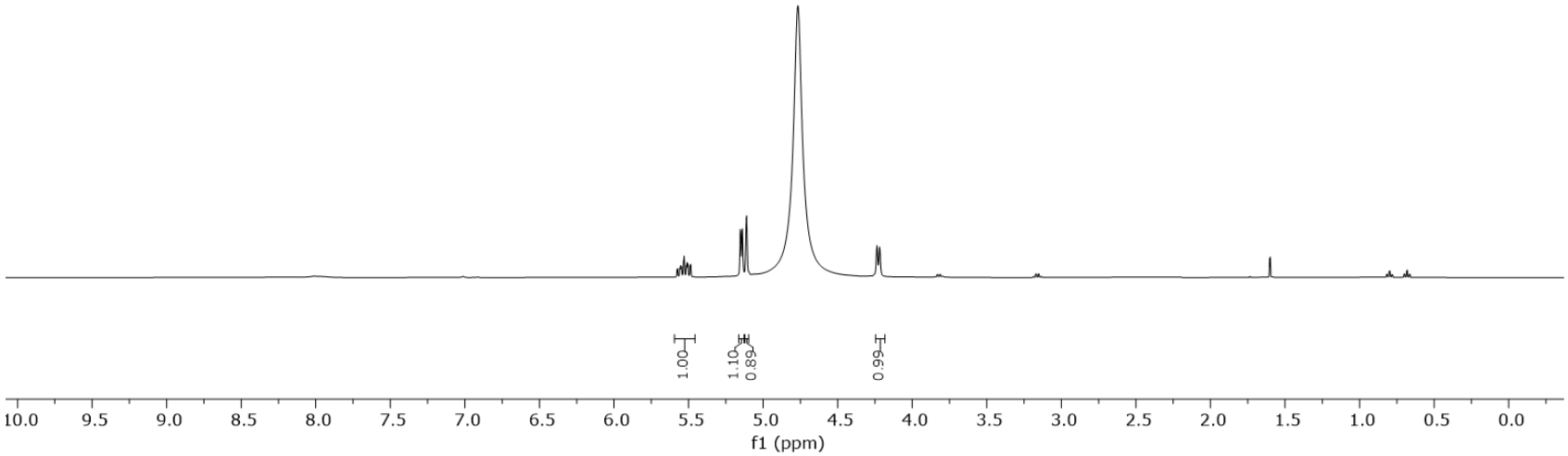

^{13}C NMR (126 MHz, D_2O)

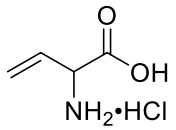

22b

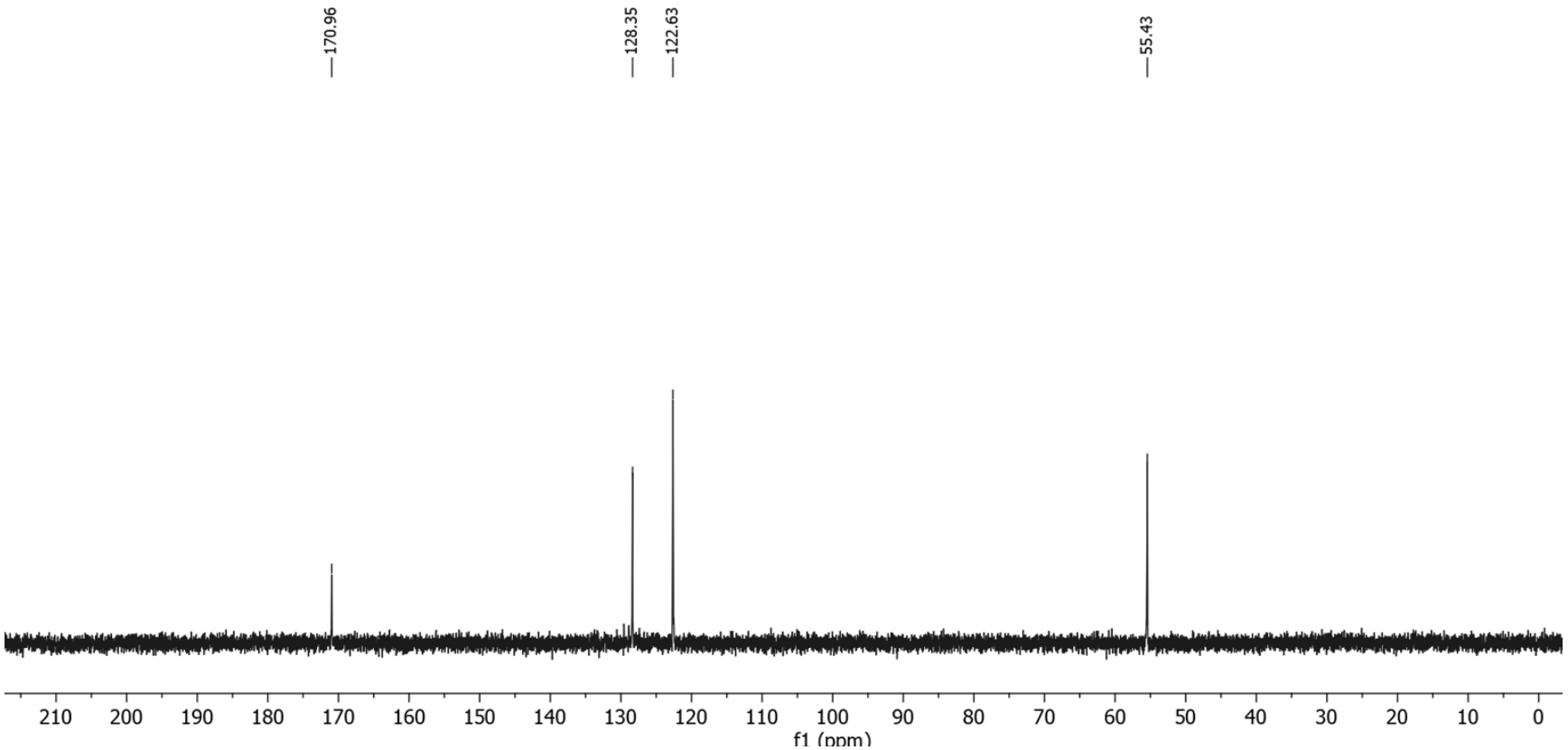

^{1}H NMR (400 MHz, D_2O)

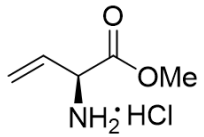

23b

^{13}C NMR (126 MHz, $CDCl_3$)

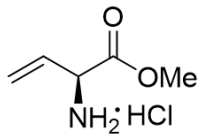

23b

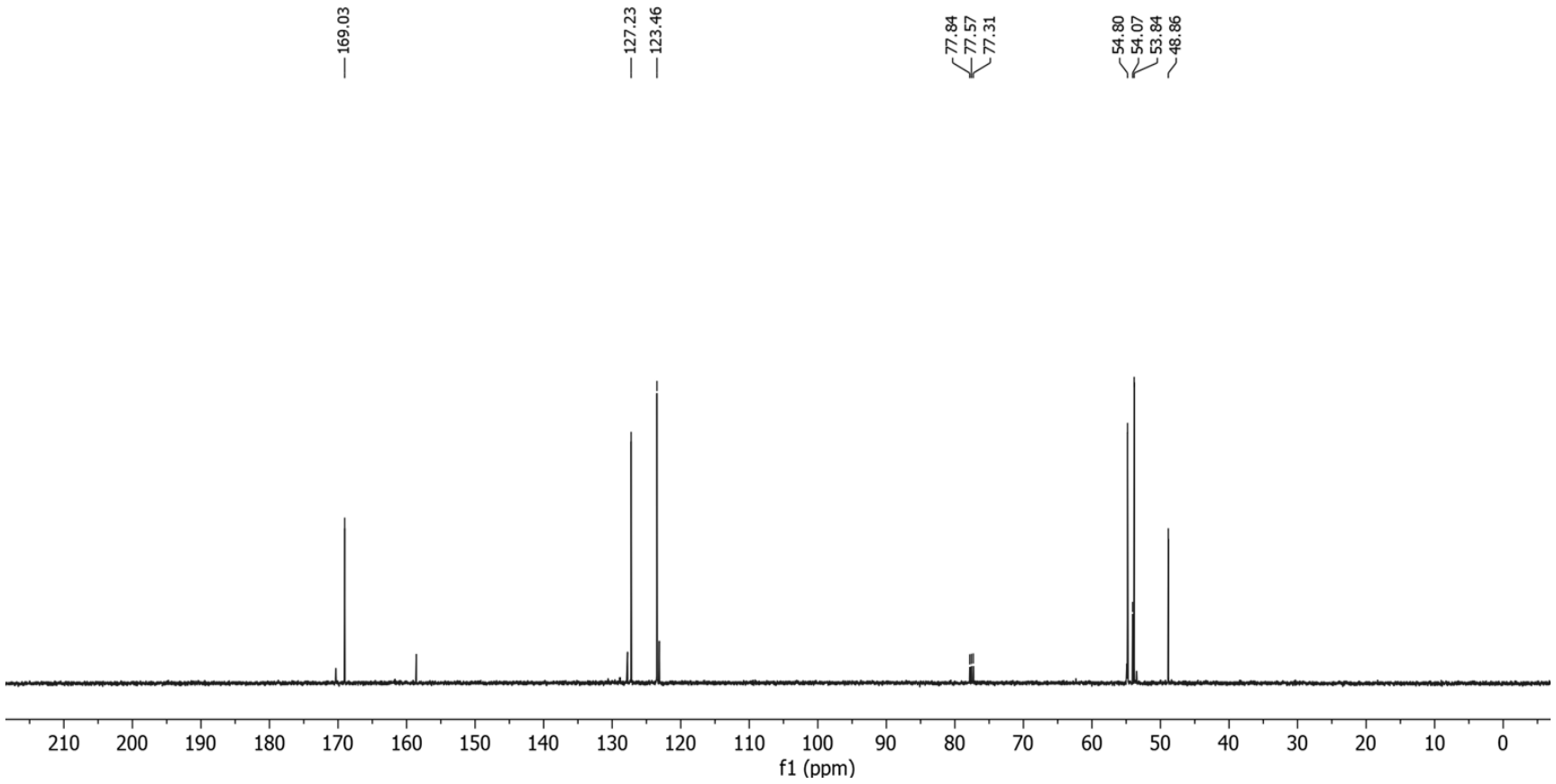

^{1}H NMR (400 MHz, $CDCl_3$)

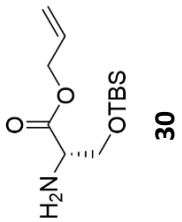

30

^{1}H NMR (400 MHz, $CDCl_3$)

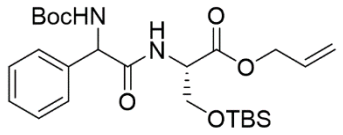

35

^{13}C NMR (126 MHz, $CDCl_3$)

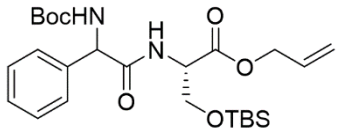

35

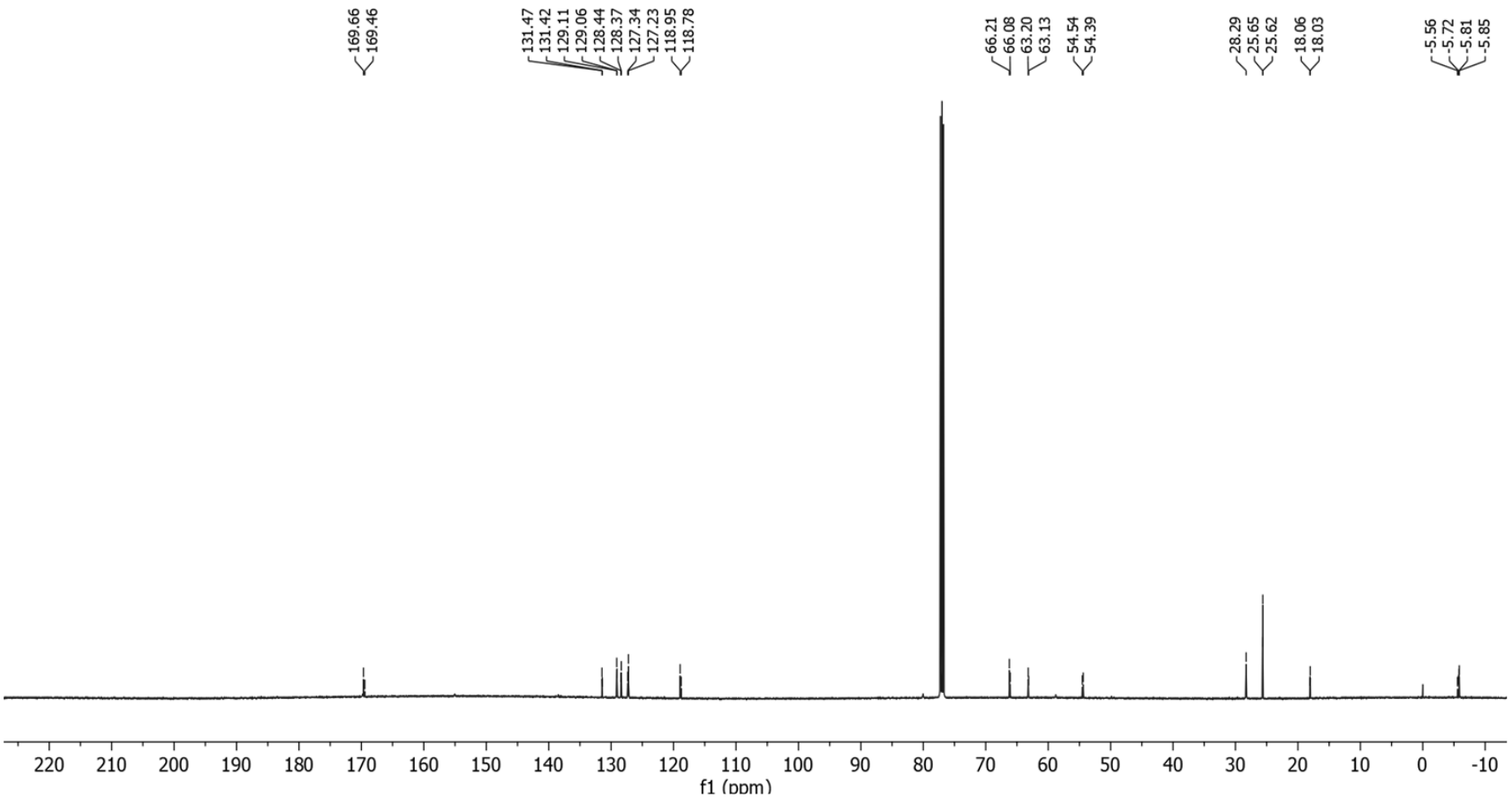

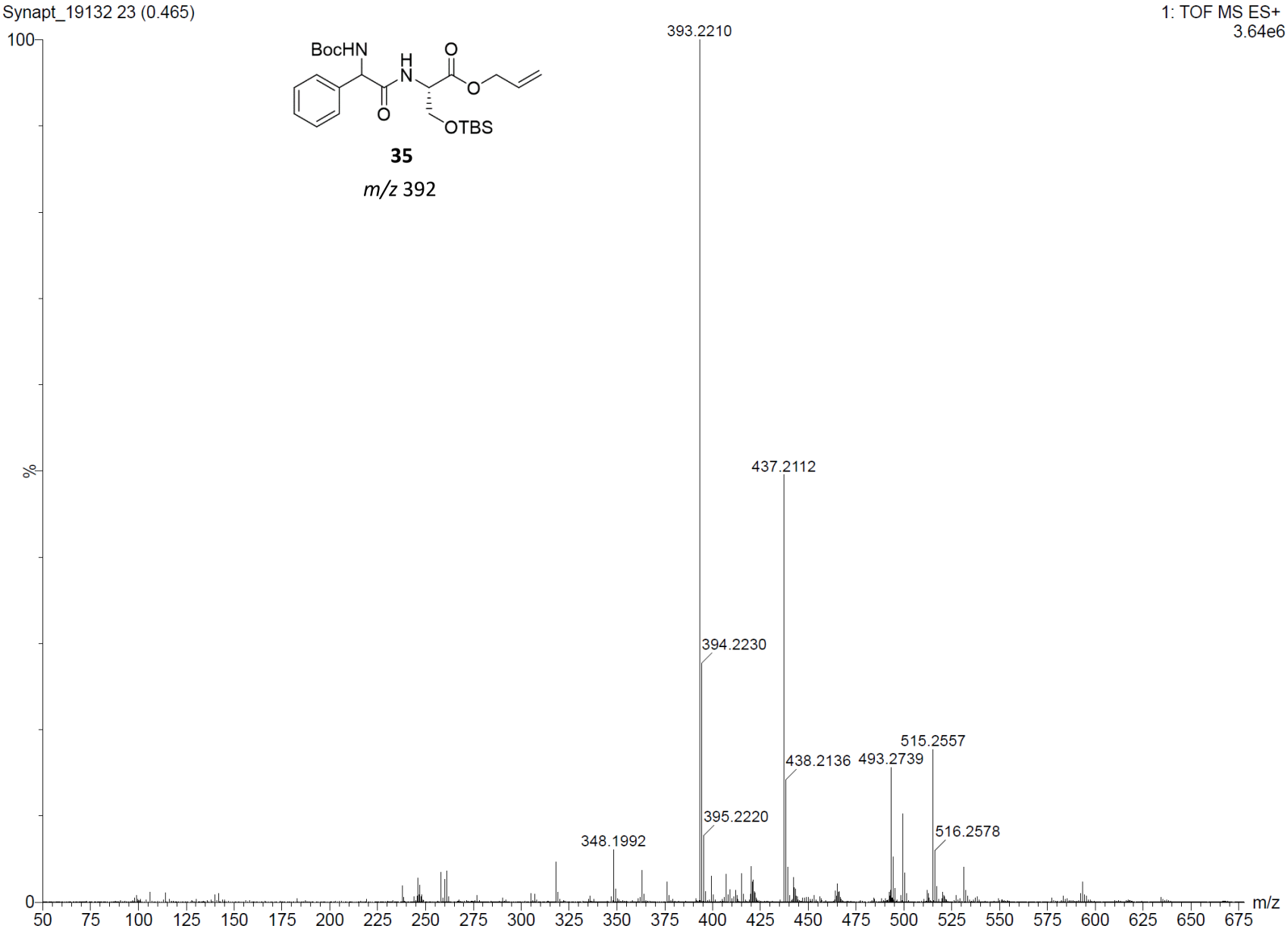
Synapt_19132 23 (0.465)
1: TOF MS ES+
3.64e6
BocHN
H
N
O
O
O
O
OTBS
35
m/z 392
393.2210
437.2112
394.2230
438.2136
493.2739
515.2557
395.2220
516.2578
348.1992
100
%
0
50 75 100 125 150 175 200 225 250 275 300 325 350 375 400 425 450 475 500 525 550 575 600 625 650 675
m/z

^{1}H NMR (400 MHz, $CDCl_3$)

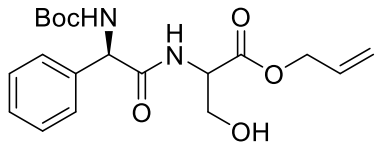

36

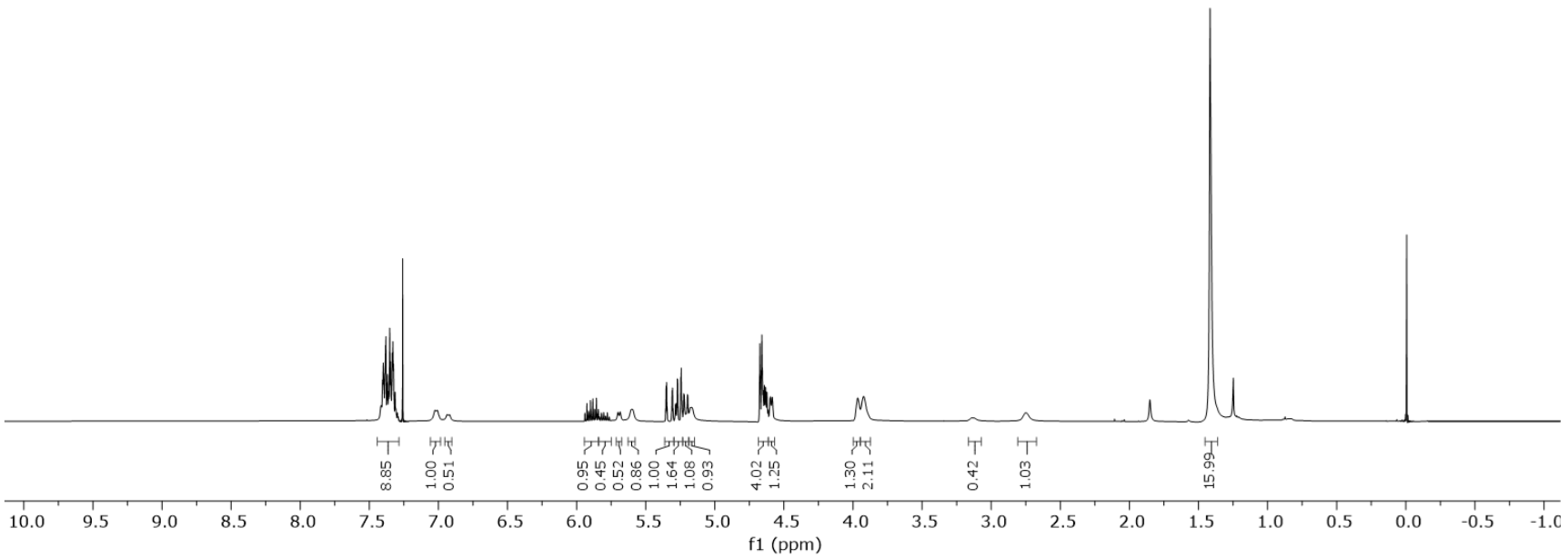

^{13}C NMR (126 MHz, $CDCl_3$)

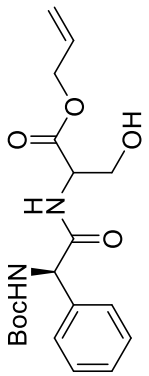

36

^{1}H NMR (400 MHz, $CDCl_3$)

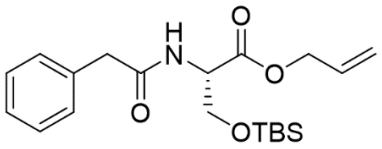

41

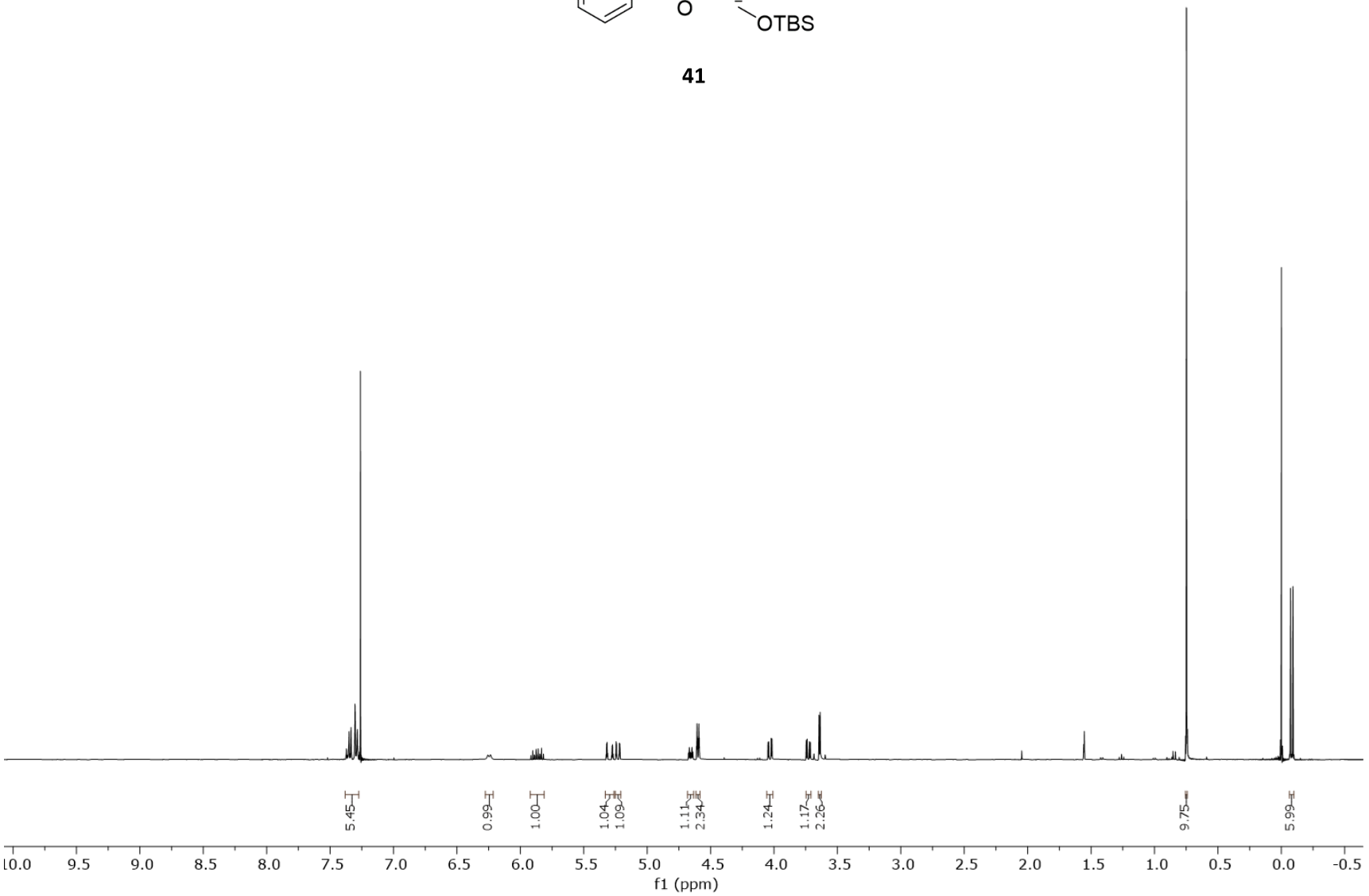

^{13}C NMR (101 MHz, $CDCl_3$)

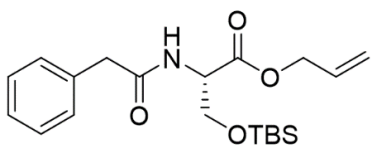

41

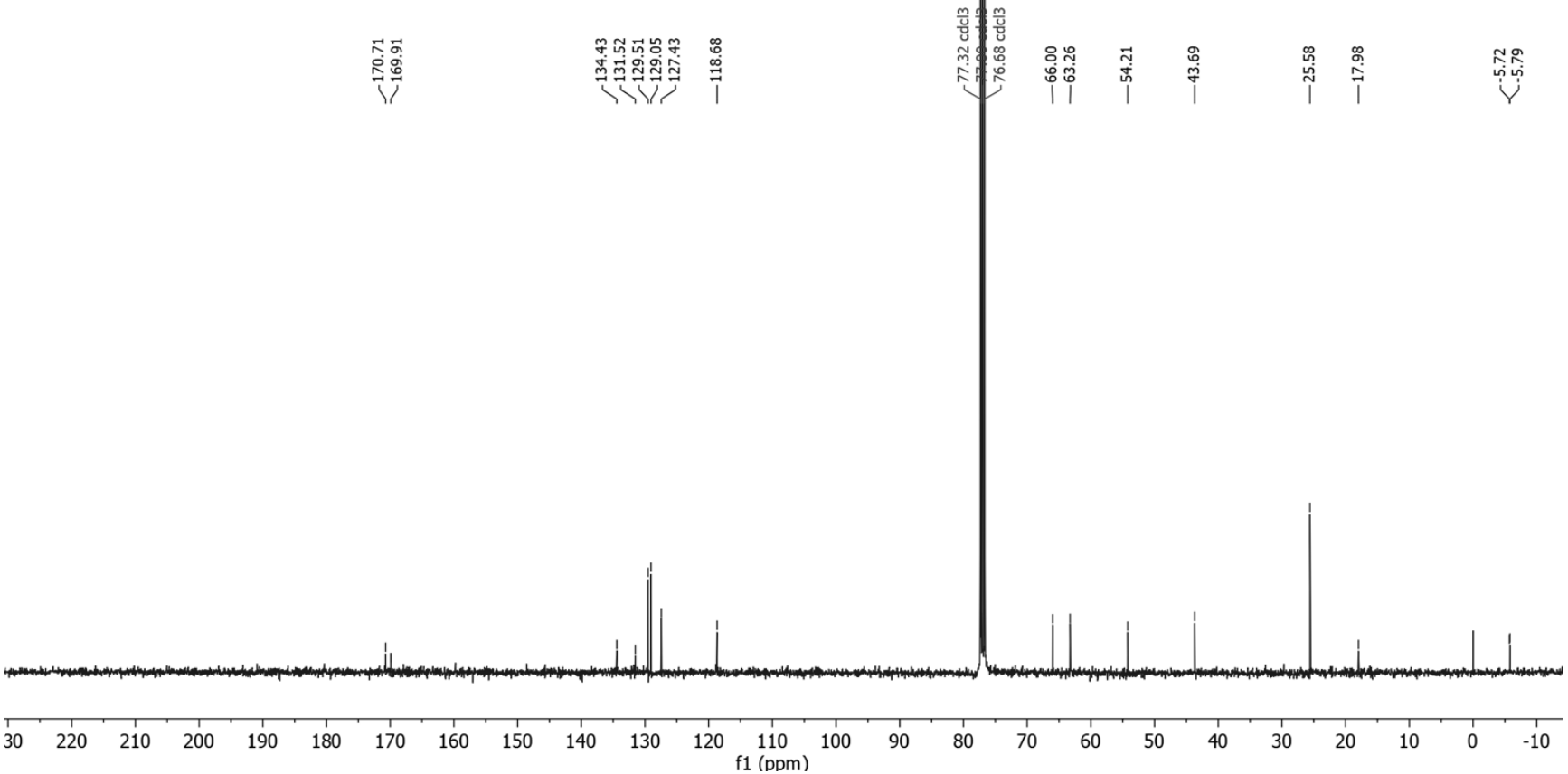

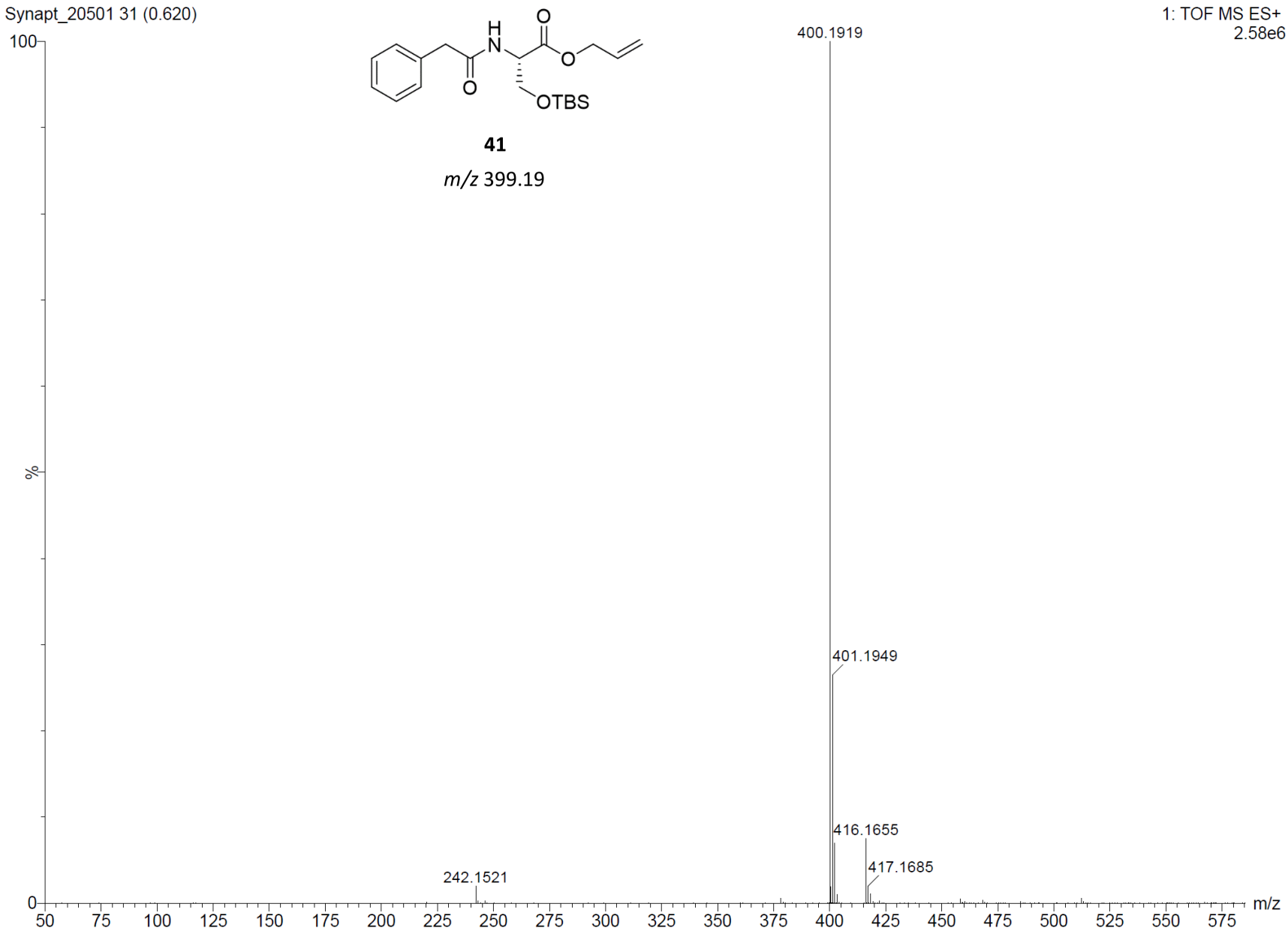
Synapt_20501 31 (0.620)
1: TOF MS ES+
2.58e6
100
%
0
400.1919
401.1949
416.1655
417.1685
242.1521
50 75 100 125 150 175 200 225 250 275 300 325 350 375 400 425 450 475 500 525 550 575
m/z
H
N
O
O
O
OTBS

41

m/z 399.19

^{1}H NMR (400 MHz, $CDCl_3$)

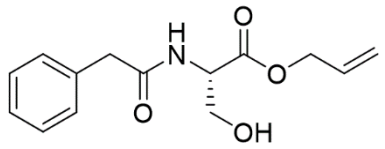

42

^{13}C NMR (126 MHz, $CDCl_3$)

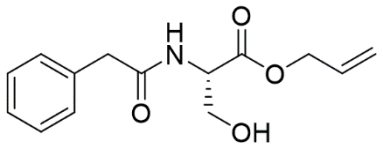

42

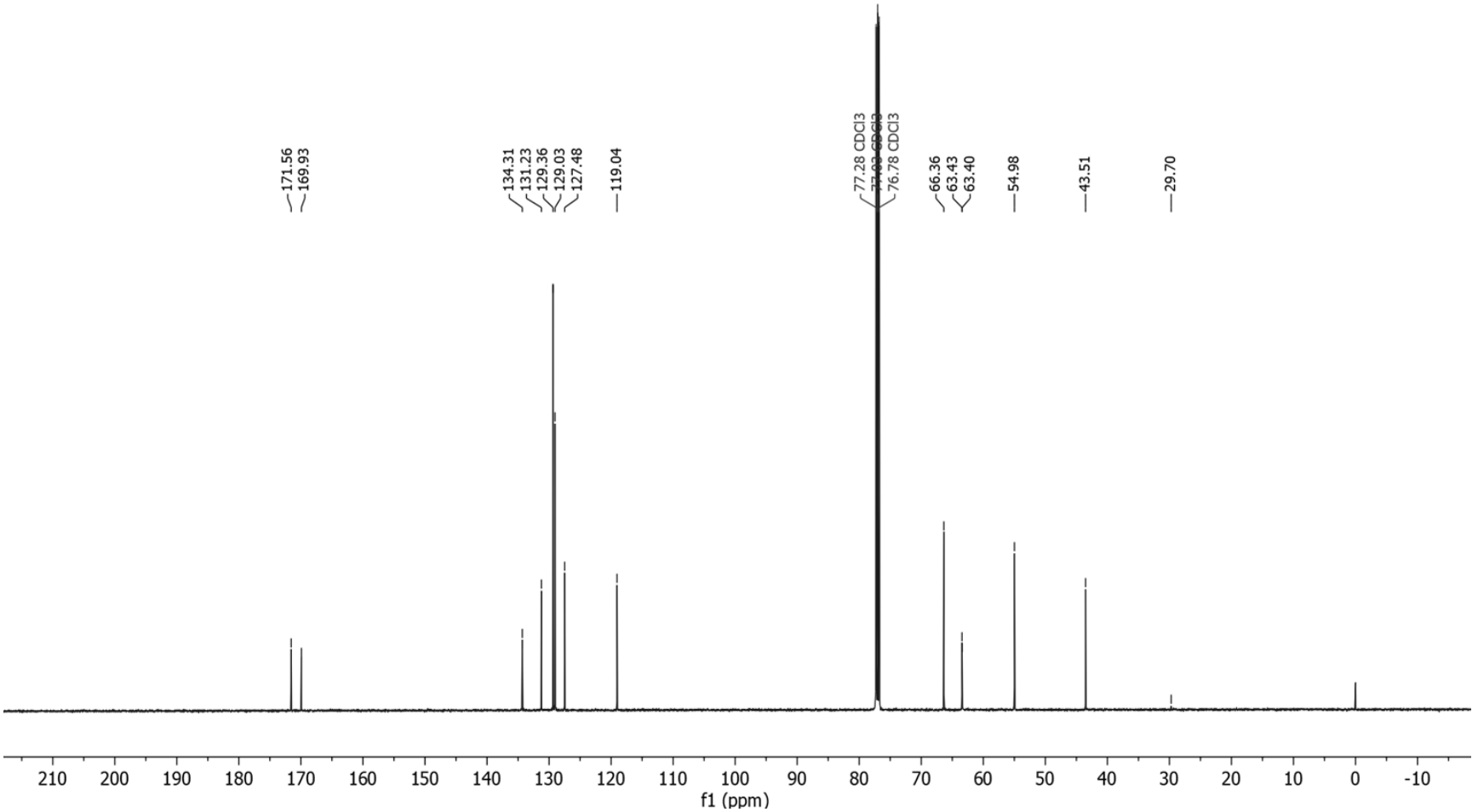

^{1}H NMR (400 MHz, $CDCl_3$)

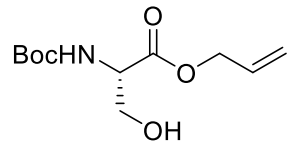

46

^{1}H NMR (400 MHz, $CDCl_3$)

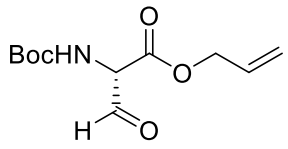

47

^{1}H NMR (500 MHz, $CDCl_3$)

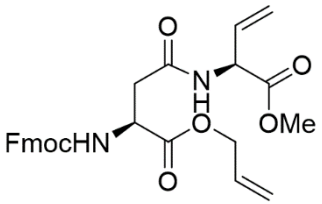

51

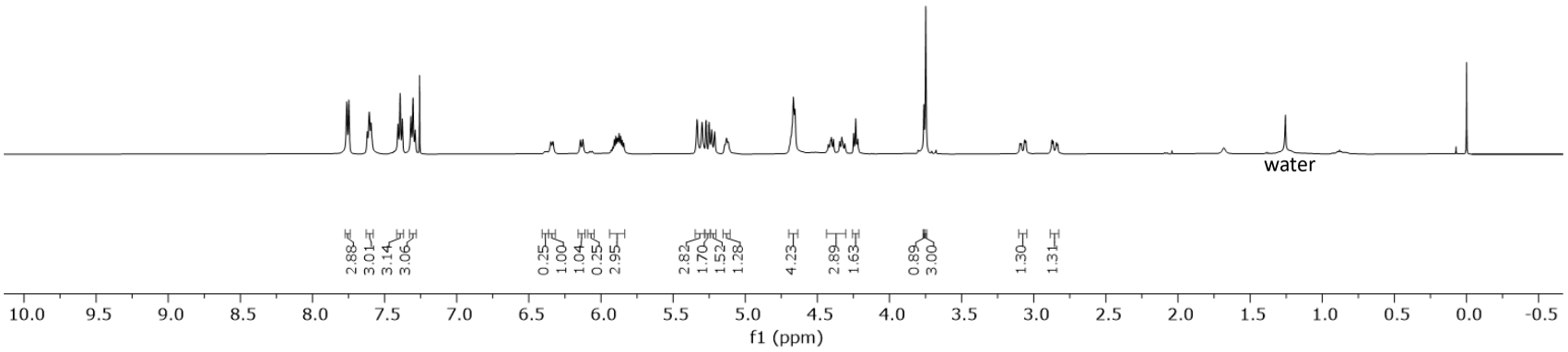

^{13}C NMR (126 MHz, $CDCl_3$)

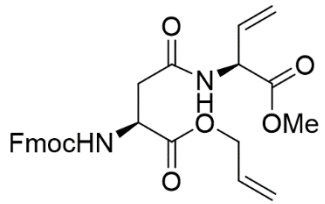

51

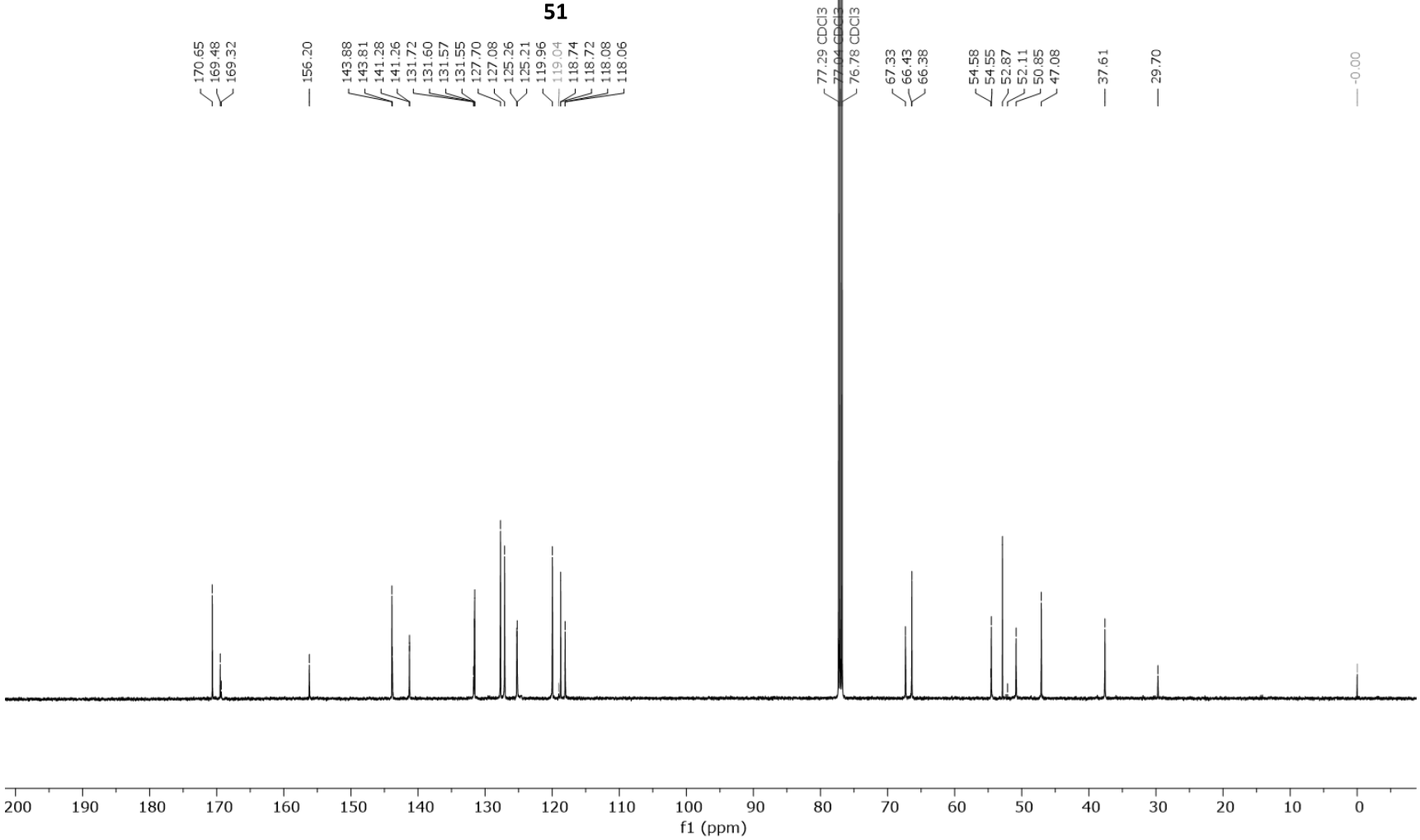

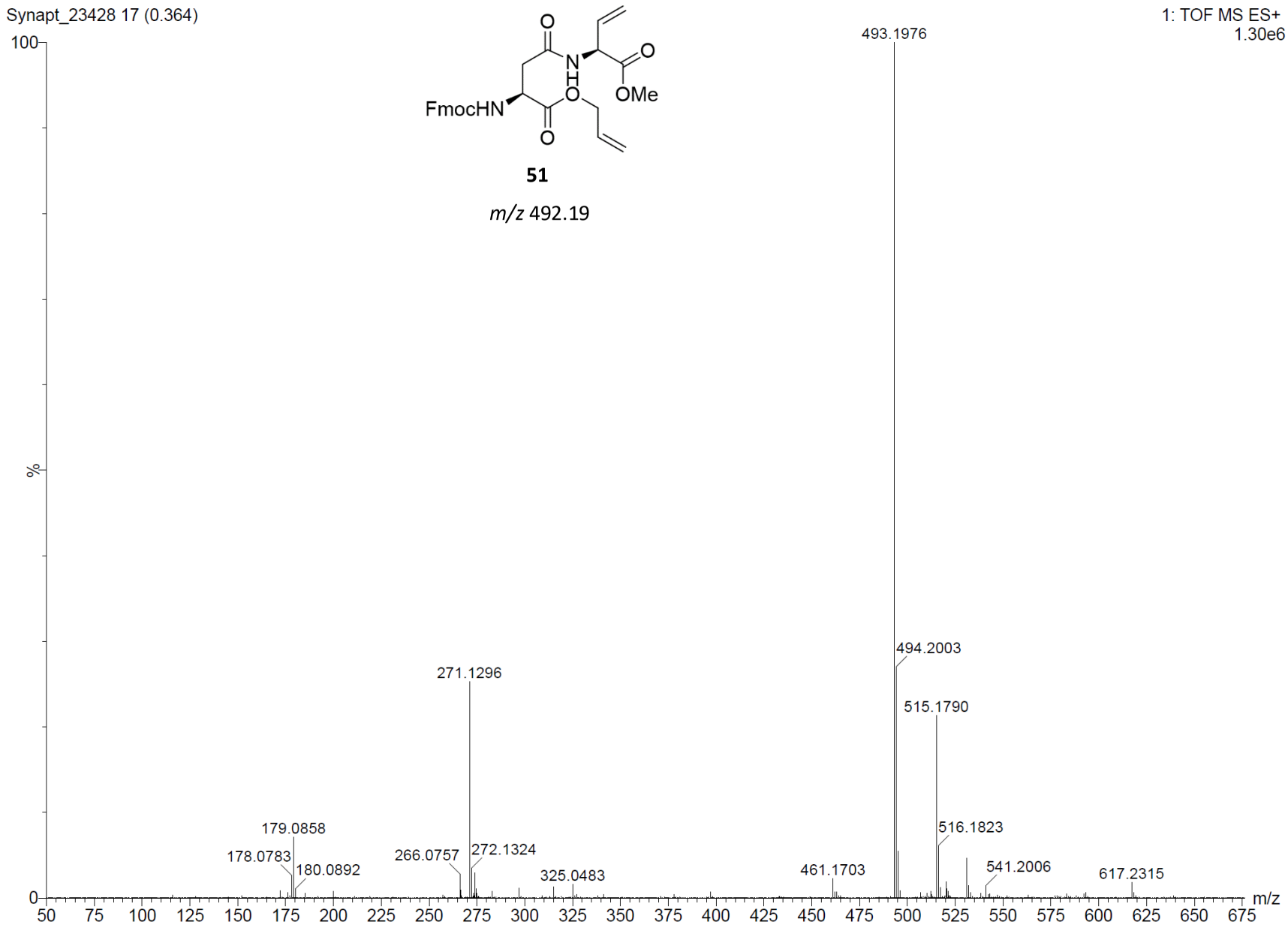
Synapt_23428 17 (0.364)
1: TOF MS ES+
1.30e6
100
%
0
493.1976
494.2003
271.1296
515.1790
516.1823
179.0858
178.0783
180.0892
266.0757
272.1324
325.0483
461.1703
541.2006
617.2315
m/z
50 75 100 125 150 175 200 225 250 275 300 325 350 375 400 425 450 475 500 525 550 575 600 625 650 675
FmocHN
O
N
H
O
O
OMe
O

51

m/z 492.19

^{1}H NMR (400 MHz, $CDCl_3$)

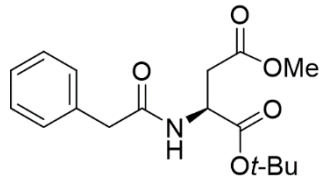

58

^{13}C NMR (126 MHz, $CDCl_3$)

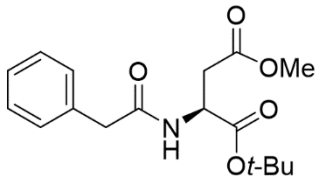

58

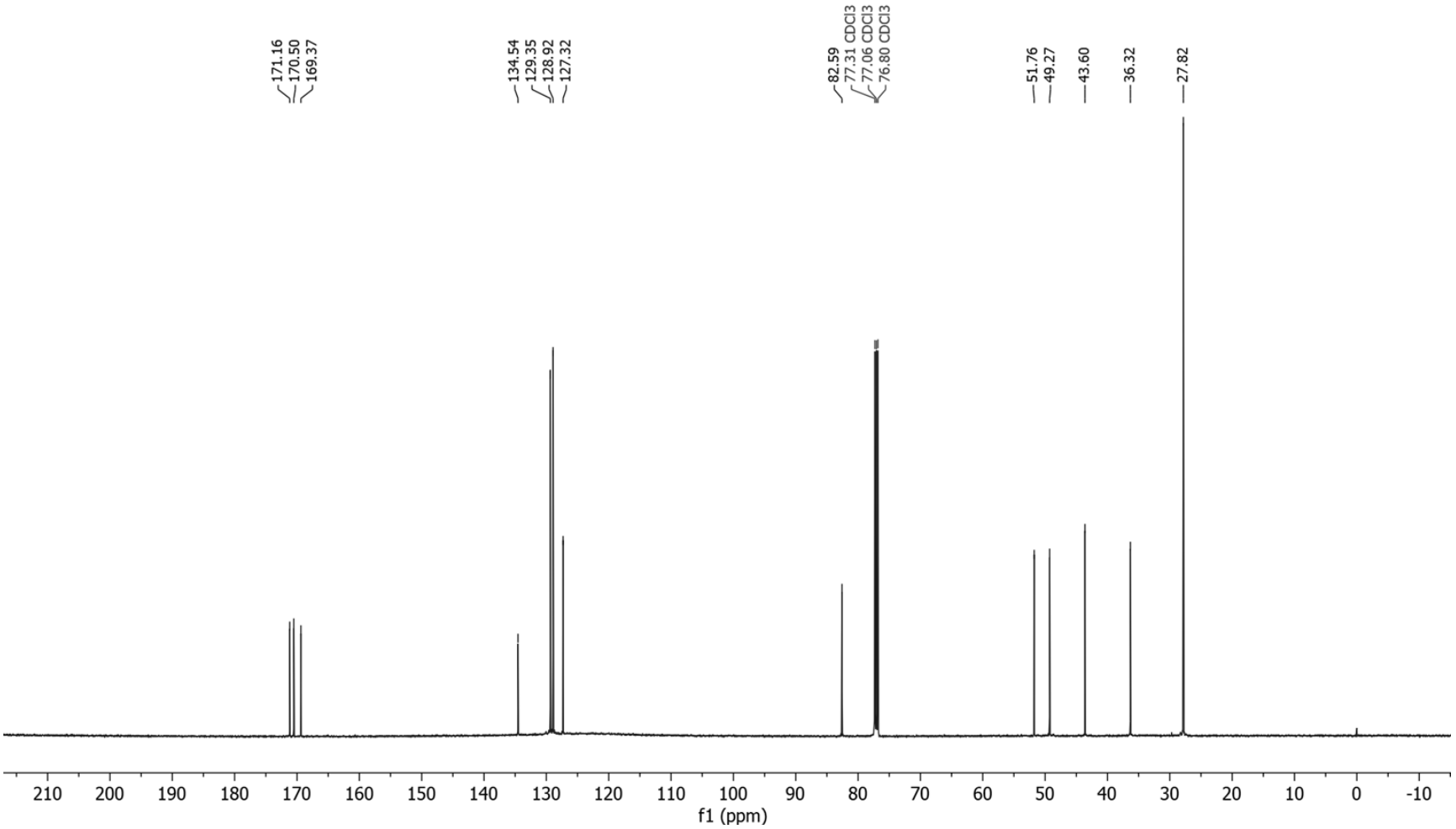

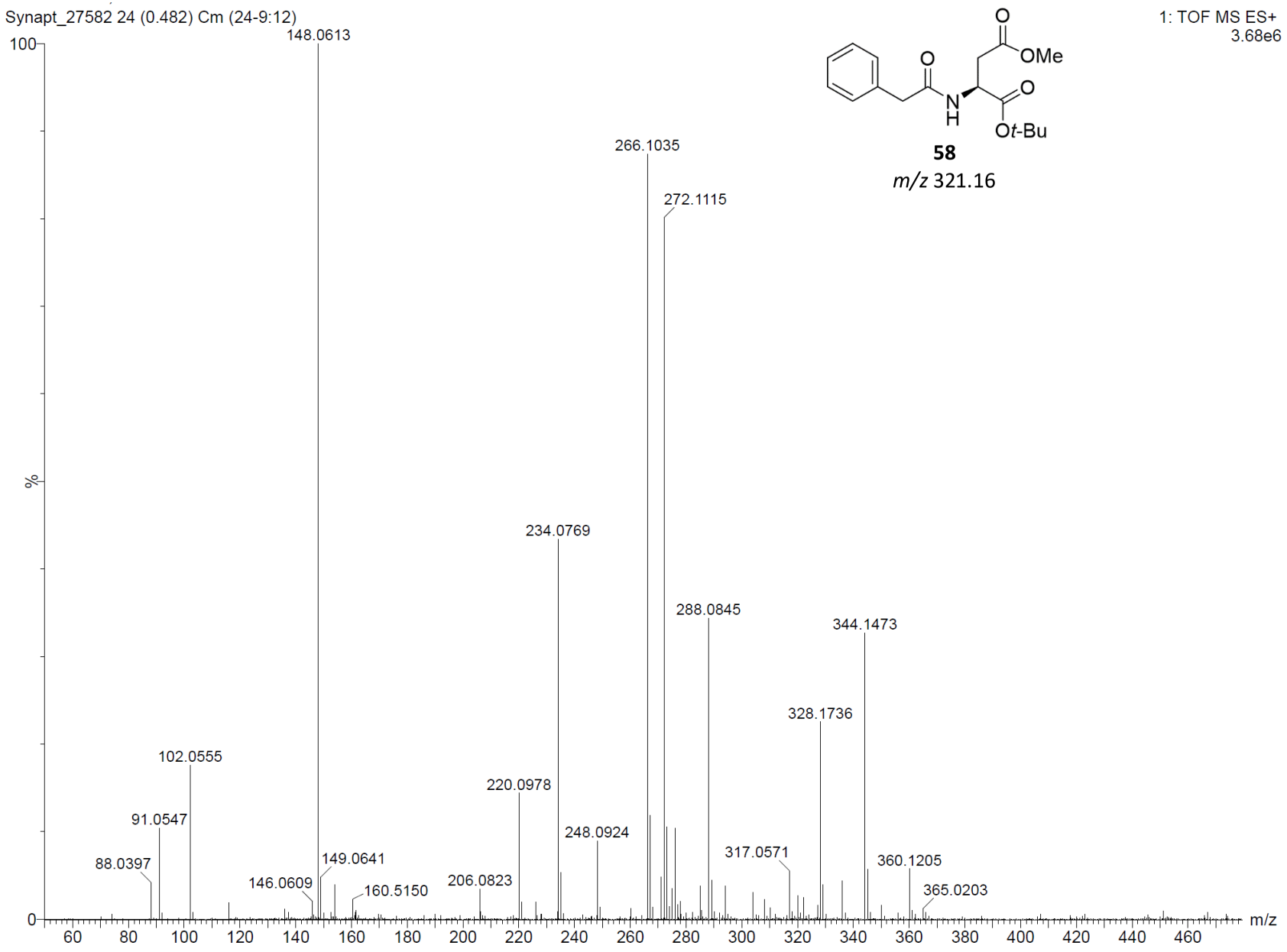
Synapt_27582 24 (0.482) Cm (24-9:12)
1: TOF MS ES+
3.68e6
148.0613
266.1035
272.1115
234.0769
288.0845
344.1473
328.1736
102.0555
220.0978
91.0547
248.0924
317.0571
88.0397
149.0641
360.1205
146.0609
160.5150
206.0823
365.0203
100
%
0
m/z
60 80 100 120 140 160 180 200 220 240 260 280 300 320 340 360 380 400 420 440 460
O
OMe
O
N
H
O
Ot-Bu

58

m/z 321.16

^{1}H NMR (400 MHz, CD_3OD)

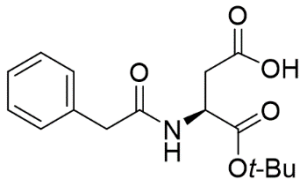

59

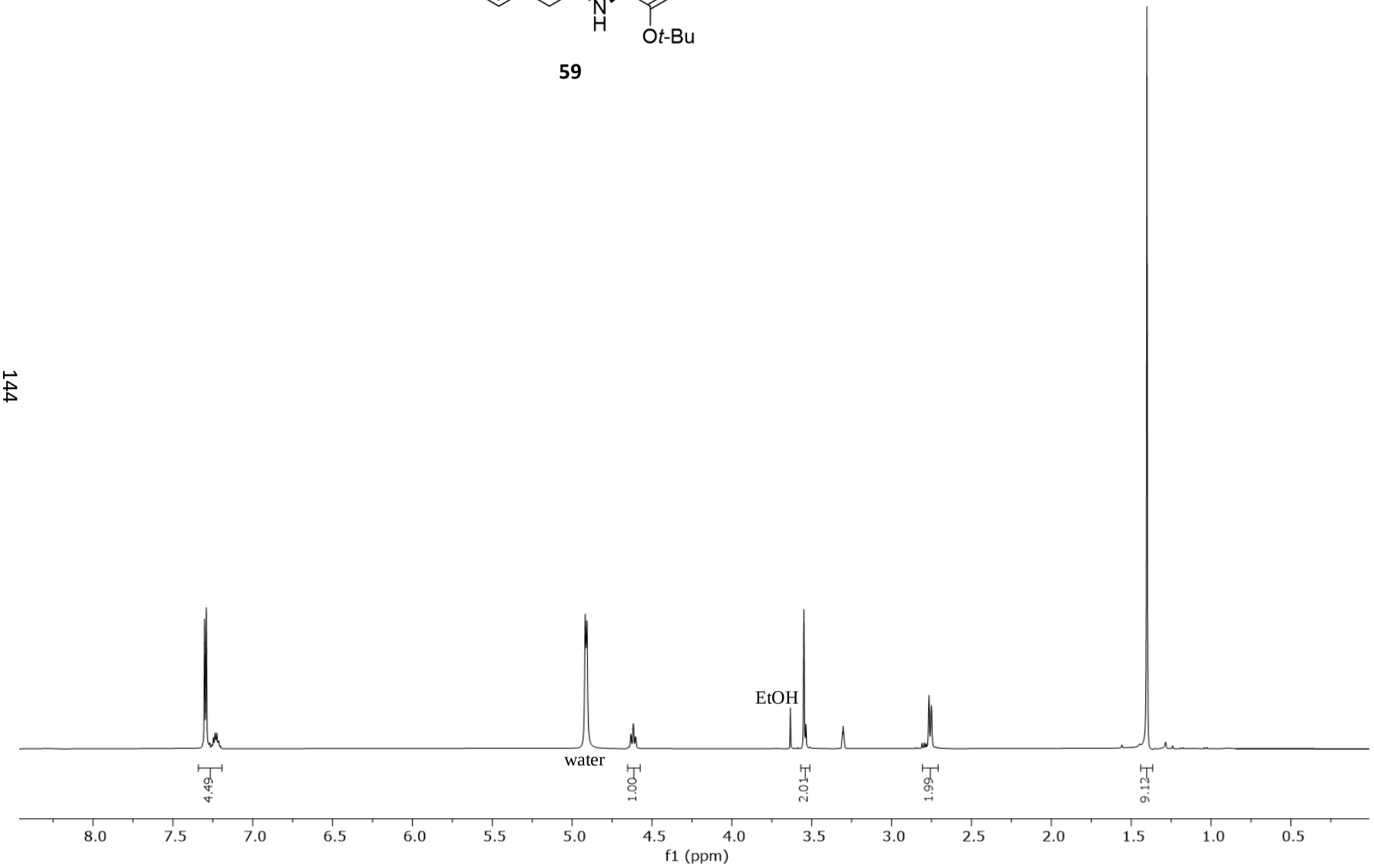

^{13}C NMR (101 MHz, CD_3OD)

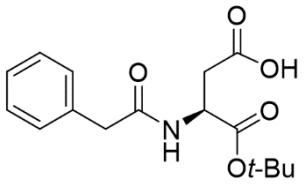

59

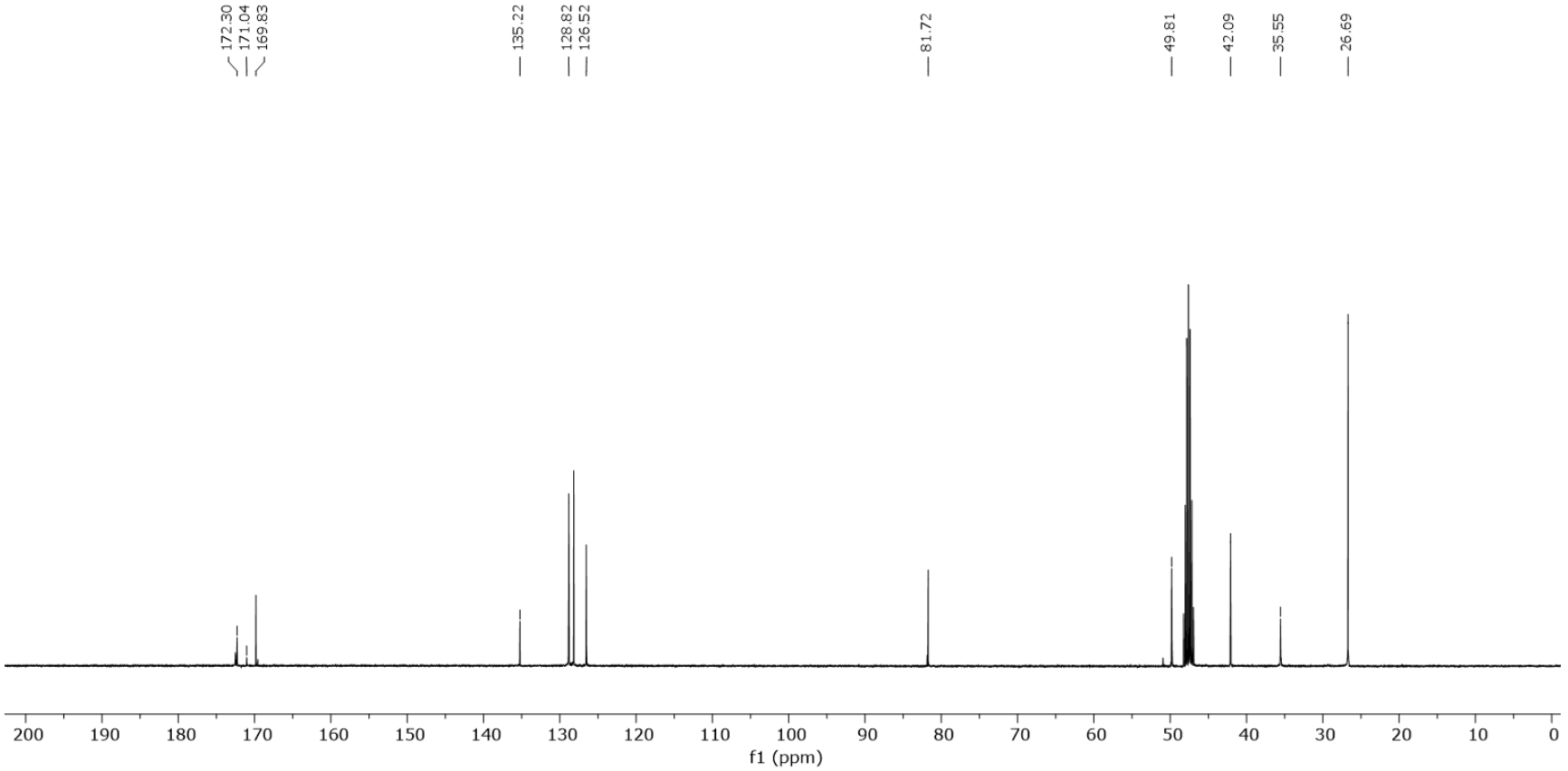

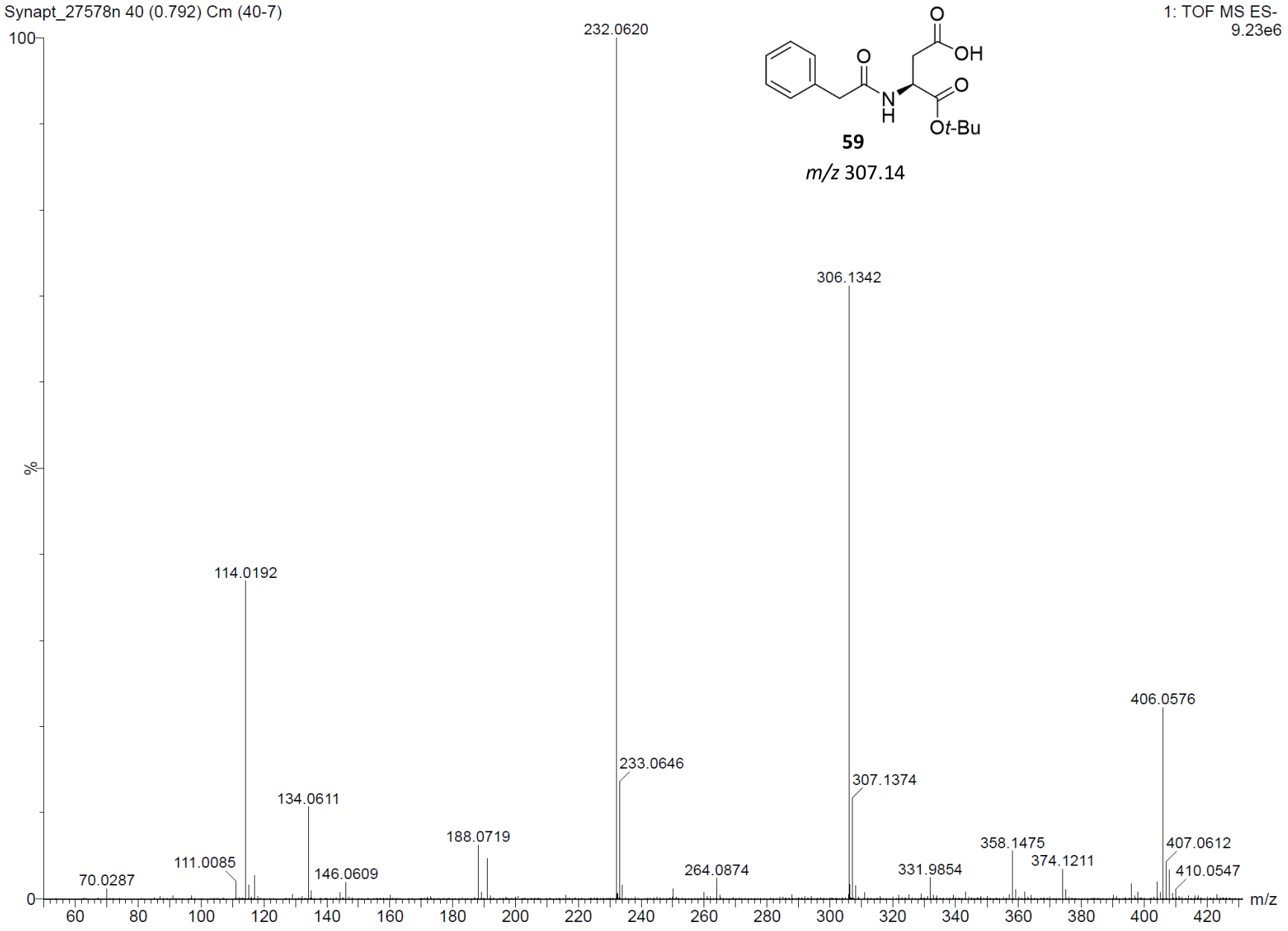
Synapt_27578n 40 (0.792) Cm (40-7)
1: TOF MS ES-
9.23e6
100
%
0
232.0620
306.1342
114.0192
233.0646
307.1374
134.0611
188.0719
406.0576
111.0085
146.0609
264.0874
358.1475
374.1211
407.0612
70.0287
331.9854
410.0547
60
80
100
120
140
160
180
200
220
240
260
280
300
320
340
360
380
400
420
m/z
O
OH
O
N
H
O
Ot-Bu
59
m/z 307.14

^{1}H NMR (400 MHz, $CDCl_3$)

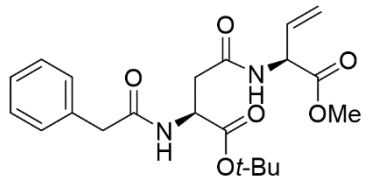

60

^{13}C NMR (101 MHz, $CDCl_3$)

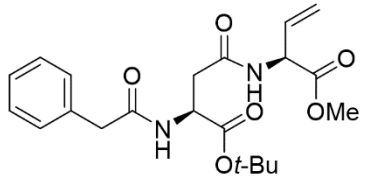

60

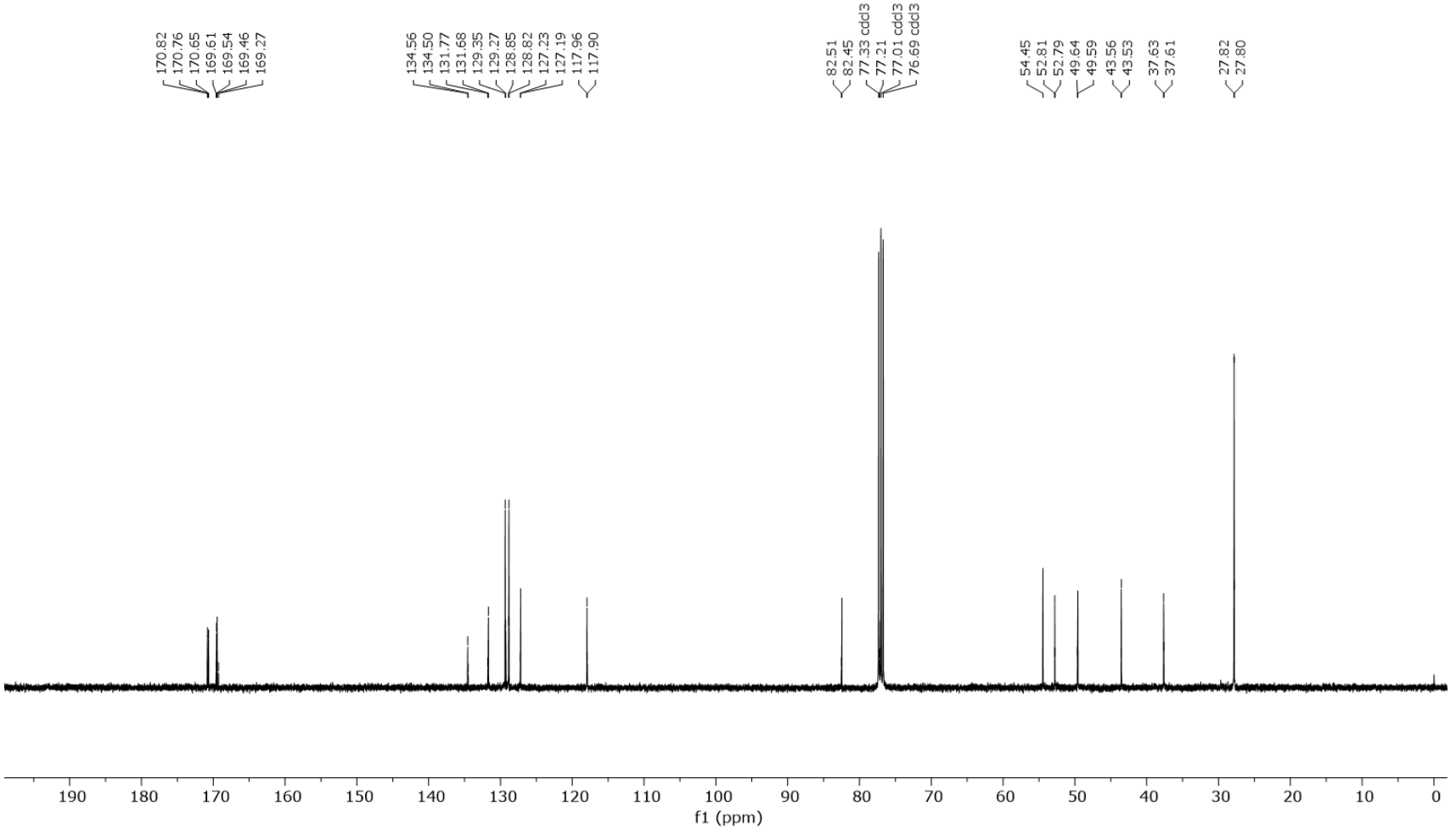

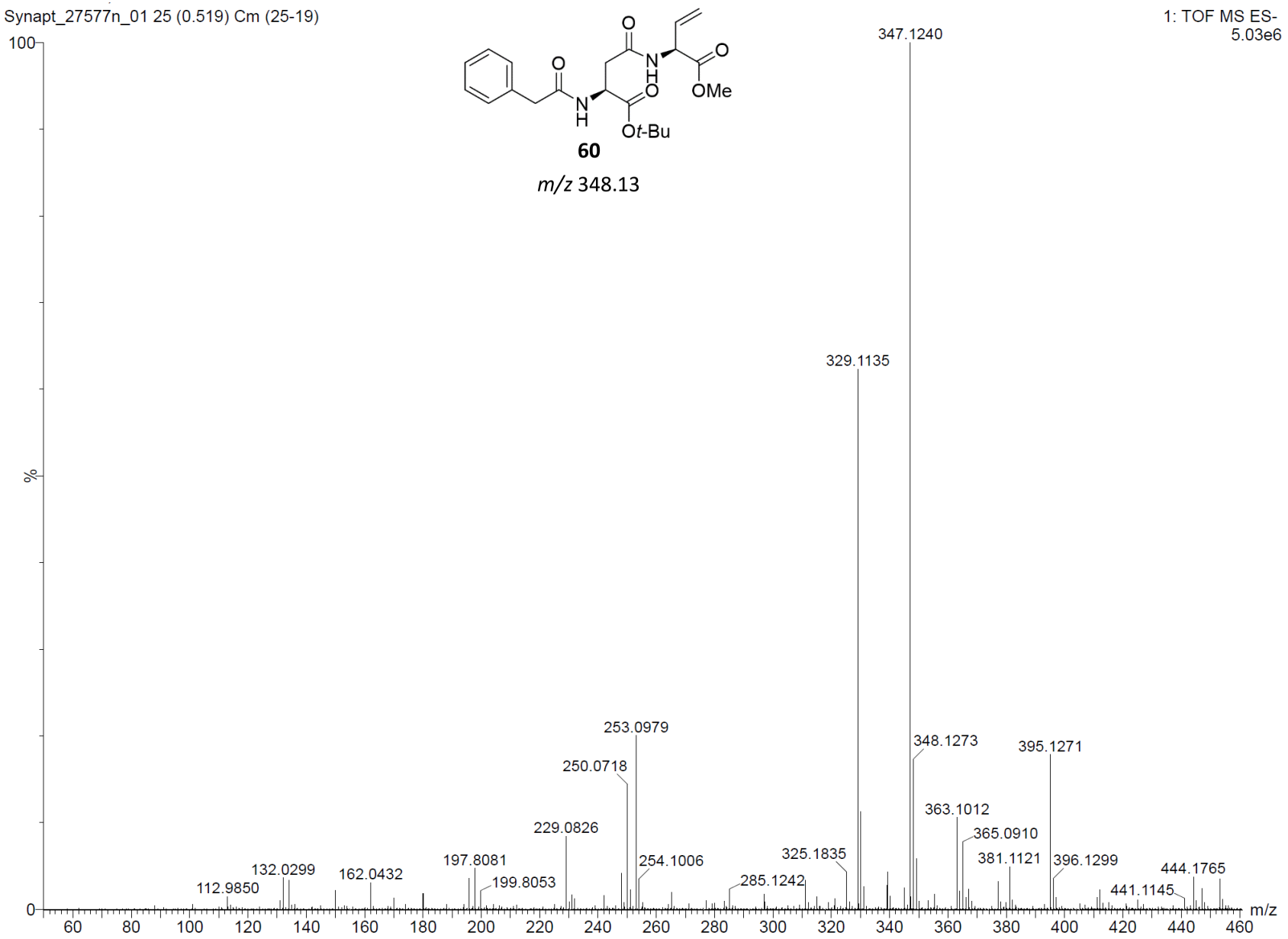
Synapt_27577n_01 25 (0.519) Cm (25-19)
1: TOF MS ES-
5.03e6
100
%
0
347.1240
329.1135
253.0979
250.0718
348.1273
395.1271
363.1012
365.0910
229.0826
381.1121
396.1299
325.1835
254.1006
444.1765
197.8081
132.0299
162.0432
199.8053
285.1242
112.9850
441.1145
60
80
100
120
140
160
180
200
220
240
260
280
300
320
340
360
380
400
420
440
460
m/z
O
N
H
O
OMe
O
N
H
O
Ot-Bu
60
m/z 348.13

^{1}H NMR (400 MHz, $CDCl_3$)

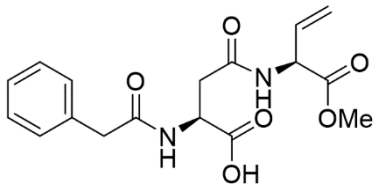

61

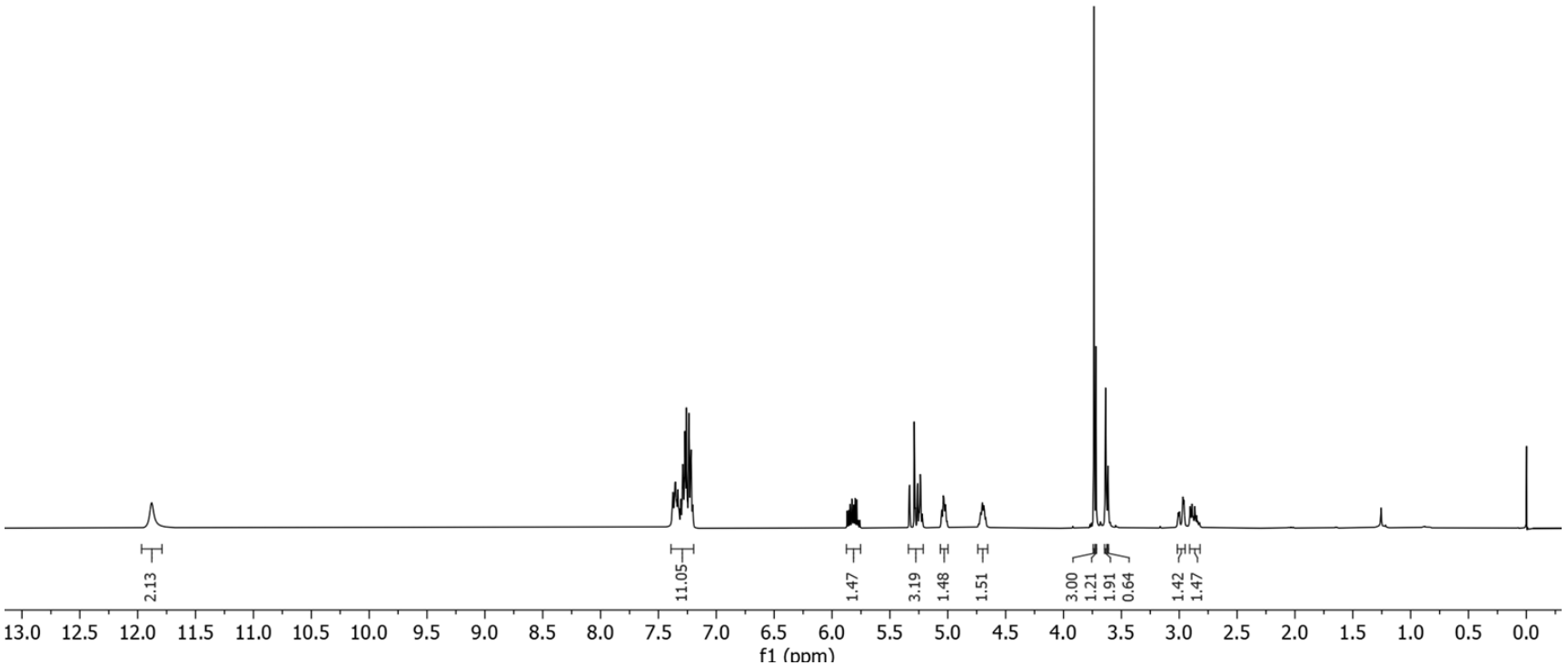

^{13}C NMR (101 MHz, $CDCl_3$)

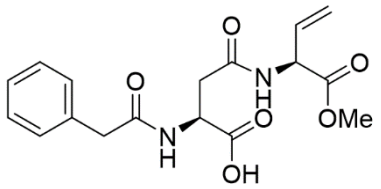

61

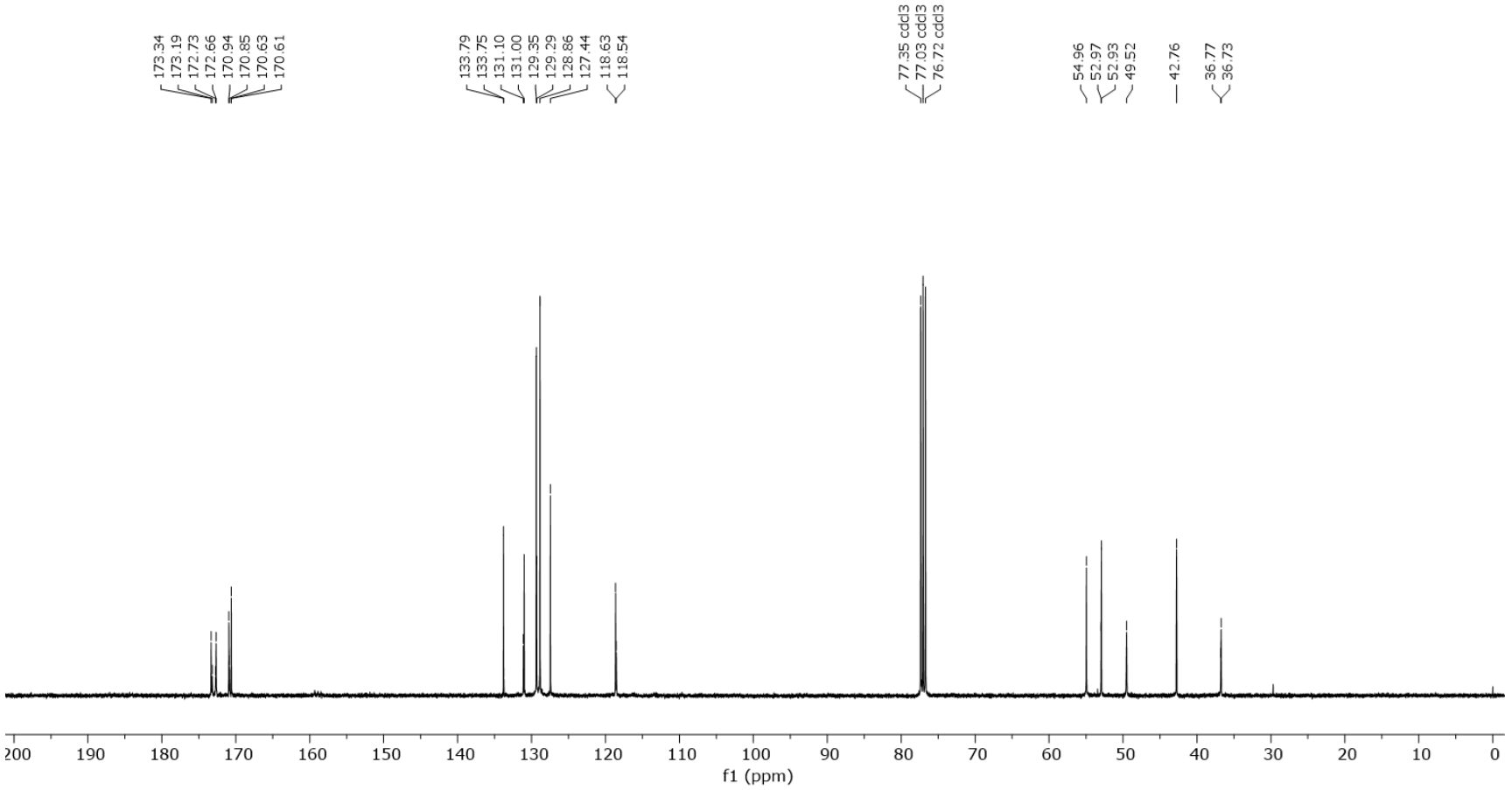

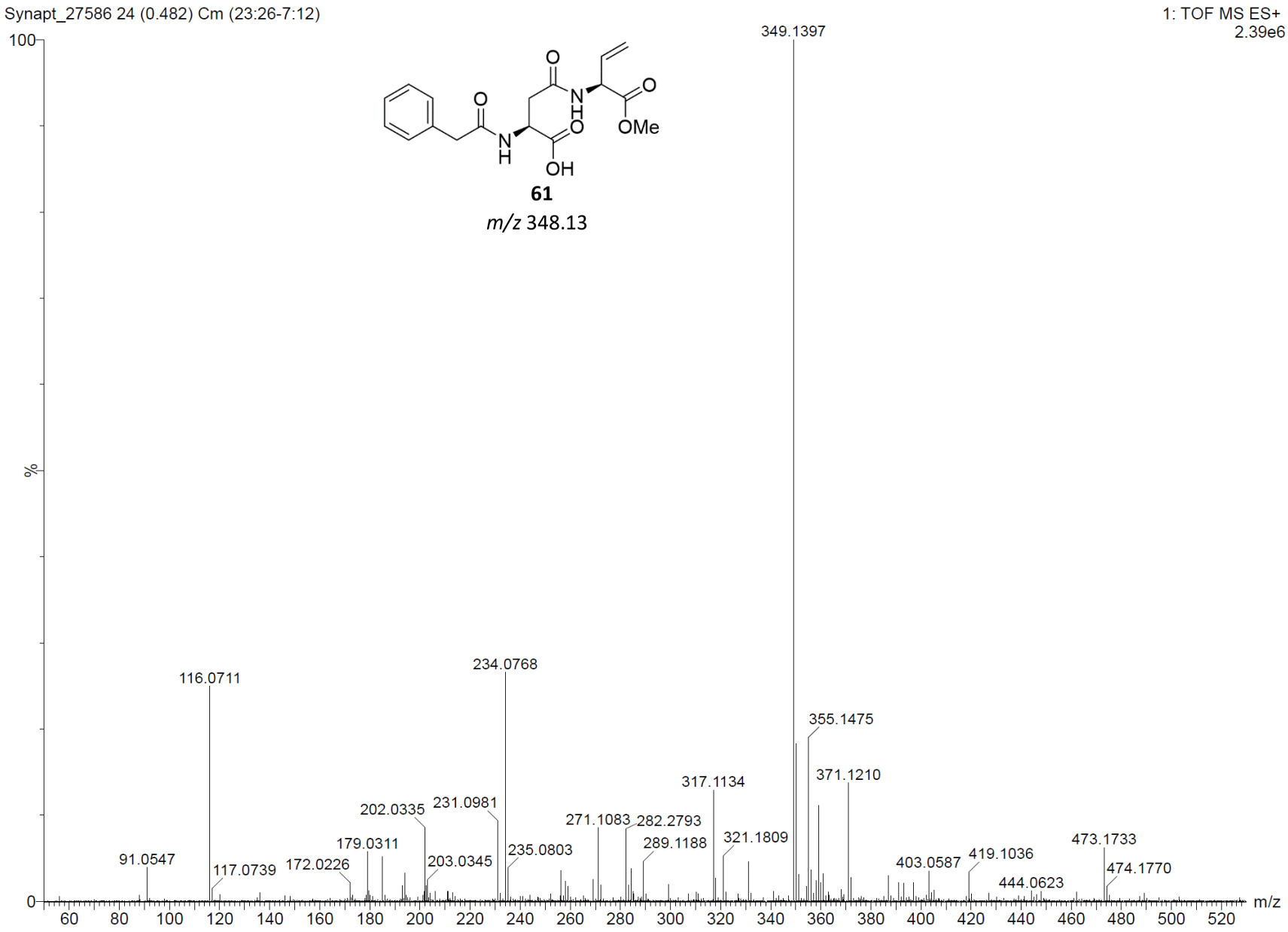
Synapt_27586 24 (0.482) Cm (23:26-7:12)
1: TOF MS ES+
2.39e6
100
%
0
349.1397
116.0711
234.0768
355.1475
371.1210
317.1134
231.0981
202.0335
271.1083
282.2793
289.1188
321.1809
179.0311
91.0547
117.0739
172.0226
203.0345
235.0803
403.0587
419.1036
444.0623
473.1733
474.1770
60 80 100 120 140 160 180 200 220 240 260 280 300 320 340 360 380 400 420 440 460 480 500 520
m/z

61

m/z 348.13

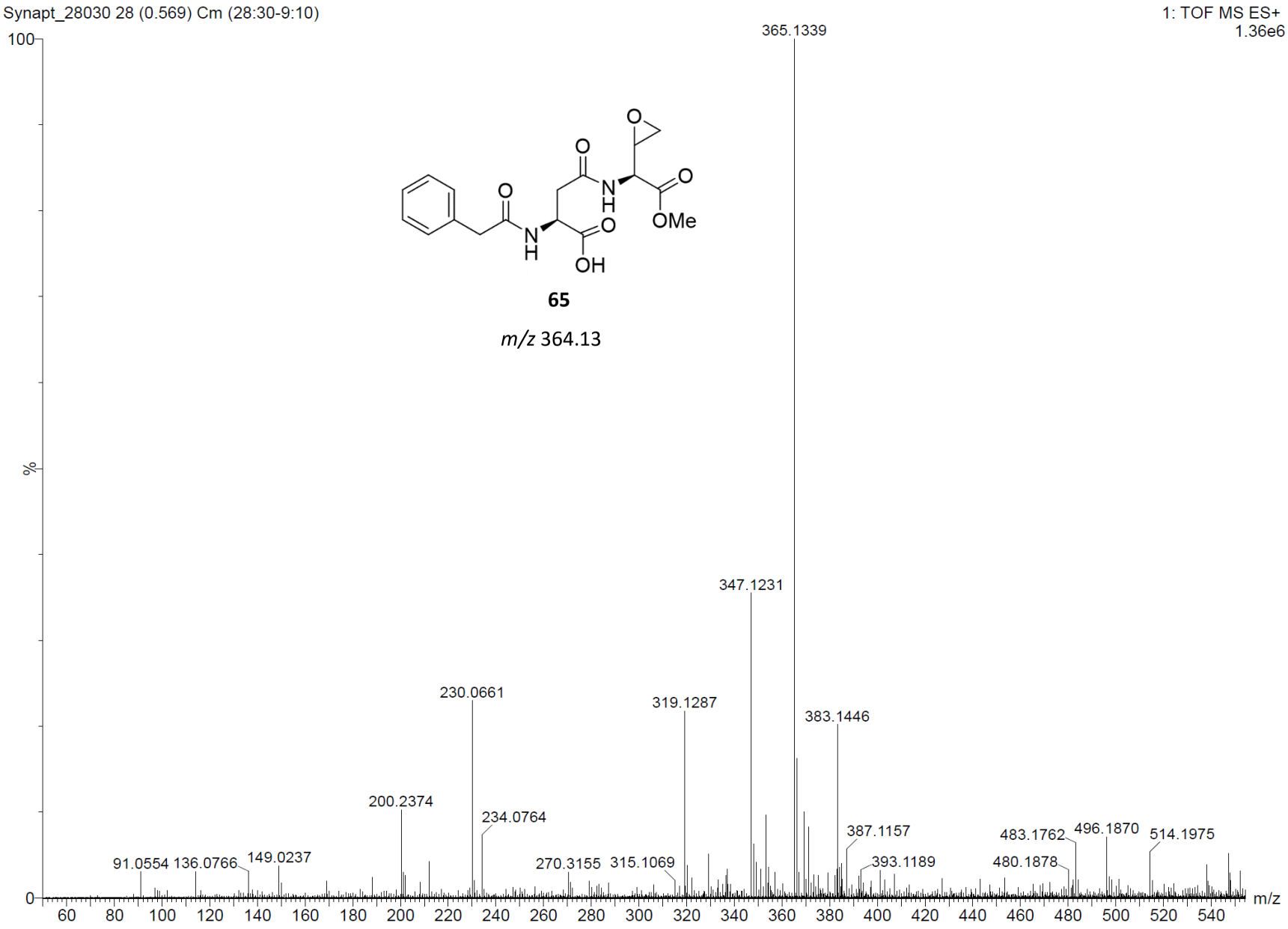
Synapt_28030 28 (0.569) Cm (28:30-9:10)
1: TOF MS ES+
1.36e6
365.1339
100
%
0
347.1231
230.0661
319.1287
383.1446
200.2374
234.0764
387.1157
483.1762
496.1870
514.1975
91.0554
136.0766
149.0237
270.3155
315.1069
393.1189
480.1878
60 80 100 120 140 160 180 200 220 240 260 280 300 320 340 360 380 400 420 440 460 480 500 520 540
m/z

65

m/z 364.13

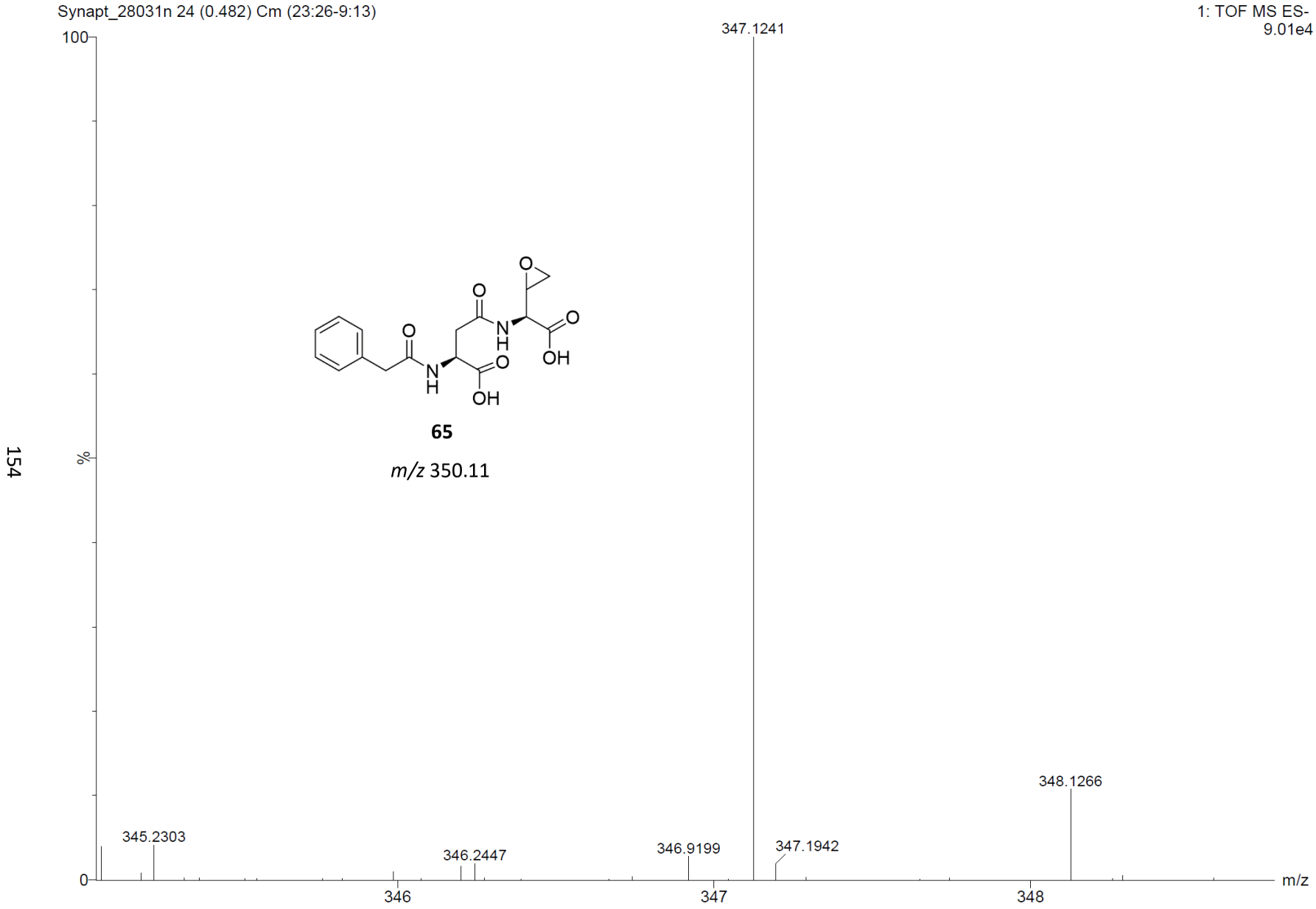
Synapt_28031n 24 (0.482) Cm (23:26-9:13)
1: TOF MS ES-
9.01e4
100
%
0
347.1241
348.1266
345.2303
346.2447
346.9199
347.1942
346
347
348
m/z
65
m/z 350.11

^{1}H NMR (400 MHz, $CDCl_3$)

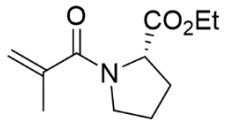

92

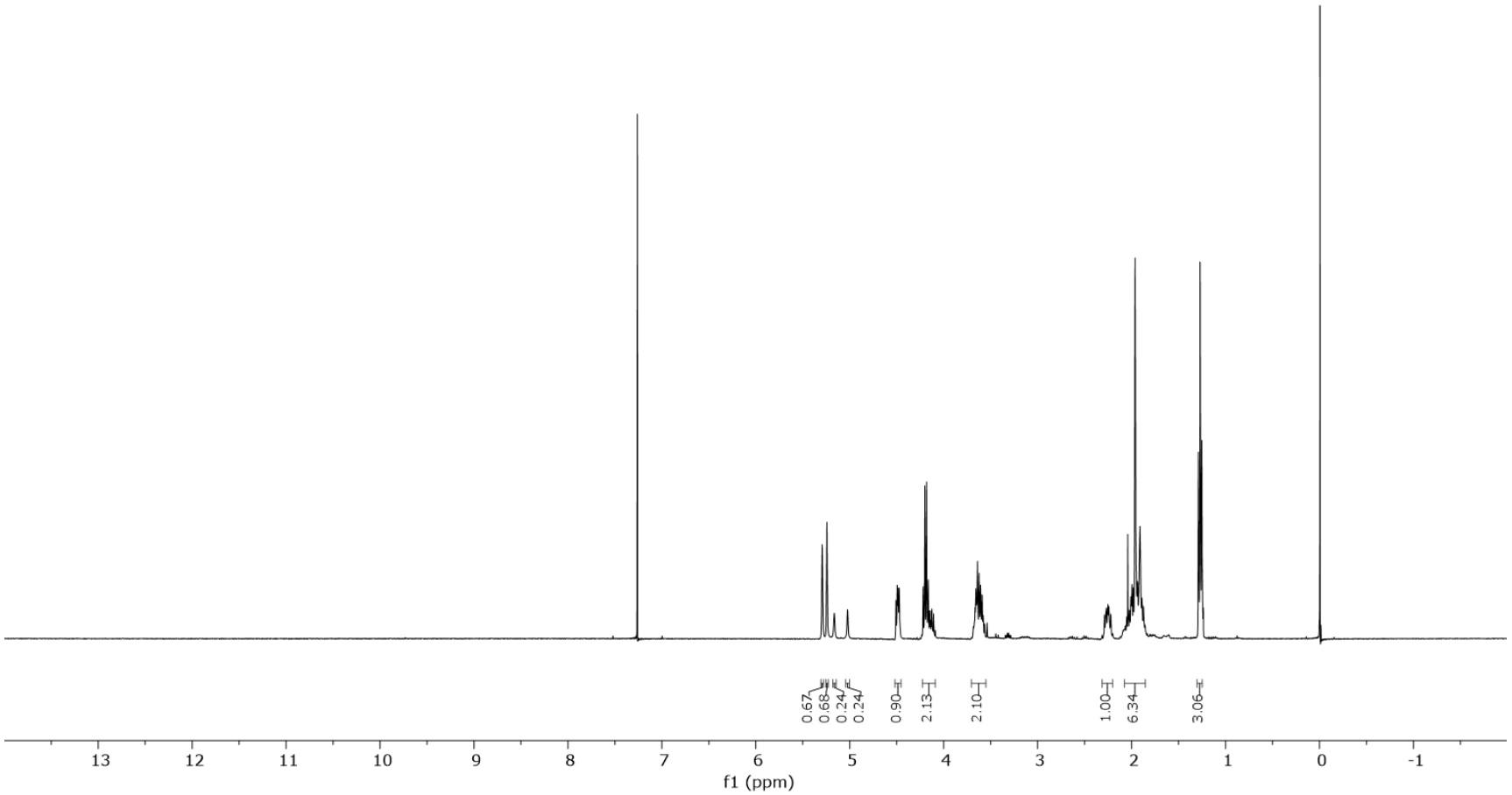

^{13}C NMR (126 MHz, $CDCl_3$)

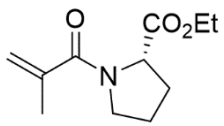

92

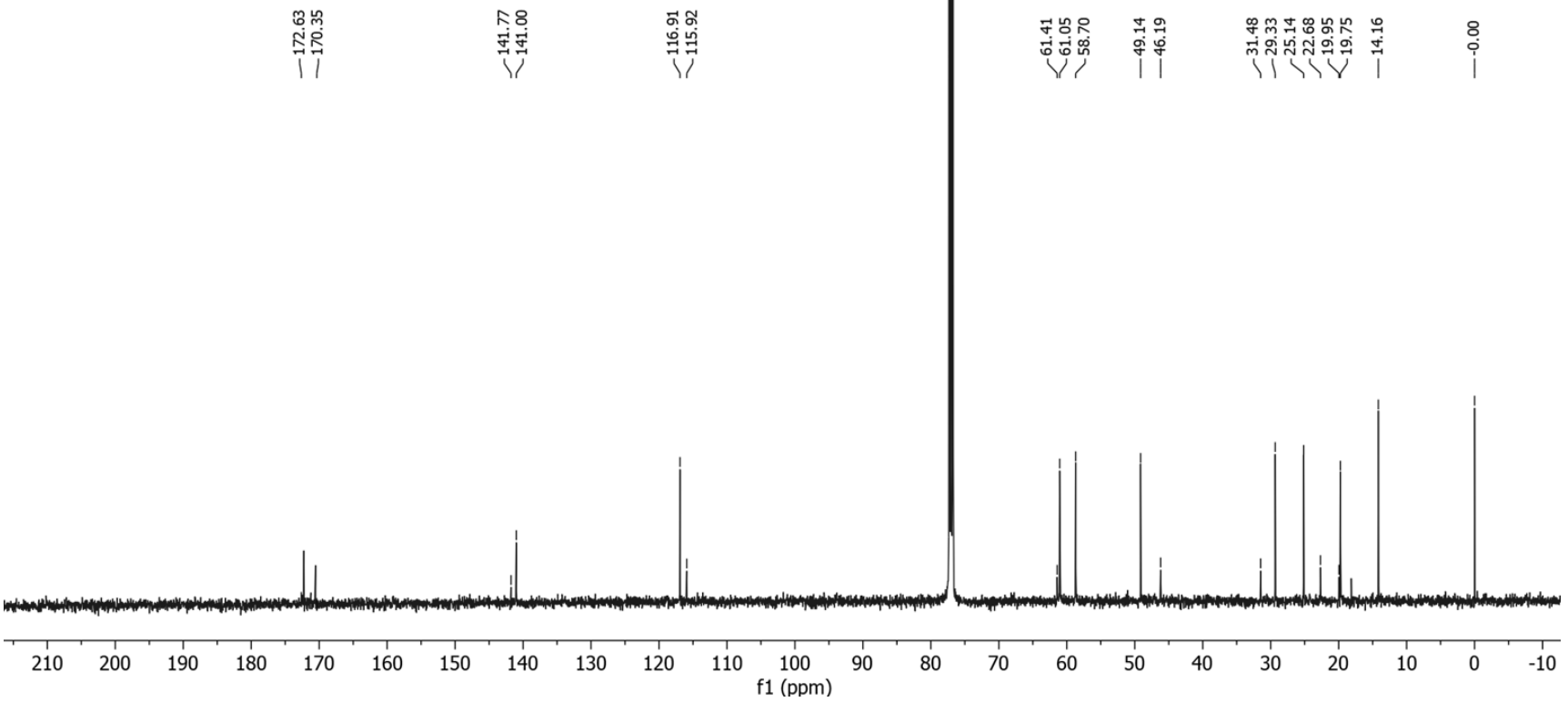

^{1}H NMR (400 MHz, $CDCl_3$)

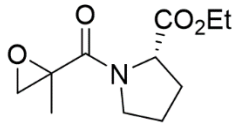

93

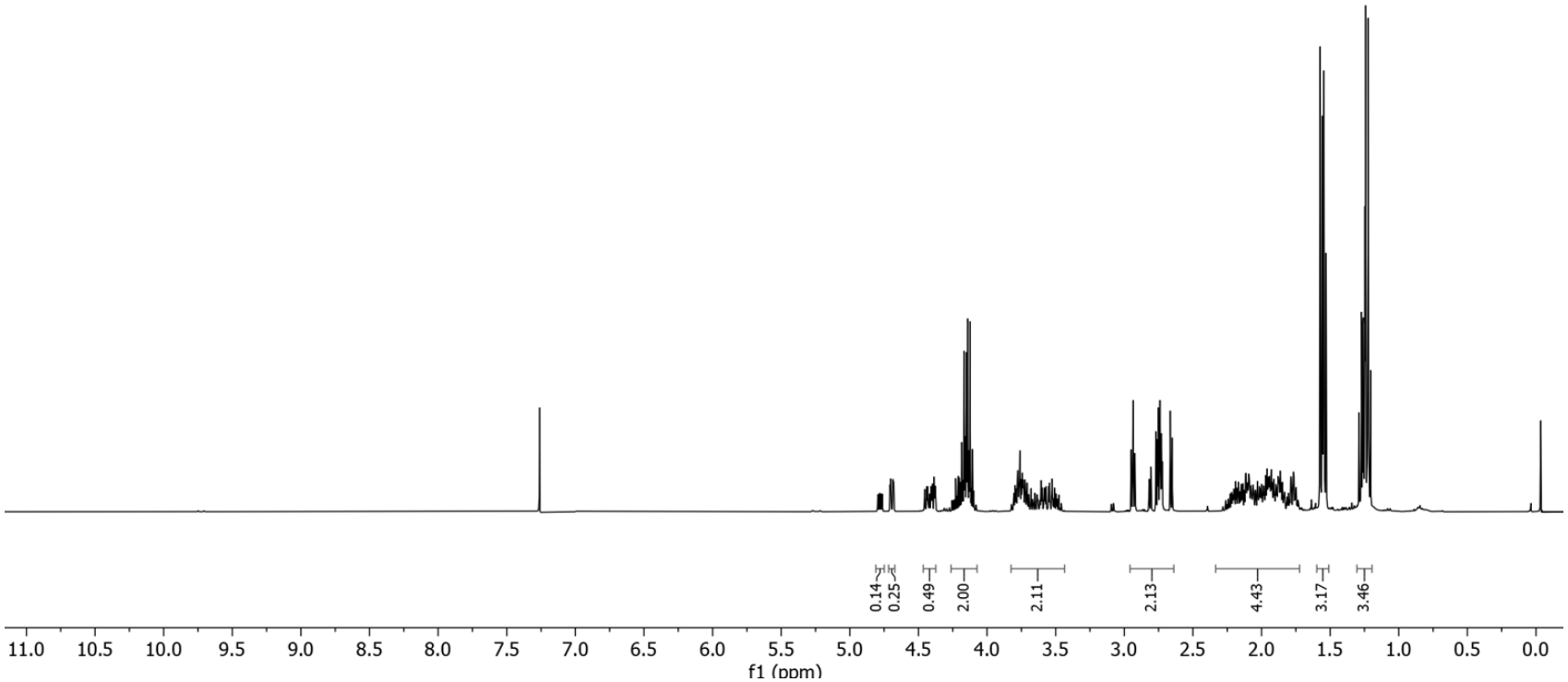

^{13}C NMR (126 MHz, $CDCl_3$)

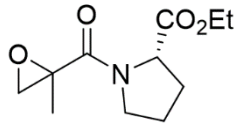

93

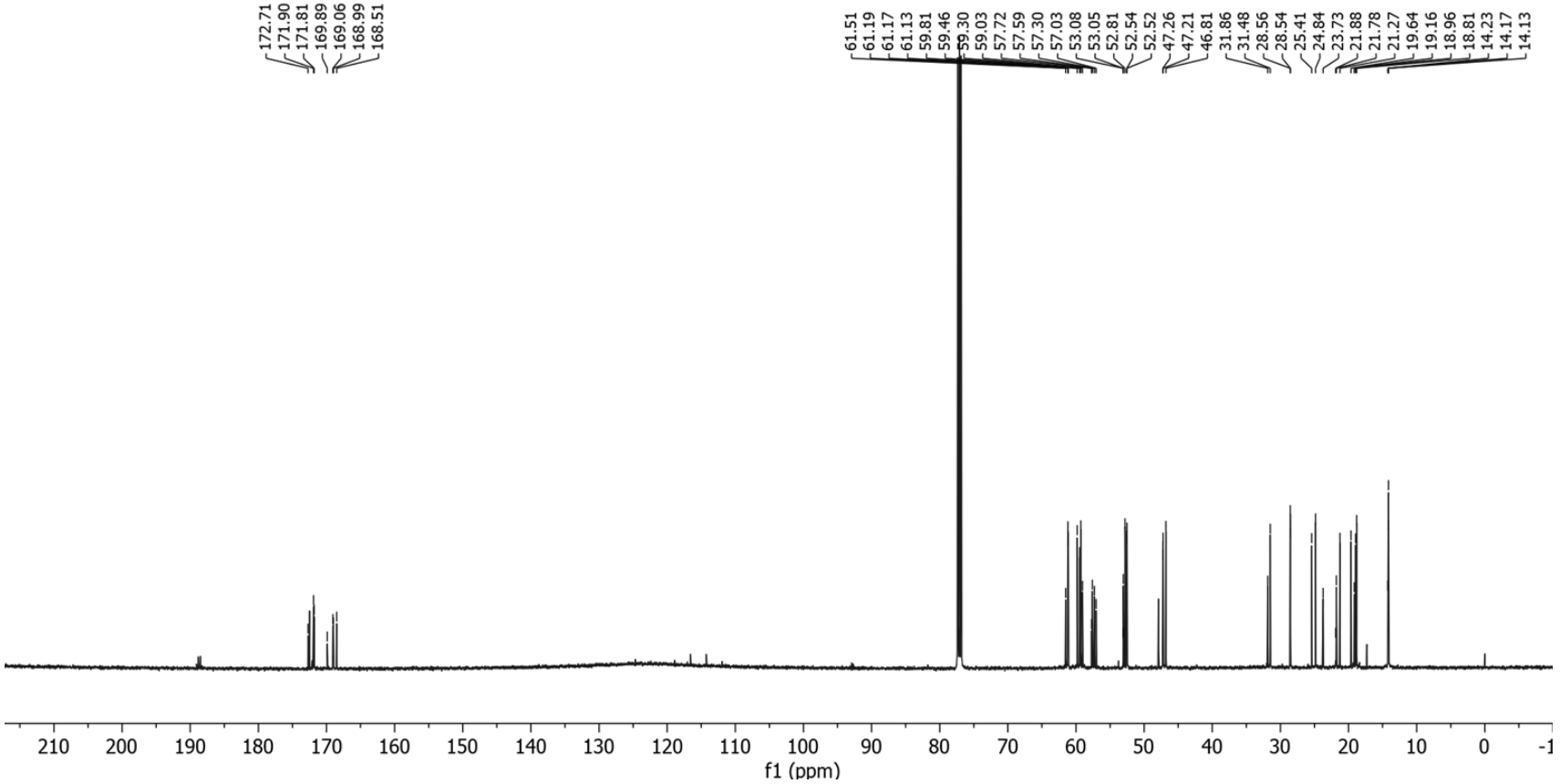

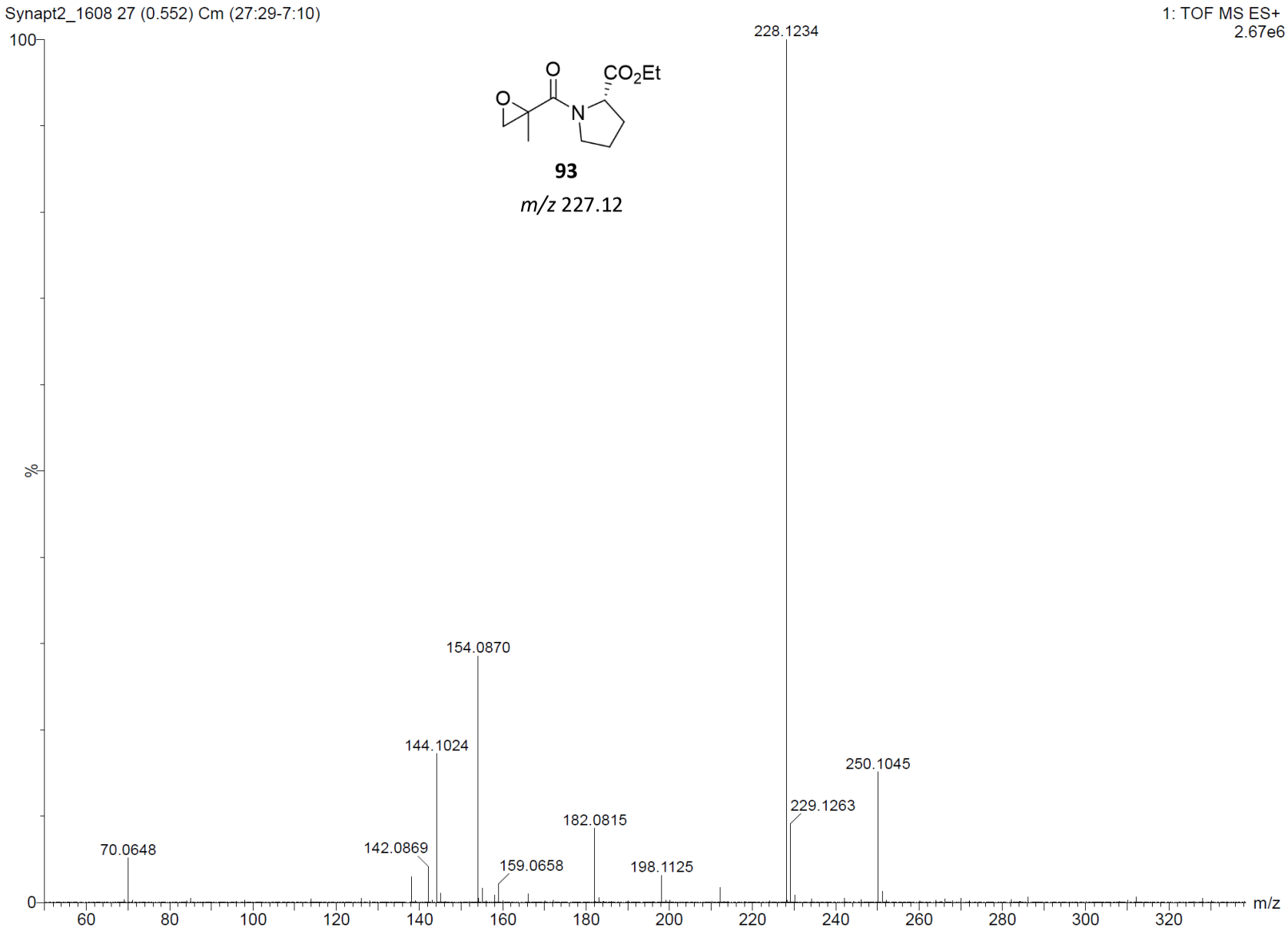
Synapt2_1608 27 (0.552) Cm (27:29-7:10)
1: TOF MS ES+
2.67e6
100
%
0
228.1234
154.0870
144.1024
250.1045
229.1263
182.0815
70.0648
142.0869
159.0658
198.1125
60
80
100
120
140
160
180
200
220
240
260
280
300
320
m/z
O
O
N
CO2Et

93

m/z 227.12

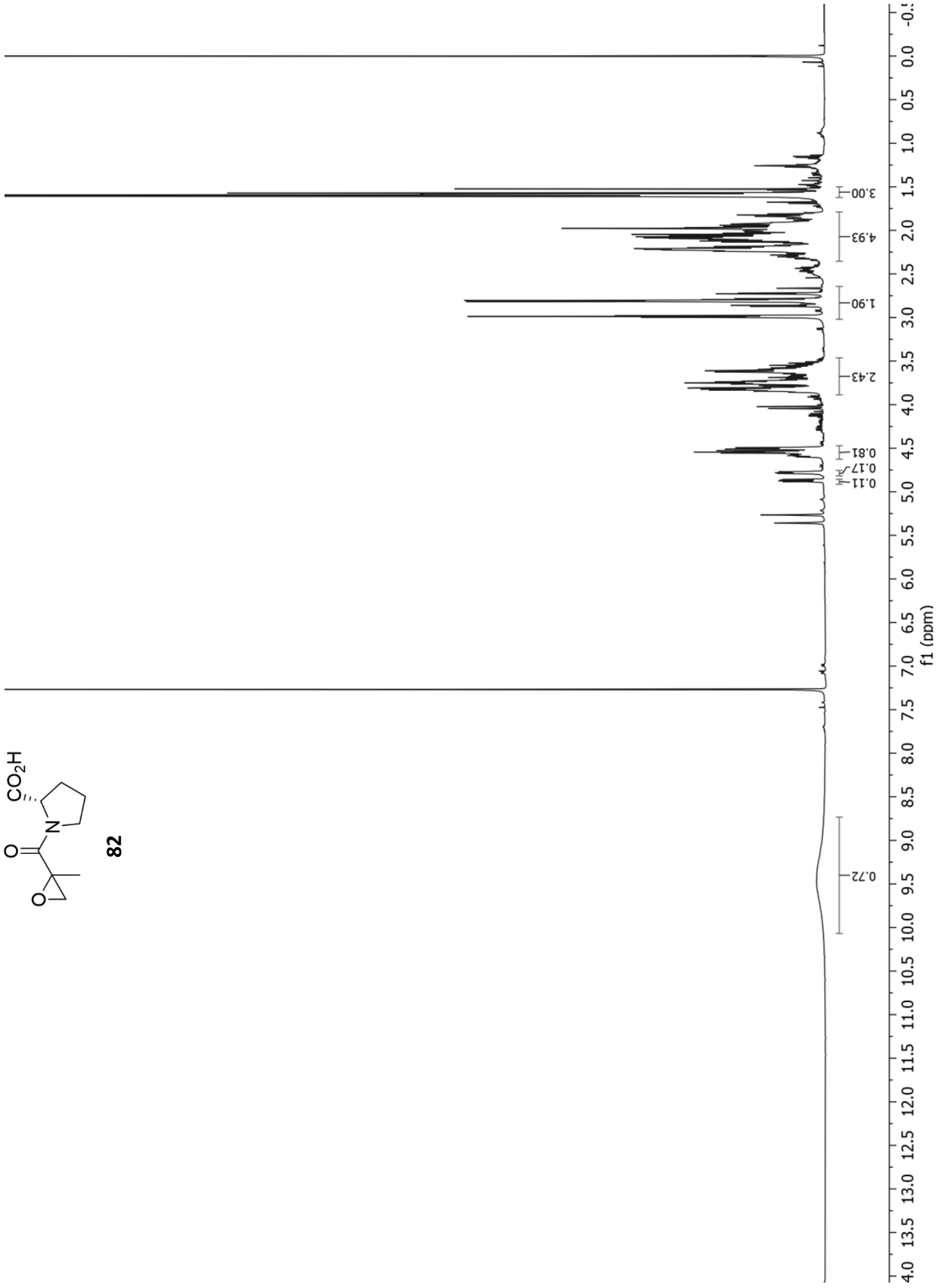
CO2H
O
N
O
82
0.72
0.11
0.17
0.81
2.43
1.90
4.93
3.00
f1 (ppm)

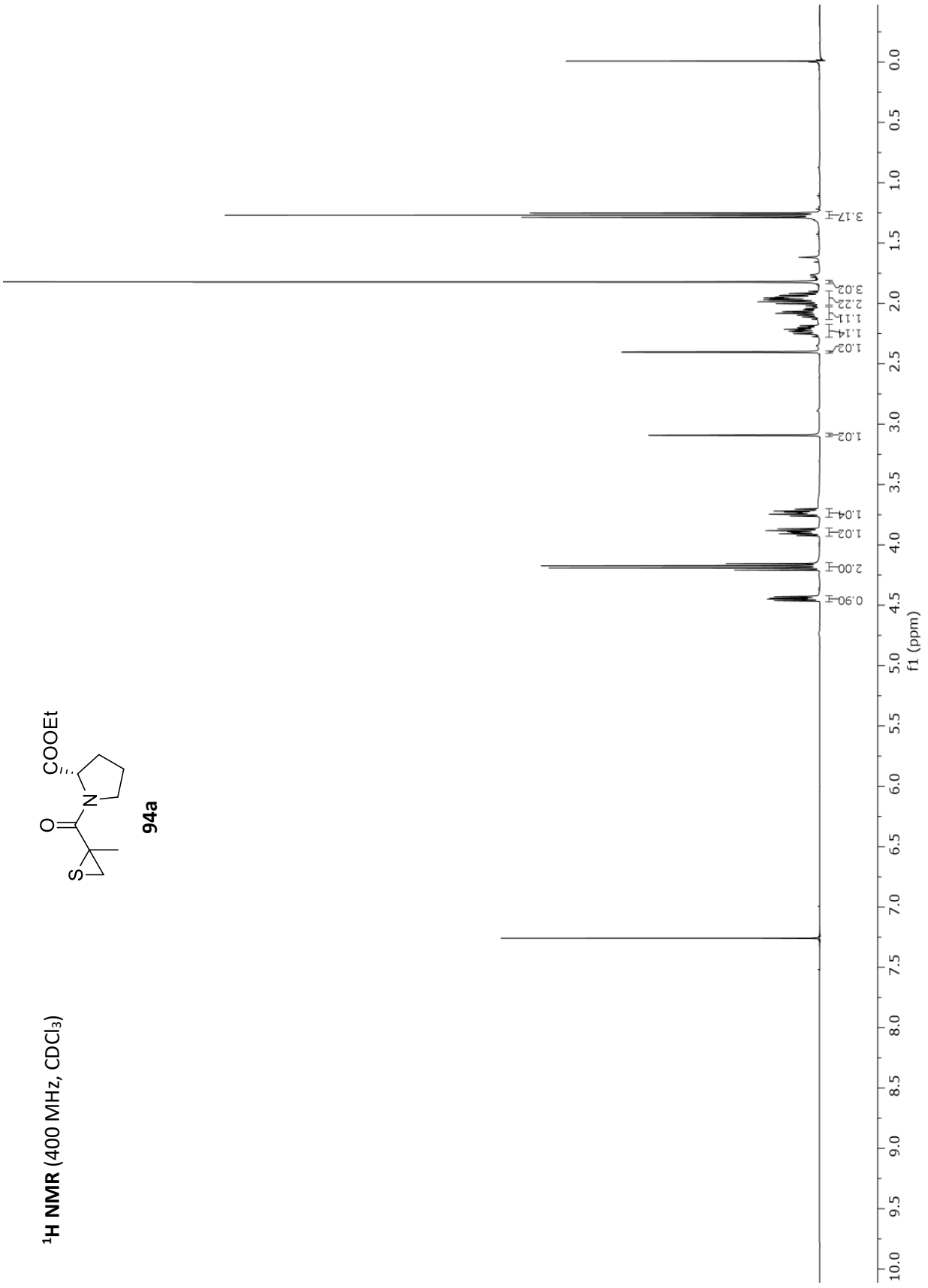

^{1}H NMR (400 MHz, $CDCl_3$)

94a

^{13}C NMR (126 MHz, $CDCl_3$)

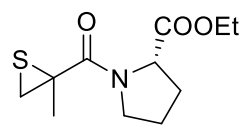

94a

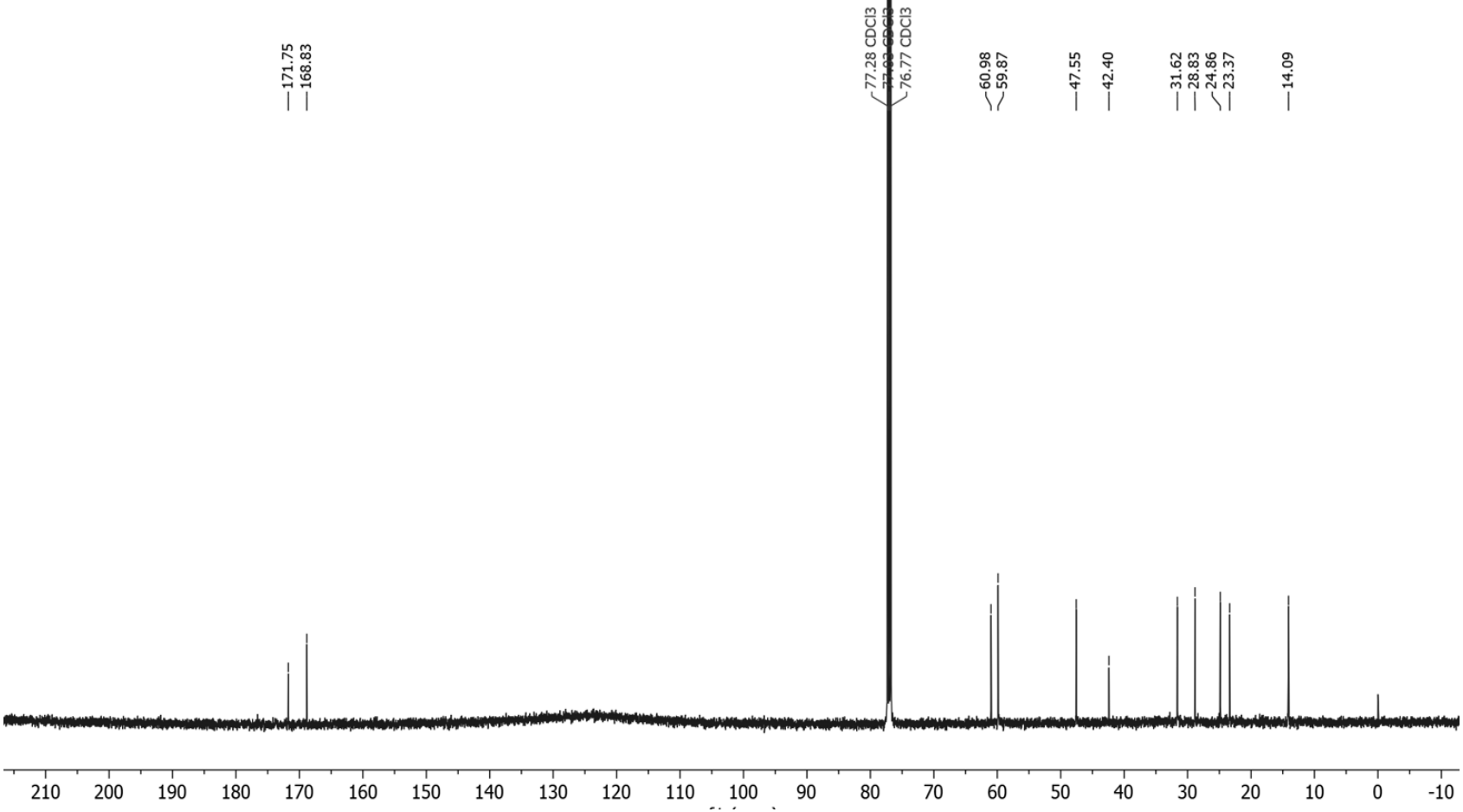

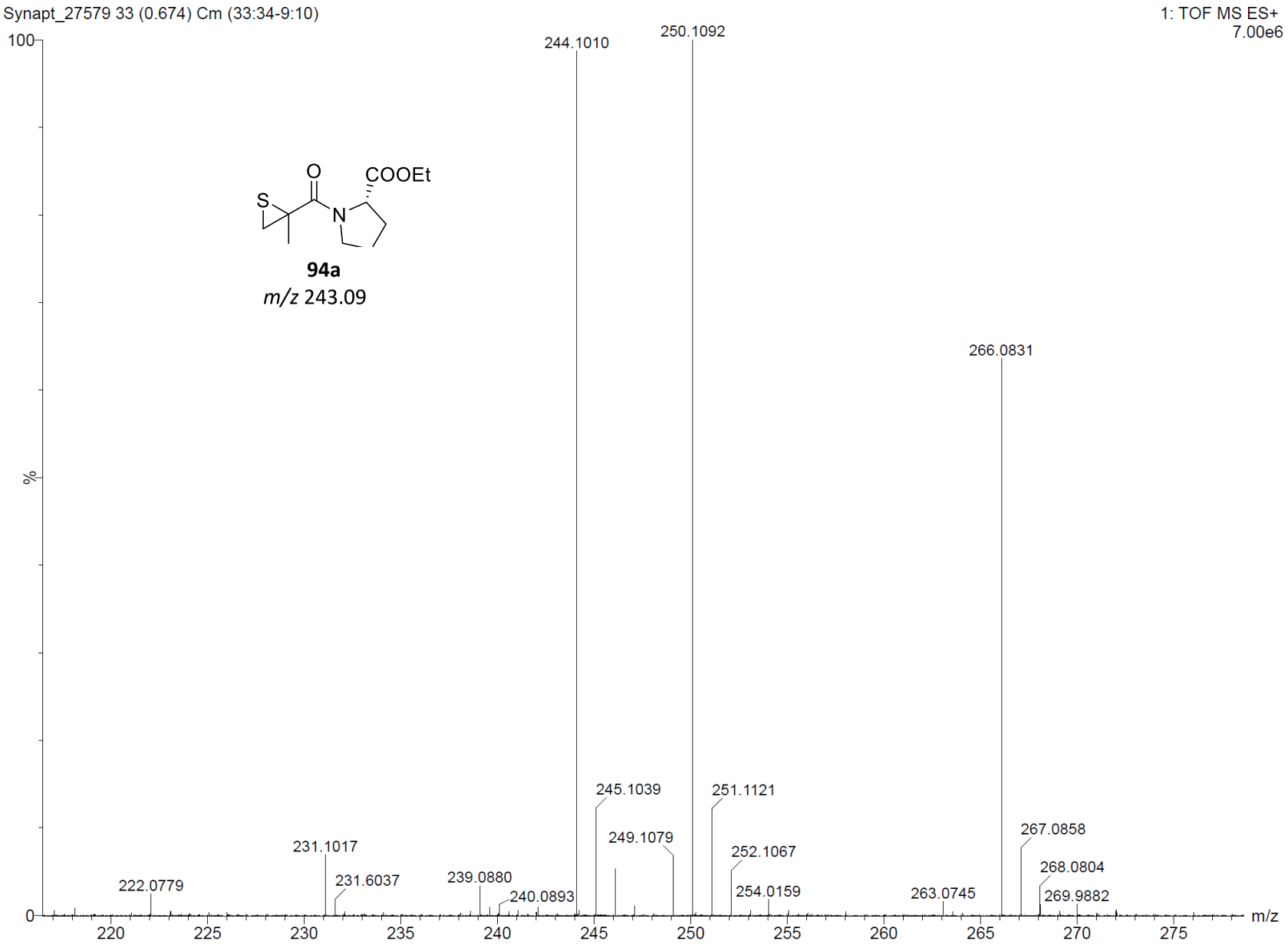
Synapt_27579 33 (0.674) Cm (33:34-9:10)
1: TOF MS ES+
7.00e6
100
%
0
O
COOEt
S
N
94a
m/z 243.09
244.1010
250.1092
266.0831
245.1039
251.1121
249.1079
252.1067
267.0858
268.0804
231.1017
231.6037
239.0880
240.0893
222.0779
254.0159
263.0745
269.9882
220
225
230
235
240
245
250
255
260
265
270
275
m/z

^{1}H NMR (400 MHz, $CDCl_3$)

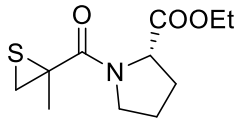

94b

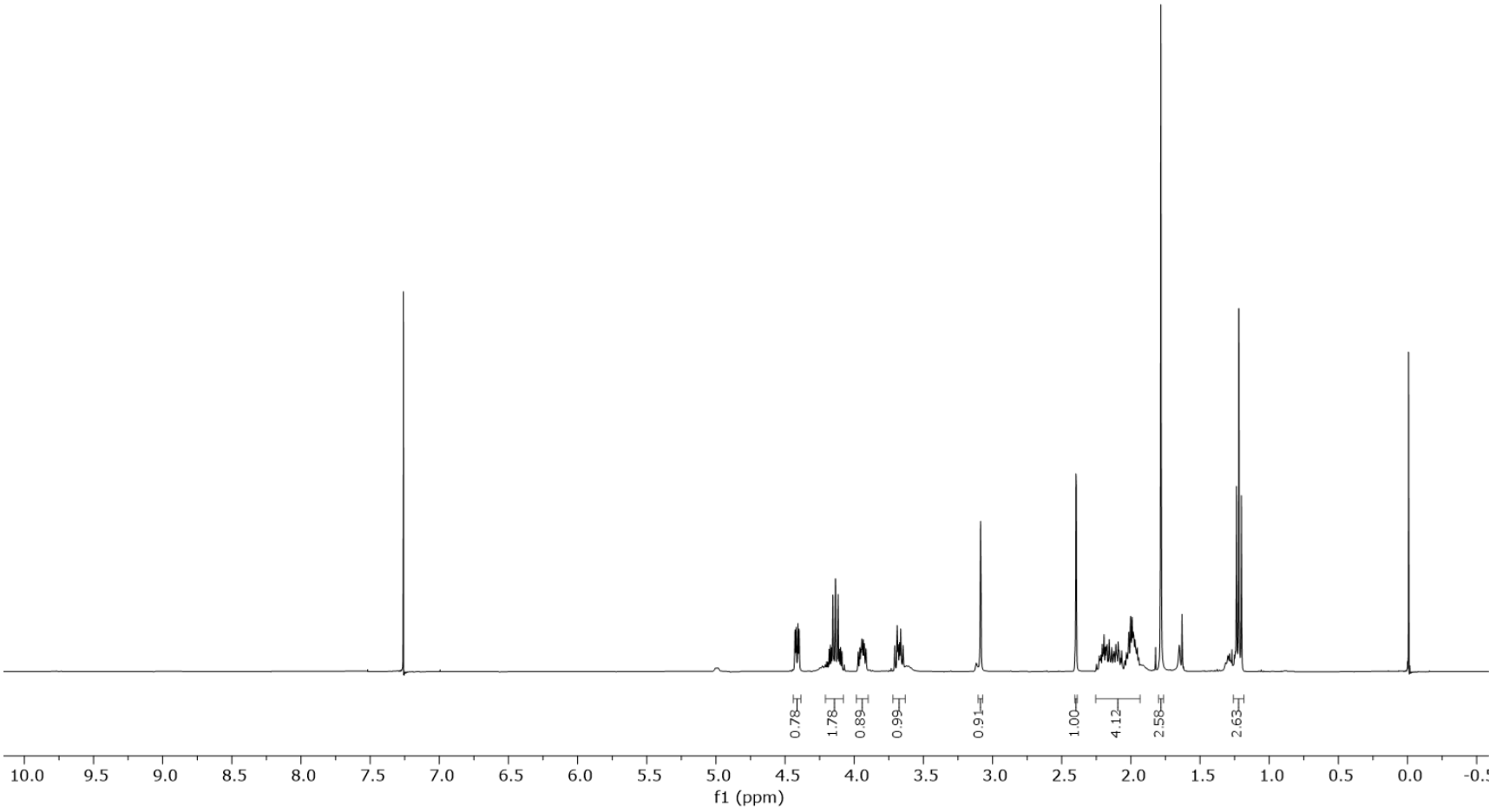

^{13}C NMR (100 MHz, $CDCl_3$)

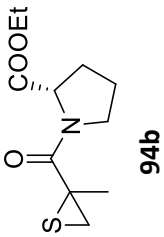

94b

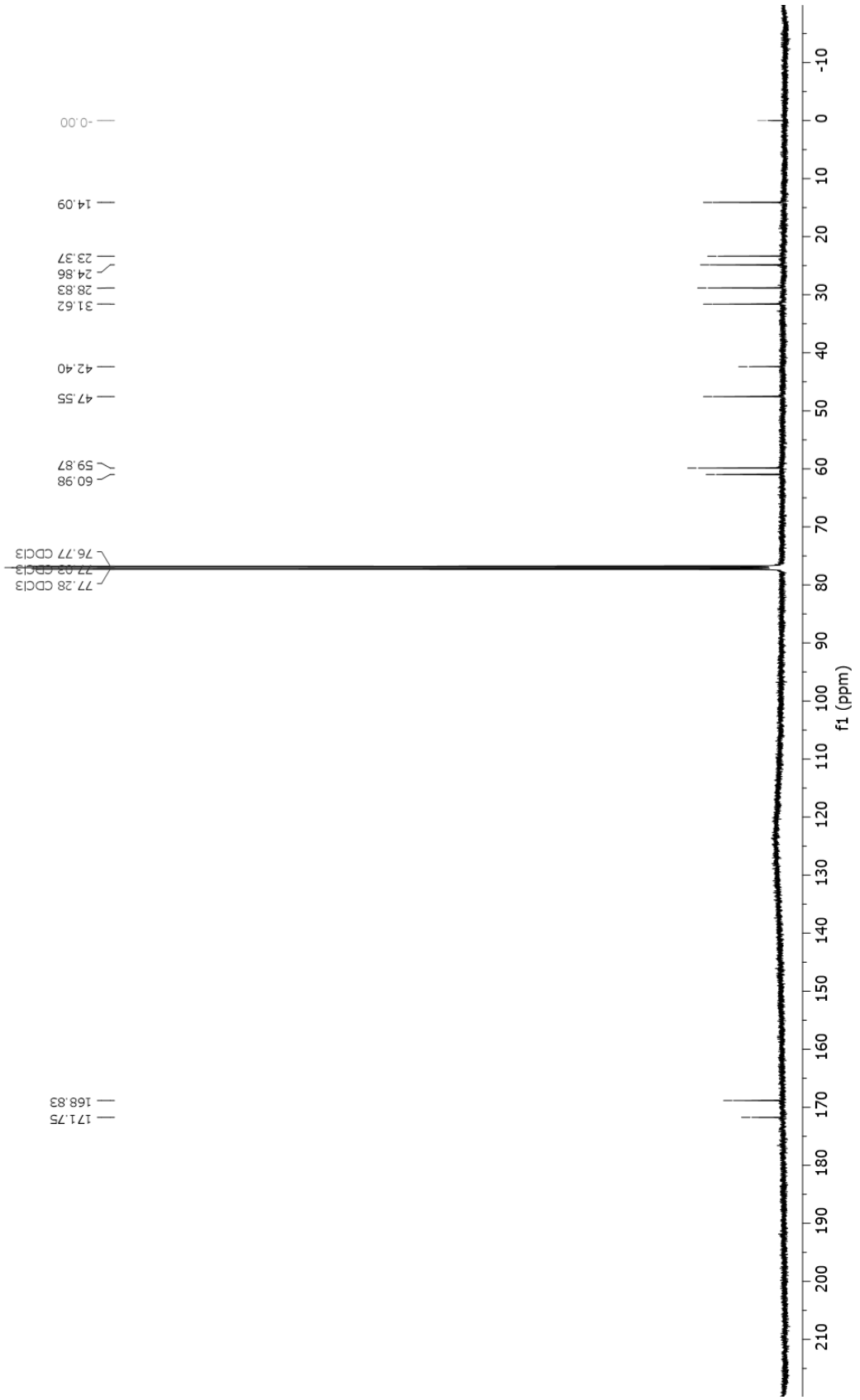

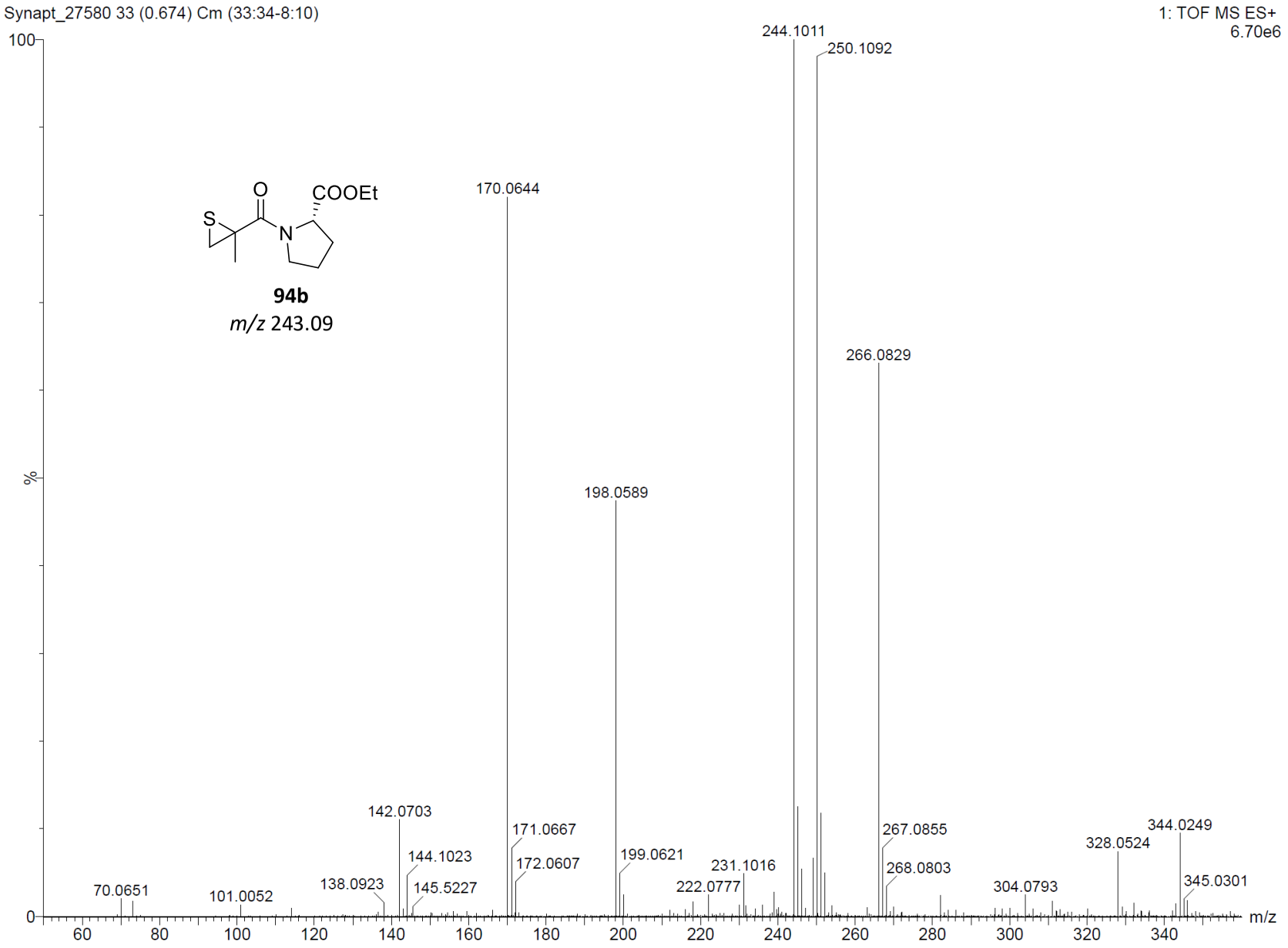
Synapt_27580 33 (0.674) Cm (33:34-8:10)
1: TOF MS ES+
6.70e6
100
%
0
244.1011
250.1092
170.0644
266.0829
198.0589
142.0703
171.0667
144.1023
172.0607
199.0621
231.1016
267.0855
344.0249
328.0524
268.0803
345.0301
304.0793
222.0777
138.0923
145.5227
70.0651
101.0052
60
80
100
120
140
160
180
200
220
240
260
280
300
320
340
m/z
O
COOEt
S
N
94b
m/z 243.09

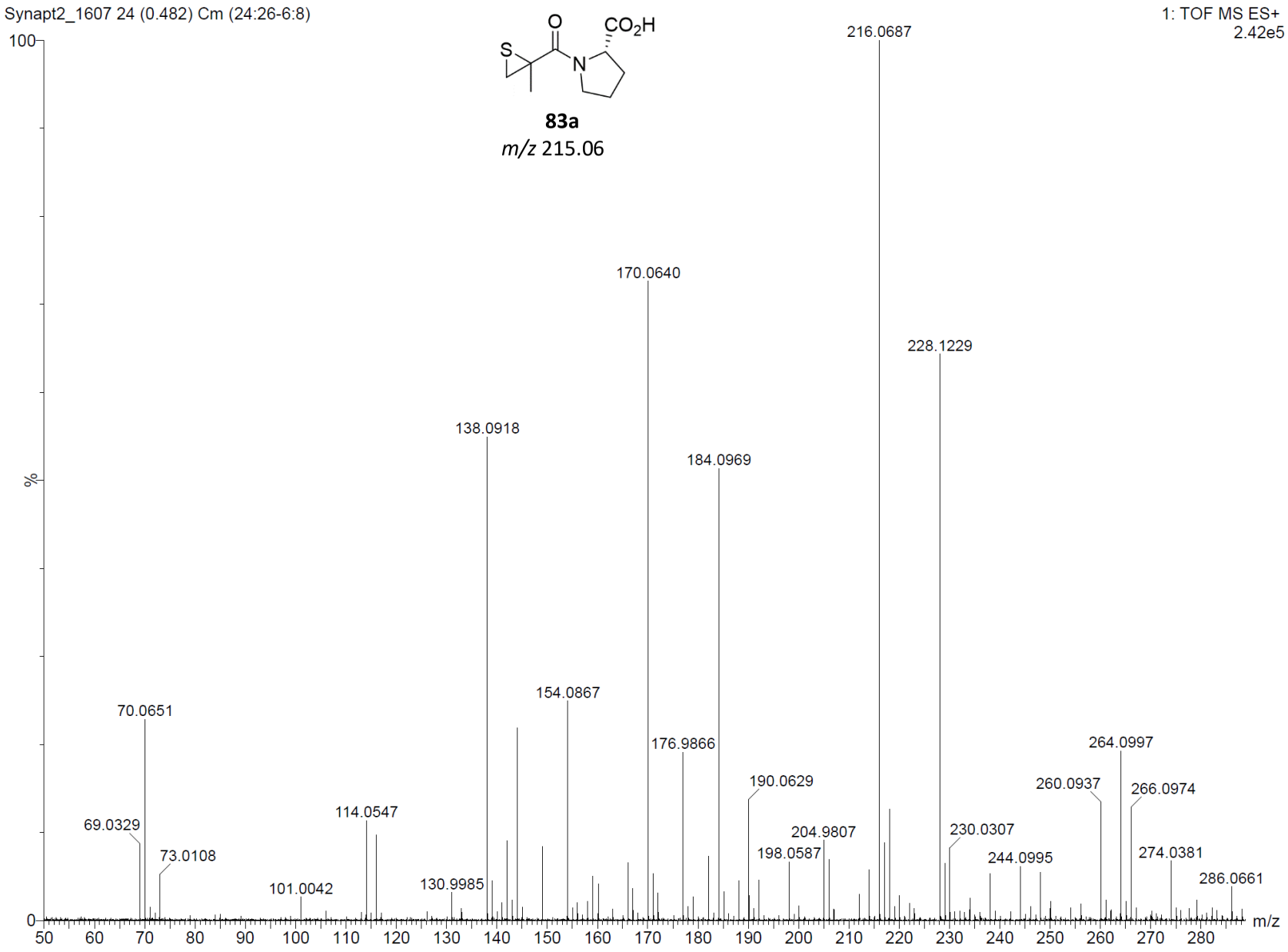
Synapt2_1607 24 (0.482) Cm (24:26-6:8)
1: TOF MS ES+
2.42e5
100
%
0
O
CO2H
S
N
83a
m/z 215.06
216.0687
170.0640
228.1229
138.0918
184.0969
154.0867
70.0651
176.9866
264.0997
190.0629
260.0937
266.0974
114.0547
69.0329
204.9807
230.0307
73.0108
198.0587
244.0995
274.0381
286.0661
101.0042
130.9985
50 60 70 80 90 100 110 120 130 140 150 160 170 180 190 200 210 220 230 240 250 260 270 280
m/z

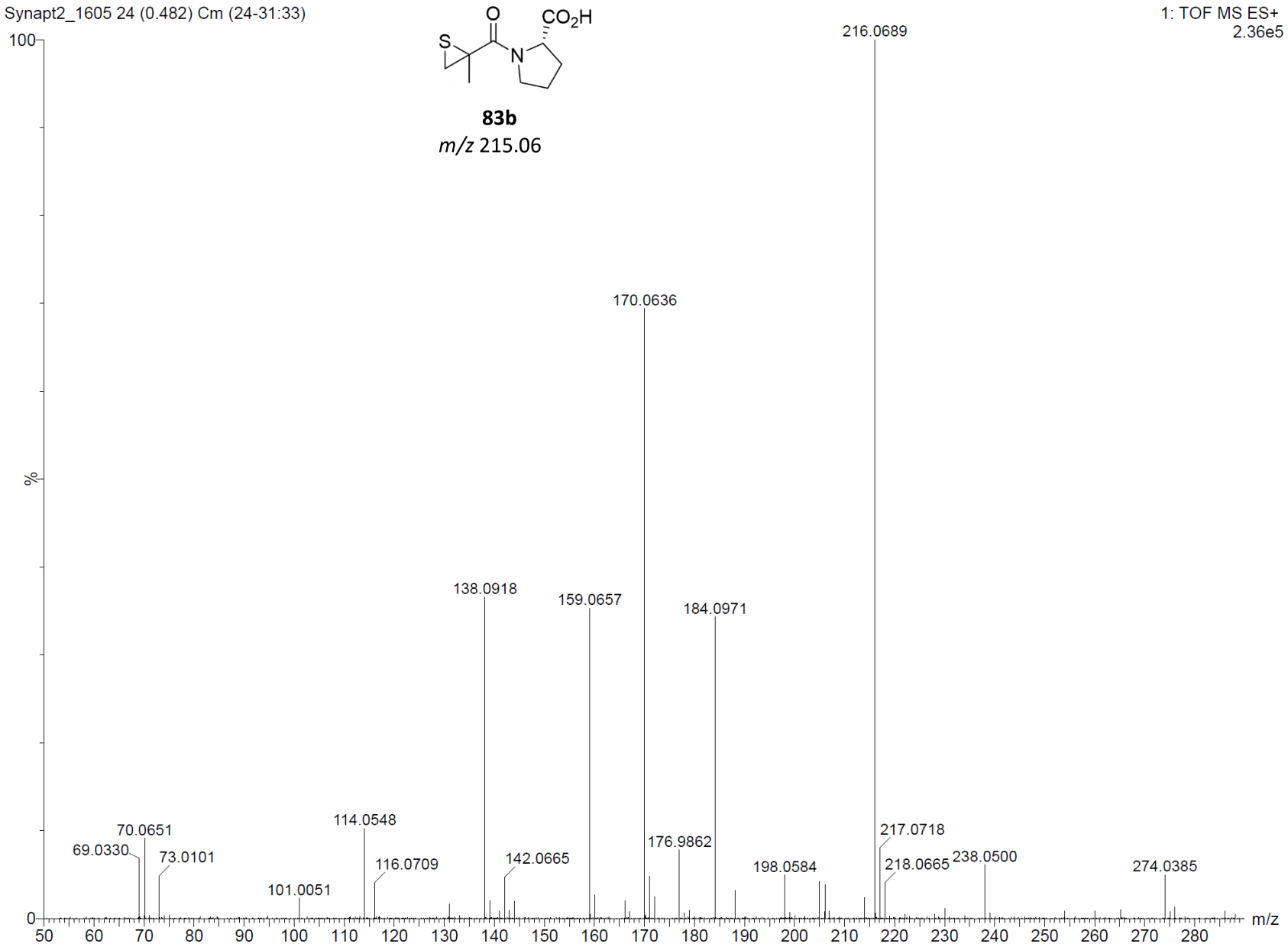
Synapt2_1605 24 (0.482) Cm (24-31:33)
1: TOF MS ES+
2.36e5
O
CO2H
S
N
83b
m/z 215.06
100
%
0
216.0689
170.0636
138.0918
159.0657
184.0971
70.0651
69.0330
73.0101
114.0548
116.0709
101.0051
142.0665
176.9862
198.0584
217.0718
218.0665
238.0500
274.0385
50 60 70 80 90 100 110 120 130 140 150 160 170 180 190 200 210 220 230 240 250 260 270 280
m/z

^{1}H NMR (400 MHz, $CDCl_3$)

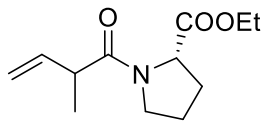

98

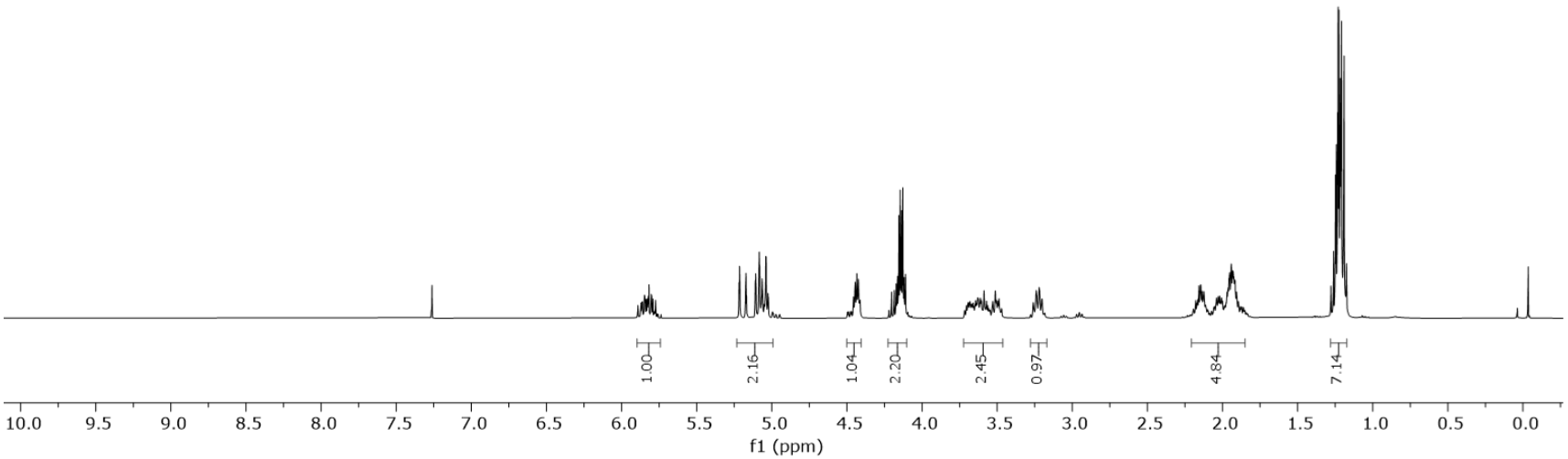

^{13}C NMR (101 MHz, $CDCl_3$)

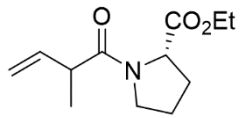

98

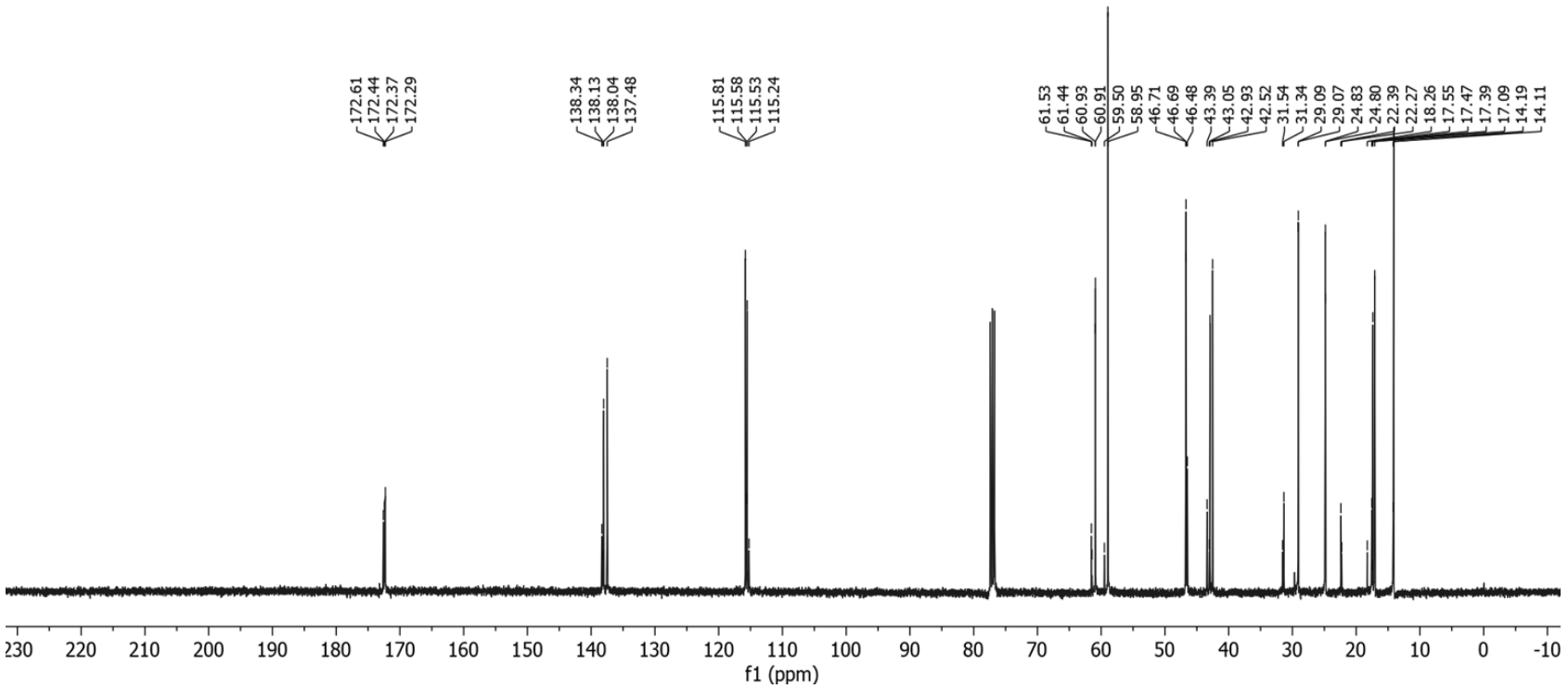

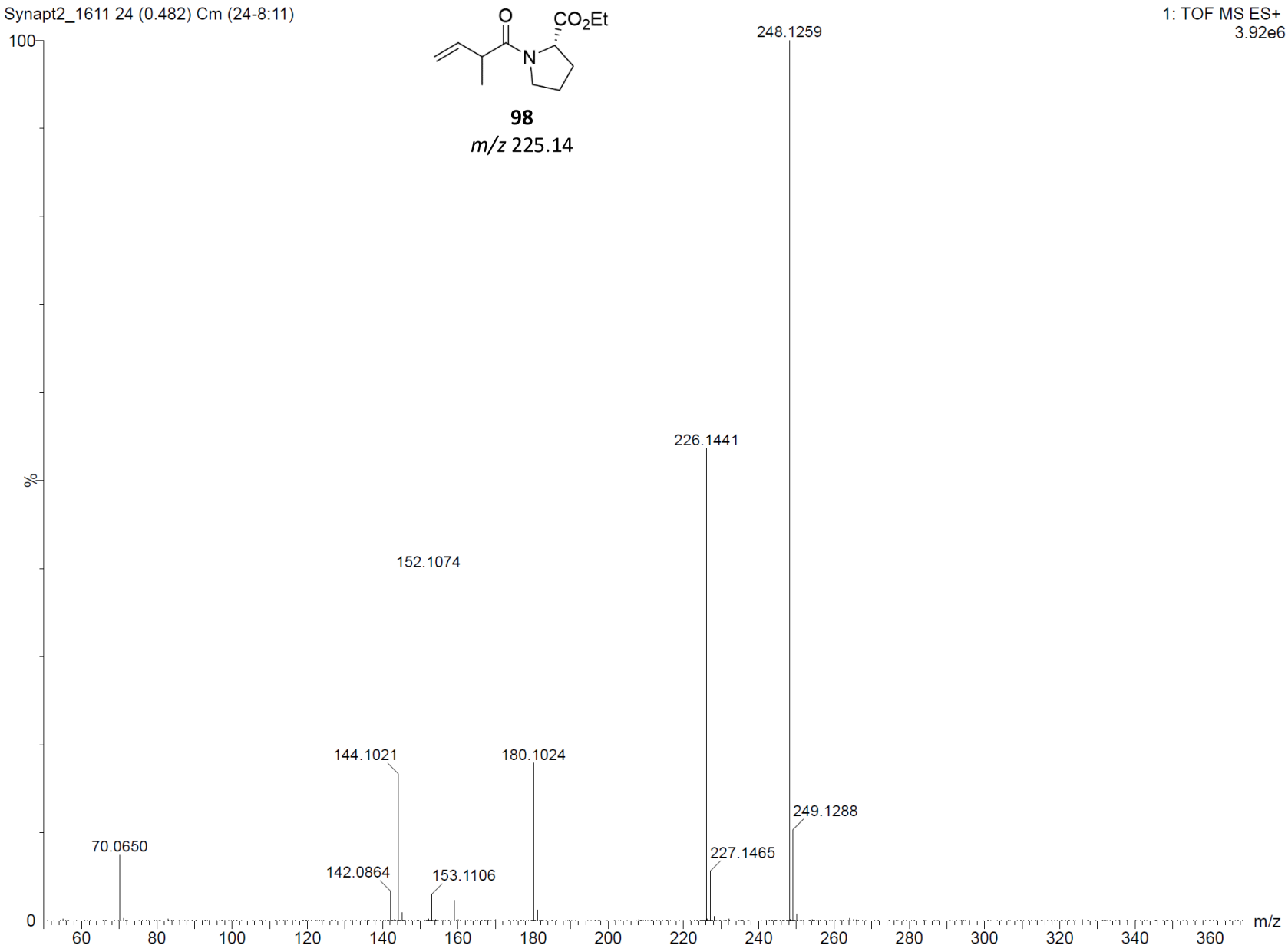
Synapt2_1611 24 (0.482) Cm (24-8:11)
1: TOF MS ES+
3.92e6
O
CO2Et
N
98
m/z 225.14
100
%
0
248.1259
226.1441
152.1074
144.1021
180.1024
249.1288
70.0650
227.1465
142.0864
153.1106
60
80
100
120
140
160
180
200
220
240
260
280
300
320
340
360
m/z

^{1}H NMR (400 MHz, $CDCl_3$)

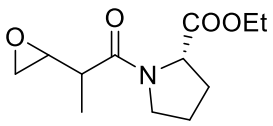

99

^{13}C NMR (101 MHz, $CDCl_3$)

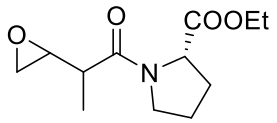

99

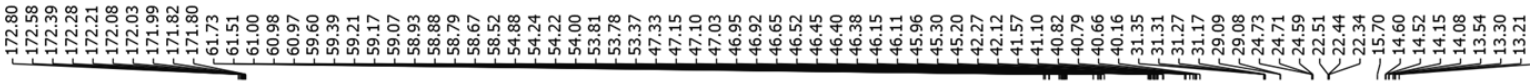

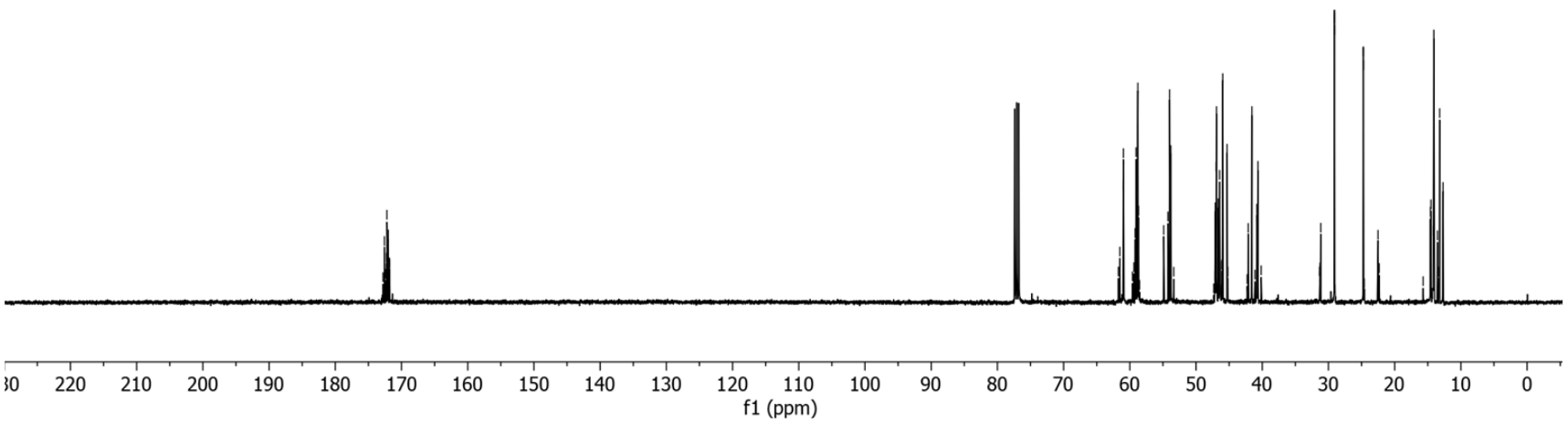

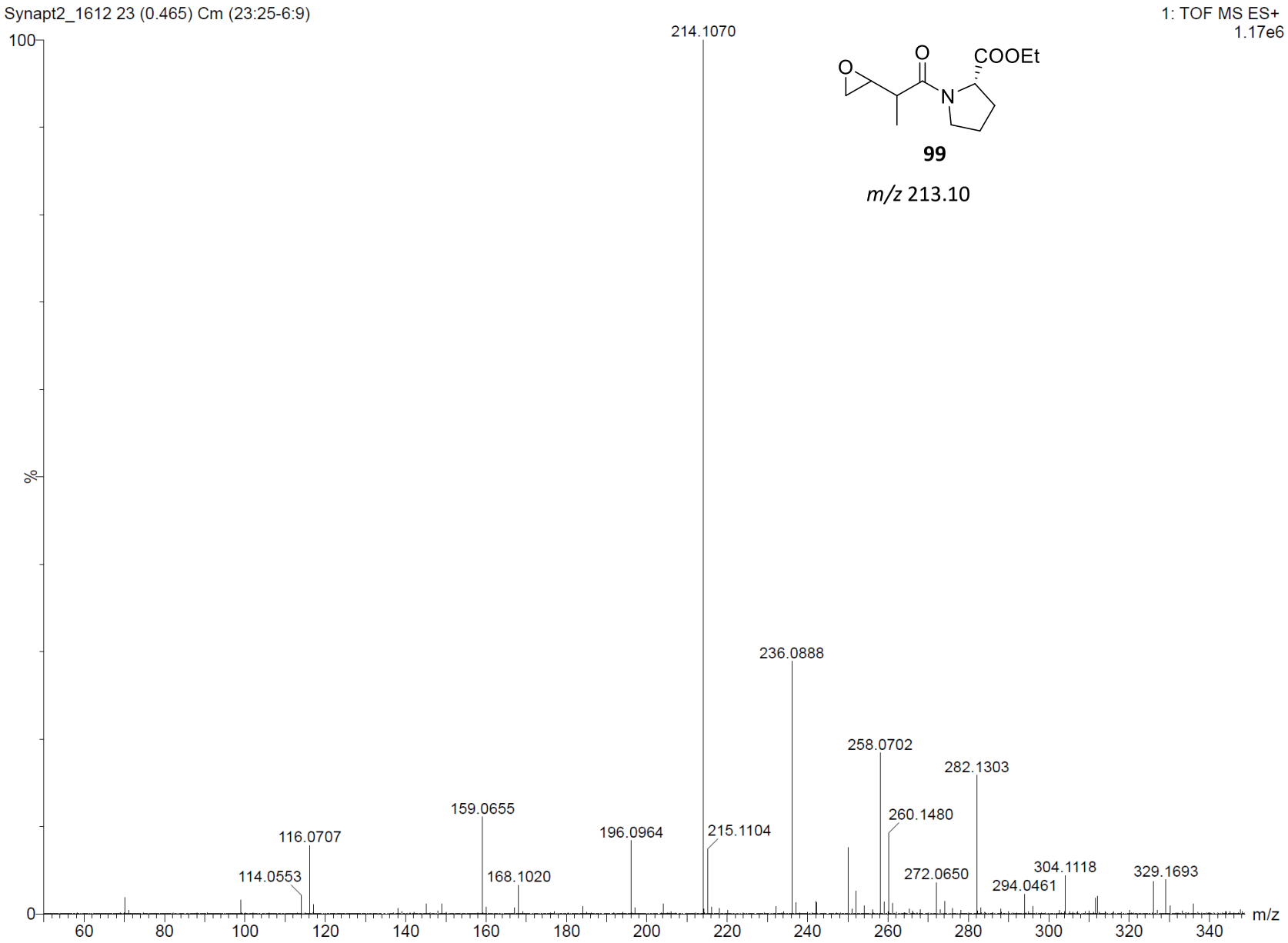
Synapt2_1612 23 (0.465) Cm (23:25-6:9)
1: TOF MS ES+
1.17e6
100
%
0
214.1070
236.0888
258.0702
282.1303
159.0655
260.1480
116.0707
196.0964
215.1104
114.0553
168.1020
272.0650
304.1118
294.0461
329.1693
60
80
100
120
140
160
180
200
220
240
260
280
300
320
340
m/z
O
O
COOEt
N
99
m/z 213.10

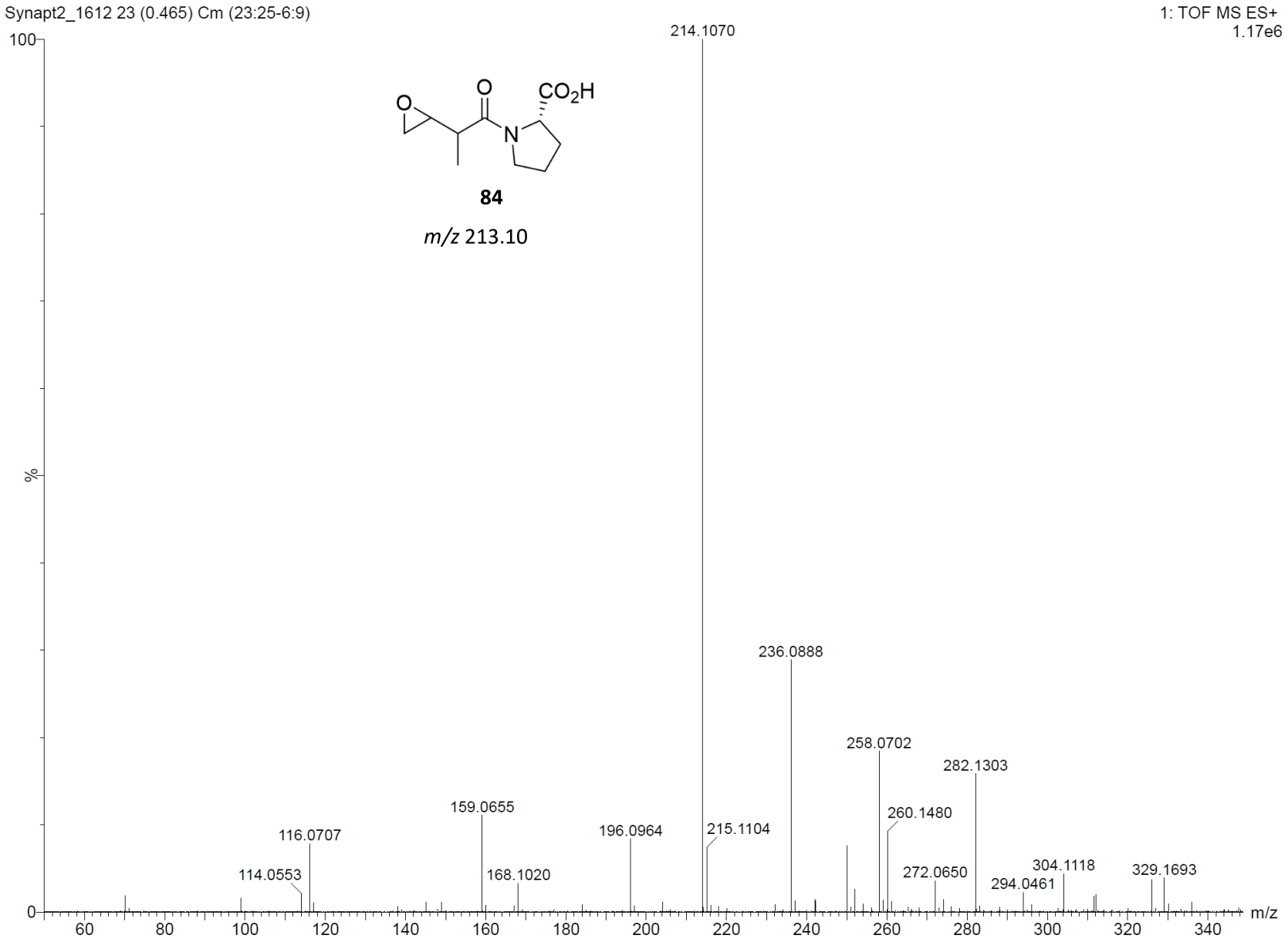
Synapt2_1612 23 (0.465) Cm (23:25-6:9)
1: TOF MS ES+
1.17e6
100
%
0
214.1070
236.0888
258.0702
282.1303
260.1480
159.0655
196.0964
215.1104
116.0707
114.0553
168.1020
272.0650
304.1118
294.0461
329.1693
m/z
60
80
100
120
140
160
180
200
220
240
260
280
300
320
340
O
O
CO2H
N
84
m/z 213.10

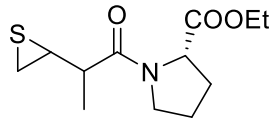
S
O
COOEt
N

100

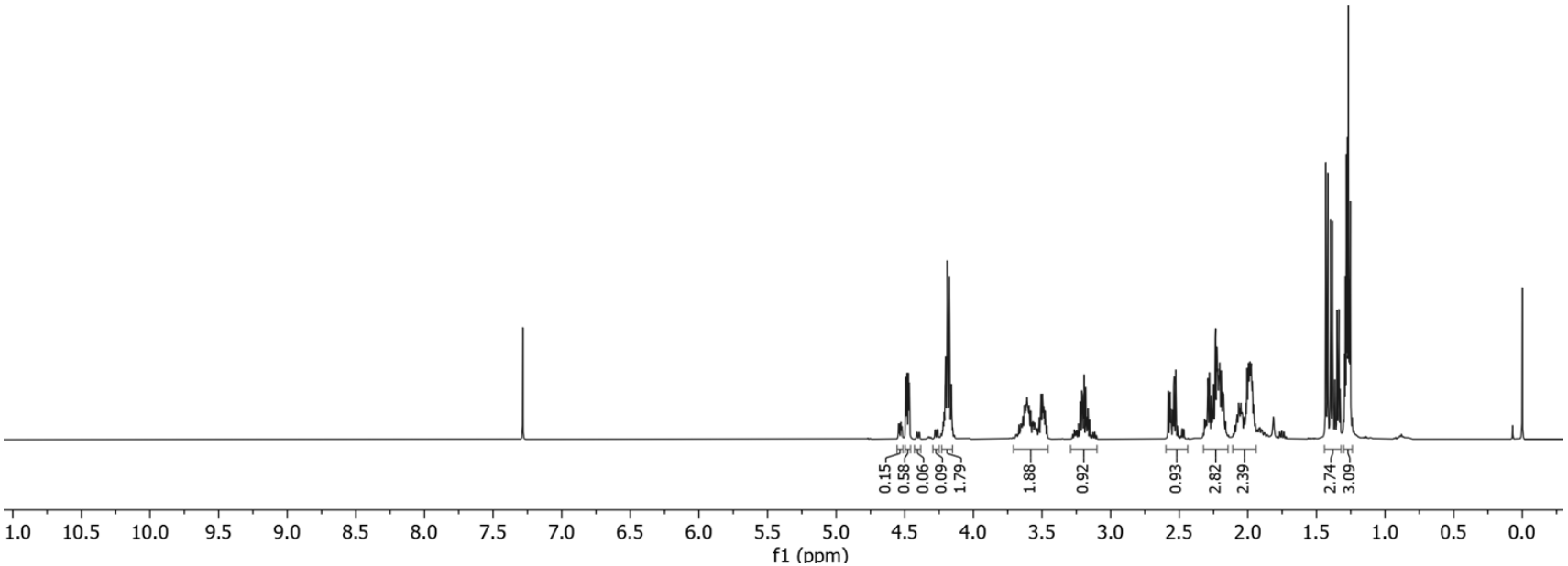
0.15
0.58
0.06
0.09
1.79
1.88
0.92
0.93
2.82
2.39
2.74
3.09
1.0
10.5
10.0
9.5
9.0
8.5
8.0
7.5
7.0
6.5
6.0
5.5
5.0
4.5
4.0
3.5
3.0
2.5
2.0
1.5
1.0
0.5
0.0
f1 (ppm)

^{13}C NMR (101 MHz, $CDCl_3$)

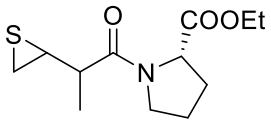

100

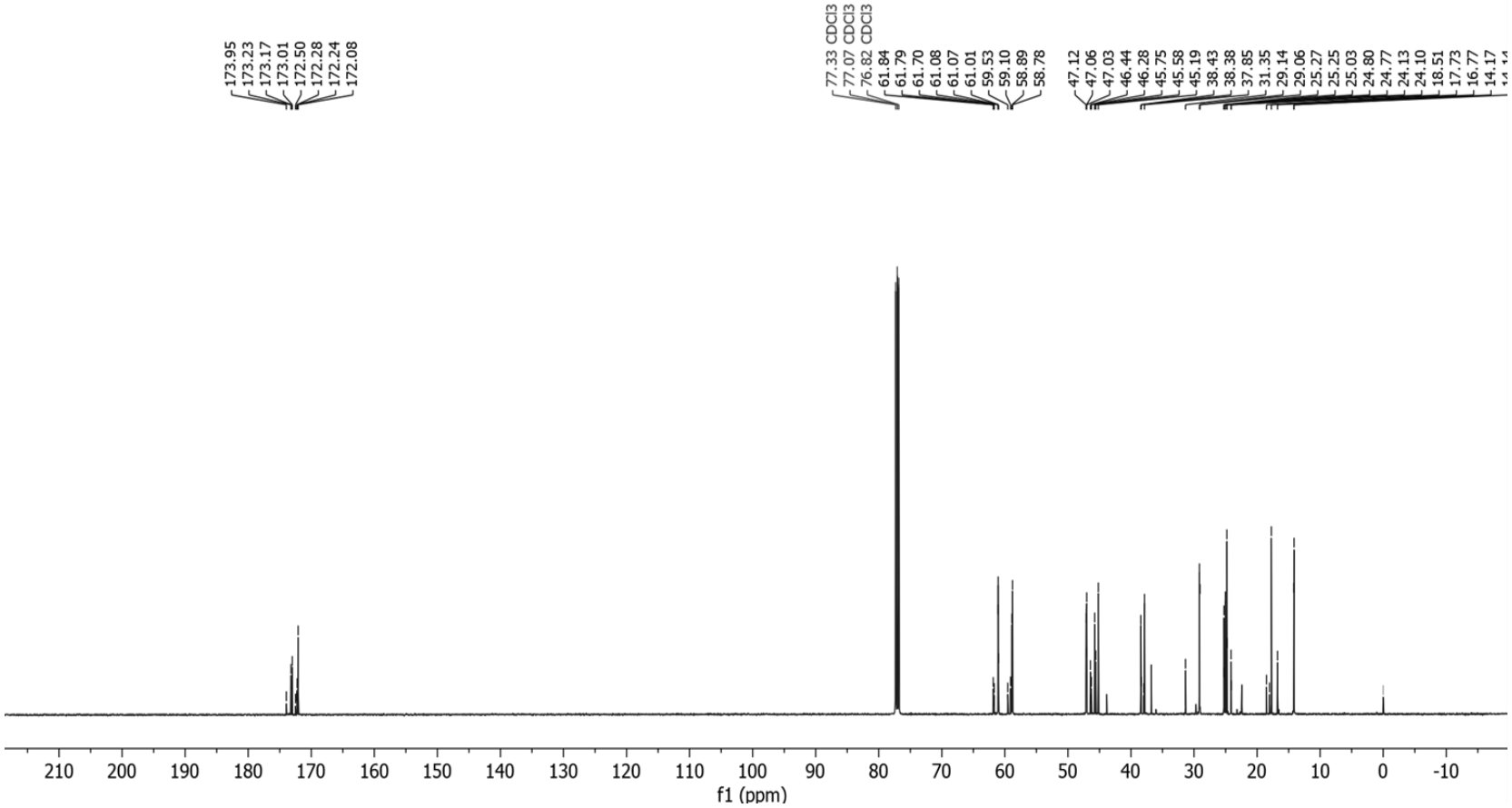

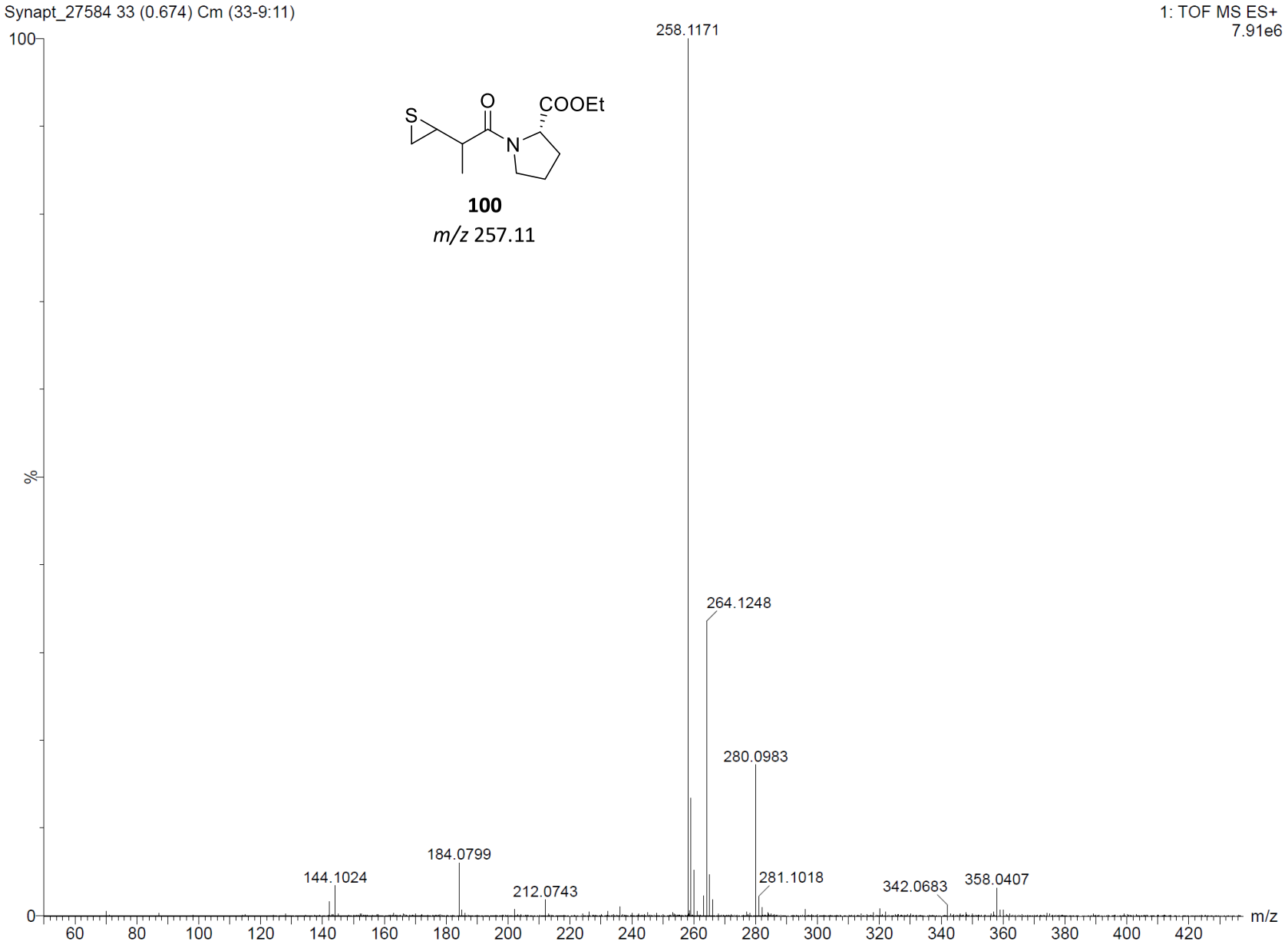
Synapt_27584 33 (0.674) Cm (33-9:11)
1: TOF MS ES+
7.91e6
100
%
0
258.1171
264.1248
280.0983
281.1018
184.0799
144.1024
212.0743
342.0683
358.0407
m/z
60
80
100
120
140
160
180
200
220
240
260
280
300
320
340
360
380
400
420
S
O
COOEt
N
100
m/z 257.11

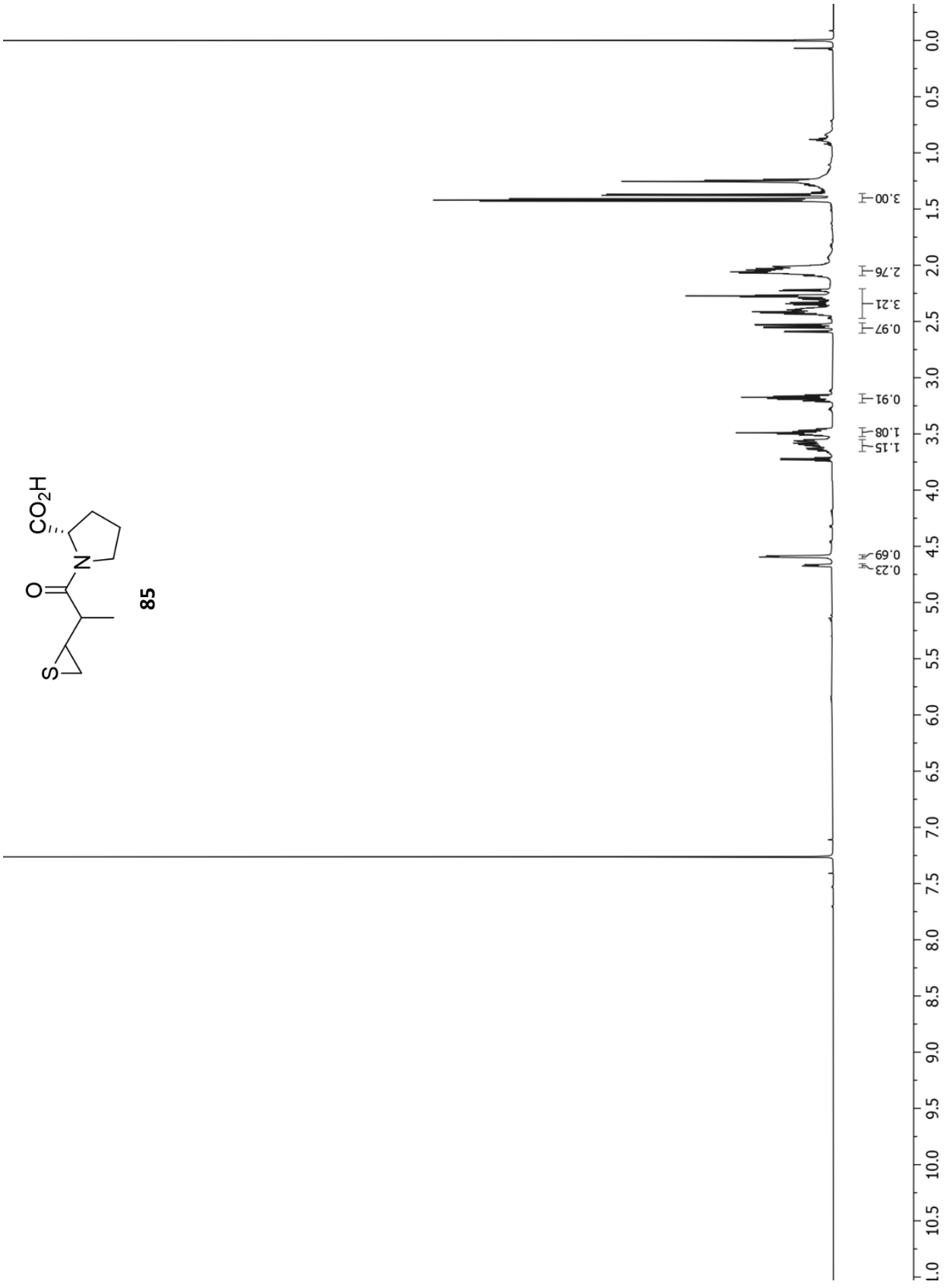
CO2H
O
N
S
85
3.00
2.76
3.21
0.97
0.91
1.08
1.15
0.23
0.69
0.0
0.5
1.0
1.5
2.0
2.5
3.0
3.5
4.0
4.5
5.0
5.5
6.0
6.5
7.0
7.5
8.0
8.5
9.0
9.5
10.0
10.5
11.0

^{13}C NMR (101 MHz, $CDCl_3$)

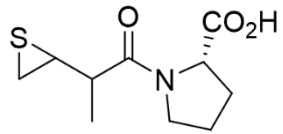

85

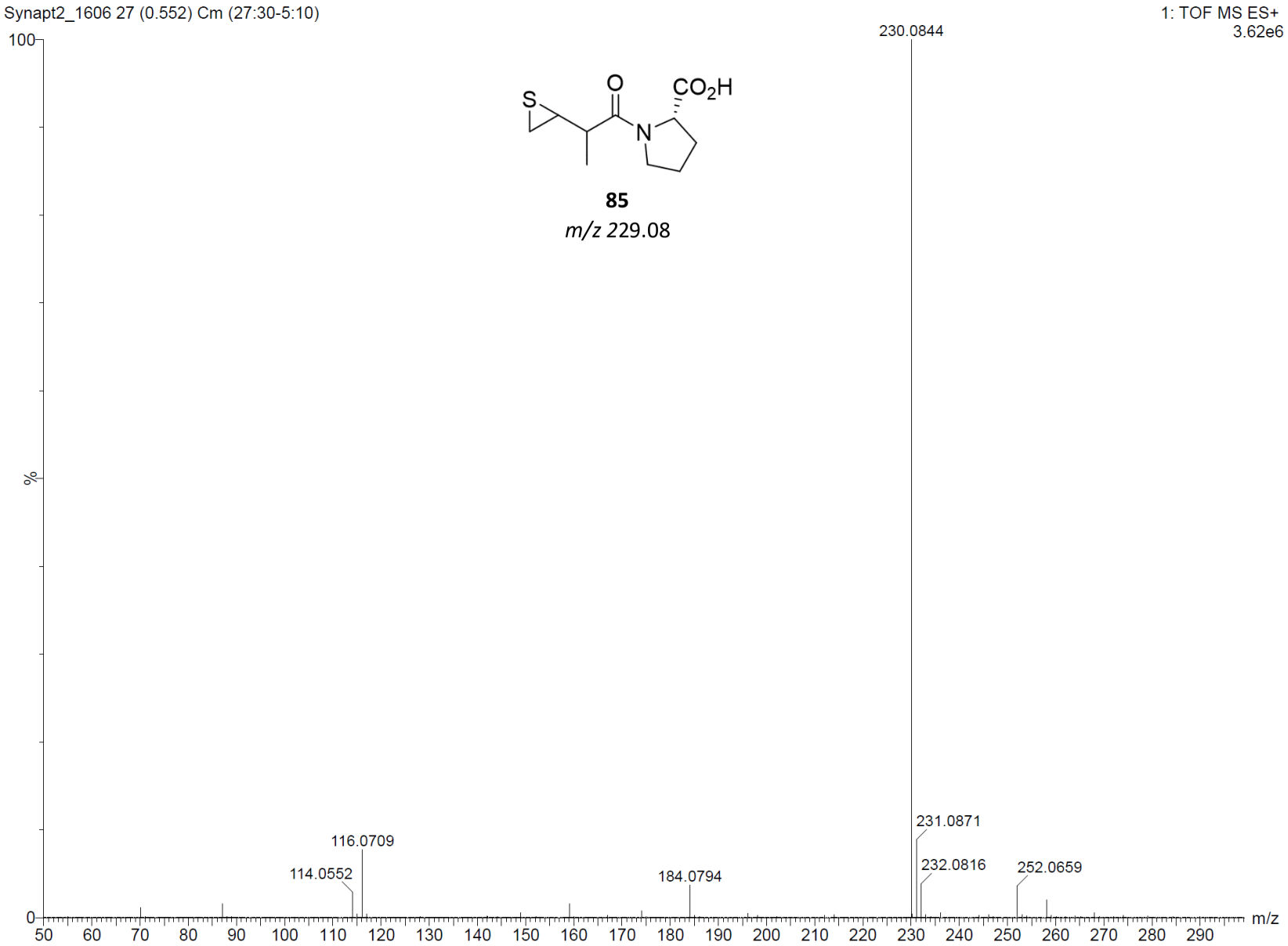
Synapt2_1606 27 (0.552) Cm (27:30-5:10)
1: TOF MS ES+
3.62e6
230.0844
100
%
0
231.0871
116.0709
232.0816
252.0659
114.0552
184.0794
m/z
50 60 70 80 90 100 110 120 130 140 150 160 170 180 190 200 210 220 230 240 250 260 270 280 290

85

m/z 229.08